MINISTRY OF EDUCATION AND SCIENCE OF UKRAINE
STATE UNIVERSITY OF INFRASTRUCTURE AND TECHNOLOGIES

TRANSPORT SYSTEMS AND TECHNOLOGIES

Issue 45

2025

МІНІСТЕРСТВО ОСВІТИ І НАУКИ УКРАЇНИ

ДЕРЖАВНИЙ УНІВЕРСИТЕТ ІНФРАСТРУКТУРИ ТА ТЕХНОЛОГІЙ

З Б І Р Н И К
Н А У К О В И Х П Р А Ц Ь

ДЕРЖАВНОГО УНІВЕРСИТЕТУ ІНФРАСТРУКТУРИ ТА ТЕХНОЛОГІЙ

СЕРІЯ

«ТРАНСПОРТНІ СИСТЕМИ І ТЕХНОЛОГІЇ»

ВИПУСК 45

Київ·2025

Collection of Scientific Papers of the State University of Infrastructure and Technologies of the Ministry of Education and Science of Ukraine: Series "Transport Systems and Technologies". № 45. Kyiv: SUIT, 2025. 173 p. DOI:10.32703/2617-9059-2025-45

e-ISSN 2617-9059
p-ISSN 2617-9040

Збірник містить статті, присвячені теоретичним, методологічним і прикладним проблемам транспортної галузі. У статтях збірника розглядаються питання транспортної інфраструктури та рухомого складу, технології та організації транспортних процесів, інформаційних та комп'ютерних технологій на транспорті, математичного моделювання об'єктів транспорту, екологічної безпеки на транспорті.

Для науковців, викладачів, студентів вищих навчальних закладів і працівників транспорту та зв'язку.

Журнал включено до міжнародних наукометричних баз даних та електронних бібліотек:DOAJ (Directory of Open Access Journals), MIAR (Information Matrix for the Analysis of Journals), ICI World of Journals (Index Copernicus),Scilit, ResearchBib, BASE (Bielefeld Academic Search Engine), ROAD (Directory of Open Access scholarly Resources), OpenAIRE (Open Access Infrastructure for Research in Europe), Crossref, Worldcat, EuroPub, Наукова періодика України, Google Scholar.

Статті збірника проходять обов'язкове подвійне сліпе рецензування членами редакційної колегії та залученими рецензентами, друкуються мовою оригіналу. Редакція не обов'язково поділяє думку автора і не відповідає за фактичні помилки, яких він припустився.

Рекомендовано до друку Вченою радою ДУІТ (протокол № 23 від 30 квітня 2025 р.).

Засновник і видавець – Державний університет інфраструктури та технологій
Ідентифікатор медіа - R30-05246

Збірник внесено до Переліку наукових фахових видань України,
в яких можуть публікуватися результати дисертаційних робіт на здобуття наукових ступенів доктора та кандидата наук у технічній галузі
(Додаток 11 до наказу Міністерства освіти і науки України 29.12.2014 № 1528)
та відноситься до категорії "Б" (відповідно до Порядку формування Переліку наукових фахових видань України, затвердженого наказом МОН України від 15 січня 2018 року № 32) періодичних фахових видань України.

https://tst.duit.in.ua/

MINISTRY OF EDUCATION AND SCIENCE OF UKRAINE

STATE UNIVERSITY OF INFRASTRUCTURE AND TECHNOLOGIES

COLLECTION OF SCIENTIFIC PAPERS

OF THE STATE UNIVERSITY OF INFRASTRUCTURE AND TECHNOLOGIES

SERIES

«TRANSPORT SYSTEMS AND TECHNOLOGIES»

ISSUE 45

Kyiv·2025

Collection of Scientific Papers of the State University of Infrastructure and Technologies of the Ministry of Education and Science of Ukraine: Series "Transport Systems and Technologies". № 45. Kyiv: SUIT, 2025. 173 p. DOI:10.32703/2617-9059-2025-45

e-ISSN 2617-9059
p-ISSN 2617-9040

The collection contains articles devoted to theoretical, methodological and applied problems of the transport industry. The articles of the collection consider the issues of transport infrastructure and rolling stock, technology and organization of transport processes, information and computer technologies in transport, mathematical modeling of transport facilities, environmental safety in transport.

For researchers, teachers, students of higher educational institutions and transport and communications workers.

Journal is included in the international scientific databases:DOAJ (Directory of Open Access Journals), MIAR (Information Matrix for the Analysis of Journals), ICI World of Journals (Index Copernicus),Scilit, ResearchBib, BASE (Bielefeld Academic Search Engine), ROAD (Directory of Open Access scholarly Resources), OpenAIRE (Open Access Infrastructure for Research in Europe), Crossref, Worldcat, EuroPub, Наукова періодика України, Google Scholar.

The articles of the collection undergo mandatory double blind peer review by members of the editorial board and invited reviewers, and are printed in the original language. The editorial board does not necessarily share the author's opinion and is not responsible for the factual errors that he made.

Recommended for publication by the Academic Council of DUIT (Minutes № 23 of April 30, 2025).

Founder and Publisher - State University of Infrastructure and Technologies
Media ID is R30-05246

The journal is included in the List of Scientific and Professional Publications of Ukraine,
in which the results of dissertations for obtaining the scientific degrees of doctor and candidate of sciences in the technical field can be published
(Appendix 11 to the order of the Ministry of Education and Science of Ukraine dated 29.12.2014 No. 1528)
and belongs to the "B" category (in accordance with the Procedure for the formation of the List of scientific specialized publications of Ukraine, approved by the order of the Ministry of Education and Science of Ukraine dated January 15, 2018 No. 32) of periodic specialized publications of Ukraine.

https://tst.duit.in.ua/

DOI: 10.32703/2617-9040-2025-45-1

UDC 004.4

***Nuru Dashdamirli*[1]**

[1]Doctoral student, Azerbaijan Technical University, pr. H. Javid 25, Baku, Azerbaijan, AZ 1148. ORCID: https://orcid.org/0009-0009-0545-7855.

*** Corresponding author**: nurudashdamirli@gmail.com.

Cross-platform development for microcontrollers: design of a virtual machine based portable programming language

The fundamental role of microcontrollers in embedded systems and the Internet of Things (IoT) environments necessitates efficient software development approaches. Resource limitations of microcontrollers, the complexity of low-level programming languages, and the challenges of implementing multitasking slow down the development process considerably. Additionally, the diversity of the microcontroller landscape creates substantial barriers to code portability, leading to increased development time to support different hardware platforms. This paper presents the design of a virtual machine-based programming approach to enable cross-platform development for microcontrollers. The proposed portable programming language integrates with a custom virtual machine, Mico8-Chip, to suit modern microcontroller applications. This allows intuitive control over peripherals and built-in support for concurrent execution. The provided abstraction layer significantly improves code portability and accelerates development by isolating application logic from underlying hardware specifics. The primary purpose of this work is to address the fragmented microcontroller ecosystem and the challenges of low-level programming by introducing a unified and portable development solution.

Keywords*: microcontroller, embedded systems, virtual machine, programming, bytecode, concurrency, Internet of Things.*

Introduction. The increasing need for smart and independent devices within the Internet of Things (IoT) ecosystem has caused a rise in the popularity of microcontroller-based systems. Microcontrollers are now widely used in many types of applications, including automation systems, wearable technologies, home appliances, medical devices, industrial equipment, and robotics. Their key advantages, such as low power use and small size, make them very important for many applications, including various IoT-based technologies [1]. However, using traditional programming methods for microcontrollers has some limits. While the C programming language and similar low-level languages are still commonly used in microcontroller systems and IoT networks, they require careful attention from programmers about important things like memory management, software security, and multitasking [2]. Although other high-level programming languages like MicroPython offer an easy-to-use way to develop software, they often have problems with program execution speed and how they use available memory, so they are not suitable for use in microcontroller environments where resources are limited [3].

A significant challenge in the domain of microcontroller programming comes from the characteristic limitations in hardware resources. These limitations typically evident as restricted Random Access Memory (RAM), small flash memory capacity, and reduced processing power compared to general-purpose computing systems. As a result, developers are required to write highly optimized code to guarantee efficient resource utilization. Furthermore, implementing complex functionalities like multitasking becomes considerably challenging due to the scarcity of available resources. When an embedded system demands concurrent execution of multiple tasks, such as processing data from sensors,

managing communication protocols, and handling user interface interactions through a control panel, the complexity of software development increases substantially. The necessity of ensuring precise memory management and the efficient scheduling of these concurrent tasks inevitably leads to delays in software development cycle.

In this paper, a new approach is proposed that integrates a portable programming language specifically designed for the microcontroller environment with a virtual machine to overcome the previously mentioned difficulties. The primary purpose of this work is to develop a comprehensive solution for cross-platform microcontroller programming that balances ease of development with resource efficiency. To achieve this, this research focuses on creating a portable, high-level programming language with a C-like syntax for microcontroller applications to enhance developer productivity and code readability. A compiler is also developed to translate this language into compact bytecode executable by the Mico8-Chip virtual machine. Additionally, the approach integrates built-in concurrency support within the language and virtual machine to simplify multitasking in embedded systems without external dependencies, demonstrating improved code portability across microcontroller architectures through the virtual machine abstraction layer. The target virtual machine, Mico8-Chip, is a redesigned version of the CHIP-8 architecture, modified to meet the requirements of modern microcontroller systems [4]. CHIP-8 is an interpreted programming language and virtual machine developed in the 1970s for use on microcomputers. CHIP-8 which was designed for the development of interactive programs and games [5]; however, it is still being used in educational environments [6]. The proposed programming language is designed to provide control of microcontroller peripherals, handling of input/output operations, and concurrent program execution. One of the important features of this approach is its built-in multitasking environment, which allows multiple applications to run simultaneously without the need for complex scheduling mechanisms.

The syntax of the proposed programming language is intentionally designed as a simplified derivative of C syntax. The motivation for this similarity is based on C's extensive application in microcontroller systems, thereby minimizing the necessity for programmers to get proficient in an entirely new syntax. Tasks developed in this programming language are converted into special bytecode and executed by the virtual machine. The proposed approach both provides easier control of the hardware in microcontroller systems and increases the portability of the code. Since the same bytecode can be used on different microcontroller platforms without changes, the efficiency and speed of software development increase significantly.

The problem statements. Despite the widespread adoption of microcontrollers in various applications, the current landscape of embedded systems development faces significant issues that decrease its efficiency. One major challenge lies in the inherent fragmentation of the microcontroller ecosystem. There are different microcontroller architectures and vendors, each often requiring specialized toolchains, programming languages, and development environments. This diversity makes it difficult for developers to port their software across different hardware platforms, leading to significant increase of effort and development costs when projects need to scale or adapt to new hardware. Valuable engineering resources are frequently spent on platform-specific optimizations and re-writes rather than on developing core application logic and new features.

Furthermore, the widespread use of low-level languages like C, while offering fine-grained control over hardware, introduces a steep learning curve and requires careful attention to low-level details. This can be particularly challenging for developers entering the embedded systems domain or those working on projects with tight deadlines. The complexity associated with manual memory management, complicated peripheral configurations, and the need to handle hardware-specific nuances can lead to increased development time and a higher likelihood of introducing subtle and hard-to-debug errors. This situation is further compounded by the growing sophistication of embedded applications, which often demand more complex functionalities and interactions, pushing the limits of what can be efficiently managed with traditional low-level programming paradigms within resource-constrained environments.

While higher-level languages offer a potential solution for simplifying development, their inherent overhead in terms of execution speed and memory footprint often renders them unsuitable for the

resource-constrained nature of many microcontroller platforms. This creates a trade-off between ease of development and performance efficiency. Developers are frequently forced to choose between the faster development cycles offered by higher-level languages and the necessary performance and resource optimization achievable with lower-level languages, often leading to compromises that may not fully satisfy the requirements of the target application. This restricts the accessibility of advanced programming concepts and tools within the embedded systems domain, potentially preventing the development of more sophisticated and feature-rich applications on microcontrollers.

The increasing demand for embedded systems to perform multiple tasks concurrently also presents a significant challenge in the context of limited resources. Implementing robust and efficient multitasking capabilities on microcontrollers using traditional methods often requires complex real-time operating systems (RTOS) or custom scheduling mechanisms. This adds another layer of complexity to the development process, demanding specialized knowledge and potentially consuming significant amounts of the already scarce memory and processing power. The need for effective concurrency management becomes even more critical in IoT applications, where devices must interact with their environment and communicate with other systems in a timely and reliable manner.

In essence, the current landscape of microcontroller development is characterized by a tension between the need for efficient resource utilization, the growing complexity of applications, and the aspiration for faster development cycles and increased code portability. These limitations collectively delay innovation, increase development costs, and complicate the creation of sophisticated and adaptable embedded systems. This paper aims to address these fundamental challenges by proposing a unique approach centered around a virtual machine-based portable language specifically designed to bridge the gap between development ease and resource efficiency in the microcontroller domain. This process involves developing a high-level programming language with a C-like syntax and an accompanying compiler that compiles this source code to bytecode for the targeted virtual machine, Mico8-Chip. This approach abstracts hardware complexities and simplifies application logic development while allowing to integrate native concurrency without relying on external scheduling mechanisms. Furthermore, it improves code portability and accelerates development cycles compared to traditional methods.

Related work. Overcoming the characteristic limitations of resource-constrained embedded systems to enable the use of higher-level programming languages has been a persistent focus of research, frequently involving the development of dedicated virtual machines. BIT and PICBIT were two of the early approaches in this domain that sought to bring the benefits of the Scheme programming language to microcontrollers. The development of BIT detailed a highly compact implementation of the Scheme programming language, focusing on achieving space efficiency and real-time garbage collection through a compact byte-code compiler and runtime system [7]. This work demonstrated the feasibility of running meaningful Scheme programs on microcontrollers with limited memory, with the limitations of relatively lower execution speed and the omission of error-checking. Further investigation into Scheme for resource-constrained devices was conducted with PICBIT, a specific adaptation of a Scheme system for the PIC microcontroller family. PICBIT utilized a 24-bit object representation and incorporated a byte-code interpreter and optimizing compiler [8]. The PICOBIT system was later modeled after these early virtual machine approaches, which included an optimizing C compiler named SIXPIC [9].

Addressing the challenge of executing Java applications on resource-constrained microcontrollers, the Darjeeling Virtual Machine was designed to provide a memory-efficient solution for environments such as wireless sensor networks. The primary objective was to design and implement a virtual machine that supports a subset of Java functionality suitable for microcontrollers. Darjeeling introduced a system comprising a runtime and offline tools that implement a modified Java Virtual Machine (JVM) designed for minimal memory usage. Key innovations of this approach include the selective omission of certain JVM features, a compact static linking model using infusions, and a unique memory model. The system also uses a basic mark-and-sweep garbage collector and supports preemptive multithreading.

Performance evaluations on AVR128 and MSP430 microcontrollers demonstrated effective operation with limited memory resources and execution speeds up to 70,000 JVM instructions per second [10].

Efforts to overcome the constraints of microcontroller environments have also led to the development of alternative JVM designs. The TakaTuka JVM specifically designed for microcontrollers with limited RAM, storage, and processing power. The TakaTuka JVM introduces techniques such as offline garbage collection, which allows deallocation of reachable but unused objects, and a variable slot size scheme for efficient memory management. The system also implements extensive Java binary optimizations, including bytecode compaction and constant pool optimizations, and utilizes a direct threading mechanism for bytecode interpretation. The main limitation of this approach is the potential restriction in dynamic adaptability due to the reliance on offline analyses for memory management [11].

Methods for improving microcontroller programming were also explored through unique virtual machine approaches, such as the OCaLustre system, which was developed as a synchronous extension to the OCaml programming language. The system works along with OCaPIC, a virtual machine designed to run OCaml bytecode on PIC microcontrollers. The primary aim was to enable safer, more expressive, and concurrent software for microcontrollers by integrating a higher-level programming model with efficient memory use. The OCaLustre system introduces nodes for deterministic concurrent tasks and features a compilation model that translates these nodes into sequential OCaml functions. Benchmarking analyses demonstrated OCaLustre's advantages in both static and dynamic resource efficiency compared to other concurrency models [12]. Later work introduced a generic virtual machine approach for programming microcontrollers with the OMicroB project. Building on earlier findings with OCaPIC, this research focused on enhancing the safety and portability of microcontroller programming by utilizing the OCaml language and the OMicroB VM, which is implemented in C. This approach involves compiling OCaml to bytecode, optimizing it with the "ocamlclean" tool, and then converting it into C code using a custom tool called "bc2c". Key findings demonstrated that the OMicroB VM could effectively execute OCaml programs on resource-constrained microcontrollers, such as the ATmega328P used in Arduino Uno boards [13].

Recognizing the potential of WebAssembly beyond web environments, its application was explored as an alternative programming platform for microcontrollers. The core objective was to enhance the efficiency, safety, and ease of programming for microcontrollers. WARDuino, a virtual machine built upon WebAssembly and improved with features such as live code updates, remote debugging, and modular runtime configuration was created and examined. The architecture of WARDuino integrates WebAssembly and Arduino functionalities, exposing hardware capabilities through specific modules. Benchmarks demonstrated that WARDuino achieved significantly faster execution compared to Espruino, a JavaScript interpreter for microcontrollers, while maintaining smaller binary sizes [14].

Researchers have also explored the feasibility and performance of implementing minimal virtual machines on microcontroller-based IoT devices. The research focused on evaluating two virtual machine architectures: a stack-based VM using WebAssembly and a register-based VM built upon extended Berkeley Packet Filters, called rBPF. Their goal was to identify solutions for process isolation and software modularity with minimal resource overhead. Evaluations demonstrated that the rBPF interpreter had a significantly smaller flash memory footprint compared to WebAssembly. However, rBPF exhibited longer execution times. The study highlighted rBPF's advantages in memory efficiency and its potential for process isolation on microcontrollers without requiring hardware memory protection units [15].

The complexity and safety issues in microcontroller programming was addressed by proposing SenseVM, a virtual machine that implements a higher-order concurrency model. The principal objective of the research was to streamline the programming of reactive and concurrent embedded systems by introducing a high-level message-passing interface based on functional programming. SenseVM introduces a concurrency model where synchronous operations are encapsulated as first-class values

called "events", which can be composed using various combinators. The virtual machine, SenseVM, is an interpreter built upon the Categorical Abstract Machine (CAM) architecture and includes a low-level bridge that interfaces with Zephyr OS for hardware-agnostic interaction. Evaluations demonstrated code portability across different microcontroller platforms, with power consumption comparable to optimized C implementations, although response times revealed a performance overhead [16].

Summing up the above works, the field of microcontroller programming has seen a significant push towards adopting higher-level languages and virtual machine technologies to address the limitations and complexities associated with traditional low-level approaches. Various studies have explored the implementation of languages like Scheme, Java, OCaml, and WebAssembly through custom-made virtual machines, each addressing the unique challenges of memory efficiency, performance, and concurrency on microcontrollers. These efforts have introduced innovative techniques in memory management, garbage collection, code optimization, and concurrency models. Different architectures have been investigated, often coupled with specialized compilers and optimization tools. While each approach presents its own strengths and limitations in terms of performance, memory usage, and portability, the overarching goal is to simplify microcontroller programming, enhance developer productivity, and enable the development of more sophisticated and safer applications for embedded systems. The main contributions of this paper are summarized as follows:

• A minimalist virtual machine-based architecture designed to enable cross-platform development for embedded systems.

• The design and implementation of a portable language specifically for microcontrollers, enabling code reuse across different hardware platforms.

• An approach that aims to balance the performance of low-level programming with the abstraction of high-level languages in the context of embedded systems.

Proposed programming language and compiler architecture. Microcontrollers typically have limited processing power and RAM resources compared to microprocessors. Therefore, it is not advisable for applications targeting microcontroller environments to carry out intensive calculations and allocate large chunks of memory. Understanding these limitations is important for selecting the right microcontroller for a specific application and designing systems that can operate effectively within these limitations. Microcontrollers are essential in devices that require low power consumption, especially for battery-powered wearable technologies. The proposed portable programming language was designed taking into account the limitations often encountered in microcontroller environments. The syntax and keywords of the language are similar to the C programming language, simplified to enable compilation into minimalistic virtual machine systems, such as Mico8-Chip, and to ensure low resource usage. Therefore, functionalities such as dynamic memory allocation and the definition of complex data models have not been integrated into the language.

To run the developed programs in the microcontroller environment, it is first necessary to convert the human-readable source code into bytecode that can be executed by a Mico8-Chip virtual machine. For this, a compiler designed for the proposed programming language is used. The compiler's conversion of source code into bytecode is a multi-stage process, which determines whether the program code is syntactically and semantically correct before execution. The compilation process goes through the following stages:

1. Reading source code. Human-readable source code is read from a file. This code is written in the syntax of the proposed language.

2. Lexical analysis. Source code is broken down into tokens. In programming languages, tokens are the smallest meaningful units processed by compilers or interpreters. Examples of tokens include keywords, operators, identifiers, and numbers.

3. Syntax analysis. Tokens are checked against the grammatical rules of the language. A syntax tree is constructed, representing the hierarchical structure of the code. This stage ensures that the code is

syntactically correct.

4. Semantic analysis. The code is checked for semantic correctness. This includes checking types, determining whether variables and functions are declared before they are used, and ensuring that function calls are correct.

5. Creation of intermediate representation code. After semantic analysis, the syntax tree is converted into intermediate representation code. Intermediate representation code is a form that can be more easily optimized and manipulated than source code.

6. Optimization. Various optimization techniques are used to improve the execution performance. This stage may include eliminating code duplication, removing unreachable code, and optimizing loops.

7. Bytecode generation. Bytecode is a low-level, platform-independent code that can be executed by the proposed virtual machine. Bytecode generation is performed based on the intermediate representation code.

All errors and warnings encountered at various stages of the compilation process are logged by the compiler. Errors result in the compilation process failing to complete, while warnings reveal potential problems in the source code. This helps in identifying and fixing problematic parts of the code. This systematic approach ensures that the source code is validated and transformed into an efficient bytecode format that is suitable for execution in the virtual machine environment (Fig. 1).

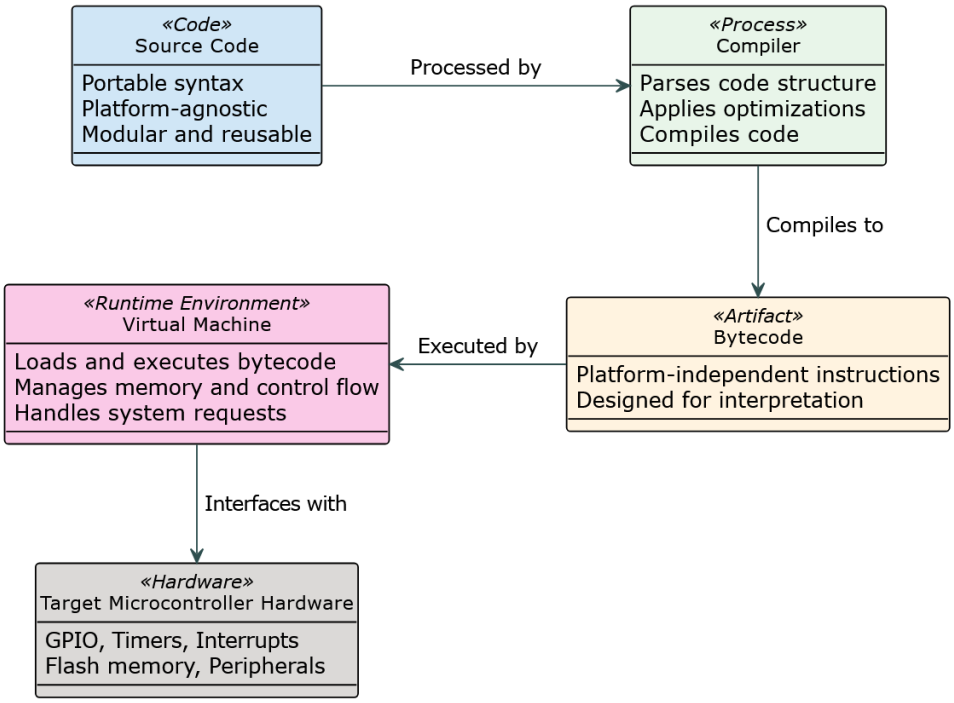

Fig. 1. **Execution flow for the proposed portable programming language for microcontrollers**

Tokens and lexical structure. The initial phase of compilation transforms unstructured text source code into a sequence of meaningful symbols that can be processed by following compiler stages. These symbols are tokens, which act as blocks of source code and are categorized based on their role in the syntax of the proposed language. The process of breaking down source code into tokens is called tokenization or lexical analysis and is the initial step in the compilation or interpretation process where the source code is scanned and tokens are identified.

The operational process of lexical analysis involves the compiler's lexer systematically reading the

source code, character by character. As it reads, it applies the defined lexical structure rules for grouping characters into lexemes and assign them the appropriate token types. For instance, upon encountering the sequence 'i', 'f', the lexer recognizes it as the keyword "if" rather than two separate identifier tokens. This recognition is based on the defined keywords list and the longest match principle. Whitespace and comments encountered during this scan are recognized and filtered out. If a sequence of characters is encountered that does not fit to any valid token pattern, a lexical error is reported. The output of this phase is a list of tokens (Fig. 2).

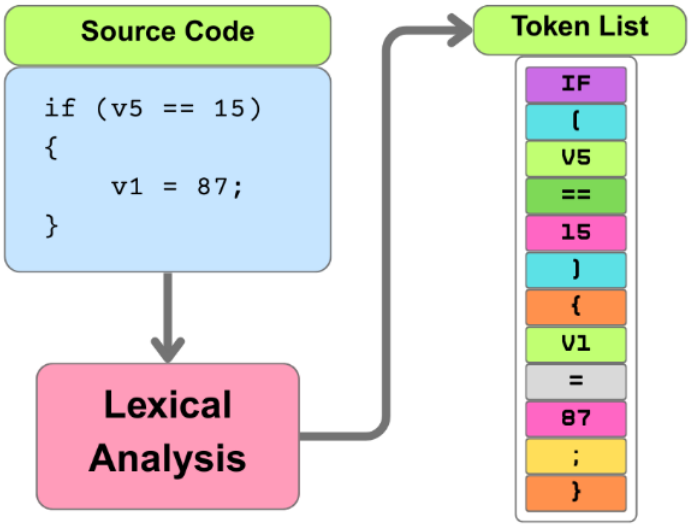

Fig. 2. **Tokenization process of the source code**

The types of available tokens are keywords, identifiers, literals, operators, and comments. Identifiers are names given to tokens such as variables, functions, and labels. Identifiers must follow certain naming conventions, starting with a letter or underscore and consisting of letters, digits, or underscores. Keywords are words with special meanings, such as "if", "else", "while", and "for", which cannot be used as identifiers. Literals represent constant values that are directly represented in the code, like integer and string literals. Operators are tokens that express operations on operands, and include arithmetic, comparison, and logical operators. There are also tokens that provide structure to the language but have no independent meaning, such as commas, semicolons, parentheses, curly braces, and square brackets. Comments are single-line or multi-line annotations that allow developers to make notes within the source code, although they do not affect the execution of the program.

The proposed language has a similar token structure to C, with the elimination of tokens that are not implemented due to different constraints of the targeted virtual machine, Mico8Chip (Fig. 3). While this limits the use of syntactic patterns, it is necessary for achieving the minimal memory and storage footprint for the virtual machine implementation and resulting executable.

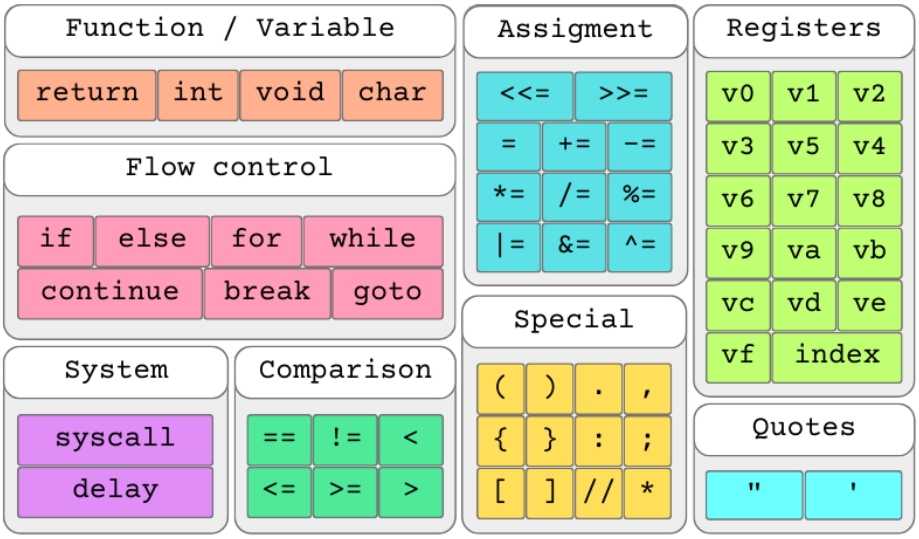

Fig. 3. **Categorization of available tokens of the proposed programming language**

Syntax analysis. The token stream produced by the lexical analysis phase serves as the input for the subsequent stage of compilation: syntax analysis. By converting the raw character data into a structured sequence of meaningful tokens, the lexical analyzer simplifies the task of the parser. The parser can then operate on these higher-level tokens rather than individual characters, allowing it to focus on verifying the grammatical structure and hierarchical relationships within the code according to the language's syntax rules. This separation is a fundamental principle in compiler design, contributing to modularity and simplifying the complexity of both the lexical and syntactic analysis phases.

The primary objective of syntax analysis is to determine if the sequence of tokens produced by the lexer conforms to the formal grammatical rules defined for the proposed programming language. This process verifies the structural correctness of the code and simultaneously constructs a hierarchical representation that reflects the relationships between the tokens, providing a structured view of the program. The syntax of the portable language is formally defined by a context-free grammar, which specifies the valid sequences in which tokens can appear to form syntactically correct language constructs such as expressions, statements, and definitions. The parser, the component of the compiler responsible for this stage, reads the token stream and applies these grammar rules to group the tokens into phrases and verify their arrangement. This process involves recognizing patterns in the token sequence that correspond to the language's syntactic constructs, ensuring that the ordering and combination of tokens strictly follow the defined grammar. As the parser successfully recognizes these constructs, it builds a hierarchical representation of the source code in the form of an Abstract Syntax Tree (AST). The AST provides a concise and abstract representation that captures the essential structure and relationships of the code while omitting unnecessary grammatical details, offering a convenient structure for following compilation phases like semantic analysis and code generation. During parsing, if the parser encounters a sequence of tokens that does not follow the language's grammatical rules, a syntax error is detected and reported to the user, indicating the location of the structural mistake. Syntax analysis serves as an intermediary phase, transforming the linear token stream into a structured representation that is crucial for understanding the program's meaning and aiding the later stages of the compilation process.

The AST of the proposed language is simpler compared to the C programming language because of the reduced number of tokens and simplicity of the design (Fig. 4).

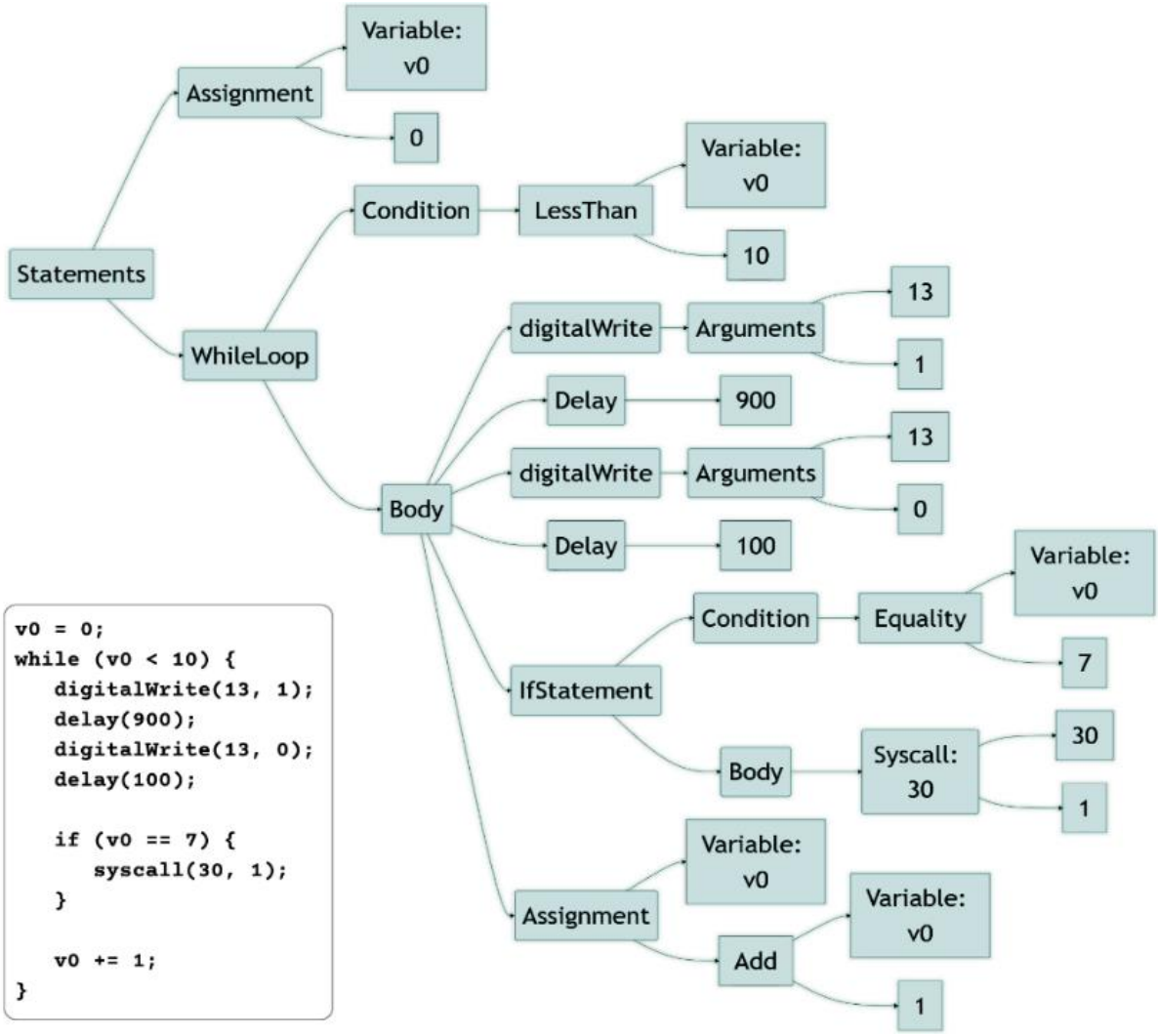

Fig. 4. **Abstract Syntax Tree of example program written in the proposed language**

Semantic analysis. Following the validation of the program's structural correctness during the syntax analysis phase, the compilation process proceeds to semantic analysis. This stage is responsible for checking the logical consistency of the source code, ensuring that it adheres to the proposed language's rules beyond just grammatical form. The input to the semantic analyzer is the AST produced by the parser. The primary goals are to detect semantic errors that are syntactically valid but logically inconsistent and to gather essential information required for following stages like intermediate code generation or optimization.

Key checks performed during semantic analysis include static type checking, which verifies that operations are applied to operands of compatible data types according to the proposed language's type system. This prevents illogical operations, such as attempting to perform arithmetic on a non-numeric value or assigning a value of an incompatible type to a variable, unless explicit and valid type coercion or casting is specified. Another important purpose of this stage is scope and declaration checking, ensuring that all identifiers for variables and functions are declared within an accessible scope before they are used and that there are no conflicting declarations within the same scope. This process involves constructing and managing a symbol table, a data structure that stores information about each declared identifier, including its type and scope. Name resolution is performed by querying the symbol table to link each use of an identifier in the code to its corresponding declaration. Additional semantic checks

include verifying correct function call arguments and ensuring control flow statements like break or return are used in appropriate contexts.

Semantic analysis performs static checks that can be done at compile time without executing the code. Unlike syntax errors, semantic errors often relate to the context in which language constructs are used. If semantic errors are detected such as using an undeclared variable or type mismatch, the compiler reports these issues to the user, providing details about the nature and location of the error. Successfully analyzed code is represented by an annotated AST, where nodes are decorated with semantic information such as resolved types and symbol table references. This enhanced representation serves as the validated and semantically meaningful input for the next stage of the compiler, building a connection between the purely structural view provided by the parser and the requirements for generating executable code for the Mico8-Chip virtual machine.

Intermediate Representation generation. After the semantic analysis process, the compiler process proceeds to generate an Intermediate Representation (IR). The IR serves as a bridge between the language-specific front-end of the compiler, which includes lexical, syntax, and semantic analysis, and the target-specific back-end, which involves optimization and code generation. Its primary purpose is to transform the program from a high-level, language-dependent structure like the AST into a lower-level, more machine-like representation that is independent of the specific target architecture, in this case, the Mico8-Chip virtual machine. IR is still more abstract than raw machine code or bytecode.

The adoption of an IR provides effective separation between the front-end and back-end. The front-end translates the source language into the IR, and the back-end translates the IR into the target code. This modularity is important for compiler development and maintenance. For instance, adding support for a new source language only requires building a new front-end that targets the existing IR, and supporting a new target architecture requires only building a new back-end that uses the existing IR. The IR is the representation at which many compiler optimizations are performed. IRs are designed to provide opportunities for optimization more effectively than either the source-level AST or the final target code. These optimizations include dead code elimination and loop transformations. Performing optimizations on a single IR allows them to be language-independent and target-independent, reducing redundant implementation effort. IRs can take various forms, ranging from graphical structures, to tree-based IRs simpler than the AST, to various forms of linear code. The compiler of the proposed portable language generates the IR by traversing the semantically analyzed AST and translating the high-level constructs into a sequence of simpler, sequential operations. This step systematically breaks down complex statements and expressions into a more elementary form that is closer to the operations the target virtual machine can execute (Fig. 5).

The IR generated at this stage then becomes the input for the subsequent optimization phase, where various algorithms are applied to improve the code's efficiency. Following optimization, the IR serves as the basis from which the final Mico8-Chip bytecode is generated. Therefore, the IR acts as an intermediate format that standardizes the program representation for both optimization and target code generation, contributing to the compiler's modularity, efficiency, and portability.

Bytecode generation. Bytecode generation is the final stage in the compiler pipeline, following the generation and optimization of the IR. This phase is responsible for translating the optimized IR into the specific instruction set that the target virtual machine, the Mico8-Chip, can directly interpret and execute. It represents the final transformation of the source code program into its portable, executable form. The input to this stage is the optimized IR code produced by the compiler's front-end, and the output is the sequence of bytes containing the Mico8-Chip bytecode.

The core task of bytecode generation is to map the operations and control flow structures expressed in the optimized IR onto the opcodes defined by the Mico8-Chip virtual machine's instruction set architecture. This involves iterating through the IR and, for each operation or sequence of operations, selecting the appropriate Mico8-Chip opcodes that perform the equivalent function. This selection

process must consider the specifics of the Mico8-Chip's architecture, including its register set, memory model, and available operations. Control flow constructs within the IR, such as conditional branches, loops, and function calls are translated into the corresponding jump and branch instructions of the Mico8-Chip virtual machine, requiring careful management of addresses within the target bytecode space. Data access operations specified in the IR are mapped to the instructions for loading from and storing to memory.

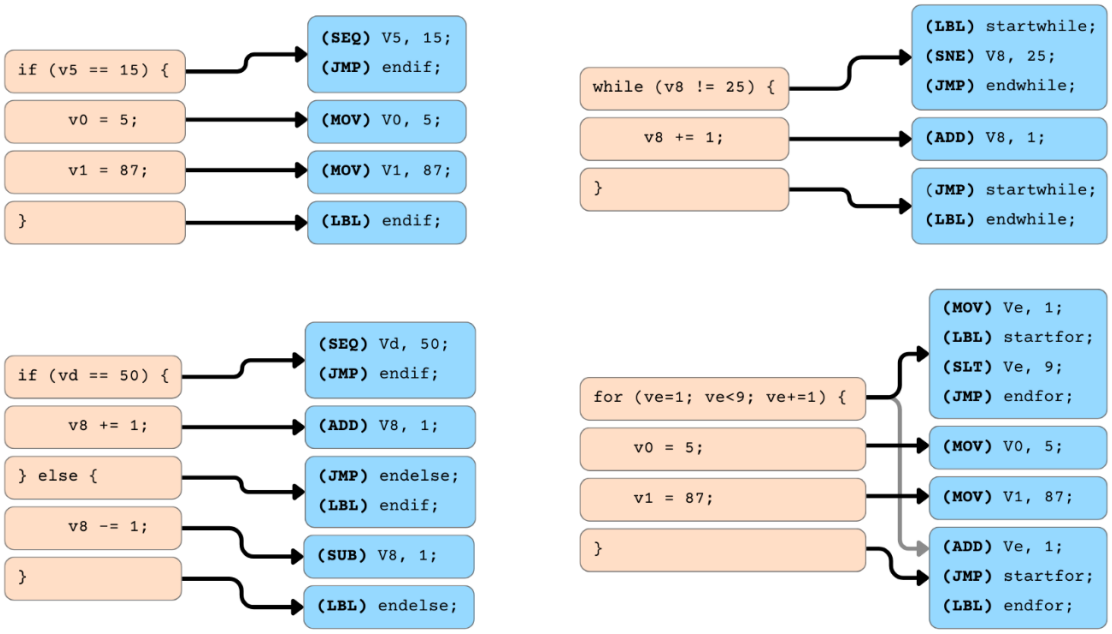

Fig. 5. **Example conversion of "if", "while", "if-else", and "for" blocks to IR code**

This phase is the most target-dependent part of the compiler's back-end, as it is intimately tied to the specific instruction set of the Mico8-Chip virtual machine. While the preceding IR provides a degree of abstraction, effective bytecode generation requires a detailed understanding of the operations, operand types, and encoding formats. The output is a linear sequence of 16-bit opcodes, formatted precisely as expected by the Mico8-Chip interpreter. This bytecode contains the compiled program logic and data in a form that is ready to be loaded into the Mico8-Chip virtual machine running on a microcontroller. The portability of the compiled program across different microcontroller platforms is achieved because the Mico8-Chip virtual machine, which interprets this bytecode, is designed to abstract away the underlying hardware differences, executing the same bytecode regardless of the specific microcontroller it is running on. Thus, bytecode generation concludes the compilation process by producing the artifact that enables cross-platform execution via the virtual machine.

Experimental results. The Mico8-Chip virtual machine is implemented in the C programming language for each specific microcontroller platform. However, benchmarking of the virtual machine's runtime performance is outside the scope of this paper, as the primary focus is on the design of the portable programming language and its compiler. Evaluating the virtual machine's execution efficiency depends heavily on its specific native implementation for each microcontroller architecture, a separate research effort from the language and compiler design presented.

Evaluation of compilation speed on host development platforms revealed it does not create a practical bottleneck. A large source file exceeding 20,000 lines (~600 kilobytes) compiles in under one second on a standard workstation, resulting in a bytecode ~150 kilobytes in size. The Mico8-Chip virtual machine’s typical 8 kilobyte bytecode limit already renders such large source files unrealistic for the

target. Moreover, the compiler's implementation in Python suggests even faster speeds are achievable with a compiled language, supporting that host compilation time is not a limiting factor in the development workflow.

A set of programs was developed using the proposed portable language and compiled into Mico8-Chip bytecode for testing purposes. As demonstrated by the data presented in Table 1, the generated bytecode for these programs has comparable size to functionally equivalent code implemented manually at a low level, such as hand-crafted Mico8-Chip instruction sequences or highly optimized low-level code. This competitive code size is achieved while offering developers the advantage of working with a higher level of abstraction through the proposed language's syntax, which improves source code clarity, increases readability, and reduces the complexity associated programming for the target virtual machine.

Table 1. **Compiled size of example programs**

Example program written in the proposed language	Bytecode size
Blinking an LED with a simple delay mechanism	10 bytes
Controlling an LED with a button click event	14 bytes
Outdoor light activation when it is dark outside	16 bytes
Servo motor control using two separate buttons	34 bytes
Ultrasonic distance measurement for object detection	52 bytes
Animated lights on an RGB LED array display	68 bytes
Basic sound-sensitive alarm system for security purposes	82 bytes
Periodic watering system designed for indoor plants	102 bytes
6 button sound pad with system calls for audio playback	140 bytes
Toggling a device on and off with hand clapping	176 bytes
Temperature and humidity logger for environmental monitoring	192 bytes
Automated feeding system for domestic pets	234 bytes
Controlling IoT devices using system calls	310 bytes

Conclusion and future work. The increasing complexity of microcontroller-based systems within the Internet of Things and other embedded applications highlights significant challenges associated with traditional development approaches. As discussed in this paper, the characteristic resource constraints of microcontrollers, coupled with the complexity of low-level programming and the fragmentation of the hardware landscape, decrease developer productivity and limit code portability. These factors require repetitive development efforts when targeting different platforms. This paper presented the design and implementation of a virtual machine-based portable programming language aimed at addressing these fundamental challenges. The core purpose of this paper was to create a cross-platform development solution for microcontrollers. The program codes written in this language compiles to bytecode for Mico8-Chip virtual machine, a re-engineered architecture based on CHIP-8, adapted to meet the demands of modern microcontroller systems. Mico8-Chip virtual machine includes a built-in concurrent task execution environment and to serves as the universal execution target for the proposed language. The language features C-like syntax, incorporating features necessary for embedded development. Through this work, the compiler pipeline of this language was detailed, which is responsible for compiling the source code into the final Mico8-Chip bytecode. This integrated approach

directly addresses the problem of code portability, as demonstrated by the ability to generate uniform bytecode for different microcontroller platforms, and lowers development complexity by offering a higher level of abstraction.

In conclusion, this work contributes a programming language that address the issue of fragmentation and portability in the microcontroller ecosystem. By providing a consistent compilation target and execution environment, the system simplifies the development process, reduces porting effort, and makes embedded programming more accessible while remaining mindful of the limitations of the target hardware. The effectiveness of the designed compiler pipeline in generating compact code for resource-constrained environments is demonstrated by the bytecode sizes of various example programs, as presented in Table 1. The small bytecode sizes for various functional programs confirm that the solution successfully balances high-level abstraction with the memory constraints of microcontrollers. This directly contributes to achieving the goal of accelerating development without significant performance or memory overhead, thus making embedded programming more accessible and portable across diverse hardware platforms.

Several paths exist for future research and development. Expanding the feature set of the portable language to include more complex data structures or standard libraries would enhance its applicability. Further optimizations to the compiler's back-end and the Mico8-Chip interpreter could potentially reduce execution overhead and memory footprint. Porting the Mico8-Chip virtual machine to a wider array of microcontroller families would broaden the system's reach. Additionally, exploring advanced features like developing integrated debugging and profiling tools could further enhance the system's utility for embedded software engineers. This research provides a solid foundation for continued exploration into high-level, portable development paradigms for the ever-growing domain of microcontroller-based systems.

REFERENCES

1. Wu, Z., Qiu, K., & Zhang, J. (2020). A Smart Microcontroller Architecture for the Internet of Things. *Sensors*, 20(7), 1821. https://doi.org/10.3390/s20071821.
2. Krishnamurthy, J., & Maheswaran, M. (2016). Programming frameworks for Internet of Things. In *Internet of Things* (pp. 79-102). Morgan Kaufmann. https://doi.org/10.1016/B978-0-12-805395-9.00005-8.
3. Bell, C. (2024). *MicroPython for the Internet of Things: A Beginner's Guide to Programming with Python on Microcontrollers Second Edition*. Apress eBooks. https://doi.org/10.1007/978-1-4842-9861-9.
4. Dashdamirli, N. (2025). Hybrid scheduling approach for concurrent task execution on microcontroller-based systems. *Romanian Journal of Information Technology and Automatic Control*, 35(1), 79–90. https://doi.org/10.33436/v35i1y202506.
5. Priyadarshini, S. B. B., Mahapatra, A., Mohanty, S. N., Nayak, A., Jena, J. P., & Samanta, S. K. S. (2022). myCHIP-8 emulator: An innovative software testing strategy for playing online games in many platforms. In *Optimization of Automated Software Testing Using Meta-Heuristic Techniques* (pp. 133-154). Cham: Springer International Publishing. https://doi.org/10.1007/978-3-031-07297-0_9.
6. Cruz, N., Ruiz-Ferrández, M., Redondo, J. L., Álvarez, J., & Ortigosa, P. (2019). Applications of chip-8, a virtual machine from the late seventies, in current degrees in computer engineering. In *EDULEARN19 Proceedings* (pp. 1720-1729). IATED. https://doi.org/10.21125/edulearn.2019.0501.
7. Dubé, D., & Feeley, M. (2005). BIT: A Very Compact Scheme System for Microcontrollers. *Higher-Order and Symbolic Computation*, 18(3), 271-298. https://doi.org/10.1007/s10990-005-4877-4.
8. Feeley, M., & Dubé, D. (2003, November). PICBIT: A Scheme system for the PIC microcontroller. In *Proceedings of the Fourth Workshop on Scheme and Functional Programming* (pp. 7-15).
9. St-Amour, V., & Feeley, M. (2010). PICOBIT: A Compact Scheme System for Microcontrollers. *Implementation and Application of Functional Languages*, 1-17. https://doi.org/10.1007/978-3-642-16478-1_1.
10. Brouwers, N., Corke, P., & Langendoen, K. (2008, December). Darjeeling, a Java compatible virtual machine for microcontrollers. In *Proceedings of the ACM/IFIP/USENIX Middleware'08 Conference Companion* (pp. 18-23). https://doi.org/10.1145/1462735.1462740.
11. Aslam, F. (2011). *Challenges and Solutions in the Design of a Java VirtualMachine for Resource Constrained Microcontrollers* (Doctoral dissertation, University of Freiburg).

12. Varoumas, S., Vaugon, B., & Chailloux, E. (2016, January). Concurrent Programming of Microcontrollers, a Virtual Machine Approach. In *8th European Congress on Embedded Real Time Software and Systems (ERTS 2016)* (pp. 711-720).
13. Varoumas, S., Vaugon, B., & Chailloux, E. (2018, January). A generic virtual machine approach for programming microcontrollers: the OMicroB project. In *9th European Congress on Embedded Real Time Software and Systems (ERTS 2018)*.
14. Gurdeep Singh, R., & Scholliers, C. (2019, October). WARDuino: a dynamic WebAssembly virtual machine for programming microcontrollers. In *Proceedings of the 16th ACM SIGPLAN International Conference on Managed Programming Languages and Runtimes* (pp. 27-36). https://doi.org/10.1145/3357390.3361029.
15. Zandberg, K., & Baccelli, E. (2020, December). Minimal virtual machines on iot microcontrollers: The case of berkeley packet filters with rbpf. In *2020 9th IFIP International Conference on Performance Evaluation and Modeling in Wireless Networks (PEMWN)* (pp. 1-6). IEEE. https://doi.org/10.23919/PEMWN50727.2020.9293081.
16. Sarkar, A., Krook, R., Svensson, B. J., & Sheeran, M. (2021, September). Higher-order concurrency for microcontrollers. In *Proceedings of the 18th ACM SIGPLAN International Conference on Managed Programming Languages and Runtimes* (pp. 26-35). https://doi.org/10.1145/3475738.3480716.

Нуру Дашдамірлі[1]

[1]Докторант, Азербайджанський Технічний Університет, пр. Г.Джавід, 25, Баку, Азербайджан, AZ 1148. ORCID: https://orcid.org/0009-0009-0545-7855.

Крос-платформенна розробка для мікроконтролерів: проєктування переносимої мови програмування на основі віртуальної машини

Фундаментальна роль мікроконтролерів у вбудовуваних системах та середовищах Інтернету речей потребує ефективних підходів до розробки програмного забезпечення. Обмеження ресурсів мікроконтролерів, складність мов програмування низького рівня та проблеми реалізації багатозадачності значно уповільнюють процес розробки. Крім того, різноманітність екосистеми мікроконтролерів створює суттєві бар'єри для портативності коду, що призводить до збільшення часу розробки для підтримки різних апаратних платформ. У цій статті представлено розробку підходу програмування на основі віртуальної машини, що забезпечує кроссплатформенну розробку для мікроконтролерів. Пропонована мова програмування, що переноситься, інтегрується з користувальницькою віртуальною машиною Micо8-Chip для відповідності сучасним додаткам мікроконтролерів. Це забезпечує інтуїтивне керування периферійними пристроями та вбудовану підтримку паралельного виконання. Наданий рівень абстракції значно покращує переносимість коду та прискорює розробку, ізолюючи логіку застосування від базових апаратних особливостей.

Ключові слова*: мікроконтроллер, вбудовані системи, віртуальна машина, програмування, байт-код, паралелізм, інтернет речей.*

DOI: 10.32703/2617-9040-2025-45-2

UDC 656.2.07:006.3:502.17

Olena Bal[1*], Volodymyr Tverdomed[2], Oresta Kovalchuk[3], Liliia Solodiak[4], Nataliia Borys[5]

[1]Candidate of technical sciences, Associate Professor, Head of Department of Railway Transport, Lviv Polytechnic National University, Stepana Bandery str., 12, Lviv, 79000; Judicial expert, Lviv Scientific Research Institute of Forensic Science, st. Lypinsky, 54, Lviv, 79024. ORCID: https://orcid.org/0000-0003-2188-4098

[2]Candidate of technical sciences, Associate Professor, director of the Kyiv Educational and Scientific Institute of Railway Transport of the National Transport University, M. Omelyanovicha-Pavlenko St., 1, Kyiv, 01010. ORCID: https://orcid.org/0000-0002-0695-1304.

[3] Head of the sector, Lviv Scientific Research Institute of Forensic Science, Lypinsky Str., 54, Lviv, 79024; Postgraduate student, National Transport University, Educational and Scientific Kyiv Institute of Railway Transport, M. Omelianovycha-Pavlenka Str., 1, Kyiv, 01010. ORCID: https://orcid.org/0000-0002-8570-313X.

[4] Candidate of technical sciences, Associate Professor of the Department of Railway Transport, Lviv Polytechnic National University, Stepana Bandery str., 12, Lviv, 79000. ORCID: https://orcid.org/0000-0001-9492-6549.

[5] Master of the Department of Railway Transport, Lviv Polytechnic National University, Stepana Bandery str., 12, Lviv, 79000. ORCID: https://orcid.org/0009-0004-0452-4896.

*Corresponding author: olena.m.bal@lpnu.ua.

Implementation of TSI requirements in railway infrastructure modernization projects of Ukraine in the context of EU transport system integration

The article is devoted to the analysis of technical and institutional aspects of the implementation of the requirements of the Technical Specifications for Interchangeability (TSI) in projects for the modernization of the railway infrastructure of Ukraine with financial support from the European Union within the framework of the Connecting Europe Facility (CEF) program. The current regulatory and institutional framework is analyzed, barriers and risks are identified, and models of cooperation with European certification bodies are proposed. The main attention is paid to the project "Modernization of the Mostyska-Lviv railway connection" as a representative example of integration into the TEN-T network. The article substantiates the feasibility of implementing a pilot model of cooperation between Ukrainian institutions and European certification bodies to confirm the compliance of design solutions with the TSI requirements. Special attention is paid to the issues of ensuring traffic safety, risk management, environmental safety, and compliance with functional safety standards, which are critically important for the certification of infrastructure facilities and obtaining funding from the EU. The pilot model of cooperation between Ukrainian participants and European certification bodies proposed in the article can become a scalable tool for ensuring TSI compliance. Institutional support from ERA and CINEA, technical dialogue, national capacity building and a multidisciplinary approach to project evaluation are the determining conditions for Ukraine's full participation in the European railway system.

***Keywords**: TSI, CEF, TEN-T, railway infrastructure, safety, environmental safety, conformity assessment, certification, European integration.*

Introduction. The integration of Ukraine's railway infrastructure into the European Union's transport system has become a strategic priority in the context of the country’s European integration agenda and the need for post-crisis reconstruction. As a full participant in the Connecting Europe Facility (CEF) programme since 2023, Ukraine has secured EU financial support for several cross-border and domestic infrastructure projects aimed at increasing interoperability and capacity [1].

A key requirement for these modernization projects is compliance with the Technical Specifications for Interoperability (TSI) [2], which establish harmonized standards across EU Member States for railway subsystems, including infrastructure, energy, control-command and signalling, and rolling stock. Meeting TSI requirements ensures seamless operation across national borders and promotes safe, reliable, and efficient rail transport throughout the trans-European transport network (TEN-T).

The TEN-T policy [3] plays a central role in the EU's long-term strategy for sustainable and interconnected transport across the continent. The extension of the core TEN-T corridors into the territory of Ukraine [4] highlights the strategic importance of integrating key routes such as Poland–Lviv, Romania–Chernivtsi–Lviv, Chop–Uzhhorod–Lviv, among others. These corridors not only strengthen physical connectivity but also facilitate Ukraine's economic and political alignment with the European Union.

The Connecting Europe Facility (CEF) [5] serves as the primary financial instrument supporting the implementation of cross-border and high-impact transport infrastructure projects within the TEN-T framework. In the case of Ukraine, CEF co-funding allows for accelerated modernization of infrastructure sections that are critical for interoperability with EU railway systems, including the introduction of 1435 mm standard-gauge lines, electrification, and implementation of signalling and safety systems in line with TSI.

In addition to its role in enhancing connectivity, CEF also contributes to the European Green Deal objectives [6] and works in alignment with the policies of the Directorate-General for Climate Action (DG CLIMA). CEF-funded railway projects prioritize sustainable mobility by supporting modal shift from road to rail, which significantly reduces greenhouse gas emissions and air pollution. In the Ukrainian context, infrastructure modernization with a focus on electrification and TSI-compliant systems is not only a step toward technical interoperability, but also an essential contribution to climate resilience and environmental sustainability. The integration of environmental standards and climate mitigation goals into CEF projects reflects a broader EU commitment to developing a transport network that is both efficient and ecologically responsible.

However, the process of adapting infrastructure projects to meet TSI requirements in Ukraine faces institutional and technical challenges. The absence of notified bodies (NoBos) within the country limits the ability to conduct independent conformity assessments, requiring cooperation with European certification institutions.

This paper explores the technical and procedural aspects of implementing TSI requirements within Ukrainian infrastructure projects supported by CEF. It analyses the current legal and institutional framework, identifies barriers and risks, and proposes models for cooperation with European certification bodies. The study also outlines the broader benefits of TSI alignment, including enhanced safety, operational interoperability, and access to EU markets and transport corridors.

Analysis of recent research and problem statement. The modernization and interoperability of railway infrastructure have become strategic priorities of the European Union's transport policy, particularly within the framework of the TEN-T. The Technical Specifications for Interoperability (TSIs) represent a cornerstone of this policy, establishing harmonized standards for infrastructure, energy, control-command and signaling, and rolling stock subsystems. Their consistent implementation enables the creation of a unified, safe, and efficient railway system across the EU.

Recent publications [6-14] provide valuable insights into the technical, legal, and interoperability-related challenges of Ukraine's railway system. Their work contributes significantly to shaping a modern, EU-integrated railway infrastructure in Ukraine.

Recent research [15] and technical documentation [16-20] - developed by the European Union Agency for Railways (ERA), infrastructure managers, and international projects such as Rail Baltica [21] and ERTMS deployment [22, 23] — highlight the importance of TSI conformity for achieving seamless cross-border operations. These studies largely focus on EU Member States or accession countries with established regulatory frameworks and operational Notified Bodies (NoBos). They provide insights into conformity assessment methodologies, the roles of Designated Bodies, and the processes of authorization for placing railway subsystems into service.

However, there is a noticeable gap in the literature regarding the implementation of TSI requirements in third countries undergoing systemic transformation—particularly Ukraine. Despite Ukraine's recent accession to the Connecting Europe Facility (CEF) programme in 2023 and the launch of several modernization projects with EU co-financing, the country currently lacks accredited NoBos capable of conducting independent conformity assessments. This institutional deficit complicates the application of the European regulatory framework and creates dependency on cross-border cooperation mechanisms with EU certification institutions.

Given Ukraine's active integration into the European transport system and the launch of infrastructure projects under the Connecting Europe Facility (CEF), there is a growing need to examine the conformity assessment procedures for railway infrastructure modernization projects in the Ukrainian context. Key issues include the adaptation of national regulatory frameworks, cooperation with European certification bodies (NoBos, AsBos), technical support during project implementation, and the methodology for verifying compliance during the design, construction, and commissioning stages.

The absence of Notified Bodies in Ukraine capable of conducting full TSI conformity assessments further emphasizes the need for the development of effective international cooperation mechanisms and the strengthening of national institutional capacity. Therefore, there is a clear demand for academic analysis of both the legal and practical dimensions of TSI implementation in Ukrainian modernization projects—a gap this study seeks to address.

The purpose and tasks of the study. The purpose of this study is to investigate the implementation of the Technical Specifications for Interoperability (TSI) in Ukraine's railway infrastructure modernization projects supported by the Connecting Europe Facility (CEF), with a focus on the role of these requirements in Ukraine's integration into the EU transport system.

To achieve this purpose, the study addresses the following tasks:

- to examine the legal and institutional framework for the application of TSI in Ukraine's railway sector.
- to analyze the content and technical objectives of a representative infrastructure project financed by CEF.
- to explore the methodological aspects of conformity assessment procedures in the EU railway domain.
- to identify challenges and barriers arising from the absence of notified bodies (NoBo) in Ukraine.
- to assess cooperation models between Ukrainian stakeholders and European certification bodies for the evaluation of TSI compliance.
- to evaluate the benefits of TSI implementation, including enhanced safety, interoperability, and access to EU transport corridors.

Materials and methods of research.

1. The legal and institutional framework for the application of TSI in Ukraine's railway sector.

The implementation of the Technical Specifications for Interoperability (TSI) in Ukraine is governed by a hybrid legal framework shaped by both national legislation and Ukraine's international commitments under the EU–Ukraine Association Agreement.

At the national level, the Law of Ukraine *"On Technical Regulations and Conformity Assessment"* [24] establishes the general legal foundation for the harmonization of national technical regulations with European standards, including the procedures for conformity assessment. This law is complemented by specific technical regulations, such as the "*Technical Regulation on the Safety of Railway Infrastructure"* [25], which partially transposes the provisions of Directive (EU) 2016/797 [16] and the related TSIs into Ukrainian law.

While the current Law of Ukraine *"On Railway Transport"* [26] outlines the overall legal and organizational framework for the sector, it was adopted prior to Ukraine's commitment to European integration and does not yet fully reflect the principles of market liberalization, interoperability, and safety management as stipulated by EU railway legislation. In this regard, the adoption of a new, modernized law on railway transport—harmonized with the provisions of Directive (EU) 2016/797 [16],

Directive (EU) 2016/798 [17], and Directive 2012/34/EU [27] — is a critical step toward enabling the full implementation of the TSI framework in Ukraine and ensuring legal compatibility with the EU railway acquis.

Institutionally, The Ministry for Development of Communities and Territories of Ukraine is responsible for policy coordination in the railway sector and for aligning sectoral legislation with the EU acquis. The State Service for Transport Safety of Ukraine (Ukrtransbezpeka) acts as the national supervisory authority. However, Ukraine currently lacks a Notified Body (NoBo) for railway subsystems assessment, which prevents full implementation of TSI conformity procedures domestically. This institutional gap necessitates cooperation with European NoBos, especially in CEF-funded projects.

The legal framework also includes references to relevant EU delegated and implementing acts, including:

- Commission Delegated Regulation (EU) 2019/777 on common specifications for the register of infrastructure [28];
- Commission Implementing Regulation (EU) 2023/1694 on the TSI for the infrastructure subsystem [18];
- And others regulating subsystems of rolling stock, energy, and control-command and signaling.

Furthermore, under the ongoing approximation process, Ukraine is aligning with Commission Delegated Regulation (EU) 2018/762 [19], which sets common safety methods and requirements for Safety Management Systems (SMS) used by railway undertakings and infrastructure managers.

This hybrid and transitional legal-institutional structure are a key consideration in the methodology of this research, particularly in evaluating the challenges and constraints in applying TSI conformity assessment in practice. Case study data from current CEF-supported modernization projects will be analyzed in this legal context, with emphasis on how gaps in domestic capability (e.g., absence of NoBos) are addressed through international cooperation mechanisms.

2. *Analysis of the content and technical objectives of a representative infrastructure project financed by CEF*

The Connecting Europe Facility (CEF) [29] supports the development of railway infrastructure projects located on the Comprehensive and Core Networks of the Trans-European Transport Network (TEN-T). In line with the Work Programme priorities, eligible actions include both studies and works related to the construction and upgrading of cross-border sections, elimination of missing links, and capacity enhancement of existing lines to accommodate international rail traffic.

Particular emphasis is placed on:

- upgrading infrastructure to allow for 740-meter freight trains;
- removal of level crossings;
- increasing capacity at key network nodes;
- improving multimodal connections between rail and inland waterways, maritime ports, or airports;
- ensuring efficient integration of freight terminals with the TEN-T railway network;
- electrification and modernization of railway lines and traction systems.

Support is strictly limited to railway infrastructure components. Passenger station buildings and rolling stock are not eligible. Furthermore, activities related to national Class B signalling systems are excluded from funding. Deployment of interoperable components such as ERTMS [30], GSM-R, and interlockings is supported separately under the “Smart and Interoperable Mobility” section of the CEF Work Programme.

In order to receive CEF funding, all supported actions must comply with Directive (EU) 2016/797 on the interoperability of the rail system and the applicable Technical Specifications for Interoperability (TSIs). Where applicable, projects must ensure procedural alignment across borders to maximize the efficiency of the infrastructure and enhance operational compatibility.

In line with EU principles, facilities developed under CEF must remain accessible to all railway operators on a non-discriminatory basis.

This requirement is of particular relevance to Ukraine, which became eligible for CEF Transport funding in 2023. The project *Modernisation of the railway connection from Mostyska to Lviv*, implemented by JSC "Ukrainian Railways" [1] and co-financed by the CEF, must adhere to the TSI framework and interoperability rules to ensure integration with the EU rail system.

According to the official decision of the European Commission on the selection of CEF Transport projects in 2023, Ukraine has been formally included among the eligible countries for EU transport infrastructure funding. In particular, the Mostyska–Lviv railway reconstruction project was approved under the Connecting Europe Facility framework, with the requirement to comply with relevant TSIs for interoperability [1]. The priority railway corridors of Ukraine covered by CEF projects are shown in Figure 1.

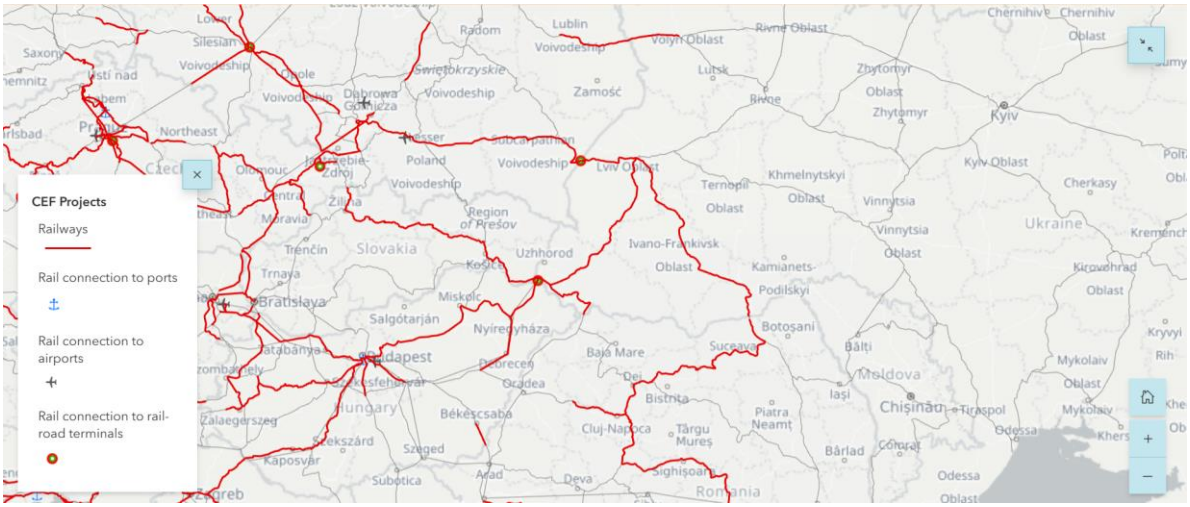

Fig 1. **Priority railway corridors of Ukraine covered by CEF projects**

Since Ukraine's accession to the Connecting Europe Facility (CEF) programme in 2023, JSC Ukrainian Railways (Ukrzaliznytsia) has gained access to EU co-financing for infrastructure projects aimed at integrating the Ukrainian railway network into the Trans-European Transport Network (TEN-T). Several projects have already been selected for funding and are being implemented in coordination with the European Climate, Infrastructure and Environment Executive Agency (CINEA).

Notable examples include:

- Modernisation of the Mostyska II – Medyka border crossing, enhancing cross-border capacity with Poland;
- Construction of a standard-gauge (1435 mm) railway link between Chop and Uzhhorod, co-financed 50% by CEF;
- The large-scale project "Modernisation of the Railway Connection from Mostyska to Lviv", officially included in the list of selected actions under CEF Transport Call 2023 [1].

All of these initiatives are subject to compliance with the provisions of Directive (EU) 2016/797 on the interoperability of the rail system and the related TSIs [31].

According to official EU publications and a 2024 report by the International Union for Road-Rail Combined Transport (UIRR) [32], part of the funding allocated to Ukraine is specifically intended for conformity assessment with TSI requirements—particularly for the Kovel–Yahodyn and Mostyska II–Lviv (Sknyliv) sections.

Ensuring compliance with TSI is not only a legal prerequisite for receiving CEF grants, but also serves as a strategic institutional indicator of Ukraine's readiness for integration into the European transport system. Without proper conformity assessment validated by authorised EU institutions, further funding and long-term infrastructure integration would be impossible.

3. The methodological aspects of conformity assessment procedures in the EU railway domain.

The conformity assessment process within the European Union's railway sector is a legally regulated mechanism designed to ensure that infrastructure projects, subsystems, and components comply with the Technical Specifications for Interoperability (TSIs), as required by Directive (EU) 2016/797 [6]. This process is particularly critical in modernization projects, where updated or reconstructed infrastructure must align with harmonized European norms to facilitate interoperability, safety, and environmental performance across the Trans-European rail Network (TEN-T).

The assessment of conformity is guided by the European Union Railway Interoperability Directive 2016/797 [6], which mandates that railway subsystems—such as infrastructure, energy, control-command and signaling, and rolling stock—must meet specific TSI requirements before being placed into service or upgraded. Each subsystem must undergo verification procedures that include both documentation and physical inspections, depending on the scope and complexity of the modernization.

Key actors involved in the conformity assessment process include:

- Notified Bodies (NoBos) - independent third-party organizations designated by EU Member States to perform assessments under TSI regulations.
- Designated Bodies (DeBos) - institutions that verify compliance with national technical rules (NNTRs) where TSI applicability is not yet fully harmonized.
- Assessment Bodies (AsBos) - entities responsible for checking the application of risk management processes, especially in the case of significant changes.

The TSI conformity assessment follows a modular approach as defined in Regulation (EU) No 2010/713 [20]. Typical modules relevant for infrastructure modernization projects include:

- EC type examination - evaluation of technical design documentation.
- Production quality assurance - assurance that the implementation during modernization aligns with approved design.
- Full quality assurance - applied to the entire lifecycle, including planning, execution, and verification stages.

In infrastructure modernization projects, a combination of modules is typically used, particularly to ensure comprehensive verification of both the design and implementation stages.

Conformity assessment in modernization projects typically follows a structured and phased approach to ensure that all technical and regulatory requirements of the applicable TSIs [31] are fully met. These phases are coordinated in collaboration with a Notified Body (NoBo) and relevant stakeholders such as project designers, construction contractors, and infrastructure managers.

1. Pre-assessment phase.

The pre-assessment phase serves as a critical preparatory stage. It includes:

- Gap analysis to determine which TSI requirements are applicable to the project, depending on the subsystem and scope;
- Mapping of existing conditions of the infrastructure section, including legacy systems, deviations from TSI norms, and interfaces with other subsystems;
- Development of a Conformity Assessment Strategy outlining which modules will be used, required documentation, and a timeline for NoBo involvement.

This phase helps minimize costly redesigns and ensures that TSI compliance is integrated into the project from the outset.

2. Design phase evaluation.

During the design phase, the Notified Body (NoBo) conducts a comprehensive assessment of the following technical and regulatory components to verify conformity with applicable Technical Specifications for Interoperability (TSIs) [31]:

A. Technical documentation:

- general arrangement drawings (GADs) of infrastructure and civil works;
- longitudinal and cross-sectional profiles of track alignments;
- site layout and zoning plans for stations, depots, and intermodal terminals;
- platform design, including height, length, and access features;
- bridge and tunnel engineering designs (if applicable).

B. Track design parameters:
- Track gauge (e.g., 1435 mm or dual gauge);
- Axle load and structural capacity (static and dynamic);
- Gradient (longitudinal slope) and minimum curvature radius;
- Super-elevation and cant deficiency values;
- Track center distance and clearances (kinematic envelope compliance);
- Ballast and substructure design;
- Turnouts and crossing systems, including compatibility with EU standards.

C. Electrification system design:
- Type of electrification system (AC 25 kV / DC 3 kV or other);
- Positioning and height of overhead contact lines (OCL);
- Catenary system type (simple, stitched, auto-tensioned, etc.);
- Mast foundations and structural calculations;
- Interface with traction power substations and feeder systems;
- Grounding and bonding schemes for safety and EMC compliance;
- Earthing, lightning protection, and surge arrestors.

D. Signalling and train control systems:
- Interlocking systems and compatibility with existing infrastructure;
- Block sections, balise placement, and detection systems;
- Interface with European Train Control System (ETCS), if applicable;
- Traffic control center architecture and remote supervision;
- Fail-safe design features and redundancy levels.

E. Environmental and climate resilience measures:
- Noise and vibration mitigation measures (e.g., noise barriers);
- Drainage and water management systems;
- Biodiversity impact assessments;
- Climate adaptation features (resilience to extreme weather, temperature ranges);
- Landscape integration and vegetation management.

F. Passenger and accessibility features:
- Compliance with PRM TSI (Persons with Reduced Mobility);
- Wayfinding systems, tactile surfaces, and signage;
- Lighting and emergency systems in passenger areas.

G. Risk and safety management documentation:
- Preliminary Safety Plan and Safety Case (if required);
- Risk assessment reports per CSM RA (Common Safety Method on Risk Evaluation);
- Hazard Identification and Hazard Logs (HAZIDs);
- Mitigation strategies for residual risks;
- Human factors and ergonomics assessments.

H. System integration and interface management:
- Interfaces between subsystems (e.g., infrastructure and energy, CCS and rolling stock);
- Interoperability with existing national or EU railway lines;
- Analysis of transitional solutions (e.g., dual-gauge sections).

I. Compliance with National Rules (if applicable):
- Evaluation of national technical rules (NNTRs) alongside TSI applicability;
- Interface with Designated Bodies (DeBos) for specific national requirements.

The outcome of this phase is typically a Design Examination Report, which determines whether the project meets TSI requirements in theory and can proceed to implementation.

3. On-site inspection and verification.

Once construction or reconstruction begins, the NoBo performs systematic inspections to verify that:

- Implemented components (tracks, switches, catenary, platforms, etc.) match the approved design.

- Construction practices and materials meet the required quality and safety standards.
- Interfaces between subsystems (e.g., infrastructure and energy) are managed in compliance with TSI requirements.
- Any deviations or non-conformities are properly documented, justified, and resolved before moving forward.

These site verifications are usually conducted at critical milestones, such as after track laying, before electrification, and before commissioning.

4. Final Validation and Issuing of Certificate

After successful completion of the construction and verification stages, the NoBo performs a final assessment of:

- The technical file, containing all project documentation, test results, inspection records, and declarations.
- The overall conformity of the subsystem or project section with the relevant TSIs.

If all conditions are met, the NoBo issues the EC Certificate of Verification, which is necessary for the Authorization for Placing into Service (APIS) by the national safety authority or ERA.

5. Documentation and compliance register.

Each conformity assessment process is accompanied by:

- A technical documentation file, as per Annex IV of Directive 2016/797 [6].
- A declaration of conformity from the applicant.
- Registration in the European Register.

These records ensure traceability, transparency, and future compatibility with EU-wide upgrades or extensions.

In Ukraine, the absence of domestic NoBos limits internal capacity for conformity assessment. Therefore, modernization projects funded by the EU (e.g., via CEF) require early involvement of European NoBos, who supervise the process and issue relevant certificates. This increases the importance of harmonized procedures and proper training of project engineers to produce TSI-compliant documentation from the design stage.

4. Implementation of the project and compliance with TSI

The successful implementation of an infrastructure project under European financial instruments, particularly the Connecting Europe Facility (CEF), requires not only adherence to construction timelines but also full compliance with the Technical Specifications for Interoperability (TSIs). TSI compliance must be ensured at every stage of project implementation—from design to commissioning:

- Design and reconstruction of railway structures:

During the design phase, a key objective is to integrate the requirements of TSI INF, TSI ENE, and TSI CCS into all technical documentation. This includes the development of track geometry, platform layouts, bridges, tunnels, overhead line systems, energy supply elements, and signalling systems in accordance with the applicable TSI versions. The reconstruction of existing infrastructure aims to align legacy assets with EU standards, including the introduction of standard gauge (1435 mm), strengthening of structural components, noise mitigation, and accessibility improvements.

- Construction of infrastructure facilities:

Construction activities must follow the TSI-compliant technical solutions approved in the design stage. This includes track laying, installation of overhead contact systems, deployment of signalling and control-command infrastructure (interlocking, train protection), and establishment of safety-critical installations. Construction works must be accompanied by rigorous technical supervision and conformity checks.

- Audit and certification of TSI compliance:

In the final stage of the project, a comprehensive audit of technical documentation and physical infrastructure components is carried out. Notified Bodies (NoBos) are involved in this process, conducting conformity assessments according to selected TSI modules. Upon successful verification, an EC Certificate of Verification is issued, which forms the basis for authorization for placing the

subsystem into service. This certificate is a legal prerequisite for the operation of the infrastructure within the EU's TEN-T network.

Thus, implementing a TSI-compliant project is a complex technical and regulatory process requiring cross-sectoral cooperation, strict adherence to legal frameworks, and integration of international expert bodies.

5. Challenges and barriers related to the absence of Notified Bodies (NoBos) in Ukraine

One of the key institutional challenges to the implementation of the Technical Specifications for Interoperability (TSIs) in railway infrastructure modernization projects in Ukraine is the absence of Notified Bodies (NoBos)—organizations officially authorized to carry out conformity assessment procedures under EU legislation.

According to the Law of Ukraine "On Technical Regulations and Conformity Assessment" [24], such procedures can only be conducted by bodies accredited by the National Accreditation Agency of Ukraine (NAAU) and officially designated by the competent authority. However, as of today, there are no entities in Ukraine with NoBo status in accordance with Directive (EU) 2016/797 [6] on the interoperability of the rail system within the EU.

Even though Ukrainian certification bodies may have the necessary technical capacity, they currently lack the legal grounds to function as NoBos because Ukraine is not a member of the EU and is not included in the NANDO (New Approach Notified and Designated Organisations) database [33]. As a result, conformity assessment procedures according to TSI modules cannot be conducted without involving accredited European structures such as TÜV Rheinland, CERTIFER and others.

The absence of NoBos compels beneficiaries - such as JSC "Ukrainian Railways" - to rely on foreign certification bodies, which significantly increases the cost of procedures, complicates logistics, and delays project implementation, especially under wartime conditions and limited site accessibility.

Compliance with TSI requirements - including those of TSI INF, TSI ENE, and TSI CCS - is a mandatory condition for the implementation of EU-funded infrastructure projects under the Connecting Europe Facility (CEF) programme. The lack of valid certificates issued by a NoBo presents risks of funding denial, delays in disbursements, and negative audit results during project progress assessments.

To address these challenges, Ukraine must implement a national strategy for integration into the European technical regulation system, including the following actions:

- create conditions for the accreditation of Ukrainian conformity assessment bodies in accordance with EU requirements, thereby strengthening national capabilities in the railway infrastructure conformity assessment sector;
- conclude mutual recognition agreements with EU Member States to facilitate Ukraine's integration into the common European railway market;
- deepen cooperation with European NoBos through joint projects, personnel exchanges, and training programmes to develop national expertise and gain practical experience aligned with EU standards;
- ensure a multidisciplinary approach to infrastructure project assessment—combining engineering, legal, environmental, and forensic-expert perspectives to comprehensively evaluate compliance with current requirements;
- incorporate TSI provisions into national construction norms, technical regulations, and industry instructions to ensure internal legal harmonization.

These tasks are reflected in Ukraine's National Transport Strategy to 2030 and the Action Plan for the Development of the Technical Regulation System until 2025 [34], which outline key steps toward adapting to EU norms and enhancing the national conformity assessment infrastructure.

Effective implementation of these measures will reduce dependence on external actors, accelerate the adoption of European standards, enhance Ukraine's institutional capacity in technical regulation, and strengthen the country's readiness for full integration into the EU transport system.

6. CEF-funded projects in Ukraine: focus on the Mostyska–Lviv section

The project "Modernisation of the Railway Connection from Mostyska to Lviv" was selected for EU co-financing under the CEF Transport Call 2023 and marks one of the first large-scale railway

infrastructure initiatives supported by the Connecting Europe Facility (CEF) on Ukrainian territory. Its main objective is to enable uninterrupted railway connectivity between the Ukrainian network and the EU system, adapted to the European standard gauge of 1435 mm.

The project covers the following activities:

- Design and technical preparation for the reconstruction of the Mostyska II – Sknyliv section;
- Feasibility studies and technical design according to the requirements of the Technical Specifications for Interoperability (TSIs);
- Preliminary environmental impact assessment (EIA);
- Development of technical documentation for conformity assessment with EU norms.

This project is strategically aligned with the expansion of the Trans-European Transport Network (TEN-T), revised in response to geopolitical changes following Russia's full-scale invasion of Ukraine. It is located along the core Baltic Sea - Black Sea - Aegean Sea Corridor, which connects Poland with southern regions of Ukraine.

According to the CEF Work Programme, priority is given to eliminating cross-border bottlenecks, increasing line capacity, and enabling 740-meter freight trains. In this context, the Mostyska-Lviv line serves as a pilot zone for EU railway integration, aiming to demonstrate a scalable model for other border connections.

Due to the absence of Notified Bodies (NoBos) in Ukraine authorized to carry out conformity assessment procedures in line with the Technical Specifications for Interoperability (TSI), we propose the implementation of a structured model of international technical cooperation within the framework of this project. This model may include the following practical steps:

- engagement of technical experts and consultants from EU Member States;
- preparation and submission of a comprehensive technical file for the certification of the "Infrastructure" subsystem in accordance with TSI INF requirements;
- application of conformity assessment modules SB, SH1, and SD as defined in Regulation (EU) No 2010/713 [20];
- establishment of cooperation with European Notified Bodies to carry out independent external audits of infrastructure solutions.

We also propose the adoption of a partnership-based interaction model, which foresees coordination between Ukrainian stakeholders (JSC Ukrainian Railways, the Ministry for Development of Communities and Territories of Ukraine, and national design and expert institutions) and European certification entities (Notified Bodies, consultancy firms, and the European Union Agency for Railways - ERA). The key principles of this model include:

- institutional support from EU bodies, in particular CINEA [35] and ERA;
- the formation of bilateral technical working groups to ensure information exchange and procedural harmonization;
- a phased approach, which allows for initial conformity assessment by EU-recognized bodies while simultaneously building national human and procedural capacity.

The implementation of this model will not only provide official confirmation of TSI compliance but also foster the systematic development of Ukraine's professional capacity in the field of railway certification. We consider the proposed model a pilot cooperation framework, which we recommend testing within the Mostyska–Lviv project and subsequently applying to other infrastructure initiatives under the TEN-T and CEF programmes.

Successful implementation of such a model will enhance Ukraine's technical reputation as a reliable EU partner and lay the groundwork for further mutual integration in the field of technical regulation for railway transport.

The proposed international cooperation model, piloted within the "Mostyska–Lviv" modernization project, can serve as a methodological template for the future implementation of EU technical standards by national infrastructure operators. Successful application of the model creates an opportunity for its replication in other key TEN-T railway sections in Ukraine.

Table 1. **Key steps of the TSI conformity model in a CEF project**

Step	Description	Responsible Actors
1. Identification of TSI requirements	Defining applicable TSI (e.g., INF, SRT)	Ukrzaliznytsia, design institutions
2. Preparation of technical file	Comprehensive technical documentation	Designers, technical consultants
3. Engagement with NoBo	Contracting a notified body	Ukrzaliznytsia, NoBo
4. External audit	Evaluation of documentation and infrastructure	NoBo, independent auditors
5. Conformity conclusion	Issuance of certification or recommendations	NoBo
6. Addressing comments	Revisions of documentation or designs	Ukrainian project stakeholders
7. Final conformity confirmation	Certification approval	NoBo, Ukrzaliznytsia

A core condition for scaling up is the development of national capacity for railway conformity assessment with TSI requirements. This includes:

- establishing qualified technical centers and training safety auditors;
- developing a regulatory framework for the future notification of Ukrainian bodies;
- creating sustainable mechanisms of coordination with ERA and CINEA;
- incorporating safety assessment procedures into infrastructure modernization plans.

In the medium term, this model supports the development of Ukraine's technical self-sufficiency, reduces reliance on foreign certification, and fosters alignment of the national regulatory system with EU standards. It also lays the foundation for a domestic market of railway conformity and safety assessment services, contributing to deeper integration with the European transport system.

7. Benefits of TSI compliance

Compliance with the Technical Specifications for Interoperability (TSIs) provides a number of strategic advantages for railway infrastructure projects, particularly in the context of Ukraine's integration into the EU transport system:

1. Enhanced Safety and Reliability

TSI implementation ensures the application of uniform safety standards throughout all stages of infrastructure design, construction, and operation. Requirements such as those in TSI INF (Infrastructure), TSI CCS (Control-Command and Signalling), and TSI ENE (Energy) prescribe harmonized technical parameters and safety procedures. This reduces the likelihood of operational failures and accidents, improves system resilience, and contributes to the overall safety culture in rail transport.

2. Interoperability with European Railway Systems

One of the key objectives of the TSI framework is to facilitate seamless cross-border operations across the EU. For Ukraine, aligning infrastructure and subsystems with TSI allows for technical and operational compatibility with neighboring railway networks. This is essential for freight corridors and international passenger services and enables full integration into the Trans-European Transport Network (TEN-T). Standardization of track gauge (e.g., 1435 mm), electrification systems, and signalling interfaces supports efficient interaction between Ukrainian and EU railway operators.

3. Economic and Environmental Advantages

TSI-compliant infrastructure promotes long-term operational efficiency by reducing maintenance costs, minimizing downtimes, and enabling higher capacity utilization. Interoperability reduces logistical bottlenecks at border points, leading to faster and more predictable transit flows. Furthermore,

the shift to electrified and standardized railway lines, as encouraged by TSI ENE, supports climate goals by reducing CO_2 emissions and dependence on diesel traction. This aligns with broader EU Green Deal objectives and the climate-oriented priorities of the CEF programme.

Overall, TSI conformity is not only a regulatory obligation within CEF-funded projects but also a key enabler of Ukraine's modernization, competitiveness, and sustainable integration into the European railway space.

8. Impact of track superstructure failures on safety indicators and TSI compliance in infrastructure modernization projects

In the implementation of railway infrastructure modernization projects, it is essential not only to ensure that design solutions meet the requirements of the TSIs, but also to guarantee that actual operating conditions align with the expected safety parameters. This is especially relevant for track superstructure elements - rails, sleepers, fastenings, ballast, and turnouts -whose failure can cause serious disruptions to train operations and pose significant risks to passenger and operational safety.

In this context, expert analysis methods and the assessment of the technical condition of track components play a vital role. These approaches are being developed as part of the research project "Development of a methodology for the forensic examination of railway track components" (State registration number: 0123U101166), conducted by the Lviv Scientific Research Institute of Forensic Expertise.

The analysis identifies common failure mechanisms, including:

- degradation of the elasticity of sleepers and ballast;
- wear or mechanical damage to rails;
- deformation and stiffness loss in turnout components;
- damage to fastenings affecting track stability.

Such defects directly influence the dynamic and loading characteristics of the infrastructure and, consequently, its compliance with the parameters established by the Infrastructure TSI (e.g., EN 13848, TSI INF 2023). These factors must be considered not only during the design phase but also during technical inspections and conformity verification prior to placing the infrastructure into service.

Introducing early detection procedures for potentially hazardous defects, along with the integration of forensic technical tools into the TSI conformity assessment process, can significantly enhance the objectivity and reliability of safety evaluations. This supports the practical implementation of the safety management principles outlined in Regulation (EU) 2018/762 [19] and Directive (EU) 2016/798 [17].

Thus, the synergy between forensic expertise on infrastructure failures and institutional practices in TSI conformity assessment forms a solid foundation for developing national approaches to ensuring railway safety in the context of Ukraine's integration into the European railway system.

9. Bridging education and practice: the contribution of master's research to infrastructure modernization in line with EU requirements"

In the process of implementing TSI requirements in infrastructure projects, the training of specialists capable of working at the intersection of technical regulation, transport safety, and European interoperability standards plays a crucial role. In preparing this article, research results developed within the framework of the second-level higher education program *"Functional Safety of Railway Transport"* (specialty J7 "Railway Transport") at Lviv Polytechnic National University were used. The thematic focus of master's theses—particularly in the areas of risk assessment and infrastructure adaptation for the 1435 mm gauge—directly corresponds to the challenges Ukraine faces in the context of TSI implementation and integration into the TEN-T system. This highlights the relevance of aligning academic training with the practical needs of infrastructure modernization under EU requirements.

Conclusions. The integration of Ukraine's railway infrastructure into the European Union transport system requires not only modernization of physical assets but also systematic alignment with EU legal and technical requirements. The implementation of the Technical Specifications for Interoperability (TSIs) is central to this process, serving as the foundation for achieving seamless, safe, and interoperable railway operations along cross-border and TEN-T corridors.

The case of the Mostyska–Lviv section, supported by the Connecting Europe Facility (CEF), demonstrates the practical challenges and solutions for ensuring TSI compliance under conditions where Ukraine lacks nationally accredited Notified Bodies (NoBos). This situation necessitates structured cooperation with European conformity assessment institutions and the application of established conformity assessment modules such as SB, SH1, and SD.

The analysis confirms that compliance with TSI requirements not only unlocks access to EU funding but also improves the technical robustness, safety, and environmental sustainability of infrastructure projects. In this context, safety remains a cross-cutting priority, especially in terms of design reliability, risk management, and conformity assessment. Environmental safety, in particular, should be more systematically integrated into planning and evaluation procedures.

Academic and expert research — such as that conducted within the Master's programme "Functional Safety of Railway Transport" — plays a critical role in developing applied methodologies for risk assessment, forensic analysis of infrastructure, and adaptation to the 1435 mm standard gauge. This knowledge base should be actively used to inform future project design, certification, and policymaking.

Ultimately, a pilot model of cooperation between Ukrainian stakeholders and European certification bodies, as proposed in this study, offers a scalable mechanism for advancing TSI compliance. Institutional support from ERA and CINEA, combined with technical dialogue, national capacity building, and a multidisciplinary evaluation framework, will be essential for Ukraine's full participation in the EU rail transport ecosystem.

REFERENCES

1. European Commission. Commission Implementing Decision C. (2024). 6940 final of 17 October 2024 on the selection of projects for EU financial assistance in the field of the Connecting Europe Facility – Transport sector. Brussels, 2024. [Online]. Available: https://transport.ec.europa.eu/document/download/744ad3f3-22e7-411f-9f04-65b20170a1c0_en?filename=C%282024%296940.pdf&prefLang=el.
2. ERA Technical Specifications for Interoperability – latest consolidated versions. Available at: https://www.era.europa.eu.
3. Regulation (EU) 2024/1679 of the European Parliament and of the Council of 13 June 2024 on Union guidelines for the development of the trans-European transport network, amending Regulations (EU) 2021/1153 and (EU) No 913/2010 and repealing Regulation (EU) No 1315/2013.
4. https://transport.ec.europa.eu/document/download/41528897-a27b-4768-ab61-c98df2681f41_en?filename=Annex3_alignment_EuropeanTransportCorridors.pdf.
5. Connecting Europe Facility (CEF) – Transport Infrastructure Programme. European Commission. Available at: https://transport.ec.europa.eu, https://eur-lex.europa.eu/legal-content/en/TXT/?uri=CELEX%3A32021R1153.
6. Lousada, S., Delehan, S., Gómez, J. M. N., Gallardo, J. M., Mandryk, O., & Khorolskyi, A. (2024). Bridging the gap: Overcoming the 85 mm railway gauge difference between Ukraine and Europe using principles of circular economy and European service quality standards. Journal of Infrastructure, Policy and Development, 8(16), 10555. https://doi.org/10.24294/jipd10555.
7. Zapara V. M., Oleniuk V. O., & Tymoshenko I. O. (2017). Technical specifications for interoperability and their implementation in high-speed traffic on the railways of Ukraine. Collection of scientific works of the Ukrainian State University of Railway Transport, (173), 12-20. https://doi.org/10.18664/1994-7852.173.2017.118183. [in Ukrainian].
8. Chernetska-Biletska, N. B., Nesterenko, G. I., Mykhaylov, E. V., Kyrychenko, I. O., Semenov, S., & O., Muzykin, M. I. (2020). Interoperability of Ukrainian railways and problems of overcoming system track jams: a textbook. Severodonetsk: Publishing house of the V. Dahl State University of Science and Technology. [in Ukrainian].
9. Kurhan, D., Kurhan, M., & Hmelevska, N. (2022). Development of the High-Speed Running of Trains in Ukraine for Integration with the International Railway Network. Acta Polytechnica Hungarica, 19(3), 207–218. https://doi.org/10.12700/APH.19.3.2022.3.16
10. Myronenko, V., Samsonkin, V., Yurchenko, O., & Pozdniakov, A. (2022, September). Ukrainian high-speed normal gauge railway: Factors of War and Peace. In International Conference TRANSBALTICA: Transportation Science and Technology (pp. 438-448). Cham: Springer International Publishing. https://doi.org/10.1007/978-3-031-25863-3_41.
11. Strelko, O., Toropov, B., Horban, A., Hrushevska, T., & Bernatskyi, A. (2024). Some Issues of the Project Analysis of Options for the Implementation of European Standard Railways in Ukraine. Transactions on Transport Sciences, 15(1), 64-70. https://doi.org/10.5507/tots.2023.023.
12. Matuszak, S., Popławski, K., Baniak, S., Gizińska, I., & Dębiec K. (2024). Running on European tracks: Modernising the rail network in western Ukraine during wartime. OSW Commentary.
13. Bal, O., Bolzhelarskyi, Y., Babyak, M., Tereshchak, Y., & Solodiak, L. (2023). Prospects of infrastructure development towards Romania, Moldova and Poland. Transport Systems and Transportation Technologies, (26), 14–29. https://doi.org/10.15802/tstt2023/293340.

14. Kurhan, M. B., Kurhan, D. M., Khmelevska, N. P., & Kovalskyi, D. L. (2025). Prospects for the Implementation of High-Speed Railway in Ukraine. Science and Transport Progress, (1(109), 65-76. https://doi.org/10.15802/stp2025/325351.
15. Joint Communication to the European Parliament and the Council on EU-Ukraine solidarity lanes to facilitate Ukraine's agricultural export and bilateral trade. Brussels, 2022.
16. Directive (EU) 2016/797 of the European Parliament and of the Council of 11 May 2016 on the interoperability of the rail system within the European Union. *Official Journal of the European Union*, L 138, 26.5.2016, pp. 44–101. [Online]. Available: http://data.europa.eu/eli/dir/2016/797/oj.
17. Directive (EU) 2016/798 of the European Parliament and of the Council of 11 May 2016 on railway safety. OJ L 138, 26.5.2016, pp. 102–119.
18. Commission Implementing Regulation (EU) 2023/1694 of 10 August 2023 amending Regulations (EU) No 321/2013, (EU) No 1299/2014, (EU) No 1300/2014, (EU) No 1301/2014, (EU) No 1302/2014, (EU) No 1304/2014 and Implementing Regulation (EU) 2019/777.
19. Commission Delegated Regulation (EU) 2018/762 of 8 March 2018 establishing common safety methods on requirements for safety management systems.
20. Regulation (EU) No 2010/713 on modules for the procedures for assessment of conformity used in the context of the TSI.
21. Rail Baltica Global Project – Technical Design Guidelines Rail Baltica joint venture RB Rail AS. https://www.railbaltica.org.
22. European Commission. Decision authorising the use of unit contributions to support the deployment of ERTMS, electric vehicles recharging infrastructure and the retrofitting of noisy wagons under CEF Transport. Brussels, 22 July 2021. [Online]. Available: https://transport.ec.europa.eu/system/files/2021-07/2021-07-22-ertms-af-noise.pdf.
23. ERA Report – "ERTMS Deployment Action Plan". European Union Agency for Railways, 2023. https://www.era.europa.eu/system/files/2022-11/keir_fitch_ec_en.pdf.
24. Law of Ukraine "On Technical Regulations and Conformity Assessment" dated 15.01.2015 No. 124-VIII. [Electronic resource]. – Access mode: https://zakon.rada.gov.ua/laws/show/124-19#Text. [in Ukrainian].
25. Cabinet of Ministers of Ukraine. Resolution No. 494 of July 11, 2013 "On Approval of the Technical Regulation on Railway Infrastructure Safety" (as amended by Resolutions No. 8 of January 13, 2016, and No. 416 of April 28, 2023). *Official Bulletin of Ukraine*. Available at: https://zakon.rada.gov.ua/laws/show/494-2013-п#Text.
26. Verkhovna Rada of Ukraine. (1996). Law of Ukraine "On Railway Transport" No. 273/96-VR, adopted on April 4, 1996. Retrieved from https://zakon.rada.gov.ua/laws/show/273/96-%D0%B2%D1%80.
27. Consolidated text: Directive 2012/34/EU of the European Parliament and of the Council of 21 November 2012 establishing a single European railway area (recast) (Text with EEA relevance) Text with EEA relevance.
28. Consolidated text: Commission Implementing Regulation (EU) 2019/777 of 16 May 2019 on the common specifications for the register of railway infrastructure and repealing Implementing Decision 2014/880/EU (Text with EEA relevance) Text with EEA relevance.
29. Regulation (eu) 2021/1153 of the european parliament and of the council of 7 July 2021 establishing a "European Cohesion Facility" and repealing Regulations (EU) No 1316/2013 and (EU) 283/2014. https://zakon.rada.gov.ua/laws/show/984_020-21#Text. [in Ukrainian].
30. Decision of 22 July 2021 authorising the use of unit contributions to support the deployment of ERTMS and conformity under CEF Transport. Available at: https://transport.ec.europa.eu/system/files/2021-07/2021-07-22-ertms-af-noise.pdf.
31. Guide for the application of the Technical Specifications for Interoperability (TSIs). Application Guide GUI/TSI/2023.
32. International Union for Road-Rail Combined Transport (UIRR). *2024 Report on Combined Transport in Europe*. Brussels: UIRR and UIC, 2024. Available at: https://www.uirr.com/media-centre/leaflet-and-studies/mediacentre/3031-uic-uirr-2024-report-on-combined-transport.html.
33. European Commission – NANDO (New Approach Notified and Designated Organisations). [Online]. Available: https://single-market-economy.ec.europa.eu/single-market/goods/building-blocks/notification-and-accreditation/nando_en.
34. Resolution of the Cabinet of Ministers of Ukraine dated September 22, 2021 No. 1145-r "On approval of the action plan for the development of the technical regulation system until 2025". [Electronic resource]. – Access mode: https://zakon.rada.gov.ua/laws/show/1145-2021-%D1%80#Text. [in Ukrainian].
35. European Climate, Infrastructure and Environment Executive Agency (CINEA). "Connecting Europe Facility – Transport." [Online]. Available: https://cinea.ec.europa.eu/programmes/connecting-europe-facility/transport-infrastructure_en.

Олена Баль[1], Володимир Твердомед[2], Ореста Ковальчук[3], Лілія Солодяк[4], Наталія Борис[5]

[1]Кандидат технічних наук, доцент, завідувач кафедри залізничного транспорту НУ «Львівська політехніка», вул. Степана Бандери, 12, м. Львів, 79000; Судовий експерт, Львівський НДІ судових експертиз, вул. Липинського, 54, м. Львів, 79024. ORCID: https://orcid.org/0000-0003-2188-4098,

[2]Кандидат технічних наук, доцент, директор Навчально-наукового Київського інституту залізничного транспорту Національного транспортного університету, 01010, м. Київ, вул. М. Омеляновича-Павленка, 1. ORCID: https://orcid.org/0000-0002-0695-1304.

[3]Завідувач сектору, Львівський науково-дослідний інститут судових експертиз, вул. Липинського, 54, м. Львів, 79024; аспірант, Національний транспортний університет, Навчально-науковий Київський інститут залізничного транспорту, вул. М. Омеляновича-Павленка, 1, м. Київ, 01010. ORCID: https://orcid.org/0000-0002-8570-313X.

[4]Кандидат технічних наук, доцент кафедри залізничного транспорту, Національний університет «Львівська політехніка», вул. Степана Бандери, 12, м. Львів, 79000. ORCID: https://orcid.org/0000-0001-9492-6549.

[5]Магістр кафедри залізничного транспорту, Національний університет «Львівська політехніка», вул. Степана Бандери, 12, м. Львів, 79000. ORCID: https://orcid.org/0009-0004-0452-4896.

Впровадження вимог TSI у проєктах модернізації залізничної інфраструктури України в контексті інтеграції до транспортної системи ЄС

Стаття присвячена аналізу технічних та інституційних аспектів імплементації вимог Технічних специфікацій взаємозамінності (TSI) у проєктах модернізації залізничної інфраструктури України за фінансової підтримки Європейського Союзу в межах програми «Механізм «Сполучення Європи» (CEF). Проаналізовано чинну нормативну та інституційну базу, визначено бар'єри й ризики, запропоновано моделі співпраці з європейськими органами сертифікації. Основну увагу приділено проєкту «Модернізація залізничного сполучення Мостиська–Львів» як репрезентативному прикладу інтеграції до мережі TEN-T. У статті обґрунтовано доцільність впровадження пілотної моделі співпраці між українськими інституціями та європейськими сертифікаційними органами задля підтвердження відповідності проєктних рішень вимогам TSI. Окрему увагу приділено питанням забезпечення безпеки руху, управління ризиками, екологічної безпеки та дотримання стандартів функціональної безпеки, що є критично важливими для сертифікації інфраструктурних об'єктів та отримання фінансування з боку ЄС. Запропонована у статті пілотна модель співпраці між українськими учасниками та європейськими сертифікаційними структурами може стати масштабованим інструментом забезпечення відповідності TSI. Інституційна підтримка з боку ERA та CINEA, технічний діалог, нарощування національного потенціалу та мультидисциплінарний підхід до оцінювання проєктів є визначальними умовами повноцінної участі України в європейській залізничній системі.

Ключові слова: *TSI, CEF, TEN-T, залізнична інфраструктура, безпека, екологічна безпека, оцінка відповідності, сертифікація, європейська інтеграція.*

DOI: 10.32703/2617-9040-2025-45-3

UDC 629.4.048

Vadym Ishchenko[1], Nadiya Braikovska[2], Iurii Shcherbyna[3], Yuri Demchenko[4]

[1]Associate Professor, Head of Department, Wagons and Wagon Management of Railways Department, National Transport University, 1, M. Omelianovycha-Pavlenka str., Kyiv, 01010, Ukraine, Ukraine. ORCID: https://orcid.org/0000-0002-5559-4251.

[2]Professor, Wagons and Wagon Management of Railways Department, National Transport University, 1, M. Omelianovycha-Pavlenka str., Kyiv, 01010, Ukraine. ORCID: https://orcid.org/0000-0003-1556-4020

[3]Associate Professor, Wagons and Wagon Management of Railways Department, National Transport University, 1, M. Omelianovycha-Pavlenka str., Kyiv, 01010, Ukraine. ORCID: https://orcid.org/0000-0002-9574-2757

[4]Senior lecturer, Wagons and Wagon Management of Railways Department, National Transport University, 1, M. Omelianovycha-Pavlenka str., Kyiv, 01010, Ukraine. ORCID: https://orcid.org/0009-0006-3809-4323.

***Corresponding author:** ischenko_vm@gsuite.duit.edu.ua

Modern requirements for refrigeration agents in transport air conditioners

The Scientific advances, changes in national legislation in the field of combating the effects of global warming and market requirements have stimulated the development of fourth generation refrigerants. In contrast to the first and second generation refrigerants, which provided, along with the principle possibility of achieving a refrigerating effect, such qualities as durability and operational safety, the third and fourth generations include environmental constraints in a significant way. The identification of a link between leaks of traditional second-generation chlorofluorocarbon (CFC)-based refrigerants and the destruction of the protective atmospheric layer of ozone gave rise to the third generation of refrigerants. The Vienna Convention and the Montreal Protocol were the reaction of the world community, leading to the banning of ozone-depleting substances (ODS). At the same time, hydrochlorofluorocarbons were considered as temporary or transient and hydrofluorocarbons (HFCs) as long-term working bodies. Interest in the natural refrigerants ammonia, carbon dioxide, hydrocarbons and water has increased dramatically.

Keywords: *railway transport, refrigerant, transportation air conditioners, greenhouse effect, alternative refrigerants, passenger car, refrigeration machine.*

Introduction. Exploring the trade-offs between new refrigerants, their environmental goals, safety and material compatibility.

According to international forecasts, with the existing rates of greenhouse effect growth, the average temperature of the Earth's atmosphere by 2050 may increase by 3...5 K, which may lead to an increase in the level of the world ocean by 20 cm and thereby cause irreversible environmental consequences.

The analysis of the most probable scenarios of transition to environmentally safe working bodies in refrigeration technology indicates that two main approaches to the search for substances compatible with environmental requirements are now competing, these are [5, 6]:

1. The use of natural refrigerants, which eliminates ozone-depleting substances in air-conditioning refrigeration systems;

2. Increasing the environmental safety of alternative refrigerants - fluorocarbon hydrocarbons, which have non-zero global warming potential, by adding natural components as an intermediate goal.

The development of the second scenario is unlikely, as industrialized countries, which play a significant role in the global economy, have decided to accelerate the phase-out of ozone-depleting substances compared to the timeframe stipulated by the Montreal Protocol. In particular, industrialized

countries reduced production and consumption of ozone-depleting substances by 75% in 2010 and 90% in 2015 compared to the baseline year of 1987. The final deadline for the elimination of environmentally hazardous substances is 2020.

For developing countries, this period has also shortened by 10 years and ends in 2030. Given the time required to develop and introduce new working bodies with non-zero global warming potential into industry, the prospect of using fluorocarbons and mixtures based on them seems doubtful.

The choice of future refrigerants depends to a large extent on changes in the political and legislative environment. At the end of 2007, the international community endorsed the "Bali Action Plan" (the so-called "Bali Roadmap") for discussion in 2009, much more stringent requirements to mitigate climate change after the end of the Kyoto Protocol (2008-2012). The Action Plan envisioned greenhouse gas emission reductions of 25 to 40% by 2020 and 50% (other proposals as high as 80%) by 2050. These ambitious plans contrasted with the collective commitments for 2008-2012, according to which the relative reduction of greenhouse gas emissions relative to the 1990 level will be on average about 5% for developed countries, and for some of them the specified targets were not fulfilled.

The generally accepted view is that hydrofluorocarbons - HFCs, as one of the six groups of greenhouse gases (GHGs) defined by the Kyoto Protocol contribute little to total GHG emissions compared to energy-intensive air conditioning and refrigeration systems. In 2006, HFCs and PFCs contributed slightly less than 2% to total GHG emissions. By 2010, this share had increased as R-22 was phased out and prioritized for replacement with the HFC - R - 410A refrigerant blend in new air conditioners.

Taking into account that historically the refrigerant consumption for service exceeds the factory norms, it should be expected that the HFC share will increase by 7-10%, corresponding to a two or threefold increase in HFC emissions, equivalent to the complete elimination of R-23 emissions in R-22 production. This contribution becomes quite competitive with a 50% reduction in emissions of the other greenhouse gases. The influence of factors related to energy efficiency (indirect contribution to greenhouse gas emissions) remains dominant, despite the increase in the direct contribution from refrigerant leaks.

Analysis of recent research and problem statement. The following parameters are used to analyze the environmental feasibility of refrigerant use: ODP (Ozon Depletion Potential); GWP (Global Warming Potential) or HGWP (Halocarlon Global Warming Potential) [7, 17].

Ozone depletion potential ODP is determined by the presence of chlorine atoms in the refrigerant molecule and is taken as one for R11 and R12. For CFC group refrigerants ozone destruction potential ODP≥1, for HCFCs ODP < 0.1, and for HFCs ODP = 0.

The global warming potential GWP is taken as one for carbon dioxide ($C0_2$) with a time horizon of 100 years, and the HGWP is calculated relative to the value of this parameter for R11, also taken as one.

According to the degree of activity of destruction of the Earth's ozone layer, haloid derivatives of hydrocarbons are divided into three groups:

- refrigerants with high ozone-depleting activity are chlorofluorocarbons (CFCs) R11, R12, R13, R 113, R114, R115, R502, R503, R12B1, R13B1 (or by international designation CFC12, CFC13, etc.)[3] and others. In accordance with the requirements of the Montreal Protocol, the countries are divided into 2 groups. The group consisting mainly of developed countries (so-called "non-article 5") stopped using CFC refrigerants in 1996. The "article 5" countries did it in 2010;

- refrigerants with low ozone-depleting activity are hydrochlorofluorocarbons (HCFCs) R21, R22, R141b, R142b, R (or by international designation HCFC21, HCFC22, HC, etc.), etc., whose molecules contain hydrogen. These substances are characterized by a shorter time of existence in the atmosphere compared to CFCs, and as a consequence, they have a smaller impact on ozone layer depletion. The Montreal Protocol provides for a phased reduction in their production from 1996, 2010, 2015 and 2020, with a complete phase-out by 2030 in "non-Article 5" countries, and in "Article 5" countries requires a "freeze" of 2016. Different countries have taken different decisions on this process. Most countries in Western and Central Europe have accelerated the phase-out of HCFCs, while most other developed countries have established regulations for the early use of these substances as an alternative to CFCs;

- refrigerants not containing chlorine atoms (fluorocarbons FC (FC) hydrofluorocarbons HFC (HFC), hydrocarbons (HC), etc.) are considered to be completely ozone-safe. Such are refrigerants R134, R134a, R152a, R143a, R125, R32, R23, R218, R116, RC318, R290, R600, R600a, R717 and others.

The ozone recovery trend is in direct in direct contrast to the worsening climate change situation. The new data on global warming published in the First Report of the Intergovernmental Panel on Climate Change reflects the unanimous position of the scientific community that "climate warming is undeniable; this is evident from the observed increase in the observed increase in the ozone layer.

The new global warming data published in the Intergovernmental Panel on Climate Change I report reflects the consensus of the scientific community that "climate warming is undeniable, evident from observed increases in global average air and ocean temperatures, widespread melting of snow and ice, and rising global sea levels". The scientists' assessment is that "it is most likely that the global warming observed since the mid-twentieth century is driven by increases in anthropogenic greenhouse gases" and that "the discernible effects of human activity are now spreading to other aspects of climate change, including ocean warming, increases in continental mean temperatures, and shifting winds."

The selection criteria for the fourth generation of refrigerants included, in addition to the existing criteria of safety and material compatibility, minimum ozone depletion potential (ODP), the requirement of low global warming potential GWP values (less than 150 for a cumulative 100-year period). Another environmental selection criterion is the rational lifetime of the refrigerant in the atmosphere, which is important for fluorine-containing chemical compounds. Along with this, the new generation of refrigerants should have high energy efficiency in order to avoid a cumulative increase in greenhouse gas emissions.

The Kyoto Protocol, ratified by Ukraine in accordance with the International Framework Agreement on Climate Change, sets some benchmarks for greenhouse gas (GHG) emissions based on the calculated equivalents of carbon dioxide, methane, nitrogen oxides, HFCs, perfluorocarbons (PFCs) and sulfur hexafluoride. It does not address ODS (the Montreal Protocol deals with them), although some of them are very potent GHGs. National laws and regulations on the application of the Kyoto Protocol differ, but, in general, they prohibit emissions of refrigerants.

In 2006, the European Parliament set a timetable to ban the use of fluorinated refrigerants (F-gases) with a GWP of more than 150 per 100 years in air-conditioners for new car models from 2011 and from 2017 for all new vehicles. In addition, the new rules require periodic inspection of stationary systems where HFCs are used. The European Parliament rejected a recommendation that would have banned the use of HFCs in aerosols by 2006, by 2009 for foaming, and by 2010 as refrigerants for stationary air-conditioning and refrigeration. Sufficiently strong intergovernmental support for greenhouse gas risk reduction measures predicts revised conditions in the future, especially in view of recent scientific discoveries indicating accelerating climate change.

As a direct result, the ban on the use of R134 in transportation air conditioners. The adopted low GWP deliberately allows the use of HFCs such as R152a despite its flammability.

Alternative refrigerants are generally less energy efficient than their predecessors [8]. With few exceptions, the efficiency gains of equipment using alternative refrigerants depend not on the properties of the new working fluid but on the design improvements in the equipment. Increasing constraints lead to new trade-offs between environmental performance, safety, cost and other parameters.

The emergence of new refrigerants raises questions about the trade-offs between conflicting environmental objectives and between environmental, safety and material compatibility. The rejection of ODS reduces the ability to combat climate change from direct or indirect effects, such as energy-related emissions. As an example of mutually conflicting goals, consider R1311 (CF31 (CEZl - fluorojodurocarbon, FIU), a potential low-potential refrigerant of R123 (HCFC). Both refrigerants have GWP and short atmospheric lifetime, low GWP value, low toxic by inhalation, non-flammable, can be effectively used for flame suppression. However, both have a low but not zero value of 0.011 to 0.018 for R1311 and a semi-empirical value of 0.02 for ODP R123. As an additive in mixtures of fluorinated olefins (unsaturated alkenes), to suppress their flammability and simultaneously reduce ODP and GWP, R1311 seems promising.

As an ODS, although not subject to the low ODP value, R1311 of the Montreal Protocol, as it has not been used commercially since 1992, when the protocol was last amended. R123 is the most efficient refrigerant for water chillers, apart from R11 and R141b, but the latter two have significantly higher ODP and GWP values. Nevertheless, the use of R123 as an ODS has long been banned in Europe. In addition, there is a ban on its use in new chillers in countries not specified in section 5 of the protocol by 2020, and in specified countries - by 2040. And this is despite the fact that R123 has very low environmental impact due to low ODP, very low GWP, very short lifetime in the atmosphere, low leakage from modern chillers, and is also highly efficient. The Montreal Protocol authorizes its limited use for service purposes until 2030 in countries not listed in Section 5. These examples demonstrate the conflict between two environmental goals: preserving the ozone layer and preventing climate change.

Another example of an environmental trade-off is the most common refrigerant R22. It is known that to replace R22, it is recommended, first of all, R410A - a mixture of two HFCs (R32 and R125). Although ODP of this mixture is practically equal to zero, GWP increases by 16% (from 1800 to 2100 for a century interval of time) [2].

Technology, market and policy changes affecting the choice of new refrigerants are transforming extremely rapidly. Recent toxicity tests have excluded from further consideration at least three refrigerant blends (AC-1, DP-1 and JDH) that were claimed to replace R134a. In particular, its stability and actual ozone depletion potential were questioned. These circumstances ruled out the R 1234yf/R1311 mixture, which is known as H-liquid [3, 5], as a candidate. The four blends listed above, which were named as candidates for Global Alternative Refrigerant, very quickly went from very promising testing in early 2007 to complete rejection in late 2007.

Most manufacturers also stopped looking for opportunities use of R-152a as a global alternative in direct expansion systems because, despite its limited flammability, this refrigerant is “not suitable for use in vehicles that are not specifically designed to use flammable refrigerants.”. Research continues for indirect systems where the effectiveness of R-152a is not in doubt [6], particularly for smaller vehicles and in hot climates.

The main studies of efficiency of carbon dioxide and other natural refrigerants utilization are carried out on stationary installations. Typically, CO_2 is used in the low-temperature circuit of cascade systems in industrial artificial refrigeration production, displacing ammonia.

The use of carbon dioxide is increasing, especially in European countries, both as a common refrigerant in industrial artificial refrigeration and as an intermediate coolant in systems (UNEP, 2007b). In the latter case, significant reductions in refrigerant charge weight are achieved and further prospects are opened for the use of ammonia, ammonia mixtures (e.g. R-723 mixtures of ammonia with dimethyl ether R-E170), hydrocarbons (UNEP, 2007b).

The hydrocarbon refrigerants R- 600a (isobutane) and its blends replaced R-12 and later R-134a in home refrigerators manufactured in Europe.

The search for a compromise solution among many alternative refrigerants requires the choice of an objective criterion for comparing the proposed options. There are several approaches to the problem of thermodynamic, selection of such criterion on the basis of thermodynamic, energy or technical and economic analysis. Each of the approaches is correct within the framework of appropriate assumptions. The main difficulty in selecting an objective criterion for the selection of the refrigerating system working body for vehicles is to find a compromise between pollution reduction and price, reliability and safety [3].

The concept of sustainable refrigeration adopted by the International Refrigeration Institute requires a balance between baseline characteristics such as physical (safety, functionality, risk of failure, technical support), economic (life cycle costs, return on investment, costs, profits), environmental (greenhouse gas emissions, water, air, soil pollution) and social (health, consumer safety, consumer prices) over the product life cycle.

There is no unambiguous solution or universal evaluations to ensure a trade-off between the baseline characteristics of a refrigeration machine, so the final choice is reached through agreements or demand.

The International Institute of Refrigeration has recommended the LCCP life cycle climate

characteristic as a sustainability criterion. This value is expressed in CO_2-equivalent units and takes into account the impact of direct and indirect greenhouse gas emissions on the climate during the entire life cycle (production of components, assembly, operation and disposal) of a product, in our case, a vehicle refrigeration system. LCCP criterion is a generalization of the widespread TEWI criterion (Total Equivalent Warming Impact), which considers the direct contribution from greenhouse gas emissions into the environment and only the part of indirect CO2 emission, which is a consequence of energy consumption during vehicle operation. Obviously, a detailed analysis of vehicle interactions and their impact on the climatic characteristics of the environment should reflect the full life cycle, for which an assessment should be made not only of carbon dioxide emissions during operation, but also during production and disposal processes.

To find the LCCP, the total equivalent warming impact, TENWI, is pre-calculated

$$TEWI = GWPR \cdot MR + GWPBA \cdot MBA + a \cdot E_O \cdot L, \quad (1)$$

where MR – refrigerant mass;
MBA – foaming agent weight;
E_O – average annual energy consumption during operation (kW·h);
L – the useful life of the vehicles;
a – conversion factor of energy units to CO_2, - equivalent, taken for Ukraine equal to 0.48 kg CO_2/kWh;
$GWPR$ – global warming potential of refrigerant;
$GWPBA$ – global warming potential of the foaming agent.

When calculating the LCCP, only the contribution of indirect components (E_p and E_i, i=1...N) of greenhouse gas emissions during the life cycle was taken into account, neglecting the contribution of direct effects, which are related to direct leakages due to their smallness. life cycle, neglecting the contribution of direct effects associated with direct leakages due to their smallness.

The calculated dependence has the form

$$LCCP = TEWI + a \cdot \left[\left(E_p - E_o \right) \cdot L + E_i \right]. \quad (2)$$

The TEWI calculation methodology was developed by the International Institute of Refrigeration. The TEWI parameter for a particular substance is the sum of the direct greenhouse effect potential due to the emission of this substance into the atmosphere and the indirect potential due to the emission of carbon dioxide during the production of electricity, which is required for the operation of refrigeration plants.

Currently, the choice of an alternative refrigerant for refrigeration systems depends on changes in the political and legislative environment, technology and market. The Vienna Convention and the Montreal Protocol leading to the ODS ban treat hydrochlorofluorocarbons (HFCs) as temporary or transitional and hydrofluorocarbons (HFCs) as long-term working bodies. Given these changes, R134a refrigerant is used to replace R12 refrigerant in transportation air conditioners.

The refrigerant Freon R-134a is non-toxic and not susceptible to ignition in the operating temperature range. Although when air penetrates into the working system and compresses it, mixtures of flammable gases are formed.

Unlike other refrigerants, which contain chlorofluorocarbons, which causes significant harm to the ozone layer of the Earth, the refrigerant Freon R-134a does not contain chlorine. And when it is used in air-conditioning and cooling systems, no harmful chlorine-containing compounds capable of destroying the Earth's ozone layer are emitted. This contributes to an environmentally friendly approach.

Low toxic effect is a significant characteristic of Freon R-134a refrigerant. This means that with proper use and maintenance of systems that operate on Freon R-134a, minimizes the risk of negative impact on human health and the environment. Which is essential at refrigerant sources, when small amounts of the substance may be released into the atmosphere.

Due to its low toxicity, Freon R-134a is suitable for use in enclosed spaces where people are present and does not pose a significant hazard under regulatory operating conditions.

Freon R-134a has excellent thermal properties, which makes it attractive for use in air conditioning systems. Since its high thermal conductivity allows efficient heat transfer from one part of the system to another, providing optimal cooling. Specific heat capacity of the refrigerant Freon R-134a, plays an important role in maintaining a stable temperature, which is important in processes where precise control of parameters is required.

It is not recommended to mix R-134a with R-12, due to the formation of a high-pressure azeotropic mixture, where the mass fraction of these components is one to one. The saturated vapor pressure of R-134a (1.16 MPa at 45 ºC) is slightly higher than that of R-12 (1.08 MPa at 45 ºC). According to ASNRAE classification R-134a refrigerant belongs to A1 class. Operational characteristics in medium-temperature equipment, where boiling point is -7 ºC and higher, R-134a is close to R-12.

Energy performance of R-134a in refrigeration systems, which operate at boiling point of the refrigerant below -15 ºC, is slightly inferior to R-12 (about 6% at -18 ºC). It is advisable to use refrigerants with lower boiling point or compressor with increased hourly volume, which describes the piston.

In hermetic refrigeration systems, through significant global warming potential, it is recommended to use R-134a.

When working with R-134a refrigerant it is recommended mainly only polyester refrigeration oils, which have increased hygroscopicity.

R-134a molecule has smaller sizes than R-12 molecule, which considerably increases the danger of refrigerant leaks.

R-134a is used in all countries of the world as a priority replacement of R-12 in refrigeration equipment operating in the range of average temperatures. The refrigerant is also used for retrofit of equipment operating at lower temperatures. In this case, replacement of the compressor of the refrigeration system is required to increase the cooling capacity.

For comparison of indicators and properties of refrigerant R134a with R12 we use the main requirements for modern refrigerants [7, 17]:

- environmental (ozone safety, low global warming potential, non-flammability and non-toxicity);
- thermodynamic (high volumetric cooling capacity;

low boiling point at atmospheric pressure; low condensation pressure; good thermal conductivity; low density and viscosity of the refrigerant, providing reduction of hydraulic friction losses and local resistances during its transportation; and local resistance during its transportation;

- maximum approximation to the replaced refrigerants (for alternative ozone-safe refrigerants) in terms of pressures, temperatures, specific volumetric cooling capacity and refrigeration coefficient);
- operational (thermochemical stability, chemical compatibility with materials and refrigeration oils, sufficient solubility with oil to ensure its circulation, processability of application; non-flammability and non-explosiveness; ability to dissolve water, insignificant fluidity; odor, color, etc.);
- economic (availability of commercial production, affordable (low) prices).

Thermodynamic requirements determine the performance of the refrigerant. To analyze the performance qualities we use the most important thermodynamic indices:

- differential value;
- value of temperature at the end of compression process t, °C;
- value of specific mass cooling capacity q_0, kJ/kg;
- value of specific volumetric cooling capacity q_v, kJ/m^3;
- adiabatic work of compression l, kJ/kg;
- COPε value.

Refrigerant differential is the ratio of pressure in condenser Pk to pressure in evaporator P_0 (Pk/P_0).

The greater the difference between the condenser pressure and the evaporator pressure, the more severe the compressor operating conditions are. Consequently, the absolute pressures and their difference determine the reliability and efficiency of the refrigeration machine.

The temperature values at the end of the compression process t.

The higher the temperature of the refrigerant at the end of compression, the more loads arise in the compressor, the greater the friction forces in the mating pairs increase, and the reliability and efficiency of the refrigeration machine decrease.

The values of specific mass cooling capacity q_0 are the amount of heat removed from the cooled body by one kilogram of refrigerant

$$q_0 = i_1 - i_4, \tag{3}$$

where i_1 – enthalpy of refrigerant at the end of boiling process in the evaporator, kJ/kg;

i_4 – enthalpy of the refrigerant at the beginning of the boiling process in the evaporator, kJ/kg.

The value of specific volumetric cooling capacity q_υ is the amount of heat removed from the body being cooled to reach one-meter cubic saturated vapor of refrigerant

$$q_\upsilon = \frac{q_0}{\upsilon}, \tag{4}$$

where υ – specific volume of refrigerant vapor at suction to the compressor, m^3/hour.

Adiabatic work of compression is the work that must be applied to compress one kilogram of refrigerant.

$$l = i_2 - i_1, \tag{5}$$

where i_2 – enthalpy at the end of compression process, kJ/kg;

i_1 – enthalpy at the beginning of the compression process, kJ/kg.

The value of CORε is the ratio of cooling capacities to the consumed work.

The values of thermodynamic indicators of refrigerants R12 and R134a are determined and compared at a fixed cycle of the refrigerating machine corresponding to the conditioning conditions:

- boiling point of the refrigerant in the evaporator, t_0 = +5°C;
- temperature of refrigerant suction into the compressor, t_{vc} = +20°C;
- refrigerant condensation temperature, t_c = +35°C;
- subcooling temperature of the refrigerant before the evaporator, t_p = +30°C.

By means of computer modeling of refrigerants R12 and R134a indicators in a fixed cycle of the refrigerating machine corresponding to the conditioning conditions, the following results were obtained:

- refrigerant differential in the fixed cycle of the refrigeration machine corresponding to the conditioning conditions when using R134a refrigerant is greater than R12 by 0.18% (Fig. 1);
- the temperature at the end of the compression process in the fixed cycle of the refrigeration machine corresponding to the conditioning conditions when using R134a refrigerant is 1.0% higher than R12 (Fig. 2);
- specific mass cooling capacity in the fixed cycle of the refrigerating machine corresponding to the conditions of conditioning when using refrigerant R134a is 34,8% higher than R12 (Fig. 3);
- specific volumetric cooling capacity in a fixed cycle of the refrigeration machine corresponding to the conditions of air conditioning when using refrigerant R134a is 2.8% higher than R12 (Fig. 4);
- adiabatic work of compression in a fixed cycle of the refrigerating machine corresponding to the conditions of conditioning when using R134a refrigerant is 2.81% more than R12 (Fig. 5);
- The value of COPε in the fixed cycle of the refrigerating machine corresponding to the conditioning conditions when using R134a refrigerant is higher than R12 by 0,72% (Fig. 6).

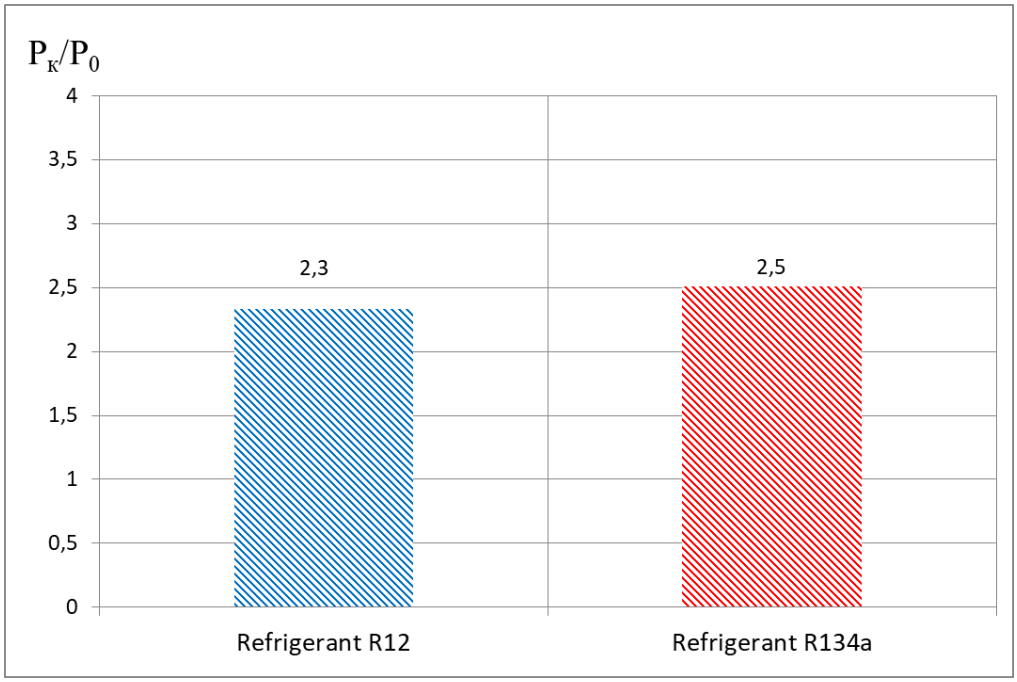

Fig. 1. **Refrigerant differential in a fixed cycle of the refrigeration machine corresponding to the conditioning conditions, using refrigerants R12 and R134a.**

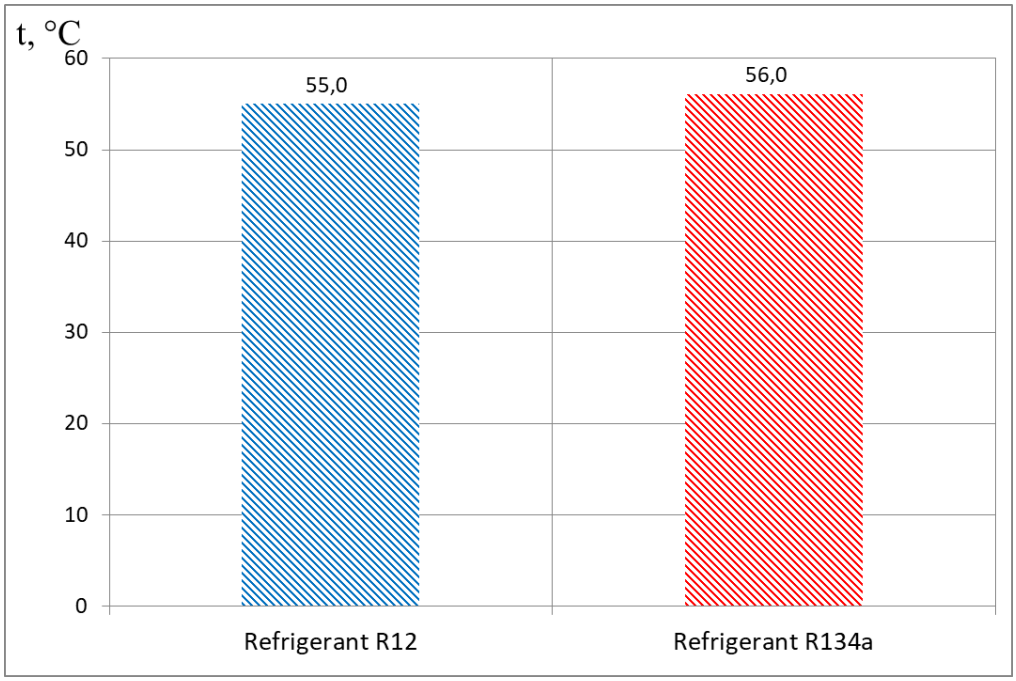

Fig. 2. **Temperature at the end of the compression process in a fixed cycle of the refrigeration machine corresponding to the conditioning conditions, when using refrigerants R12 and R134a.**

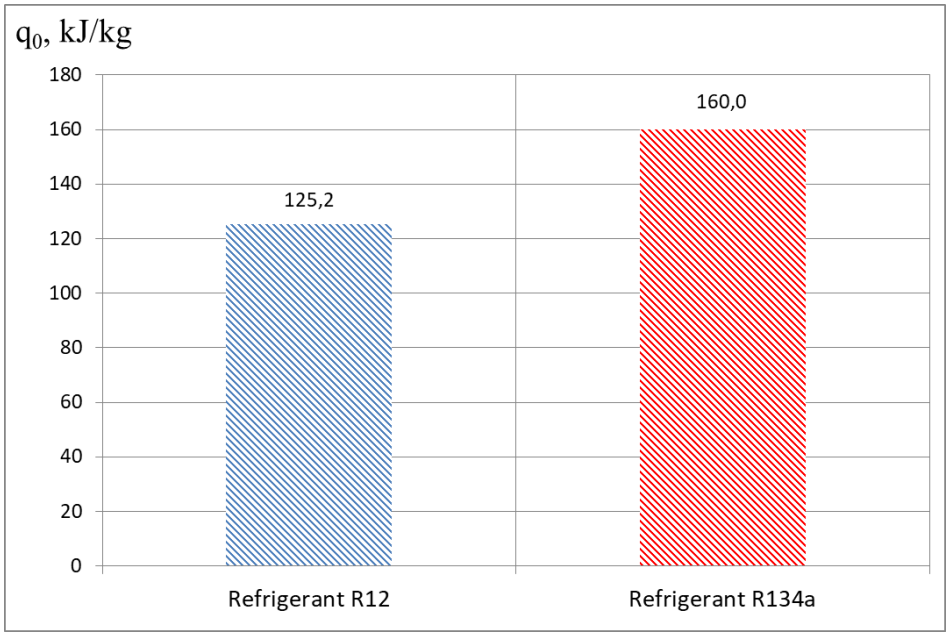

Fig. 3. **Specific mass cooling capacity in a fixed cycle of the refrigeration machine corresponding to conditioning conditions, using refrigerants R12 and R134a.**

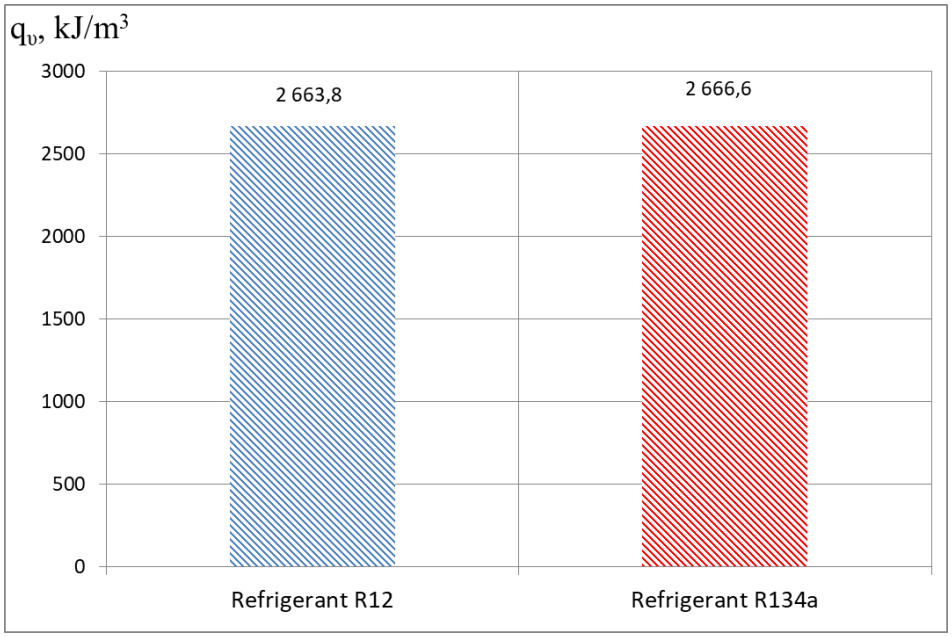

Fig. 4. **Specific volumetric cooling capacity in a fixed cycle of the refrigeration machine corresponding to conditioning conditions, using refrigerants R12 and R134a.**

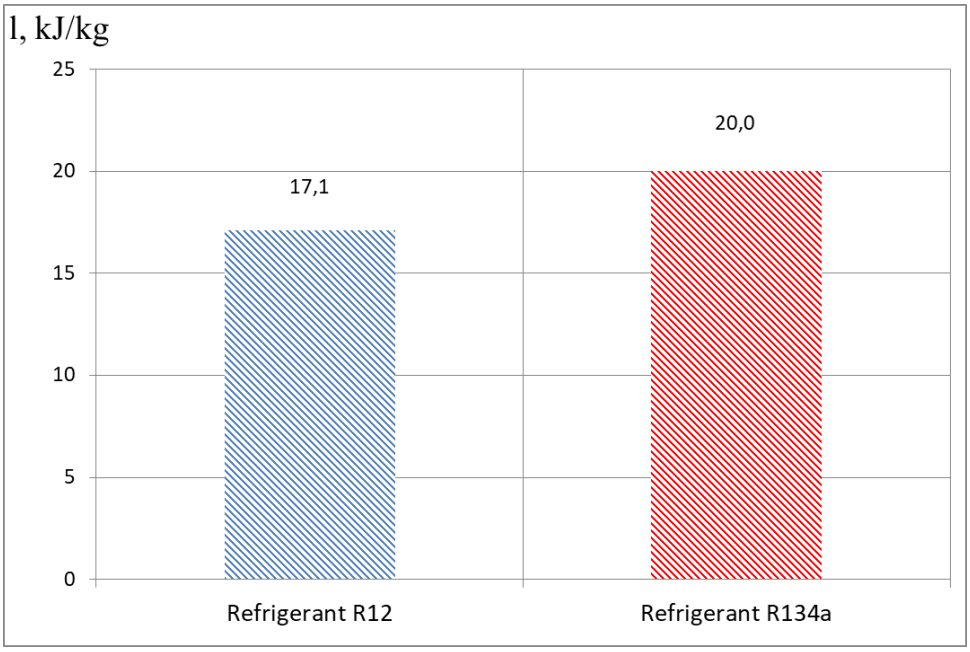

Fig. 5. **Adiabatic compression work in a fixed cycle of the refrigeration machine corresponding to conditioning conditions, using refrigerants R12 and R134a.**

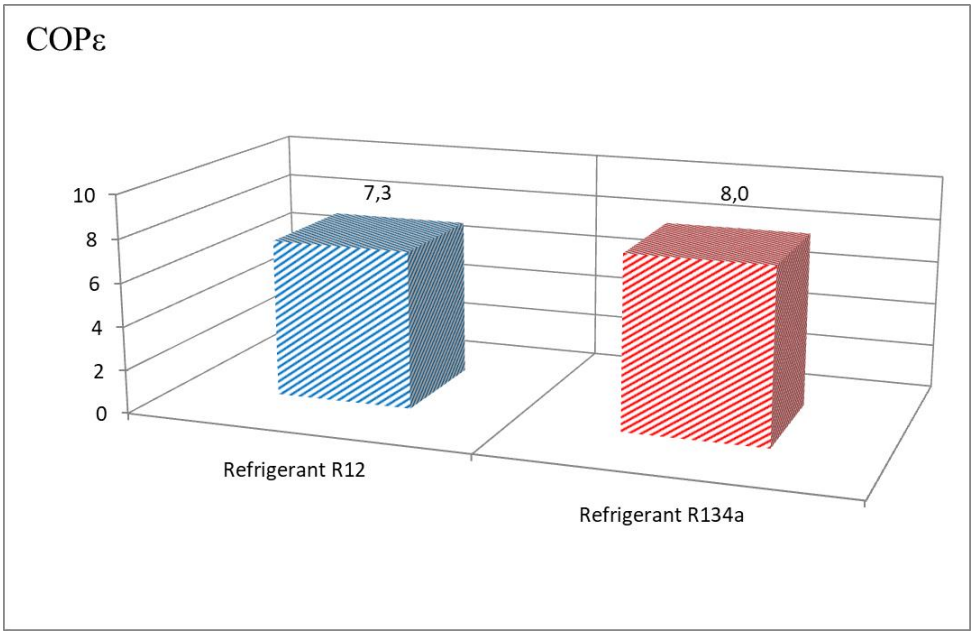

Fig. 6. **COPε value per fixed cycle for air conditioning condition, using refrigerants R12 and R134a.**

The conducted analysis of the values of weighty thermodynamic parameters of refrigerants R12 and R134a in the conditions of the fixed cycle of the refrigerating machine, corresponding to the conditioning conditions, has revealed insignificant deviations given in table 1 and has shown an insignificant discrepancy of the weightiest thermodynamic parameters. The results of the conducted thermodynamic analysis of working qualities of refrigerants R12 and R134a in the fixed cycle corresponding to the conditioning conditions, satisfies the use of refrigerant R134a as an alternative R12.

Values of refrigerant indices at fixed cycle corresponding to conditioning conditions are given in

Table 1.

Table 1. Values of indicators of refrigerants R12 in R134a in a fixed cycle corresponding to conditioning conditions

№	Parameter	Dimensionality	Refrigerant		
			R12	R134a	Divergence Δ, %
1	Differential refrigerant differential (Pк/Po)	-	2,33	2,51	0,18
2	Temperature at the end of the compression process t	°C	+55	+56	1
3	Specific mass cooling capacity q_0	kJ/kg	125,2	160	34,8
4	Specific volumetric cooling capacity q_v	kJ/m^3	2663,8	2666,6	2,8
5	Adiabatic work of compression l	kJ/kg	17,15	20	2,81
6	Value $COP_ε$	-	7,28	8,0	0,72

Practical relevance. The most important task of railway transport is the mass transportation of goods and passengers. When operating a passenger railcar fleet, it is necessary to ensure not only traffic safety but also comfortable conditions for passengers. Creating and maintaining comfortable conditions in passenger cars is achieved by air conditioning with transport air conditioners. Transport air conditioners of MAB-II type of passenger cars, which are in operation of passenger car fleet, are equipped with ventilation, water and electric heating, cooling and automatic regulation and control systems [7, 17]. A feature of these systems is the ability to adjust the air temperature in each compartment by the passengers themselves, while in other air-conditioned cars the temperature is regulated simultaneously in all rooms of the car from one temperature sensor.

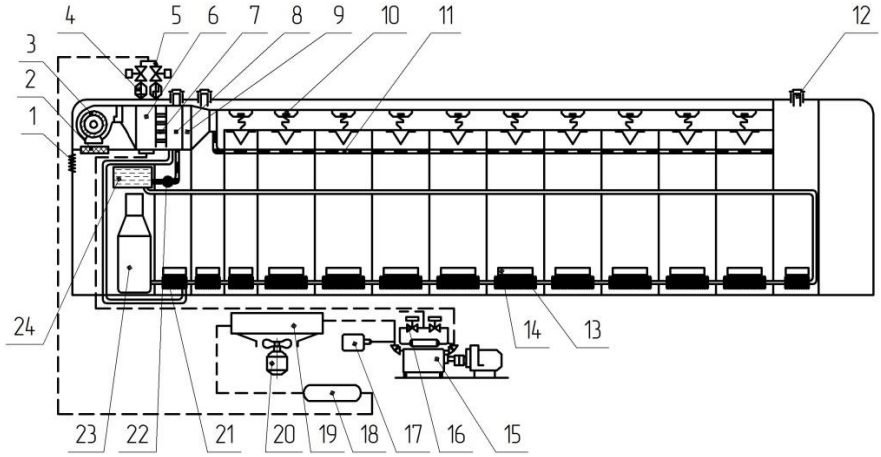

Fig. 7. **Diagram of the transport air conditioner type MAB-II:**
1 - grilles for external air; 2 - filter; 3 - ventilation unit; 4 - thermostatic valves; 5 - solenoid valves; 6 - air cooler; 7 - droplet separator; 8 - water heater; 9 - electric heater; 10 - outlet control device; 11 - perforated grille; 12 - deflector; 13 - heating battery; 14 - electric furnace; 15 - compressor; 16 - solenoid valves; 17 - pressure difference switch; 18 - receiver; 19 - condenser; 20 - condenser fan; 21 - circulation pump in the heating network; 22 - circulation pump of the heater; 23 - boiler; 24 – expander.

The refrigeration machine in the air conditioner cooling system cools the air supplied to the car by the ventilation system.

The refrigeration machine of the transport air conditioner MAB-II is a vapor compression, single-

stage compression, automated, has an aggregate design, designed for refrigerant Hladon 12 (R12). Compared to other types of refrigeration machines, this machine has a number of advantages: simple design, easy to operate, maintain and repair, and the use of alternative refrigerants. The scheme of the refrigeration machine (Fig. 8).

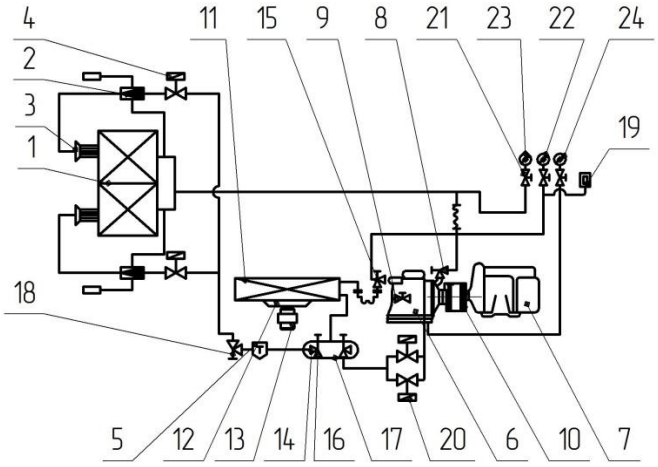

Fig. 8. **Diagram of the refrigeration machine of the transport air conditioner type MAB-II:**

1 - evaporator; 2 - thermostatic valve; 3 - liquid distributor; 4 - solenoid valve; 5 - filter-dryer; 6 - compressor; 7 - compressor motor; 8 - compressor suction shut-off valve; 9 - valve for filling the compressor crankcase with oil; 10 - flywheel coupling; 11 - condenser; 12 - condenser fan; 13-fan motor; 14-receiver; 15-compressor discharge shut-off valve; 16-angle shut-off valve at the receiver outlet; 17-angle shut-off valve of the receiver; 18-angle shut-off valve of the liquid line; 19 - high-pressure relay; 20 - electromagnetic valve for compressor capacity control; 21 - shut-off valves for pressure gauges; 22 - discharge pressure gauge; 23 - suction pressure gauge; 24 - oil pressure gauge.

By comparing the parameters of the compressor operating process and the values of COPε under operating conditions at the refrigerant boiling temperature in the evaporator t_0 = +5°C, condensation temperature in the condenser t_k = +55°C, which corresponds to the outside air temperature of more than +36°C, the following results were obtained (Fig. 9).

The refrigeration machine uses a V-type reciprocating compressor. The compressor is a 4-cylinder, V-axis, single-stage compression, block-crankcase, stuffing box, air-cooled cylinder, with a combined lubrication system, equipped with a device for regulating cooling capacity. The device for reducing the cooling capacity ensures the shutdown of two or three compressor cylinders using devices located in the cylinder heads. The cylinder diameter is 80 mm, the piston stroke is 58 mm, the crankshaft speed is 24.16sec^{-1}, and the volume described by the pistons per unit time is 112 m^3/h.

The crankshaft of the V-type compressor is connected to the shaft of a 13 kW electric motor.

The compressor is equipped with a device for reducing the cooling capacity of the unit by disconnecting two or three cylinders using lifting devices placed in their heads, and an oil heating device that facilitates start-up at low ambient temperatures.

At present transport air conditioners of MAB-II type of passenger cars are transferred to alternative refrigerant R134a.

By comparing the compressor refrigeration machine operating process parameters and COPε values on operating conditions at the refrigerant boiling temperature in the evaporator t_0 = +5°C, condensation temperature in the condenser t_k = +55°C, which corresponds to the outside air temperature of more than +36°C, in computer modeling the following results of using refrigerants R12 and R134a (Fig. 9)

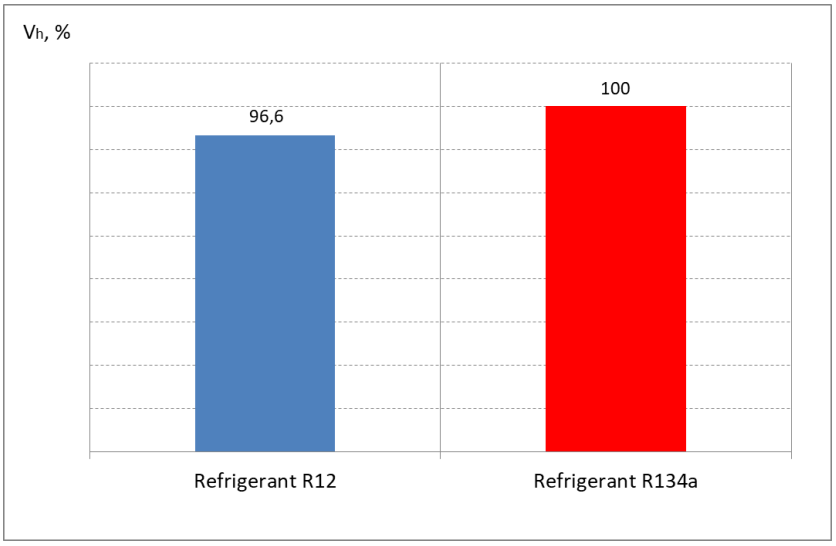

Fig. 9. **Volume described by pistons of the compressor type V for the operating mode t_0 = +5°C, t_k = +55°C when using refrigerants R12 and R134a.**

The volume described by the pistons of the compressor type V for the considered operating mode when using R134a is 100%, and when using R12 it is less by 3.4% (Fig. 9).

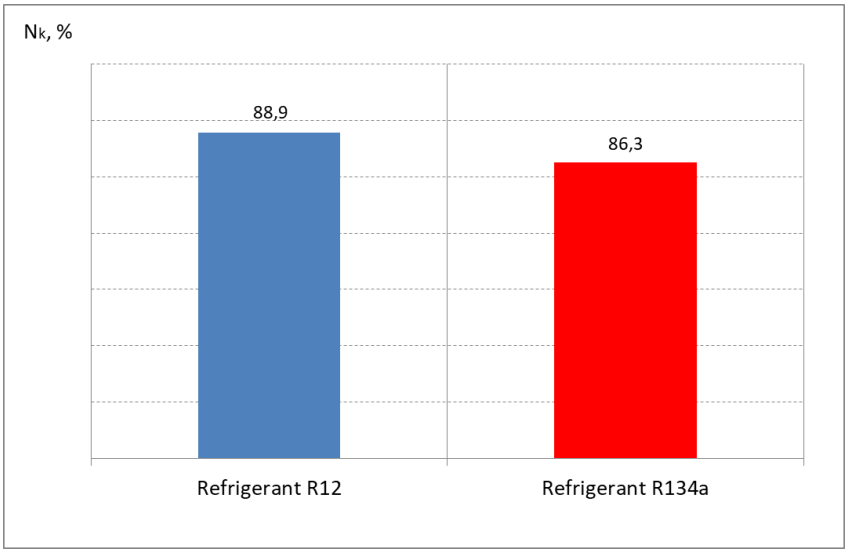

Fig. 10. **Power consumed by V type compressor for operating mode t_0 = +5°C, t_k = +55°C when using refrigerants R12 and R134a.**

The power consumed by the V type compressor for the considered operating mode when using R134a is less than R12 by 2.6% (Fig. 10).

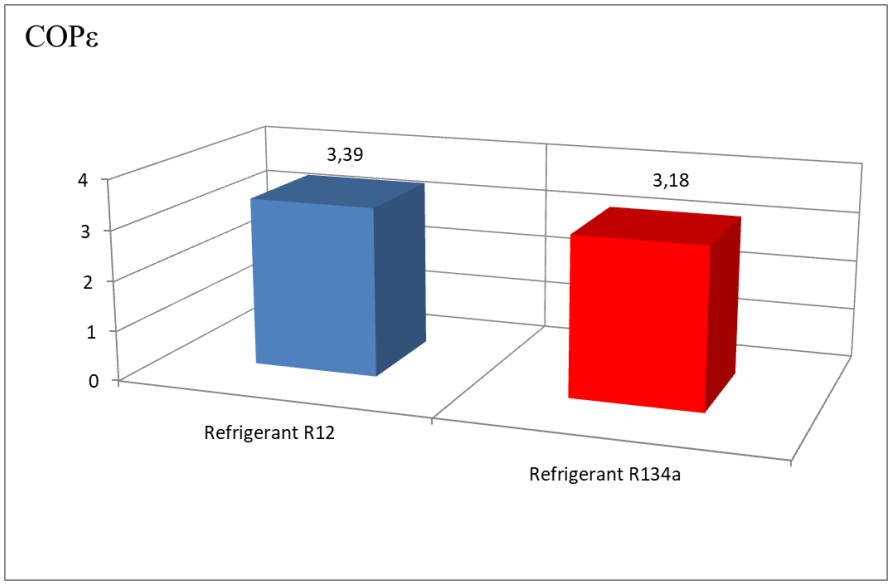

Fig. 11. **COPε value for operating mode t_0 = +5°C, t_k = +55°C when using refrigerants R12 and R134a.**

The value of COPε for the considered temperature mode when using R134a is less than R12 by 0.21% (Fig. 11).

Analysis of operating parameters of V type compressor and COPε value of refrigerating machine of transport air conditioner MAB-II of passenger car when using alternative refrigerant R134a instead of refrigerant R12 for operating conditions showed insignificant differences, which gives the reason for expediency of its application in transport air conditioner.

At present passenger cars with transport conditioners of MAB-II type, which are in the passenger car fleet, are transferred to alternative refrigerant Freon R-134a. Railway transport production enterprises have developed measures on retrofit of the refrigeration system of the transport air conditioner of MAB-II type of passenger car to the alternative refrigerant R-134a and conducted bench tests. Operational tests of passenger cars with transport conditioners of MAB-II type when using alternative refrigerant R-134a gave the confirmation about expediency of its application.

Conclusions. The following trends are currently prevailing in the development of refrigeration systems due to the risk of climate change, leading to the development of 4th generation refrigerants:

1) reduction of refrigerant emissions from refrigeration systems;

2) reducing the amount of refrigerant charged into the system;

3) increased requirements to the quality of assembly of refrigeration machines and equipment;

4) improvement of existing refrigeration machines in order to increase their energy efficiency and development of new refrigeration machines;

5) at present, the choice of alternative refrigerant for operating refrigeration machines depends on changes in the political and legislative environment, technology and market;

6) in transportation air conditioners of passenger coaches, freon R134a, which does not deplete the ozone layer, is used as an alternative refrigerant to replace refrigerant R12, but at the same time, further research on the use of natural component additives as an intermediate target is needed to reduce greenhouse gas emissions.

REFERENCES

1. Law of Ukraine "On Environmental Protection". [in Ukraine]. https://zakon.rada.gov.ua/laws/show/1264-12.
2. Yang, Z., Feng, B., Ma, H., Zhang, L., Duan, C., Liu, B., Zhang, Y., Chen, S., & Yang, Z. (2021). Analysis of lower GWP and flammable alternative refrigerants. *International Journal of Refrigeration*, *126*, 12–22. https://doi.org/10.1016/j.ijrefrig.2021.01.022.
3. Rajamanickam, C.S., & Tamil Selvan, P. (2023). An Experimental Study on the Cooling Performance of Refrigerant

(R134a/R1234yf) in Automobile HVAC System. *International Journal of Membrane Science and Technology*, *10*(1), 532–540. https://doi.org/10.15379/ijmst.v10i1.2617.
4. Kivevele, T. (2022). Propane (HC – 290) as an Alternative Refrigerant in the Food Transport Refrigeration Sector in Southern Africa – a Review. *Automotive Experiences*, *5*(1), 75–89. https://doi.org/10.31603/ae.5994.
5. Alkan, A., Kolip, A., & Hosoz, M. (2021). Energetic and exergetic performance comparison of an experimental automotive air conditioning system using refrigerants R1234yf and R134a. *Journal of Thermal Engineering*, 1163–1173. https://doi.org/10.18186/thermal.978014.
6. Hmood, K. S., Apostol, V., Pop, H., Badescu, V., & Pop, E. (2021). Drop-in and retrofit refrigerants as replacement possibilities of R134a in domestic/commercial refrigeration and automobile air conditioner applications. *Journal of Thermal Engineering*, 1815-1835. https://doi.org/10.18186/thermal.1027435.
7. Ishchenko, V. M., Shcherbyna, Yu. V., Os′mak, V. Ye., & Horlushko, Yu. V. (2021). Interchangeability of alternative refrigerants in air conditioning systems of passenger cars. Bulletin of the Volodymyr Dahl East Ukrainian National University, (2 (266)), 96-100. [in Ukraine]. https://doi.org/10.33216/1998-7927-2021-266-2-96-100.
8. İşkan, Ü., Kahraman, M. C., & Direk, M. (2023). Comparison of R134a and R516A's performance at different air velocities in two evaporator ejector cooling system. *Hittite Journal of Science and Engineering*. https://doi.org/10.17350/hjse19030000293.
9 Belman-Flores, J. M., Heredia-Aricapa, Y., García-Pabón, J. J., Pérez-García, V., & Pérez-Reguera, C. G. (2023). Drop-In Replacement of R134a in a Household Refrigerator with Low-GWP Refrigerants R513A, R516A, and R1234ze(E). *Energies*, *16*(8), 3422. https://doi.org/10.3390/en16083422.
10. Hacipaşaoğlu, S. G., & Öztürk, İ. T. (2023). Energy and exergy analysis in the ejector expansion refrigeration cycle under optimum conditions. *International Advanced Researches and Engineering Journal*, *7*(1), 23-34. https://doi.org/10.35860/iarej.1171637.
11. Baskaran, A., Manikandan, N., Tesfaye, J. L., Nagaprasad, N., & Krishnaraj, R. (2022). Exergy Performance Investigation of Eco-Friendly Refrigerant Mixtures as an Alternative to R134a in a Domestic Refrigerator. *International Journal of Photoenergy*, *2022*, 1-9. https://doi.org/10.1155/2022/4431378.
12. Ingle, D. A. H. (2024). Literature Review on Experimental Analysis of Domestic Refrigerator. *International Journal for Research in Applied Science and Engineering Technology*, *12*(5), 4154–4159. https://doi.org/10.22214/ijraset.2024.62567
13. Getie, M. Z., Lanzetta, F., Bégot, S., Admassu, B. T., & Djetel-Gothe, S. (2023). Parametric Investigation and Univariant Optimization of Domestic Stirling Refrigerator. *International Journal of Energy Research*, *2023*, 1–19. https://doi.org/10.1155/2023/3181171
14. Kravchenko, M. B., & Kokul, S. V. (2022). Optimization of the operating mode of a refrigeration machine operating on a zeotropic mixture of refrigerants. *Refrigeration Engineering and Technology*, *58*(2), 66–72. [in Ukraine]. https://doi.org/10.15673/ret.v58i2.2380.
15. Prasad, U. S., Mishra, R. S., Das, R. K., & Soni, H. (2023). Experimental and Simulation Study of the Latest HFC/HFO and Blend of Refrigerants in Vapour Compression Refrigeration System as an Alternative of R134a. *Processes*, *11*(3), 814. https://doi.org/10.3390/pr11030814.
16. Kumar, V., Kabir, R., Shannon, Z., R. Waghmare, D. P., & Flynn, D. M. (2024). Experimental study on R1234yf/R134a mixture (R513a) as R134a replacement in heat pipes. *Journal of Enhanced Heat Transfer*. https://doi.org/10.1615/jenhheattransf.2024053767.
17. Ishchenko, V. M., & Horlushko, YU. V. (2023). Improving the environmental performance of a passenger car air conditioning system by using an alternative refrigerant. *Railway transport of Ukraine*, 4, 26–33. [in Ukraine]. http://nbuv.gov.ua/UJRN/ZTU_2023_4_5.

Вадим Іщенко[1], Надія Брайковська[2] Юрій Щербина[3], Юрій Демченко[4]

[1]Доцент, Кафедра вагонів та вагонного господарства, Національний транспортний університет, М. Омеляновича-Павленка, 1, м. Київ, 01010, Україна. ORCID: https://orcid.org/0000-0002-5559-4251.

[2]Професор, Кафедра вагонів та вагонного господарства, Національний транспортний університет, М. Омеляновича-Павленка, 1, м. Київ, 01010, Україна. ORCID: https://orcid.org/0000-0003-1556-4020.

[3]Доцент, Кафедра вагонів та вагонного господарства, Національний транспортний університет, М. Омеляновича-Павленка, 1, м. Київ, 01010, Україна. ORCID: https://orcid.org/0000-0002-9574-2757.

[4]Старший викладач, Кафедра вагонів та вагонного господарства, Національний транспортний університет, М. Омеляновича-Павленка, 1, м. Київ, 01010, Україна. ORCID: https://orcid.org/0009-0006-3809-4323.

Сучасні вимоги до холодильних агентів транспортних кондиціонерів

Наукові досягнення, зміни національних законодавств у сфері боротьби з наслідками глобального потепління і вимоги ринку, стимулювали розробку холодоагентів четвертого покоління. На відміну від холодоагентів першого і другого поколінь, які забезпечували поряд із принциповою можливістю досягнення холодильного ефекту, такі якості як довговічність і безпека експлуатації, третє і четверте покоління істотно включають екологічні обмеження. Виявлення зв'язку між витоками традиційних холодоагентів другого покоління на основі хлорфторвуглеводнів (ХФВ) та руйнуванням захисного атмосферного шару озону спричинило появу третього покоління холодоагентів. Віденська конвенція і Монреальський протокол були реакцією світового співтовариства, що призвела до заборони озоноруйнівних речовин (ОРВ). При цьому ГФХУ розглядали як тимчасові або перехідні, а гідрофторвуглеці (ГФУ) - як довготривалі робочі тіла. Різко зросла зацікавленість до природних холодоагентів аміаку, діоксиду вуглецю, вуглеводнів і води.

Ключові слова: *залізничний транспорт, холодоагент, транспортні кондиціонери, парниковий ефект, альтернативні холодоагенти, пасажирський вагон, холодильна машина.*

DOI: 10.32703/2617-9040-2025-45-4

UDC 621.33: 629.4

Ievgen Riabov[1*], Liliia Overianova[2], Liliia Kondratieva[3], Oleksandr Plyutin[4], Artem Overianov[5]

[1] Assistant professor, Department of Electric Transport and Locomotive Engineering, National Technical University «Kharkiv Polytechnic Institute», Kyrpychova str. 2, Kharkiv, 61002, Ukraine. ORCID: https://orcid.org/0000-0003-0753-514X.

[2] Assistant professor, Department of Electric Transport and Locomotive Engineering, National Technical University «Kharkiv Polytechnic Institute», Kyrpychova str. 2, Kharkiv, 61002, Ukraine. ORCID: https://orcid.org/0000-0002-4827-572X.

[3] Postgraduate student, Department of Electric Transport and Locomotive Engineering, National Technical University «Kharkiv Polytechnic Institute», Kyrpychova str. 2, Kharkiv, 61002, Ukraine. ORCID: https://orcid.org/0000-0002-2788-9116.

[4] Postgraduate student, Department of Electric Transport and Locomotive Engineering, National Technical University «Kharkiv Polytechnic Institute», Kyrpychova str. 2, Kharkiv, 61002, Ukraine. ORCID: https://orcid.org/0009-0009-5199-4344.

[5] National Technical University «Kharkiv Polytechnic Institute», Kyrpychova str. 2, Kharkiv, 61002, Ukraine ORCID: https://orcid.org/0009-0003-7367-2203.

***Corresponding author:** riabov.ievgen@gmail.com

Dual-mode powered locomotives for main routes

The development of railway transport in Ukraine is associated with the improvement of transportation along the routes of pan-European transport corridors, improving rail connections with the countries of the European Union and domestic transportation. This requires the renewal of traction rolling stock, the current technical condition of which does not meet modern indicators of fuel efficiency and environmental friendliness. An analysis of traction rolling stock from world manufacturers shows the interest of railway operators in locomotives with dual-mode power supply. Such locomotives are able receive power both from the contact network and a diesel generator. This provides a number of advantages, the key among which is a reduction in the cost and transportation duration. The designs of ALP-45DP locomotives manufactured by Bombardier Transportation, Vectron Dual Mode manufactured by Siemens Mobility, EURODUAL and Class 93 manufactured by Stadler are considered. It's demonstrated that locomotives with dual-mode power supply are based on the design and components of serial locomotives. This reduces the cost of the explored locomotives, simplifies maintenance and ensures high reliability. At the same time, the presence of dual-mode power supply has influenced the application of specific design and circuit solutions. Energy storage systems, including plug-in accumulators, are promising for use on locomotives with dual-mode power supply. The use of accumulators allows both to accumulate energy during braking and power the locomotive systems, and to store energy from low-cost sources. This reduces the cost of fuel and energy resources. Basing on the analysis fulfilled, the structure of the traction system for a domestic locomotive with dual-mode power supply, which can be created by modernizing existing locomotives, is proposed and substantiated.

***Keywords**: locomotive, traction rolling stock, diesel, energy storage, plug-in hybrid power plant, traction system*

Introduction. Three international railway pan-European transport corridors No. 3, No. 5 and No. 9, the transport corridors Gdansk-Odesa (Baltic Sea Black Sea), Europe-Caucasus-Asia (TRACESA), Europe-Asia, also run through the river ports of Ukrainian railways tangent to the pan-European corridor No. 7, which runs along the Danube River [1]. In 2023, the agreement was reached on the creation of a 1520 mm gauge railway corridor between Ukraine and Lithuania [2]. In 2025, construction of a 1435 mm gauge standard from Chop to Uzhgorod [3] began, as well as preparations for the implementation of a project to build a 1435 mm Euro-gauge from the Romanian border to Chernivtsi and from Mostyska-1 station to Lviv. The development of railway connections along these routes is an important target that will accelerate European integration processes. In domestic transportation, the key tasks are the reorientation of freight transportation to rail transport, the renewal of rolling stock for passenger transportation, the replacement of carbon-emitting modes of transport, the advancing of "green" modes of transport, the development of high-speed rail traffic, etc. [4].

Analysis of recent research and problem statement. The development of domestic railway transport is not possible without updating the locomotive fleet. Currently, the main lines are electrified. At the same time, the volume of electrified sections is only 50% of the total length of Ukrainian railways, and many important routes have non-electrified sections. This requires the combined use of diesel locomotives and electric locomotives to drive trains on such routes. An alternative option is to use locomotives with dual-mode power supply, which can be powered both from the contact network and from the on-board power pack. Perhaps the first example of the use of such locomotives on trunk lines is the operation of the P32AC-DM locomotives manufactured by GE [5] and DM30AC manufactured by EMD [6]. Both locomotives are essentially diesel locomotives equipped with a current collection system from the "third rail". This is necessary for service on route sections where the application of diesel engines is impossible. In the 2000s, the BITRAC CC35600 locomotives manufactured by CAF Power [7], ALP45DP manufactured by Bombardier Transportation [8] were created. Recently, the locomotive line has been supplemented with the CLASS 88, CLASS 93, EURO9000, EURODUAL manufactured by Stadler [9], South African Class 38-000, Vectron Dual Mode and ALC-42E manufactured by Siemens [10], Euskotren TD2000 manufactured by CFD [11], Gama 111DE manufactured by PESA [12], locomotives of the BDD, EDD, EBB, BFC (Vossloh) series. and others. Dual-mode power supply technologies are used in the creation of Prima H4 (Alstom) shunting locomotives [13], HDB800 from Toshiba [14]. It is worth to note that energy storage systems are used on these locomotives, as a result of which manufacturers call them locomotives with tri-mode power supply. To a certain extent, locomotives with dual-mode power supply include electric locomotives equipped with power plants to implement the last mile function [15,16].

As can be seen from the experience in the EU and other countries, locomotives with dual-mode power supply are quite common in commercial operation, which confirms the feasibility of its use in rolling stock.

Currently, the locomotive fleet of Ukrainian railways requires significant renewal. A possible option is the application of locomotives with dual-mode power supply, since some important routes have electrified and non-electrified sections. The operation of locomotives with dual-mode power supply on such routes will ensure the improvement of rail transportation.

The exploitation of modern locomotives with dual-mode power supply compared to the technology of operating single-mode locomotives provides [17]:

– increasing the efficiency of locomotive operation due to the "coverage" of electrified and non-electrified sections by one locomotive;

– increasing traffic safety due to the presence of a dual traction system, which will ensure movement in the event of a power outage;

– simplifying the maintenance of routes on which there are electrified and non-electrified sections;

– flexibility of the system for organizing operational work due to the "universality" of the fleet in the case of freight and passenger locomotives;

– introducing alternative routes for freight and passenger trains, which in turn will lead to an increase in railway capacity and transportation efficiency;

– simplifying shunting operations when delivering target routes from door to door to ports and terminals, as well as changing the route;

– reducing harmful emissions into the environment;

– the possibility of reducing the noise level.

Thus, the use of locomotives with dual-mode power allows simplifying and accelerating rail transportation. This is important for the transport industry of Ukraine, for the development of which the growth of railway transportation is a priority.

The purpose and tasks of the research. The purpose of the article is to analyze the structures and traction systems of mainline locomotives with dual-mode power supply.

Research materials and methods. To date, foreign manufacturers have created several models of locomotives with dual-mode power supply. Below, the main characteristics of locomotives operated on main lines are considered and analyzed.

The ALP-45DP locomotive was developed and manufactured by Bombardier Transportation [8,18]. Fig. 1 shows a general view of the locomotive. The equipment layout is shown in Fig. 2. Table 1 lists the main technical parameters of the locomotive. The locomotives are putted into service on main lines in the USA and Canada.

a

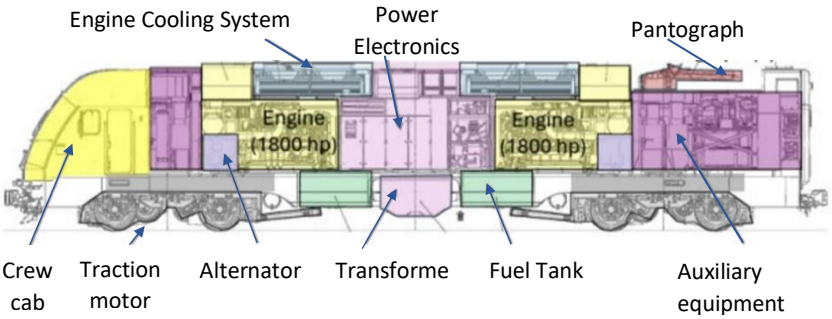

b

Fig. 1. **Locomotive ALP-45DP (photo from the Internet)**
a – general view (photo from the Internet); b) – Equipment placement [8]:

The ALP-45DP locomotive is designed using technologies developed and used in the TRAXX family of locomotives and the ALP-46 electric locomotive [20]. The body is made with a single cab. To meet the requirements of the Association of American Railroads [21], the locomotive body has a reinforced structure. The reinforcement of the body structure was also caused by the use of equipment with a greater weight. To access the internal equipment, the locomotive body has been designed with a removable roof. The locomotive bogies have a reinforced frame structure due to the greater axial load. This also caused the strengthening of the spring suspension and hydraulic vibration dampers. The transmission of longitudinal traction and braking forces between the body and bogies is carried out through two longitudinal inclined pull rods connected to the body in the area of the fuel tanks. This provides high

traction properties of the locomotive. The locomotive is equipped with disc and shoe brakes, which provides high braking efficiency.

To ensure high power in autonomous mode, the locomotive uses two high-speed 12-cylinder Caterpillar 3512C HD engines with a capacity of 1567 kW, each of which has a traction asynchronous generator. This solution provides a power plant capacity of over 3000 kW, and also allows movement in the event of a malfunction of one diesel engine.

The set of electrical equipment is similar to the ALP-46 electric locomotive. The main electrical equipment is located in the middle part of the body. The pantograph is situated on the roof in the rear part. A feature is the placement of the traction transformer under the locomotive body, between the fuel tanks.

Table 1. **Technical parameters of the ALP-45DP locomotive [19]**

Parameter	Value
Type of vehicle	Passenger locomotive
Track gauge	1435 mm
Clearance gauge	AMTRAK
Wheelset arrangement	B_0–B_0
Length over coupler, mm	21 800
Width, mm	3310
Virtual distance between bogie centers, mm	13 250
Axle base, mm	2800
Wheel diameter, mm	1118 (new)/ 1046 (fully worn)
Axle load, t	32.66
Total weight, t	130.64
Converter type	IGBT, water cooled
Traction converters	2 x MITRAC TC 3350
System voltage	25 kV/60 Hz, 12 kV/25 Hz
Head-end power (HEP) – train supply capability	1100 kVA, 3 x 480 V/60 Hz
Max. traction power «Electric mode», kW Max. traction power «Diesel mode», kW	4000 2x1567
Max. rheostatic braking power, kW	1200
Max. Starting tractive effort, kN	316
coefficient of adhesion	1:4.06
Max. Brake force (electric brake), kN	150
Brake resistor power, kW	1300
Fuel capacity (usable), l	6044…6800
Max. Service speed «Electric mode», km/h Max. Service speed «Diesel mode», km/h	201 160

Fig. 2 shows a diagram of the traction system of one trolley.

When operating from the contact network, the propulsion electric drive is powered from the traction transformer via four-quadrant converters (active rectifiers). When it powered from a diesel generator, three of the four phases are used, which are formed by two four-quadrant converters. Compared to synchronous generators of any type, this is a cost-effective solution, which, however, became possible and economically viable only thanks to the use of already existing four-quadrant converters. The diesel engines are started by an asynchronous generator, and the active converter is used at that as an inverter. For this purpose, the DC bus can be powered by a battery and one of the phases of the four-quadrant converter as a boost converter in a corresponding other bogie.

By operation under the contact network the energy is regenerated during electrodynamic braking. The rheostatic brake is as well available with a capacity of 2x650 kW.

The locomotive is equipped with a three-phase train power supply system with a capacity of 1100 kVA (1000 kW), regardless of the power mode.

The drive technology is designed in such a way that switching between modes can occur even while the train is moving, without any interruption in the train's power supply. For certain operators, the change can only occur when stopping at a station, to prevent the locomotive from running without power for the 100 seconds required for this.

The Vectron Dual Mode locomotive was developed by Siemens Mobility. Fig. 3 displays the general view (Fig. 3a) and the equipment layout (Fig. 3b). Table 2 consists the technical parameters of the locomotive.

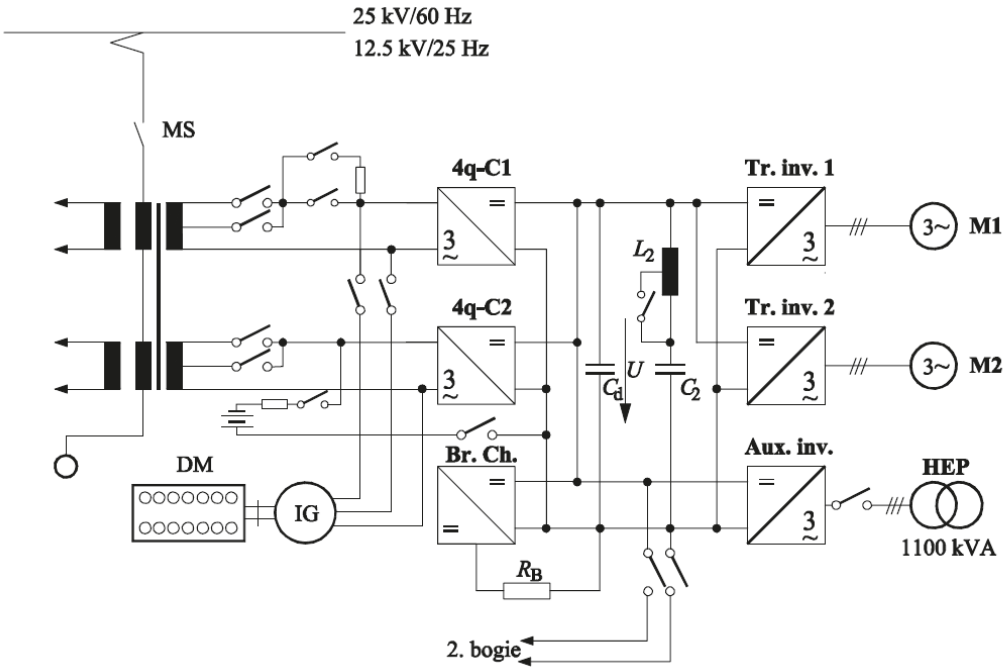

Fig. 2. **Diagram of the traction system of one trolley [19]**

MS – main switch; 4q-C1, 4q-C2 – four-quadrant converters; Br.Ch. – brake converter; R_B – braking resistor; C_d, C_2 – filter; L_2 – inductance; Tr.inv.1, Tr.inv.2 – traction inverters; Aux.inv. – auxiliary inverter; M1, M2 – traction motors; HEP – electric train supply; DM – diesel motor; IG – generator

The aim of the Vectron Dual Mode locomotive was to create a modern, environmentally friendly and powerful mainline locomotive that combines the advantages of diesel and electric traction [22]. This provided operators with the opportunity to make long trips with the same locomotive, which could overcome both electrified and non-electrified sections.

The Vectron Dual Mode locomotive is an evolution of the existing Vectron DE locomotive, to which appropriate equipment was added to ensure its operation from the catenary network. The traction properties of the locomotive in both modes are approximately the same, since the main area of application of the locomotive is driving trains moving under diesel traction. Fig. 4 represents the traction and braking characteristics of the Vectron Dual Mode.

а

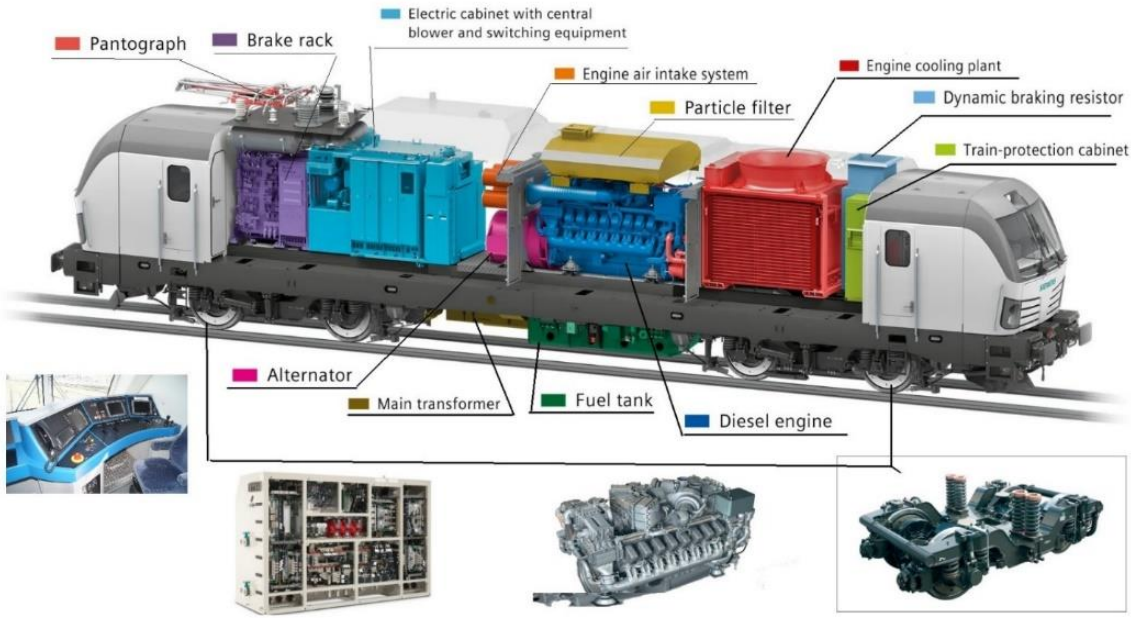

б

Fig. 3. **Vectron Dual Mode Locomotive**
a – general view (photo from the Internet); b – equipment placement [22]

The locomotive is designed as a mainline locomotive with two end cabs. The driver's cabs are identical to the Vectron E locomotive or the previous Vectron DE locomotive. The engine cabinet (Fig. 3b) is divided into three separate chambers by two partitions. The electrical chamber, located behind the driver's cab, contains the most important electrical functional components. These include the converter (with integrated equipment for switching between electric mode and diesel mode), the auxiliary system module, the pneumatic brake equipment and the air cleaning system for the diesel engine. In the middle of the locomotive is the diesel engine compartment, which is completely closed. This ensured its soundproofing. The diesel engine with an exhaust system and the preheating/heating support device for the diesel engine is located in the diesel compartment. Directly above the diesel engine is a particulate filter that acts as a silencer. Inside the particulate filter are individual replaceable filter elements. This arrangement of the particulate filter above the engine minimizes the number and length of exhaust pipes with high thermal load, as well as heat radiation to the engine compartment. A preheating/heating maintenance device with an installed thermal output of 35 kW ensures a smooth start of the diesel engine. The start itself is carried out using a starting system based on double-layer capacitors, so-called Ultra-Caps. Unlike conventional starter batteries, these energy storage devices are smaller and lighter, practically maintenance-free and have significantly better properties at low temperatures. Directly below the engine system is a 2,600-liter fuel tank, which can be filled from both sides, as well as a main transformer with a corresponding cooling system. The third segment of engine compartment contains

the diesel cooling system, braking resistor and standard protection cubicle. All engine room components are located in the center.

Two through side passages provide good access for maintenance or changing direction. The essential feature of the less complex system is the usage of only one diesel engine and the intelligent combination of all components, fewer and easily replaceable individual modules. This results in a small number of interfaces, which in turn minimizes the number of possible electrical and mechanical sources of error, such as oil, coolant or fuel leaks.

Table 2. **Technical parameters of the Vectron Dual Mode locomotive**

Parameter	Value
Area of application	Freight / Passenger
Wheelset arrangement	B_0-B_0
Vehicle length (length over buffers), mm	19975
Track gauge, mm	1435
Fuel tank volume (usable), l	2600
Wheel diameter. mm	1100 (new) / 1020 (worn)
Wheelset load, t	22.5
Weight (max.), t	90
Voltage system	AC 15 kV, 16.7 Hz
Diesel engine power (at the crankshaft), kW	2400
Traction power at the wheel rim, kW Electric mode (max.) Diesel mode	 2400 2000
Starting tractive effort, kN	300
Electric braking power at the wheel rim, kW Electric mode (max.) Diesel mode	 2100 1700
Electric braking effort, kN	150
Train protection	PZB, ready for ETCS
Traction gear type	Cog-wheel-hollow shaft
Gear ratio	1:5.1
Train power supply	1000 V, 22 Hz resp. 16.7 Hz; 480 kVA
Max. Speed, km/h	160
Double traction	Via WTB ÖBB: with same-type vehicles as well as Vectron E, Vectron DE, and ER20
Operation ambient temperature	-30°C….+40°C

The cooling system of the main transformer has three fans that can be switched on and off separately as required. The main transformer is characterized by a particularly compact design. The absorption circuit choke is also located in the transformer tank, which is filled with synthetic ester. This minimizes the noise level, especially at train stations. The side cooling tower system serves exclusively for cooling the diesel engine. The main features of the cooler are the infinitely variable cooling fan with hydrostatic drive and highly efficient aluminum radiators. The cooling system performance is designed for high loads, so the diesel engine does not experience any reduction in performance at outside temperatures of up to 35°C. For inspection and maintenance of the cooling system, access to the interior is possible at the same level via the end service door.

In contrast to purely electric locomotives, a locomotive with a powerful diesel engine requires a significantly higher air flow rate. The locomotive body is therefore specially adapted to the requirements of the diesel engine air supply. The combustion air is specially drawn in through an opening on the side of the electrical chamber. To meet the high air requirements for the diesel engine cooler and the brake resistor, large intake openings are locating in the cooler compartment.

The locomotive is powered by a 4000 series diesel engine from MTU Friedrichshafen, which is already used on the Vectron DE. The engine is a 16-cylinder V-engine. When idling, the engine control unit switches off the cylinders, meaning that in this operating mode the engine operates only with 8 cylinders at a time, which also minimizes fuel consumption in this operating mode. The engine is two-stage with turbocharging. The proportional reduction in exhaust emissions in the engine is achieved by recirculating the cooled exhaust gases. By choosing a large diesel engine that has been specially optimized for operation by railway, it can be perfectly tuned to the optimum maximum tractive effort with minimized fuel consumption, while adhering to the specified exhaust emission limits using the appropriate engine control parameters. The diesel engine used in the Vectron Dual Mode complies with the European Stage V emissions standard.

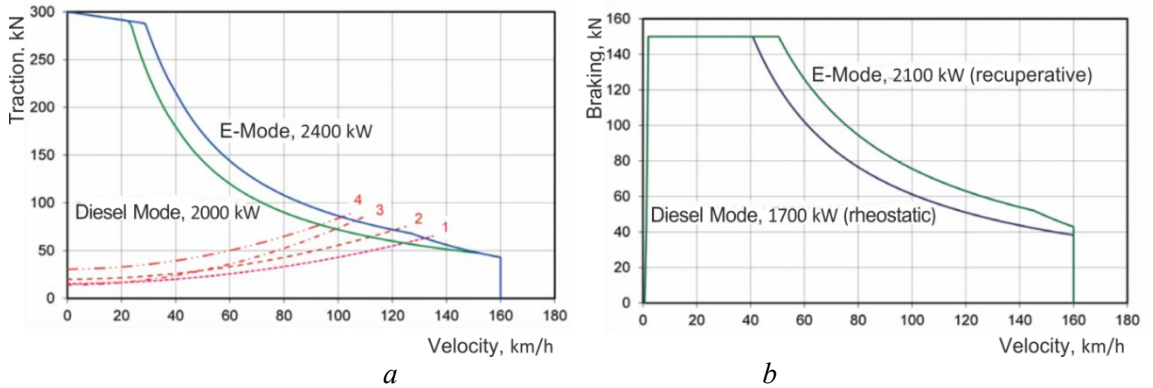

a *b*

Fig. 4. **Traction and braking characteristics of the Vectron Dual Mode locomotive [22]**
a – traction characteristics; b – braking characteristics:
4 Vectron DM + loaded container train/block train 2,500 t hauled load on flat route;
3 Vectron DM + mixed freight train 1,200 t hauled load on flat route;
2 Vectron DM + loaded container train/block train 1,600 t hauled load on flat route;
1 Vectron DM + loaded container train/block train 1,200 t hauled load on flat route

The Vectron Dual Mode bogie is a further development of the long-proven SF3 Eurorunner ER20 bogie. It has been adapted to current standards and the maximum speed has been increased from 140 km/h to 160 km/h. This means that not only freight but also regional passenger traffic is fully covered. In addition, the maximum permissible axle load has been increased to 22.5 t. Since the locomotive is primarily intended for freight transport, the sand supply system has been designed in such a way that sand is supplied to the front wheels of both bogies in both directions of travel (8-fold sprinkling). In addition, the drive clutch control has been further improved to achieve the highest possible use of tractive force.

Fig. 5 displays a diagram of the traction system of the Vectron Dual Mode locomotive.

The propulsion system of the locomotive consists of a three-phase synchronous generator G with independent excitation, high-voltage equipment, a transformer, a power converter with IGBT power semiconductors and four three-phase asynchronous traction motors powered by the converter. The central converter unit, which was essentially borrowed from the Vectron DE, contains all the electrical equipment for the locomotive controlling. Two traction motors are powered by a pulse-controlled inverter from the DC intermediate circuit. The intermediate circuit is powered by a contactless three-phase synchronous generator via an uncontrolled rectifier bridge. The converter unit also contains an auxiliary power inverter that feeds an auxiliary network of 3x440 V, 60 Hz from the intermediate circuit to power internal consumers. The arrangement of the pulse inverters and auxiliary converters on a common intermediate circuit allows auxiliary systems to be powered by the regenerated braking energy during electrodynamic braking and thus ensures that the locomotive operates with optimized energy consumption. The roof segment above the power converter located a current collector, a main switch with an attached earthing conductor and two arresters for overvoltage protection. The design of the high-

voltage equipment takes into account the possible option of a locomotive powered by a 25 kV network. The braking energy during electrodynamic braking is fed back into the energy overhead network during electric operation (regenerative braking). When operating on a diesel engine, excess braking energy that cannot be used to power the auxiliary systems is dissipated via the brake drive and the braking resistor (rheostatic braking). The braking resistor is designed in the form of a tower, as in the electric versions of the Vectron. This has allowed for an increase in power to 1,700 kW. This proven braking resistor was adopted from the Vectron DE without modification. The Vectron Dual Mode drive consists of the proven hollow shaft gear drive, which is already used as standard in all Siemens Eurorunner ER20 diesel locomotives. It differs from the drive of the Vectron electric locomotive variants in that the nominal power is adapted to the diesel engine. This results in weight savings, which is important for a dual-mode locomotive.

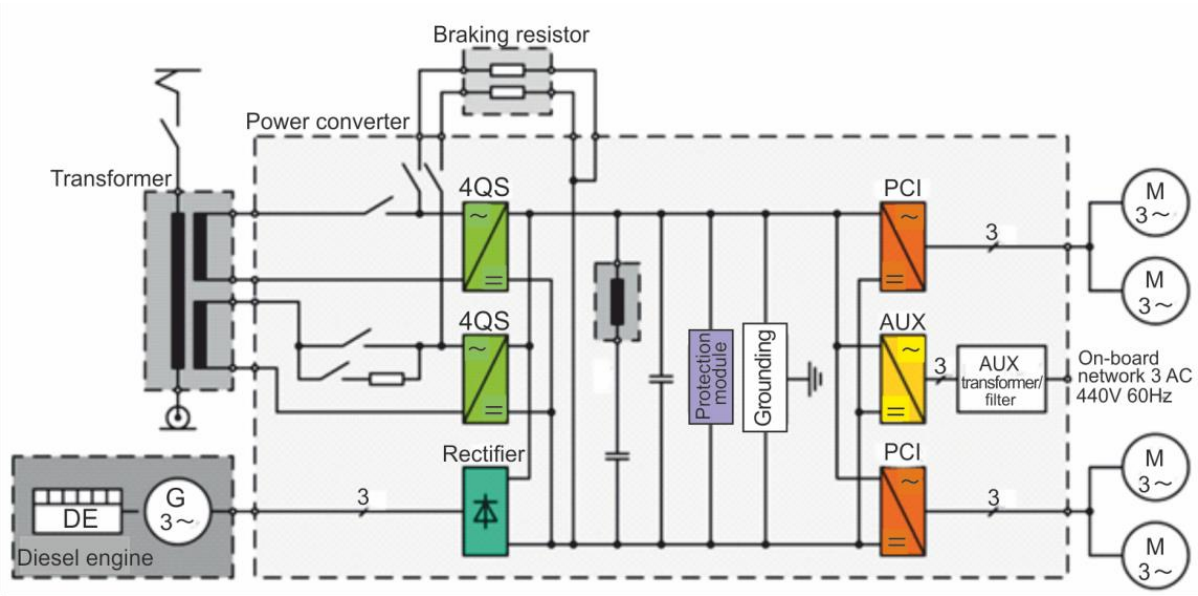

Fig. 5. **Diagram of the traction system of the Vectron Dual Mode locomotive [22]:**
4QS – four-quadrant converter; G – generator; PCI – pulse-controlled inverter;
AUX – auxiliary power inverter; M – traction motor

An important function of a dual-powered locomotive is the switching between electric and diesel operation. This switching is possible for the Vectron Dual Mode while in motion. The intermediate circuit remains charged and the auxiliary systems are continuously powered. The duration of the interruption of traction during the switch is minimal and amounts to a few seconds and therefore does not affect the movement. The switchover process is initiated by the train driver via the display and is largely automatic. Due to safety requirements, the driver must perform several operations/confirmations. For example, he must look after the lifting of the pantograph to ensure that the locomotive is under the contact wire. The corresponding preheating/heating maintenance concept ensures that the diesel engine is always ready to start with little wear.

As an evolution of the series is the Vectron Dual Mode Light locomotive with a less powerful diesel engine.

The EURODUAL locomotive was developed by Stadler. Fig. 6 shows the general view (Fig. 6a) and the design structure (Fig. 6b) of the EuroDual locomotive. Table 3 shows the technical parameters of the locomotive.

The EURODUAL locomotive is based on proven models such as EURO4000 and EUROLIGHT (Fig. 6b). The following advantages were achieved when creating the locomotive:

– multi-purpose locomotive for freight and passenger transportation;

– AC, DC or multi-system contact network;

– AC traction system with IGBT;
– for various engine powers up to 3000 kW;
– high starting tractive effort of 500 kN, both in diesel and electric modes(with each single axle control);
– high wheel-rail adhesion;
– remote radio control for effective shunting work;
– extremely low track forces due to the most modern design of the three-axle bogie with support-frame suspension of traction electric motors;
– equipped with the latest version of ETCS BL3.4.0 and all national class B systems;
– designed for (digital) automatic coupling;
– monocoque construction made of high-strength steel;
– multi-unit operation possibility;
– cross-border operations;
– reduced environmental impact.

a

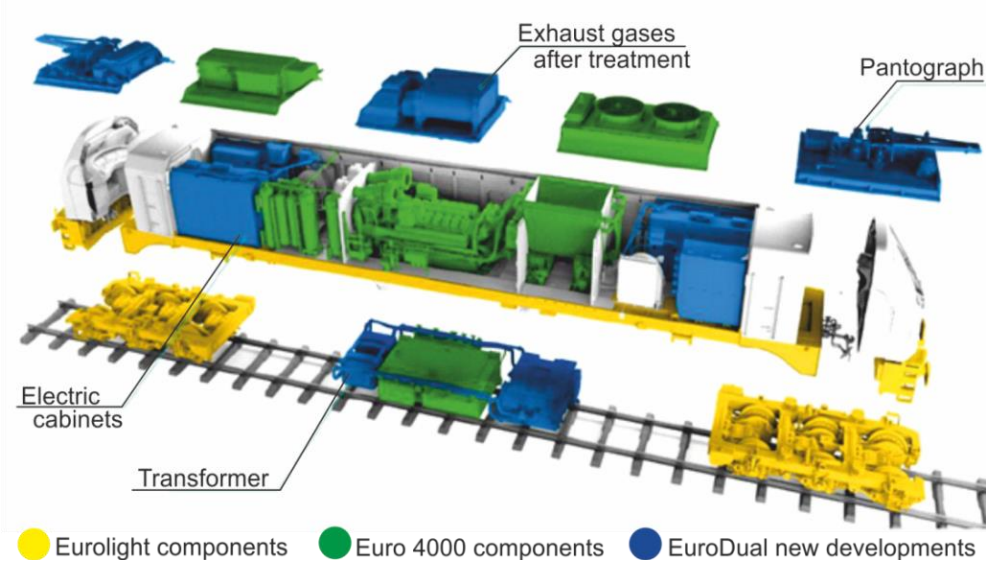

b

Fig. 6. **EURODUAL locomotive:**
a – general view (photo from the Internet); b – locomotive design [23]

In autonomous operation, the power source is the CAT C175-16 ACERT TM diesel engine, which is derived from the successful Caterpillar C175 series, which is commonly used in diesel-generator sets and heavy earthmoving equipment. The C175-16 engine is a 16-cylinder V-cylinder four-stroke engine with a cylinder diameter of 175 mm and a stroke of 220 mm, a working volume of 84.7 liters and a

power of 3755 h.p. (2800 kW) at 1740 rpm. It uses electronically controlled fuel injection, which allows for precise adjustment of the injection according to the requirements applied to the engine. The injection strategy, which is possible at this engine, can be changed depending on the load, speed, engine temperature, air temperature and fuel temperature. The engine is equipped with four turbochargers with two-stage cooling and weighs 11 tons. CAT engines meet European 2012 IIIB emission standards by replacing the muffler with a diesel particulate filter. Engine maintenance can be performed at intervals of 1,000 hours between minor maintenance (oil change) and of 18,000 hours between heavy work (overhaul).

Table 3. **Technical parameters of the EURODUAL locomotive**

Parameter	Value
Locomotive type	Dual-mode: Electric / Diesel-electric
Track gauge, mm	1435 (1520)
Axle arrangement	C_0-C_0
Length, m	23.02
Width, m	2.900
High,	4.290
Virtual distance between bogie centers, m	17.60
Wheel Base, m	3.60
Service weight, t	123
Friction weight, t	123
Axle load, t	20.5
Coefficient of adhesion	1:2.41
Electric power supply	DC (1500 V, 3000 V), AC (25 kV 50 Hz and 15 kV 16.7 Hz) Multisystem
Diesel engine	CAT C175-16, IIIB (Emission level according to EU standard EC 26/2004 Stage IIIB)
Engine power, kW	Up to 3000
Electric power at wheel rim, kW	Up to 7000
Starting tractive effort, kN	500
Fuel tank, l	Up to 4000
Transmission	AC/AC
Maximum speed, km/h	120
Brake system	Mechanic: Pneumatic Dynamic: Regenerative/ rheostatic 2 distributors, one per bogie Bail off functionality
Suspension	Primary: Coil springs Secondary: Rubber metal Vertical and horizontal dampers

Some components of the diesel generator are made of aluminum rather than steel to reduce weight. The ABB generator was specifically designed for use with the C175 engine and is attached directly to it. The engine/generator assembly uses a flexible five-point mounting system.

The traction system is built using ABB equipment. ABB's Bordline CC1500 DE converter is a latest-generation device used in the Swiss manufacturer's double-decker trains. It was therefore logical for Stadler to use it for its Euro Dual. The traction converter control must not only optimize the voltage waveforms supplied to the engines, but also ensure that the transmission is not a source of disturbances, oscillations or harmonic pollution for the power supply side. Using modern IGBT technology that controls each traction motor individually, the Bordline CC1500 DE generates a wave-like quasi-sinusoidal current, which reduces harmonic losses, acoustic noise and mechanical stress on the traction

motor. On the EuroDual, the converter control must minimize generator waveform distortion to reduce wear and optimize fuel efficiency.

According to ABB, the secret to the compactness and power density of these ABB traction converters is basing on their internal liquid cooling, modular design and carefully manufactured aluminium or stainless steel housings. This has allowed two of them to be installed in the Euro Dual, one per bogie. Each channel has its own rectifier to create a DC intermediate power supply, a brake chopper and drive operation electronics (AC800 PEC) with manual control, two traction inverters and an auxiliary inverter.

The EURODUAL locomotive can operate in the following operating modes [24]:

– Last Mile operation;
– Diesel service with electrified stations;
– Dual operation on electrified and non-electrified lines;
– Diesel detour to avoid highly populated areas (e.g. cities) and stop time;
– Power-boost with diesel engine on electrified lines;

A further development of Stadler locomotives is the implementation of energy storage systems in the power plants of locomotives. For example, an energy storage system can be used on the EuroDual locomotive, which will provide a tangential power of 2400 kW [25]. The layout of the equipment of such a locomotive is provided in Fig. 7.

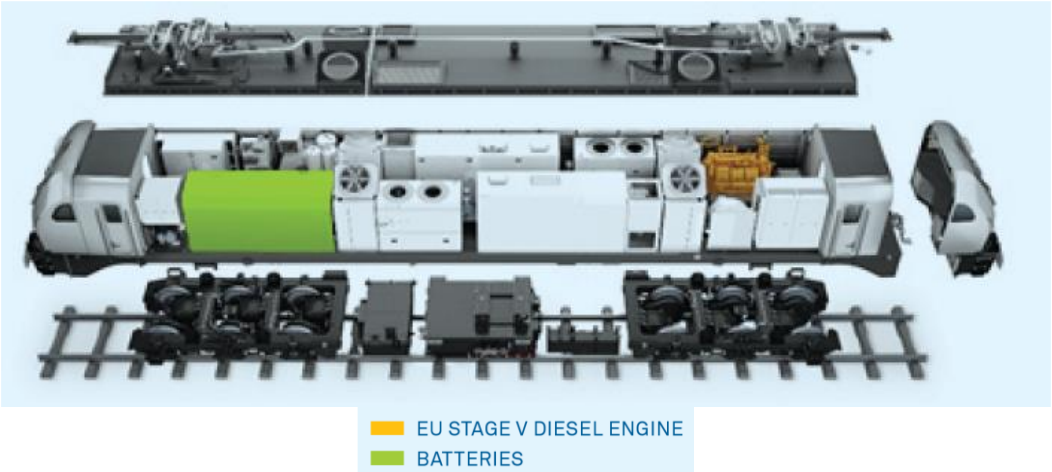

Fig. 7. **Design of a locomotive with an energy storage device [25]**

Energy storage devices in the traction system were used by creation of the *Class 93 locomotive* (Fig. 8).

Table 4 represents the main technical parameters of the locomotive. Fig. 9 displays a diagram of the traction system.

The locomotive is equipped with a Caterpillar C32 diesel engine, which has a power of 900 kW at 1800 rpm, and an energy storage system consisting of two traction batteries with a power of 200 kW each. A hybrid operation mode with a diesel engine and batteries is possible, which provides a combined power of 1300 kW.

Fig. 8. **General view of the Class 93 locomotive (photo from the Internet)**

Table 4. **Technical parameters of the Class 93 locomotive**

Parameter	Value
Axle arrangement	B_0-B_0
Weight, t	86
Track gauge, mm	1435
Maximum speed, km/h	180
Maximum tractive effort, kN	290
Continuous traction force, kN	229
Power in power supply mode from the catenary network 25 kV, 50 Hz	4000 кВт
Diesel engine power, kW	900
Power of the energy storage system, kW	2x200
Power in hybrid mode (diesel/battery), kW	900+400
Power in booster mode when powered from the catenary network, kW	4600
Fuel tank capacity, l	3600

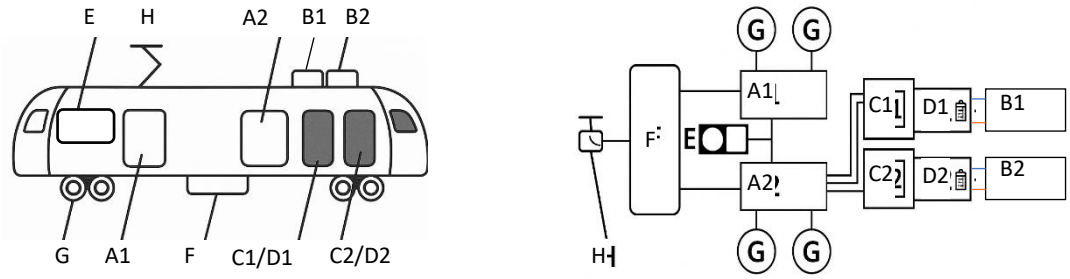

Fig. 9. **Diagram of the traction system of a Class 93 locomotive [26]**
A1, A2 – Compact converter; B1, B2 – Battery thermal management system; C1, C2 – Energy Storage System (ESS) filter; D1, D2 – Energy Storage System; E – Diesel generator unit; F – Transformer; G – Drive motors; H – Pantograph with main circuit breaker

The Caterpillar C32 diesel engine is a 12-cylinder, four-stroke, turbocharged engine with mechanical-electrical unit injection (MEUI) to meet Stage V emissions.

The traction batteries are an energy storage system (ESS) consisting of two lithium titanate oxide (LTO) traction batteries. These batteries can be charged from the overhead contact line or from the diesel engine. In ESS mode, the power is supplied as follows: energy from the batteries is supplied to a DC-DC converter, where the voltage is stepped up. The output current is fed into the DC link, and the current

from the link is then inverted to AC by the traction and auxiliary inverters to power the traction motors and auxiliary loads respectively.

The Class 93 locomotive is equipped with four asynchronous AC traction motors. These motors are force-cooled and are individually controlled by four separate traction inverters. When operating at constant load, the motor has a rated power of 1050 kW at rotational frequency of 1281 rpm. This provides a rated electrical power of 4 MW when powered by the catenary, which can be increased to 4.6 MW in "Boost" mode.

Class 93 locomotives have an electrodynamic brake. When operating from the catenary, energy will be regenerated to the catenary. When the locomotive is operating in diesel or hybrid mode, the energy from the electrodynamic braking will be used to power the load of auxiliary systems and power the passenger cars or to charge the batteries.

Basing on the conducted analysis, two approaches can be distinguished to creating locomotives with dual-mode power supply for mainline operation. In the first case, the traction characteristics of the locomotive do not differ much when powered by the contact network and in diesel operation. Such locomotives are oriented for use on routes with predominantly non-electrified sections. In the second case, the power of the locomotive when powered by the contact network significantly exceeds the power when operating on diesel. Such locomotives are operated on routes with a predominant share of electrified sections. However, the power of the diesel is sufficient for movement on main lines. Another option is to use a diesel generator to provide the last mile function. In this case, the power of the diesel generator is sufficient for shunting operations with the train. An example is the TRAXX AC3 locomotive with a capacity of 5600 kW, where a diesel generator with a capacity of 240 kW is used. Thus, the option of a locomotive with dual-mode power supply is determined by the conditions of its operation.

For Ukrainian railways, it is considered as reasonable to use the above mentioned approaches, in which some of the locomotives will be diesel locomotives with the ability to be powered from the contact network, and some will be electric locomotives equipped with a sufficiently powerful diesel generator set or a low-power diesel engine to provide the last mile function. Given that Ukrainian railways are electrified with both alternating and direct current, it will be rational to provide power from these both power supply systems.

Usage of a plug-in energy storage device as part of a hybrid traction system will contribute to reducing costs for fuel and energy resources. This will occur, firstly, as a result of the accumulation of energy during electrodynamic braking and its subsequent use to power the traction system and auxiliary consumers. Secondly, since the plug-in storage device can be charged from a low-cost energy source, in autonomous driving mode, there is a possibility of longer-term power supply with low-cost energy.

Basing on the analysis of the designs of locomotives with dual-mode power supply, the following option for structure of traction system can be proposed (Fig. 10).

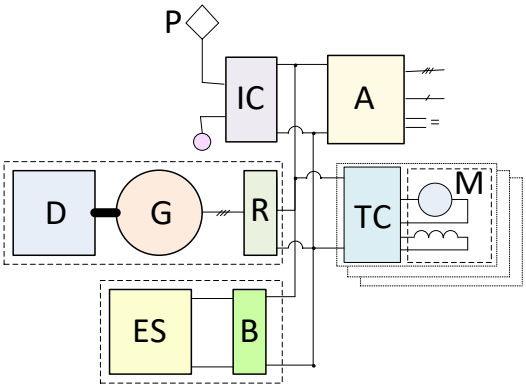

Fig. 10. **Plug-in hybrid traction system diagram using traction collector electric motors**
P – current collector; IC – input converter; A – auxiliary systems power supply; D – diesel;
G – generator; R – rectifier; TC – traction converter; M – traction electric motor;
ES – energy storage; B – matching converter

The scheme shown in Fig. 10 can be applied in the case of using a traction electric drive with AC electric motors. In this case, the traction converters are autonomous voltage inverters that power and control the traction electric motors. In the case of usage of high-voltage traction inverters operating at a voltage of 4000 V, it is reasonable to connect them directly to the contact network. In this case, a pulse voltage regulator is not used. The voltage of the intermediate circuit is chosen to be about 3000…4000 V.

It is foreseeing that a locomotive with a dual-mode power supply should be a freight-passenger one. In this case, single section is used in passenger operation mode, and for hauling of freight trains, locomotives are operated in a system of multiple units. In the case of locomotives application mainly with freight trains, it would be reasonable to create a specialized two-section locomotive.

Conclusions. Currently, the operation of dual-powered locomotives is advisable on routes with combination of electrified and non-electrified sections. The advantages of application of dual-powered locomotives are the reduction of costs by purchasing of such locomotive (one instead of at least two types of locomotives); reduction of travel time due to the elimination of locomotive changes; reduced track use fees, since you can move less on any tracks; reduced costs for diesel fuel, maintenance and repair of a diesel engine; decrease of harmful emissions.

Analysis of the designs of dual-mode locomotives demonstrated that when creating them, typical components from serial locomotives are kept in design. This reduces the cost of designing and manufacturing such locomotives. At the same time, the design of certain components and elements of the locomotive is adapted and optimized for operation from two power sources.

As further evolution of propulsion systems of dual-powered locomotives is the implementation of energy storage devices. This allows you to accumulate energy during electrodynamic braking and use it in traction mode. As a result, the consumption of fuel and energy resources and harmful emissions are reduced. When using a plug-in energy storage device, which can be charged with low-cost energy, the greatest reduction in the cost of fuel and energy resources is achieved.

The creation of a domestic locomotive with dual-mode power supply is possible by modernizing existing locomotives. The proposed generalized diagram of the traction system takes into account the possibility of powering of the locomotive from the AC and DC contact network and provides the application of a plug-in hybrid power plant.

Acknowledgements. The article was prepared as part of the research work “Energy management in plug-in hybrid traction systems of rail rolling stock equipped with a multi-motor traction electric drive”, funded by the Ministry of Education and Science of Ukraine (No. S/r 0125U001619).

REFERENCES

1. Kharchuk, O.H., Kryvenko, O.M. (2017). International railway transport corridors of Ukraine and the role of the «LISKA» UDCTS in their development. *International scientific journal «Internauka», 2, 15(37),* 63-68. [in Ukrainian].
2. Ukrzaliznytsia presents its logistics capabilities at the leading international exhibition Transport logistic 2023 in Munich. [Electronic resource]. Access mode: https://www.uz.gov.ua/press_center/up_to_date_topic/607214/. [in Ukrainian].
3. Temporary changes in the schedule of passenger trains heading to Zakarpattia. [in Ukrainian]. [Electronic resource]. Access mode: https://www.uz.gov.ua/press_center/up_to_date_topic/664282/.
4. Postanova Kabinetu Ministriv Ukrainy vid 27.12.2024 r. №1550 «Pro Natsionalnu transportnu stratehiiu Ukrainy na period do 2030 roku» [Resolution of the Cabinet of Ministers of Ukraine dated December 27, 2024 No. 1550 “On the National Transport Strategy of Ukraine for the period until 2030”]. [in Ukrainian]. [Electronic resource]. Access mode: https://zakon.rada.gov.ua/laws/show/1550-2024-%D0%BF#Text.
5. GE Genesis Locomotive. [Electronic resource]. Access mode: https://web.archive.org/web/20110717194014/http://www.vergarastudio.com/pdf/GE_Genesis_Locomotive.pdf.
6. Dual Mode Locomotive DE 30 AC/DM 30 AC. [Electronic resource]. Access mode: https://img1.wikia.nocookie.net/__cb20150215203135/obts/images/0/02/1998.xBBx~LHxx.AARx_1m435~0022m86_EMDx.DM30.PDF.
7. Elektrische Drehstromlokomotiven aus europäischer Produktion. [Electronic resource]. Access mode: https://www.elektrolokarchiv.de/index.php?nav=1409329&lang=1.
8. CSR Locomotive Report KISS EMU «Radiography». Class ALP-45DP Locomotive InnoTrans Megareport, Part 2. In The Birthplace Of The Gravitas. *Railvolution, Vol. 10, 6/10,* 53-58. [Electronic resource]. Access mode:

https://static1.squarespace.com/static/561e6ed5e4b039248a6a94aa/t/565f6990e4b0860912bcf262/1449093520706/ALP-45DP+Article+Railvolution-2010.pdf.
9. STADLER. Solutions. Rolling Stock. [Electronic resource]. Access mode: https://www.stadlerrail.com/en/solutions/rolling-stock.
10. SIEMENS. Vectron Dual Mode – keeps going where the wire ends. [Electronic resource]. Access mode: https://www.mobility.siemens.com/global/en/portfolio/rolling-stock/locomotives/vectron/dual-mode.html.
11. TD2000. Locomotoras de tracción dual de Euskotren. [Electronic resource]. Access mode: https://www.ingeteam.com/Portals/0/Catalogo/Sector/Documento/PRD_165_Archivo_td2000bb-2.pdf.
12. Gama Dual Power 111 DE. [Electronic resource]. Access mode: https://pesa.pl/en/produkty/lokomotywy/gama-dualpower-111de/.
13. Traxx Shunter locomotives: Modularity and tractive effort. [Electronic resource]. Access mode: https://www.alstom.com/solutions/rolling-stock/locomotives/traxx-shunter-locomotives-modularity-and-tractive-effort.
14. Kinoshita, H., Ogawa, K. (2021). Series Hybrid Locomotive Equipped with Energy-Saving Electrical Equipment for European Market. *Toshiba Review, 76,* 4. [Electronic resource]. Access mode: https://www.global.toshiba/content/dam/toshiba/migration/infrasolution/www/infrastructure/en/railway/assets/pdf/Toshiba%20Review%20(Hybrid%20Locomotive).pdf.
15. Alstom delivers first Traxx Universal DC locomotive with Last Mile to Polo Logistica at Vado Ligure site. [Electronic resource]. Access mode: https://www.alstom.com/press-releases-news/2024/5/alstom-delivers-first-traxx-universal-dc-locomotive-last-mile-polo-logistica-vado-ligure-site.
16. Locomotives for RCH, Hungary. [Electronic resource]. Access mode: https://crrczelc-europe.com/mainline-locomotive-rch-hungary/.
17. Overianova, L., Plyutin, O., Riabov, Ie. (2024, December). Locomotives with dual power supply. In: *2nd International Scientific and Technical Conference "Progressive Technologies of Transport", Kharkiv, December 5-6, 2024: Abstracts of reports. –Kharkiv: UkrDUZT, 17.*
18. ALP-45DP Locomotive Procurement. [Electronic resource]. Access mode: https://stvinc.com/project/alp-45dp-dual-powered-locomotive-procurement/.
19. Canetta, D., Bikle, Dr. U. (2010). ECO4 Superior Products: Dual Powered Locomotives ALP-45DP for the North American Railways. *12th WCTR, July 11-15, 2010 – Lisbon, Portugal.* [Electronic resource]. Access mode: https://www.wctrs-society.com/wp-content/uploads/abstracts/lisbon/selected/02421.pdf.
20. Brugger, P., Schwendt, L., Spillmann, M., & Vitins, J. (2009). Die Zweikraft-Lokomotive ALP45DP – eine Innovation für den amerikanischen Markt. *Schweizer Eisenbanhn-Revue, 11*, 560-563. [Electronic resource]. Access mode: https://documents.epfl.ch/users/a/al/allenbac/www/documents/Fich1109.pdf.
21. Standard AAR S-580. Locomotive Crashworthiness Requirements. Association of American Railroads. (2008).
22. Brade, I., Emde, J., Röpper. M., Schurr, J. (2021). Vectron Dual Mode – keeps going where the wire ends. ZEVrail. *TAGUNGSBAND SFT GRAZ 2021*,145.
23. 3 Jahre Betriebseinsatz EuroDual bei der HVLE. [Electronic resource]. Access mode: https://www.static.tu.berlin/fileadmin/www/10002264/ews/2023_wise/2023-10-16-folien.pdf.
24. Stadler - Locomotive bi-mode Euro Dual. [Electronic resource]. Access mode: https://mediarail.be/Materiel_roulant/Bi-mode/Stadler%20Euro%20Dual/Euro%20Dual_01.htm.
25. STADLER. Eurodual Battery Hybrid Locomotive. [Electronic resource]. Access mode: https://a.storyblok.com/f/269997/x/6c89da103d/eurodual_en.pdf.
26. The future of UK traction arrives. [Electronic resource]. Access mode: https://www.therailwayhub.co.uk/68192/the-future-of-uk-traction-arrives/.

Євген Рябов[1*], Лілія Овер'янова[2], Лілія Кондратьєва[3], Олександр Плютін[4], Артем Овер'янов[5]

[1] Доцент, Кафедра електричного транспорту та тепловозобудування, Національний технічний університет «Харківський політехнічний інститут», вул. Кирпичова, 2, м. Харків, 61002, Україна. ORCID: https://orcid.org/0000-0003-0753-514X.

[2] Доцент, Кафедра електричного транспорту та тепловозобудування, Національний технічний університет «Харківський політехнічний інститут», вул. Кирпичова, 2, м. Харків, 61002, Україна. ORCID: https://orcid.org/0000-0002-4827-572X.

[3] Аспірантка, Кафедра електричного транспорту та тепловозобудування, Національний технічний університет «Харківський політехнічний інститут», вул. Кирпичова, 2, м. Харків, 61002, Україна. ORCID: https://orcid.org/0000-0002-2788-9116.

[4] Аспірант, Кафедра електричного транспорту та тепловозобудування, Національний технічний університет «Харківський політехнічний інститут», вул. Кирпичова, 2, м. Харків, 61002, Україна. ORCID: https://orcid.org/0009-0009-5199-4344.

[5] Національний технічний університет «Харківський політехнічний інститут», вул. Кирпичова, 2, м. Харків, 61002, Україна. ORCID: https://orcid.org/0009-0003-7367-2203.

***Автор,відповідальний за листування**: riabov.ievgen@gmail.com.

Локомотиви з дворежимним живленням для магістральних маршрутів

Розвиток залізничного транспорту України пов'язаний з удосконаленням перевезень маршрутами пан'європейських транспортних коридорів, покращенням залізничного сполучення з країнами Євросоюзу та внутрішніми перевезеннями. Це потребує оновлення тягового рухомого складу, поточний технічний стан якого не відповідає сучасним показникам паливної ефективності та екологічності. Аналіз тягового рухомого складу світових виробників показує зацікавленість залізничних операторів у локомотивах з дворежимним живленням. Такі локомотиви можуть отримувати живлення від контактної мережі та дизель-генератора. Це надає ряд переваг, ключовими серед яких є зниження вартості та тривалості перевезень. Розглянуто конструкції локомотивів ALP-45DP виробництва Bombardier Transportation, Vectron Dual Mode виробництва Siemens Mobility, EURODUAL та Class 93 виробництва Stadler. Показано, що локомотиви з дворежимним живленням базуються на конструкції і вузлах серійних локомотивів. Це зменшує вартість досліджуваних локомотивів, спрощує обслуговування та забезпечує високі показники надійності. Водночас наявність дворежимного живлення вплинула на використання специфічних конструктивних і схемотехнічних рішень. Перспективними для застосування на локомотивах з дворежимним живленням є системи накопичення енергії, у тому числі plug-in накопичувачі. Використання накопичувачів дозволяє як акумулювати енергію при гальмуванні і живити системи локомотиву, так і запасати енергію від джерел з низькою вартістю. Це зменшує вартість паливно-енергетичних ресурсів. На основі проведеного аналізу запропоновано і обґрунтовано структуру тягової системи для вітчизняного локомотиву з дворежимним живленням, який може бути створений шляхом модернізації наявних локомотивів.

***Ключові слова**: локомотив, тяговий рухомий склад, дизель, накопичувач енергії, plug-in гібридна енергетична установка, тягова система.*

DOI: 10.32703/2617-9040-2025-45-5

UDC 656.1

Fuad Dashdamirov[1*], Turan Verdiyev[2]

[1]Associate professor, Director of the Institute of Logistics and Transport, Azerbaijan Technical University, pr. H. Javid 25, Baku, Azerbaijan, AZ 1148. ORCİD: https://orcid.org/0000-0003-3781-3542.

[2]Doctoral student, research fellow at the Institute of Logistics and Transport, Azerbaijan Technical University, pr. H. Javid 25, Baku, Azerbaijan, AZ 1148. ORCİD: https://orcid.org/0000-0002-9520-5038.

*Corresponding author: dr.fuad@mail.ru

Study of the ınfluence of coordınated regulatıon on the traffıc flow parameters on ıntersectıng streets

The article studies the nature of changes in traffic flow parameters on the intersecting streets when using coordinated regulation to organize uninterrupted traffic on city highways. The influence of the "green wave" mode on the traffic flow parameters is analyzed. Traffic delays on intersecting streets were compared before and after the implementation of coordinated regulation. Traffic delay values at intersections were determined and analyzed in a comparative manner using the Webster and HCM 2010 methodology and simulation tests. Measurements were carried out based on real values (speed and traffic intensity on sections) taken at 7 intersections of the street network of the city of Baku. For simulation tests, a coordinated regulation model built in the PTV VISSIM program was used. Using the created micromodel, the results of the impact of the implementation of coordinated regulation on traffic delays on main and intersecting streets were tested. The total time losses on the street where the "green wave" is implemented and on intersecting streets were estimated for the options before and after the coordination of traffic light modes. Based on the values determined by all three methods, it was found that after the implementation of coordinated regulation on the main street the delay time of vehicles increases on intersecting streets. The proposed approach can help to evaluate the effectiveness of coordinated regulation in terms of time losses before its implementation on city streets.

Keywords: *coordinated regulation, traffic flow, traffic parameters, delay, intersection, modeling, PTV VISSIM*

Introduction. Traffic jams and delays on city roads are considered the main problems of urban transport infrastructure. The rapid growth in the number of vehicles requires the implementation of various regulatory and organizational measures in cities. Before moving on to constructive solutions, experts often try to solve the problem by optimizing the organization of traffic. One of such solutions is coordinated regulation ("green wave"), which is introduced to ensure the smooth movement of traffic flows on the main streets of the city. In most large cities in the world, this regulation regime has been adopted as one of the main solution tools and is widely used. However, experience shows that the very organization of such regulation is associated with certain problems.

The main consequences that may arise as a result of the introduction of coordinated regulation on the streets include:

- a large loss of time for pedestrians when crossing the road;
- difficulties for cyclists in areas with high speed;

- increased harm to the environment as a result of increased speed and increased emissions;
- increased exhaust emissions due to delays when making a left turn from the opposite side;
- inefficiency for public transport (especially buses) moving in mixed traffic;
- difficulty adapting to changing conditions due to traffic speed and other parameters;
- inefficiency for traffic on an intersecting street at low traffic volumes on the main road;
- reduced opportunities to ensure safety due to reduced driver attention;
- reduced opportunities to ensure the movement of emergency vehicles;
- increased delay time in intersecting directions;
- inefficiency of time saved on movement on the street due to long delays at the last traffic light;
- efficiency only for streets with certain geometric parameters;
- negative impact on the stimulation of mobility solutions that improve the quality of life, such as walking and cycling.

As can be seen, there are certain negative consequences of coordinated regulation on city streets. However, special attention should be paid to delays and congestion caused by traffic flows on intersecting streets.

Analysis recent research and problem statement. Traffic signal coordination on streets is implemented to improve mobility. Lee and Tarko [1] note that this mobility solution does not include safety measures. In their study, the authors used a logarithmic model of short-term crash probability to examine the impact of coordinated traffic flow on highways on side and rear-end collisions. The studies showed that traffic signal coordination has a significant impact on crashes. Reducing the distances between intersections reduces the number of crashes, and a separate right-turn lane reduces the risk of crashes. Yue et al. analyzed the impact of traffic signal coordination on road safety using a model implemented in the PTV VISSIm program [2]. The authors analyzed the number of traffic conflicts on three Nevada highways under different traffic intensities. The studies showed that the introduction of a "green wave" for unsaturated traffic flows can reduce the number of conflicts. However, no significant differences in the number of conflicts are observed in saturated flows. A study of 121 intersections in Ohio assessed the relationship between traffic signal performance (percentage of green signals) and safety using vehicle trajectory data. It was found that a one percent increase in the number of people driving on green lights reduced the number of crashes by 1.12% [3].

An analysis and evaluation of busy signalized intersections in Baghdad was conducted using Synchro 9. The author estimated the reduction in delays on major streets and queues at intersections in front of traffic signals when using coordinated regulation [4].

There is experience in using modeling programs such as Aimsun, SUMO, Paramics and others to analyze, evaluate and optimize traffic management at intersections and streets [5, 6, 7]. Using Anylogic software, it is possible to analyze, evaluate and improve traffic management at intersections of various configurations [8, 9, 10].

Bencat and Janota consider it appropriate to use a hybrid and multi-method approach, given the complexity of the systems being modeled. The Anylogic environment is considered as such a modeling environment. The authors compare the delay time for existing and designed options based on the values of traffic flow intensity taken from the intersection [11].

In the work of Sutanhaya and Putra, a microsimulation approach was applied using VISSIM software. The T-test was used to test the validity of the simulation. The objective of the study is to improve the efficiency of intersections by coordinating traffic lights. In the simulation tests, it was found that after the implementation of coordinated scheduling, the queue length was reduced by 18.52%, delays by 21.41%, and fuel consumption by 5.15% [12].

In their study, Rida and Hasbi propose an algorithm for wireless network architecture that operates according to changing traffic patterns to reduce queues at intersections, create a green wave system and prioritize traffic on low-traffic streets. The authors use SUMO to model the traffic flow [13].

Delays are considered as one of the key metrics in assessing the service level at a signalized intersection. Kumar et al. compared the delays predicted using the HCM2000 methodology at an intersection with the delays predicted theoretically and found that there was no good correlation between the observed and predicted values. Therefore, the authors recommend using the site-based values to measure the service level [14].

There are a number of studies devoted to assessing vehicle delays at signalized intersections. For example, Huang et al. simplified the analytical formula for the case of uniform vehicle arrival distribution and obtained a linear relationship between time and vehicle location [15]. Ramesh and Molugaram proposed an alternative planning method that takes into account parameters such as delay, queue length, and service level at 4 major intersections in Hyderabad city [16]. In a study that measured traffic delays and service levels at each of three intersections in Ilorin, the average delay time at the intersections was determined and modifications to taxi and bus stop locations and parking areas were suggested [17].

Working on a dynamic car equivalent model to optimize delays for heterogeneous traffic flows at a signalized intersection, Roy et al. found that turning vehicles required more space and took longer [18].

As can be seen, the issue of assessing traffic flow parameters, especially delays, on streets intersecting with signalized streets has been understudied.

The purpose and objectives of the study. The main objective of the study is to analyze changes in traffic flow delays on intersecting streets by assessing and analyzing them using various methods when implementing coordinated traffic flow regulation on streets and avenues in order to ensure uninterrupted traffic flow, as well as determining time losses on main and intersecting streets in order to assess the effectiveness of the regulation regime. For this purpose, traffic flow delays at entrances to the main street and intersecting streets on the selected main street of the city were assessed and compared, and a methodology for assessing time losses of vehicles and traffic flow as a whole on the section under consideration was developed.

Materials and methods of research. The main parameters of traffic flows are the speed of traffic flow, hourly traffic intensity and traffic density. The following relationship exists between these three parameters [19]

$$q = kv, \tag{1}$$

where q - traffic intensity, veh/hour;

v - speed, km/hour;

k - is density, veh/km.

The traffic flow parameters under consideration are significantly affected by traffic control on the street, especially delays at controlled intersections. The speed of traffic is reduced due to delays at the entrances to intersections. Since the traffic intensity is generally constant, the traffic density increases.

At intersections controlled by traffic lights, the delay time according to the traditional Webster model is calculated based on the operating mode of the traffic light as follows [20]

$$d = \frac{c(1-\lambda)^2}{2(1-\lambda x)} + \frac{x^2}{2q(1-x)} - 0.65\left(\frac{c}{q^2}\right)^{1/3} x^{2+5\lambda}, \tag{2}$$

where d - is the average delay time of one vehicle at each entrance, s;

c - is the cycle length, s;

q - is the traffic flow, veh/h;

λ - is the share of the green cycle in the overall phase, %;
x - is the saturation factor (the ratio of intensity to capacity).

In the formula, the first term is the average delay of vehicles arriving in different distributions, the second term is the delay due to the randomness of vehicles, and the third term is the correction term, the amount included in the model to take into account specific road conditions.

Modified forms of Webster's model have also been used in various studies. [21, 22].

According to the HCM 2010 methodology, the average delay time of each vehicle at intersections controlled by traffic lights is determined as follows [23]

$$d = d_{un} + d_{ovs} + d_{leave}, \tag{3}$$

where d_{un} - is the delays of vehicles arriving with uniform distribution and is determined as follows

$$d_{un} = \frac{0.5C(1-\frac{g}{C})^2}{(1-\frac{g}{C}X)} \frac{(1-P)f_p}{1-\frac{g}{C}}, \tag{4}$$

where X - the ratio of traffic volume and capacity;
C - cycle length, s;
g - is the duration of the green light, s;
f_p - is progression adjusment factor;
d_{ovs} - is the delay under congested traffic conditions and is determined as follows

$$d_{ovs} = 900T\left[(X-1) + \sqrt{(X-1)^2 + \frac{8KIX}{T_c}}\right], \tag{5}$$

where T - is the assesment period;
K - is increment delay factor 0.4-0.5 (0.5 for fixed-time signals for the M/D/1 queuing system);
I - is upstream filtering adjusment factor (1 for an isolated intersection).
d_{lea} - is the delays occurring when leaving the queue before the intersection and is determined as follows

$$d_{leave} = \frac{3600Q_b}{c} - 1800T(1-X), \tag{6}$$

where c - is capacity of intersection aproach, veh/h;
Q_b - is the queue length at the beginning of assesment period, veh.

As an alternative to analytical methods for calculating traffic delays, it is possible to propose determination by means of simulation models using computer programs. Simulation models allow one to evaluate the effectiveness of serious design and organizational measures on streets and roads before their implementation. In addition, using these models, one can successfully test various options for improving traffic organization. The fastest and most cost-effective solution to reduce traffic delays is to improve the performance of traffic lights at intersections. The various simulation programs used for

simulating traffic flows, such as SUMO, Aimsun, CORSİM, Paramics, SimTraffic, PTV Vissim, differ somewhat in their functionality [24]. It is noted that PTV Vissim is increasingly used as a modeling tool in studies related to the analysis, evaluation and improvement of traffic flows [25]. PTV Vissim is more suitable for implementing the verification of various solutions, since it has more necessary functions.

Primary data were obtained by live observation on Bakikhanov Street, one of the main transport arteries of Baku, where the coordinated traffic light mode is implemented. In real life, there are serious queues and delays on intersecting streets. For example, in Figure 1 is shown a satellite image of one of the Bakikhanov Street intersections.

Fig. 1. **Satellite image of one of the Bakikhanov Street intersections.**

In Figure 2 is shown a traffic organization scheme on Bakikhanov Street in Baku.

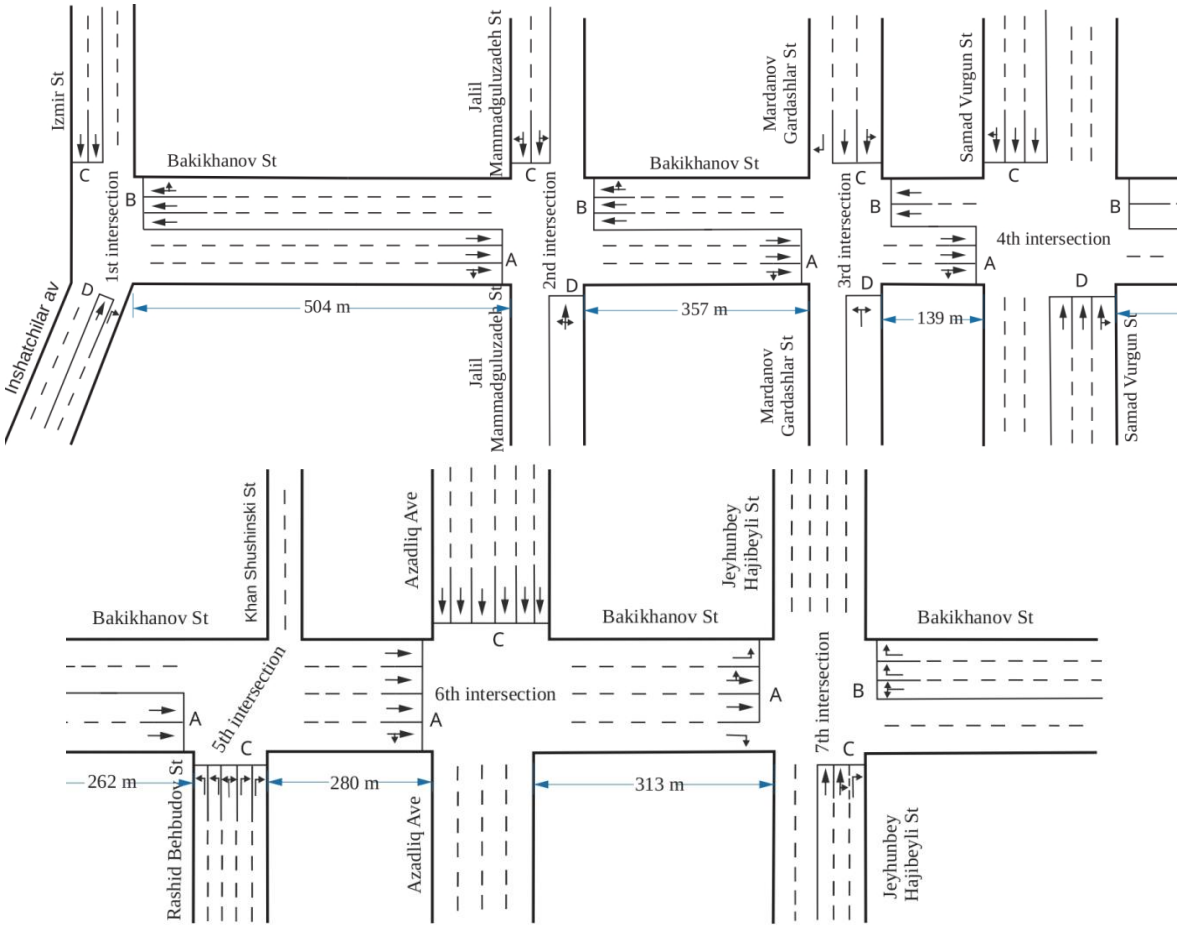

Fig. 2. **Traffic management scheme on Bakikhanov Street with traffic directions indicated**

Table 1 shows the actual traffic intensities in the directions at intersections.

Table 1. **Traffic intensity values by directions at intersections**

At the 1st intersection		At the 2nd intersection		At the 3rd intersection		At the 4th intersection		At the 5th intersection	At the 6th intersection	At the 7th intersection	
Traffic intensity, veh/h											
B		A	B	A	B	A	B	A	A	A	B
2473		2308	1958	2082	776	2230	744	2100	3215	2774	788
C	D	C	D	C	D	C	D	C	C	C	
655	1007	542	256	1684	198	1166	1010	1415	1850	666	

There are seven intersections on Bakikhanov Street where traffic light control is used. These are intersections with Izmir, Rashid Behbudov, Jeyhun Hajibeyli, Jalil Mammadguluzade, Mardanov Gardashlari, Samad Vurgun streets and with Azadlig Avenue. The cycles of traffic lights are adjusted along the street to coordinate the work of traffic lights. The estimated duration of the cycle is 120 seconds. A micromodel was created in the PTV VISSIM software to test the movement of the traffic flow and to determine vehicle delays. The coordinated traffic control schedule on Bakikhanov Street in Baku, constructed in the program in accordance with the actual traffic light operation mode, for direction A (from Izmir Street to J. Hadzhibekov) is shown in Figure 3.

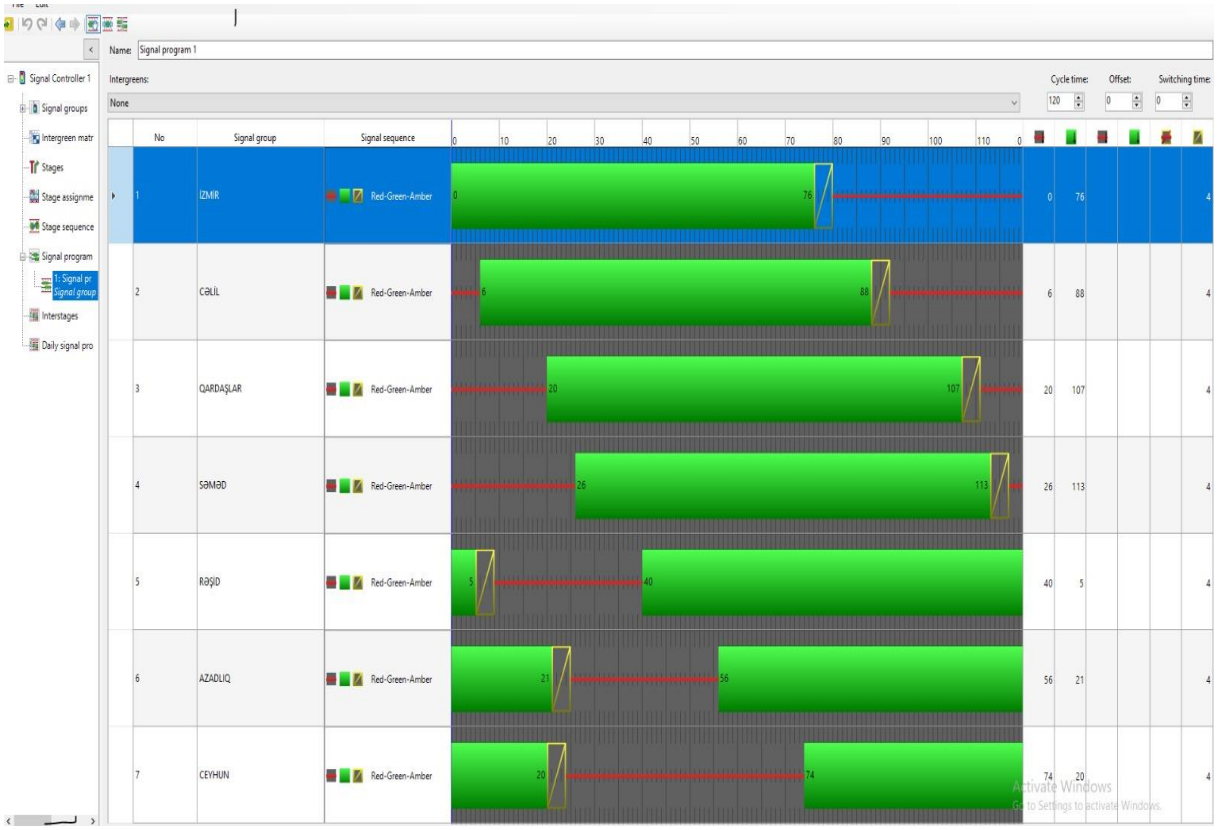

Fig. 3. **Coordinated traffic control schedule on Bakikhanov Street in Baku**

In the Figure 4 is shown queues at intersected direction at the four intersections (1th intersection with Izmir avenue, 5th intersection with R. Behbudov street, 6th intersection with Azadliq avenue, 7th

intersection with Jeyhun Hajibeyli street) in results of testing of micromodel of traffic, built using the PTV VISSIM program the implementation of coordinated traffic on main street.

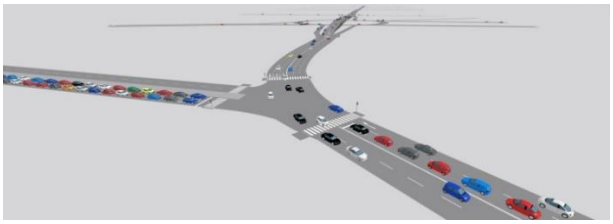

1th intersection with Izmir avenue

5th intersection with R.Behbudov street

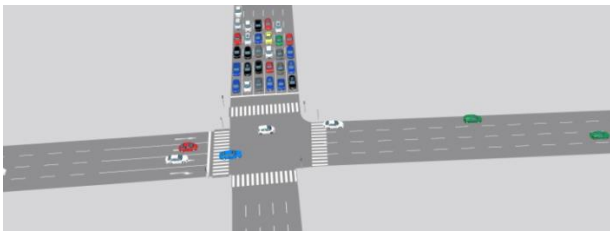

6th intersection with Azadliq avenue

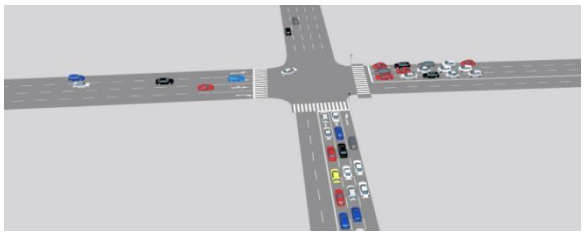

7th intersection with Jeyhun Hajibeyli

Fig. 4. **Queue at intersected direction in results of testing of micromodel (3D)**

As can be seen from Figure 4, the results obtained from simulation experiments on streets intersecting with Bakikhanov Street also show that queues are formed in front of traffic lights on the intersecting streets. Therefore, it is necessary to calculate isolated traffic light operation modes based on the actual traffic flow intensities at all intersections and compare the obtained values using the proposed methods.

By applying the proposed simulation model, it is possible to compare the obtained delay time values with those obtained from analytical reports and determine the conditions for the effectiveness of the green wave on the main street in terms of time losses. Based on the above formulas and simulation experiments, a mathematical model was created to determine the total time losses on the street section where coordinated traffic control is applied. Thus, in general, the delay time of entering intersections where coordinated traffic control is applied can be determined as follows in accordance with the Webster and HCM 2010 methodology

$$\sum d = \sum_{j}^{m} \sum_{i=1}^{n} N_{vi} d_i \,, \tag{7}$$

where d_i - is the vehicle delay time at the stop line i;

N_{vi} - is the number of vehicles at the stop line i.

The delay time obtained using the model created with PTV VISSIM will be determined as follows:

$$\sum d = \sum_{j}^{m} \sum_{i=1}^{n} D_i \,, \tag{8}$$

where D_i - is the delay time of all vehicles at the stop line i.

Discussion. The values of delays at the entrances to the intersections of the main and intersecting streets as a result of tests conducted using the model, as well as those calculated using the Webster and

HCM 2010 methodologies before and after the implementation of coordinated regulation at the intersections are given in Table 2 and Table 3.

Table 2. **Values of delay time on the main street**

	At the 1st intersection	At the 2nd intersection		At the 3rd intersection		At the 4th intersection		At the 5th intersection	At the 6th intersection	At the 7th intersection	
	Delay time per vehicle before the implementation of coordinated regulation, sec										
	B	A	B	A	B	A	B	A	A	A	B
Webster	15.3	13.5	12.8	9.8	10.8	9.7	8.4	11.3	7.2	15.9	31.9
HCM 2010	14.7	12.6	13.2	11.1	9.9	9.7	8.4	10.1	8.1	15.6	37.8
PTV VISSIM	15.8	14.4	12.2	17.3	10.3	10.7	10.7	12.5	9.3	14.9	42.8
	Delay time per vehicle after the implementation of coordinated regulation, sec										
	B	A	B	A	B	A	B	A	A	A	B
Webster	9.9	9.5	9.9	6.9	6.4	7.0	7.3	7.6	6.7	14.9	35.0
HCM 2010	10.1	7.1	7.5	5.7	4.9	6.0	4.9	8.0	7.8	14.7	38.9
PTV VISSIM	12.5	8.7	7.8	11.7	5.1	8.3	4.9	8.2	7.9	14.1	46.7

Table 3. **Values of delay time on intersecting streets**

	At the 1st intersection		At the 2nd intersection		At the 3rd intersection		At the 4th intersection		At the 5th intersection	At the 6th intersection	At the 7th intersection
	Delay time per vehicle before the implementation of coordinated regulation, sec										
	C	D	C	D	C	D	C	D	C	C	C
Webster	24.7	24.3	19.5	19.9	12.4	11.9	13.8	13.9	23.4	14.1	33.3
HCM 2010	16.1	16.9	19.5	19.2	12.1	12.5	13.9	13.9	24.3	14.6	32.9
PTV VISSIM	18.7	13.1	19.3	20.9	17	10.7	16.8	17	24.6	18.6	34.2
	Delay time per vehicle after the application of coordinated regulation, sec										
	C	D	C	D	C	D	C	D	C	C	C
Webster	28.7	27.9	28.5	28.2	22.5	22.9	23.3	20.3	27.3	17.3	31.8
HCM 2010	22.2	21.1	28.9	28.6	24.9	26.4	24.9	24.8	34.7	28.6	39.7
PTV VISSIM	26.7	18.7	24.3	30.1	31.0	27.6	24.8	27.7	33.5	29.5	42.9

As can be seen from Table 2, the results obtained when calculating traffic delays on the main street using different methods do not differ significantly. However, after the implementation of coordinated regulation on the main street, a decrease in delays was noted. Only at the seventh intersection in the direction B (intersection with J. Hajibeyli), or more precisely at the entrance to Bakikhanov Street, an increase in delays is observed. This is due to the start of the coordinated mode.

Based on the data in Table 3, it can be said that after the implementation of coordinated regulation on intersecting streets with the main street, the average delay time per vehicle increases when calculating using all three methodologies. This increase is felt even more strongly with the growth of the intensity of vehicle traffic in these directions. Delays on intersecting streets are more pronounced at intersections with high intensity and density of traffic. For example, for the sixth intersection in the direction C, the delays per one vehicle, calculated by the Webster, HCM 2010 methodologies and obtained from the simulation experiment in PTV VISSIM for the isolated mode are 14.1, 14.6 and 18.6 seconds,

respectively. But after implementation the coordinated regulation, the delays increase to 17.3, 28.6 and 29.5 seconds, respectively. This is approximately twice as much as the values obtained from the isolated mode of operation.

Using formulas (7) and (8) the results of calculating the total traffic delays on the main highway and intersecting streets, based on the values of Tables 2 and 3, as well as on the values of traffic intensity at intersections, are shown in Table 4.

Table 4. **Total delay time at intersections before and after the implementation of coordinated regulation**

	Total delay time, hour		
	with Webster methodology	with HCM2010 methodology	with simulation tests
Before the implementation of coordinated regulation	127,2	124,92	139,9
After the implementation of coordinated regulation	128,9	136.25	149,36

As can be seen from Table 4, the total time losses of vehicles when traveling along the main and intersecting streets did not decrease when comparing the variant where isolated regulation was used at intersections with the variant where coordinated regulation was used on the main street. The results obtained during the simulation experiments for considered case show that this time even increases by about 10 hours. From this, it can be concluded that when implementing coordinated regulation on main streets, it is necessary to take into account not only the time losses on this street, but also the time losses on intersecting streets. In this regard, the proposed methodology can be used for verification of effectiveness of coordinated regulation.

Conclusion. In order to reduce vehicle delays on city streets, a coordinated traffic light control mode ("green wave") organizes. Despite its high efficiency on main streets, this solution has certain drawbacks. One of these drawbacks is an increase in traffic delays on intersecting streets.

The calculated values of the delay time using different methods for real traffic light operation modes on streets intersecting with the main street, where coordinated control was used, show that the use of such a mode increases the average delay time on intersecting streets, and in some cases the total delay time on the main and intersecting streets. Therefore, when implementing the "green wave", it is necessary to analyze and verify the total time losses at street intersections using a simulation experiment.

REFERENCES

1. Li, W., & Tarko, A. P. (2011). Effect of arterial signal coordination on safety. *Transportation research record*, *2237*(1), 51-59. https://doi.org/10.3141/2237-06.
2. Yue, R., Yang, G., Zheng, Y., Tian, Y., & Tian, Z. (2022). Effects of traffic signal coordination on the safety performance of urban arterials. *Computational Urban Science*, *2*(1), 3. https://doi.org/10.1007/s43762-021-00029-4.
3. Kabir, R., Remias, S. M., Lavrenz, S. M., & Waddell, J. (2021). Assessing the impact of traffic signal performance on crash frequency for signalized intersections along urban arterials: A random parameter modeling approach. *Accident Analysis & Prevention*, *149*, 105868. https://doi.org/10.1016/j.aap.2020.105868.
4. Abdulstaar, Z.A. (2023). Effect of Signal Coordination on The Traffic Operation of Urban Corridor. *Tikrit Journal of Engineering Sciences*, *30*(1),12-24. https://doi.org/10.25130/tjes.30.1.2.
5. Fabian, P., Čulík, K., Kalašová, A., & Černický, Ľ. (2024). The Impact of Road Realignment on the Traffic Load in the Surrounding Area. *Vehicles*, *6*(4), 1942-1962. https://doi.org/10.3390/vehicles6040095.
6. Yu, C., Chen, J., & Xia, G. (2022). Coordinated control of intelligent fuzzy traffic signal based on edge computing distribution. *Sensors*, *22*(16), 5953. https://doi.org/10.3390/s22165953.
7. Rida N., Ouadoud, M., &Hasbi, A. (2020). Coordinated Signal Control System in Urban Road Network. *İnternational journal of Online and biomedical Engineering*, *16*(10), 1-19. https://doi.org/10.3991/ijoe.v16i10.15473.

8. Liu, Y., & Song, Y. (2022). Research on simulation and optimization of road traffic flow based on Anylogic. In *E3S Web of Conferences* (Vol. 360, p. 01070). EDP Sciences. https://doi.org/10.1051/e3sconf/202236001070.
9. Kazmi, S. M. M., Sun, X., Yu, H., Pettersen, J. A., & Thordarson, D. S. (2022). *Proceeding of the 32nd conference of fruct association*. (p. 369-365). https://fruct.org/publications/volume-32/acm32/.
10. Dashdamirov, F., Aliyev, A., Verdiyev, T., & Javadli, U. (2023, June). Improving Intersection Traffic Management Solutions by Means of Simulation: Case Study. In *Recent Developments and the New Directions of Research, Foundations, and Applications: Selected Papers of the 8th World Conference on Soft Computing, February 03–05, 2022, Baku, Azerbaijan, Vol. II* (pp. 279-286). Cham: Springer Nature Switzerland. https://doi.org/10.1007/978-3-031-23476-7_25.
11. Benčat, G., & Janota, A. (2020). Road traffic modelling based on the hybrid modelling tool AnyLogic. *Journal of civil engineering and transport,* 2(2), 73-89. https://doi.org/10.24136/tren.2020.006.
12. Suthanaya, P. A., & Putra, R. (2023). Traffic signal coordination based on VISSIM software (case study of Sudirman road in Denpasar city, Indonesia). In *E3S Web of Conferences* (Vol. 445, p. 01004). EDP Sciences. https://doi.org/10.1051/e3sconf/202344501004.
13. Rida, N., & Hasbi, A. (2022). A collaborative road traffic regulation approach using a wireless sensor network. *International Journal of Service Science, Management, Engineering, and Technology (IJSSMET)*, *13*(1), 1-19. https://doi.org/10.4018/IJSSMET.290330.
14. Kumar, R. P., & Dhinakaran, G. (2012). Estimation of delay at signalized intersections for mixed traffic conditions of a developing country. *International journal of civil engineering*, *11*(1). 53-59. http://ijce.iust.ac.ir/article-1-595-en.html.
15. Huang, J., Li, G., Wang, Q., & Yu, H. (2013, November). Real time delay estimation for signalized intersection using transit vehicle positioning data. In *2013 13th International Conference on ITS Telecommunications (ITST)* (pp. 216-221). IEEE. https://doi.org/10.1109/ITST.2013.6685548.
16. Ramesh, A., & Molugaram, K. (2018). Evaluation of delay characteristics at signalized intersections for improvement in level of service. *International journal for traffic and transport engineering*, *8*(3), 309-319. http://dx.doi.org/10.7708/ijtte.2018.8(3).05.
17. Wasiu, J., Owolabi, A., & Popoola, O. (2015). Determination of Traffic Delay at Selected Intersection within Ilorin Metropolis. *American Journal of Engineering Research (AJER)*, *4*(9), 176-180.
18. Roy, B., Suma, S. A., Hadiuzzaman, M. D., Barua, S., & Mashrur, S. K. (2021). Optimization of Delay Time at Signalized Intersections Using Direction-Wise Dynamic PCE Value. *International Journal of Transportation Engineering*, *8*(3), 279-298. https://doi.org/10.22119/ijte.2020.225672.1514.
19. Knoop, V. L. (2021). *Traffic Flow Theory: An Introduction with Exercises*. TU Delft OPEN Publishing. https://doi.org/10.5074/t.2021.002.
20. Webster, F.V. (1958). *Traffic Signal Settings. Department of Scientific and Industrial Research, Road Research Technical Paper No. 39*. Her Majesty's Stationary Office, London, England. https://trid.trb.org/View/113579.
21. Hoque, S., & Imran, A. (2007). Modification of Webster's delay formula under non-lane based heterogeneous road traffic condition. *Journal of Civil Engineering*, *35*(2), 81-92.
22. Raval, N. G., & Gundaliya, P. J. (2012). Modification of Webster's delay formula using modified saturation flow model for non-lane based heterogeneous traffic condition. *Highway Research Journal*, *5*(1), 41-48.
23. Manual, H. C. (2000). Highway capacity manual. *Washington, DC*, *2*(1), 26-27. https://onlinepubs.trb.org/Onlinepubs/trnews/rpo/rpo.trn129.pdf.
24. Akkaya, S., & Engin, T. (2022). Traffic simulation software overview. *Akıllı Ulaşım Sistemleri ve Uygulamaları Dergisi*, *5*(2), 157-168. https://doi.org/10.51513/jitsa.1090209. [in Turkish].
25. Qadri, S. S. S. M., Gökçe, M. A., & Öner, E. (2020). State-of-art review of traffic signal control methods: challenges and opportunities. *European transport research review*, *12*, 1-23. https://doi.org/10.1186/s12544-020-00439-1.

Фуад Дашдамірov[1], Туран Вердієв[2]

[1]Доцент, директор Інституту Логістики та Транспорту, Азербайджанський Технічний Університет, пр. Г. Джавід, 25, Баку, Азербайджан, AZ 1148. ORCİD: https://orcid.org/0000-0003-3781-3542.

[2]Докторант, науковий співробітник Інституту Логістики та Транспорту, Азербайджанський Технічний Університет, пр. Г. Джавід, 25, Баку, Азербайджан, AZ 1148. ORCİD: https://orcid.org/0000-0002-9520-5038.

Вивчення впливу координованого регулювання на параметри транспортного потоку на вулицях, що перетинаються.

У статті досліджується характер зміни параметрів транспортних потоків на вулицях, що перетинаються, при застосуванні узгодженого регулювання для організації безперебійного руху на міських магістралях. Проаналізовано вплив режиму "Зеленої хвилі" на параметри руху транспортних потоків. Затримки транспортного потоку на вулицях, що перетинаються, порівнювалися до і після впровадження узгодженого регулювання. Значення затримки руху на перехрестях визначалися та аналізувалися порівняно з використанням методології Webster та HCM 2010 та імітаційних тестів. Вимірювання проводилися на основі реальних значень (швидкості та інтенсивності руху на ділянках), взятих на 7 перехрестях вуличної мережі міста Баку. Для імітаційних випробувань використовувалася модель координованого регулювання, побудована у програмі PTV VISSIM. За допомогою створеної мікромоделі перевірено результати впливу впровадження узгодженого регулювання на затримки руху на основних вулицях, що перетинаються. Оцінено сумарні втрати часу на вулиці, де реалізується «зелена хвиля», і на вулицях, що перетинаються, для варіантів до і після узгодження режимів роботи світлофорів. На підставі значень, визначених за всіма трьома методиками, встановлено, що впровадження узгодженого регулювання на вулиці, що розглядається, дозволило скоротити загальні втрати часу. Однак на вулицях, що перетинаються, збільшується час затримок транспортних засобів. Запропонований підхід може допомогти оцінити ефективність координованого регулювання з погляду втрат часу до його впровадження на міських вулицях.

Ключові слова: координоване регулювання, транспортний потік, параметри руху, затримка, перехрестя, моделювання, PTV VISSIM

DOI: 10.32703/2617-9040-2025-45-6

UDC 004.925.5

Oleksandr Gertsiy[1], Serhii Karnatov[2], Vitaliy Gladish[3], Valentyna Tkachenko[4]

[1]Assistant professor, Automation and Computer-Integrated Transport Technologies Department, National Transport University, M. Omelyanovicha-Pavlenko St., 1, Kyiv, 01010, Ukraine. ORCID: https://orcid.org/0000-0002-8634-5880.

[2]Postgraduate student, Automation and Computer-Integrated Transport Technologies Department, National Transport University, M. Omelyanovicha-Pavlenko St., 1, Kyiv, 01010, Ukraine. ORCID: https://orcid.org/0009-0006-6254-6166.

[3]Postgraduate student, Automation and Computer-Integrated Transport Technologies Department, National Transport University, M. Omelyanovicha-Pavlenko St., 1, Kyiv, 01010, Ukraine. ORCID: https://orcid.org/0009-0003-5801-056X.

[4]Assistant professor, Associate Professor, Department of Transport Law and Logistics, National Transport University, 2, Mykhailo Omelyanovich-Pavlenko str, Kyiv, 01010, Ukraine. ORCID: https://orcid.org/0000-0001-5147-0772.

Corresponding author: gertsiy_oa@gsuite.duit.edu.ua.

Modeling an Image Clustering Algorithm For Detecting Overheated Railway Axle

This paper presents an approach to image identification based on a clustering algorithm for detecting the thermal characteristics of railway axle boxes. The study analyzes the potential of clustering algorithms in the task of digital image identification. The principles of the proposed algorithm are described in the context of image segmentation and compression, as well as pattern recognition in the transportation domain. A block diagram of the algorithm is provided along with an explanation of its operational principles. A scheme for implementing a machine vision system using the proposed algorithm is suggested for the detection of overheated axle boxes in railway transport. Experimental modeling was conducted for image segmentation based on color models in the infrared spectrum to identify regions with elevated temperatures in the MATLAB environment. For the experiment, thermal images of rolling stock axle boxes were selected one representing a normal condition and the other representing an overheated condition. The simulation results demonstrated that segmentation based on image color models allows for accurate delineation of the thermal characteristics of axle box images. The study confirmed that the use of the proposed algorithm and its software implementation for thermographic cameras is effective for recognizing temperature indicators. Additionally, the algorithm enables image compression, which increases data processing speed and facilitates the monitoring of thermal characteristics of rolling stock at high speeds.

Keywords: *thermographic images, clustering, segmentation, monitoring, modeling, temperature indicators, axle box.*

Introduction. Currently, the field of graphical image identification has gained significant popularity among researchers and scientists. This is due to the growing number of practical applications of such tasks in everyday human activity. Examples include text recognition, fingerprint identification, license plate detection, facial recognition, and more. An important factor contributing to the popularity of image identification is the continuous development of theoretical and mathematical frameworks [1]. Among the key approaches for solving recognition problems are: classification using decision functions and distance metrics; support vector machines; neural networks; various statistical methods; and clustering algorithms.

In computer science, cluster analysis can be used to detect boundaries or recognize objects by dividing a digital image into distinct regions [2].

In the transportation sector, cluster analysis can be applied in pattern recognition for supporting control, operations, and modeling of transportation systems [3]. For instance, it can be used to determine scenarios in decision support systems based on traffic simulation, where scenario clustering procedures may assist in real-time weather-responsive traffic management (WRTM) by rapidly classifying current or forecasted weather conditions into predefined categories and suggesting appropriate WRTM strategies that can be tested through real-time traffic simulation prior to deployment [4]. Additionally, clustering algorithms can be used in image processing and visualization systems to assess railway traffic safety [5].

Analysis of recent research and problem statement. Clustering, or cluster analysis, in the context of identification tasks, refers to the process of partitioning a given sample of objects into non-overlapping subsets (clusters) such that each cluster consists of similar objects. The similarity between objects is determined based on a selected metric, which is chosen according to the clustering criterion.

The input data for the clustering procedure is a set of objects, each defined by a vector of features. In such algorithms, the vectors typically represent pixels or neighborhoods of pixels. The vector set may include the following components [1, 2]:

- intensity values;
- color codes or color characteristics;
- computed feature descriptors;
- textural characteristics.

The clustering algorithm itself can be described as a function a: X→Y, which maps any object $x \in X$ to a cluster number $y \in Y$. In some cases, the set Y (i.e., the number of clusters) is known in advance; however, more often, the objective is to determine the optimal number of clusters according to a specific clustering quality criterion.

Nevertheless, the solution to the clustering problem is inherently ambiguous due to several reasons:

- there is no universally optimal clustering quality criterion;
- the number of clusters is generally unknown and must be determined based on some subjective criteria;
- the result of clustering strongly depends on the chosen metric, which is also typically subjective and defined by an expert [6].

This ambiguity necessitates flexible data processing tools, which must be considered during the development of methods for graphical image identification.

Researchers and scientists worldwide are actively working on this issue within the domain of digital image processing. In particular, the segmentation of color images based on clustering for identification purposes has gained widespread popularity [7].

For example, in the railway industry, a well-known system for detecting overheated axle boxes is widely used for inspecting wagons and locomotives to detect technical malfunctions, especially overheated axle boxes [8]. The operational principle of this equipment is based on measuring the temperature of axle boxes as trains pass by infrared sensors. However, this system has several drawbacks: detecting overheated axle boxes may trigger false alarms when transporting hot cargo (e.g., sinter pellets), in the event of hot water leakage from passenger car heating systems, or when passing through the system while braking with friction brakes (due to heating of the brake pads) [9].

In one of the studies, the authors present a machine vision system for efficient monitoring, analysis, and representation of visual data obtained from multiple cameras [10]. This solution aims to enhance the safety of daily railway transportation in two key ways:

1. by evaluating a wide range of safety requirements using image analysis algorithms capable of processing large-scale train images, and
2. by assisting train safety operators in detecting any potential malfunctions within the train. The system utilizes high-speed visible and thermal cameras that monitor the train as it passes beneath a railway frame structure.

Therefore, instead of using outdated systems for detecting overheated axle boxes, technical vision systems based on thermographic cameras could be implemented [11]. Thermographic cameras detect radiation in the infrared range of the electromagnetic spectrum (approximately 0,9–14 μm) and generate images based on this radiation, which allows for the identification of overheated or undercooled objects. In such images, color serves as an indicator of temperature level. For example, blue indicates that the object's temperature is around 27-28 °C, violet indicates 29-31 °C, orange indicates 32-34 °C, yellow indicates 35-36 °C, and white represents temperatures above 36 °C, etc.

The advantages of such cameras include the following:

- the ability to display visual images, which aids in comparing temperatures across large surfaces;
- the capability to detect malfunctioning components before failure occurs;
- effective temperature measurement in areas where other methods are either impossible (e.g., low thermal capacity objects) or pose health risks;
- non-destructive testing;
- facilitation of defect detection (such as cracks) in columns or other metallic parts;
- the ability to visualize heat at a rate of one frame per second, even with relatively low spatial resolution [12].

To implement a machine vision system for detecting overheated axle boxes on railways, a structural diagram is presented in Fig. 1. The operating principle of this system is as follows: when a wheelset approaches sensor S1, it sends a signal to the control system CS (which records the serial number of the wheelset) and to the thermographic cameras C1 and C2 to initiate image capture. The cameras process the thermal images and, depending on the results, send a high-level signal to the CS if an excessive temperature is detected. The CS associates the wheelset number with the side of the axle box, logs the inspection results into the database, and for instance sends a signal to a controller, which in turn marks the axle box with paint or sends a signal to the train operator to reduce speed, and so on [13, 14].

Thus, the key challenge is the development of a high-quality image recognition algorithm - specifically for thermographic images that is both fast-acting and effective in the presence of other thermal interferences typically found in railway environments.

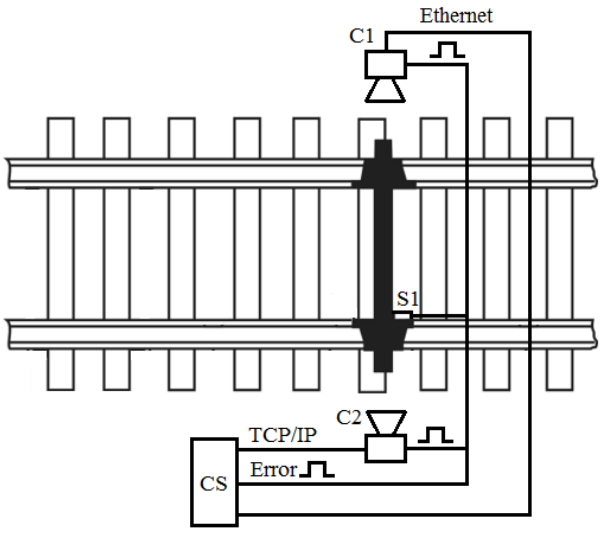

Fig. 1. **Structural Diagram of the Implementation of a Machine Vision System for Detecting Overheated Axle Boxes in Railway Transport**

The purpose and tasks of the study. To analyze the operating principle of the k-means clustering algorithm in image recognition tasks, and to conduct experimental modeling of this algorithm by

segmenting thermal images based on color in order to recognize the thermal characteristics of the studied objects using the MATLAB environment.

Materials and methods of research. The k-means clustering algorithm partitions a set of elements in an *n* - dimensional vector space into *k* clusters, in which each object belongs to the cluster with the nearest mean value. This method yields exactly *k* distinct clusters with the greatest possible separation. The optimal number of clusters *k*, which results in the highest degree of separation, is not known a priori and must therefore be derived from the data. The goal of k-means clustering is to minimize the total intra-cluster variance or the sum of squared error (SSE) function [15, 16]:

$$J = \sum_{j=1}^{k} \sum_{i=1}^{n} \left\| x_i^{(j)} - c_j \right\|^2, \quad (1)$$

where J – objective function;
k – number of clusters;
n – number of observations;
$x_i^{(j)}$ – observation i;
c_j – centroid of the cluster j;
$\left\| x_i^{(j)} - c_j \right\|^2$ – distance function.

Algorithm Description. The process begins by assigning objects to clusters. The number of clusters *k* is selected, and at the initial step, these points are considered the "centers" of the clusters. Each cluster corresponds to one center. The initial centroids can be selected in one of the following ways:

- selecting *k* observations to maximize the initial distance;
- randomly selecting *k* observations;
- selecting the first *k* observations.

As a result, each object is assigned to a specific cluster. Next, an iterative process begins. The cluster centers are recalculated and are considered to be the coordinate-wise means of their respective clusters. The objects are then reassigned based on the updated centers.

The simulation will be carried out in the Jupyter Notebook environment using the Scikit-learn library.

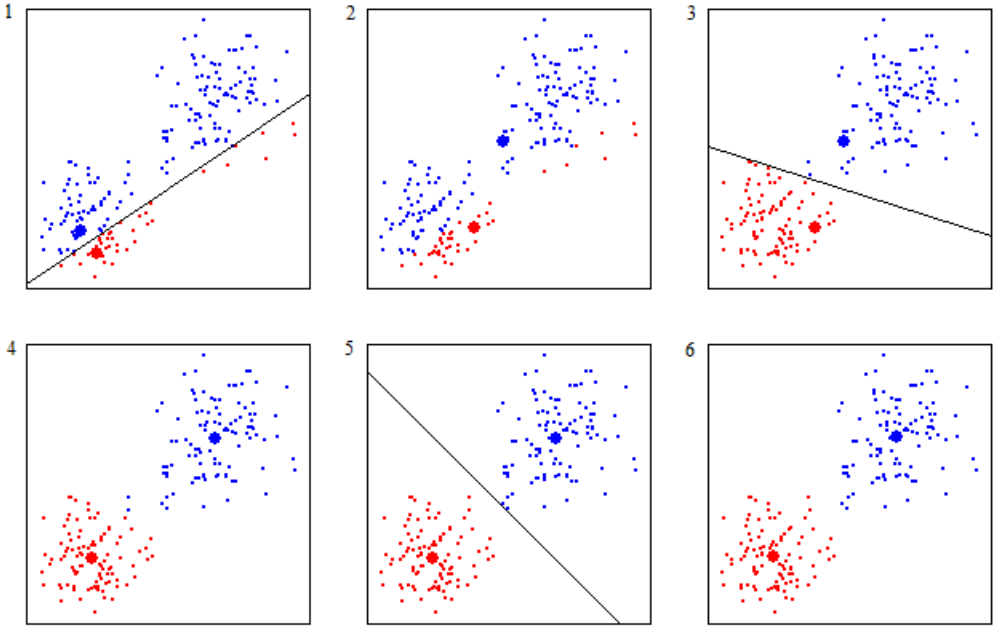

Fig. 2. **Illustration of the Operation of the K-Means Algorithm**

This process of computing cluster centers and redistributing objects continues until one of the following conditions is met:

- the cluster centers have stabilized, i.e., all observations belong to the same cluster as in the previous iteration;
- the number of iterations reaches the predefined maximum.

Figures 2 and 3 illustrate the working principle of the *k*-means algorithm (where *k*=2) and its block diagram [14, 17].

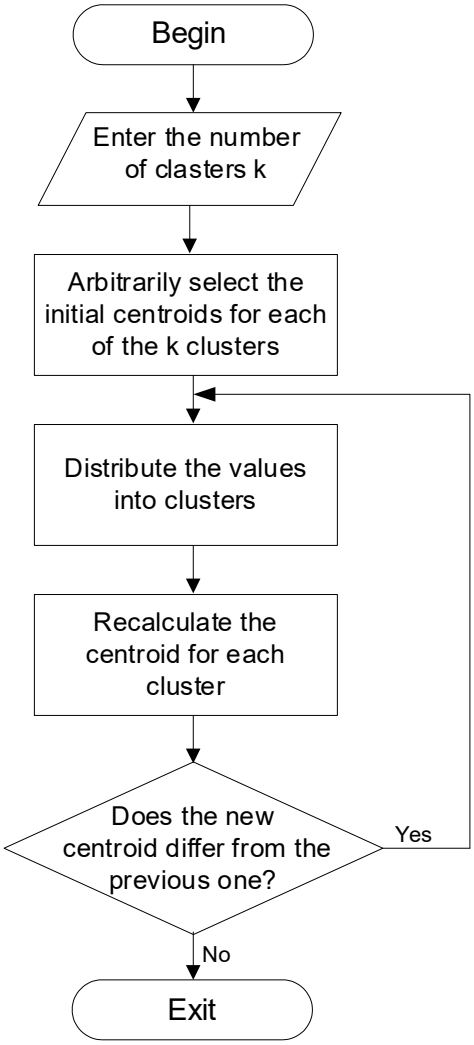

Fig. 3. **Block diagram of the k-means algorithm**

The simulation (Table 1) illustrates how the algorithm works on synthetic datasets. The essence of the simulation is as follows:

- in the Jupyter Notebook environment, four datasets are generated using the scikit-learn package, namely: datasets.make_blobs, datasets.make_gaussian_quantiles, datasets.make_circles, and datasets.make_moons;
- we apply the K-means algorithm, which uses the Euclidean distance metric, to each data type, and gradually increase the number of clusters from 2 to 5 to see how the algorithm behaves on different data types with different values of the k parameter.

Note. The number of clusters does not exceed 5, since we know in advance that the number of 'correct' clusters, for example, for data of type datasets.make_blobs is 5, in other cases no more than 2.

From Table 1, we can conclude that the K-means algorithm performed best for data of the datasets.make_blobs type with K=5. Each cluster is defined solely by its centre, which means that each cluster has a convex shape. As a result, the K-means algorithm can describe relatively simple shapes. In addition, the K-means algorithm assumes that all clusters have the same 'diameter' in a sense, it always draws the boundary between clusters so that it passes exactly in the middle between the cluster centres. This can sometimes lead to unexpected results, as shown in Table 1 on the datasets.make_gaussian_quantiles data.

Table 1. **Illustration of how the K-means algorithm works with artificially generated data**

Type of input data / Number of clusters	datasets.make_blobs	datasets.make_gaussian_quantiles
K = 2	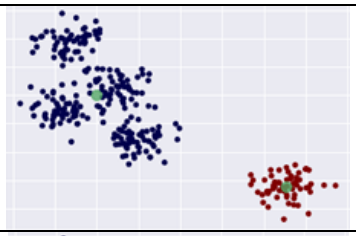	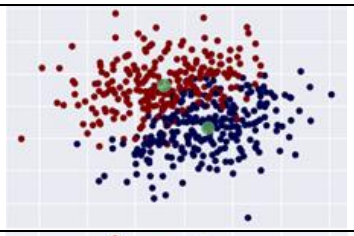
K = 3	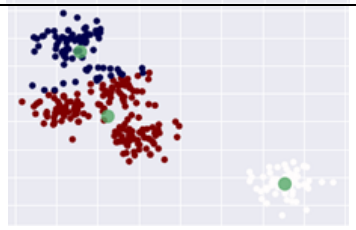	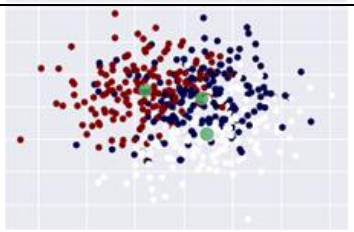
K = 4	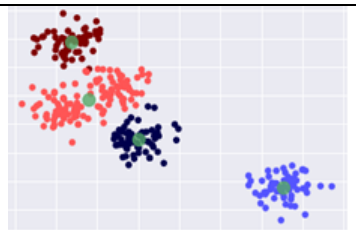	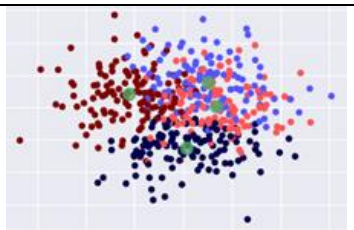
K = 5	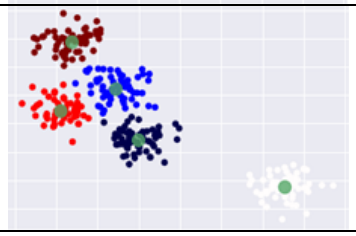	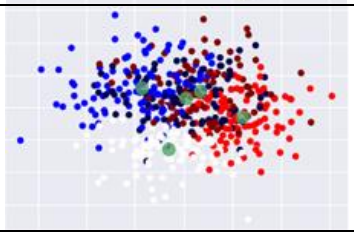

Segmentation of an object image consists in dividing it into spatially connected areas (segments). Global and local pixel connectivity maxima of quantized images are determined, and then regions adjacent to these maxima are formed. The set of these regions forms a spatial set of objects. In the process of image segmentation, several incorrectly classified elements (the so-called speckle noise)

inevitably appear. After thresholding, such errors can be eliminated. If the brightness level of any image element is higher than the maximum level of its neighbors, then it is likely due to noise. It can be replaced by the maximum brightness level of neighboring elements. A similar operation, filtering, can be applied if the brightness level of an element is lower than the minimum level of its neighbors. Another possibility is to replace each level value with the average or median value of neighboring elements.

Let's consider the procedure for segmenting objects by determining the connectivity of image elements [18-21]. The mask matrix formed by selecting each minimal element will be called a cut, and the total connectivity value of a cut element will be called internal cut connectivity, and the total connectivity value between elements of neighboring cuts will be called intercut connectivity.

The value of internal cut connectivity $f(k)$ will be determined by the formula.

$$f(k)=\sum_{j=1}^{M-1}\sum_{i=1}^{N-1}\left(a_{ij}^{k}\wedge a_{ij+1}^{k}+a_{ij}^{k}\wedge a_{ij-1}^{k}+a_{ij}^{k}\wedge a_{i-1j}^{k}+\ldots+a_{ij}^{k}\wedge a_{i+1j+1}^{k}\right). \quad (2)$$

Next, we determine the global and local values of internal cut connectivity. The values of internal cut connectivity are determined at the time points t_{k_1-1}, t_{k_2}, t_{k_3+1}. These time points correspond to cuts k_1-1, k_2, k_3+1. The number of such cuts is $v=\overline{1,w}$, which corresponds to the general case. Let us define the functions of internal cut connectivity as follows:

$$f(k_v,k_{v+1})=f(k_v,k_{v+1}),\ldots,f(k_{v+p_1-1},k_{v+p_1}),\ldots,f(k_{v_1-1},k_{v_1}),\ p_1=\overline{1,l_1} \quad (3)$$

$$f(k_v,k_{v-1})=f(k_v,k_{v-1}),\ldots,f(k_{v+p_2},k_{v+p_2-1}),\ldots,f(k_{v_2+1},k_{v_2}),\ p_2=\overline{1,l_2}\ . \quad (4)$$

Functions of intercut connectivity $f(k_{v+p_1-1},k_{v+p_1})$ and $f(k_{v+p_2},k_{v+p_2-1})$ can be written as follows:

$$f(k_{v+p_1-1},k_{v+p_1})=\sum_{j=0}^{M-1}\sum_{i=0}^{N-1}\left(a_{ij}^{k_{v+p_1-1}}\wedge a_{ij+1}^{k_{v+p_1}}+a_{ij}^{k_{v+p_1-1}}\wedge a_{ij-1}^{k_{v+p_1}}+a_{ij}^{k_{v+p_1-1}}\wedge a_{i-1j}^{k_{v+p_1}}+\ldots+a_{ij}^{k_{v+p_1-1}}\wedge a_{i+j+1}^{k_{v+p_1}}\right). \quad (5)$$

Similarly, you can write the intercut connectivity function

$$f(k_{v+p_2},k_{v+p_2-1})=\sum_{j=0}^{M-1}\sum_{i=0}^{N-1}\left(a_{ij}^{k_{v+p2}}\wedge a_{ij+1}^{k_{v+p2-1}}+a_{ij}^{k_{v+p2}}\wedge a_{ij-1}^{k_{v+p2-1}}+a_{ij}^{k_{v+p2}}\wedge a_{i-1j}^{k_{v+p2-1}}+\ldots+a_{ij}^{k_{v+p2}}\wedge a_{i+1j+1}^{k_{v+p2-1}}\right). \quad (6)$$

The general segmentation scheme can be represented by sequential or parallel definition of sequences of intercut connectivity functions:

$$f(k_v,k_{v+1}),f(k_{v+2},k_{v+3}),\ldots,f(k_{w-1},k_w) \quad (7)$$

and

$$f(k_v,k_{v-1}),f(k_{v-2},k_{v-3}),\ldots,f(k_2,k_1). \quad (8)$$

The determination of the intercut connectivity functions in accordance with formulas (7) and (8) is carried out until

$$f(k_v,k_{v+1})=\delta,\ f(k_{v+2},k_{v+3})=\delta,\ f(k_{w-1},k_w)=\delta\ , \quad (9)$$

or

$$f(k_v,k_{v-1})=\delta,\ f(k_{v-2},k_{v-3})=\delta,\ f(k_2,k_1)=\delta\ . \quad (10)$$

Practically, the threshold δ in expressions (9), (10) is formed for each function of intercut connectivity $f\left(k_{v+p_1+1}, k_{v+p_1}\right)$ and $f\left(k_{v+p_2+1}, k_{v+p_2}\right)$. The process of determining the functions of intercut connectivity in accordance with expressions (3) and (4) is carried out until $f\left(k_{v+p_1+1}, k_{v+p_1}\right)=\delta$ or $f\left(k_{v+p_2+1}, k_{v+p_2}\right)=\delta$. Moreover, in the roughest approximation, the elements of the cuts k_{v+p_1}, k_{v+p_2} for which the functions of intercut connectivity $f\left(k_{v+p_1+1}, k_{v+p_1}\right)=\delta$ and $f\left(k_{v+p_2+1}, k_{v+p_2}\right)=\delta$, respectively, are uninformative elements and should be excluded from the original image.

If $f\left(k_{v+p_1+1}, k_{v+p_1}\right)\neq\delta$ or $f\left(k_{v+p_2+1}, k_{v+p_2}\right)\neq\delta$, then iterative determination of the intercut connectivity functions is performed in accordance with expressions (3) and (4).

Let's consider an example for a particular case. Let *v=2*, then for the cut k_2, the intercut connectivity functions take the following form:

$$f\left(k_2, k_{2+1}\right)=f\left(k_2, k_{2+1}\right), f\left(k_{2+1}, k_3\right), \ldots, f\left(k_{2+p_1-1}, k_{2+p_1}\right), \ldots, f\left(k_{l_1-1}, k_{l_1}\right) \quad (11)$$

$$f\left(k_2, k_{2-1}\right)=f\left(k_2, k_{2-1}\right), f\left(k_{2-1}, k_{2-2}\right), \ldots, f\left(k_{2+p_2}, k_{2+p_2-1}\right), \ldots, f\left(k_{l_2+1}, k_{l_2}\right). \quad (12)$$

At the same time, for expressions (10) and (11), we sequentially define the functions of intercut connectivity: from $f\left(k_2, k_{2+1}\right)$ to $f\left(k_{l_1-1}, k_{l_1}\right)$ and from $f\left(k_2, k_{2-1}\right)$ to $f\left(k_{l_2+1}, k_{l_2}\right)$.

Let's assume that

$$f\left(k_2, k_{2+1}\right)\neq\delta, f\left(k_{l_1-2}, k_{l_1-1}\right)\neq\delta, \text{ and } f\left(k_{l_1-1}, k_{l_1}\right)=\delta$$

$$f\left(k_2, k_{2-1}\right)\neq\delta, .. f\left(k_{l_2+2}, k_{l_2+1}\right)\neq\delta \text{ and } f\left(k_{l_2+1}, k_{l_2}\right)=\delta. \quad (13)$$

This means that in the cuts k_{l_1} and k_{l_2}, some elements are uninformative. There are two possible solutions. The first is to directly remove the noise elements from the cuts. The second option is the most promising. When implementing it, it should be assumed that the cuts k_{l_1} and k_{l_2} define noise elements as the product of single elements by the value of an element, for example, selected by the average value. Thus, it is not the values of single elements themselves that are subtracted from the original image (image fragment), but the single elements of the cuts k_{l_1} and k_{l_2} multiplied by the corresponding values of the minimum elements for this cut.

Thus, for all cuts with the maximum value of the internal cut connectivity function between cuts k_{1l_1} and k_{2l_2}, k_{2l_2} and k_{1l_1}, k_{2l_1} and k_{3l_1}, k_{3l_1} and k_{2l_1}, as well as between cuts k_{1l_2} and its preceding cut and k_{3l_2} and its following cut, and vice versa for the last two pairs of cuts. For the sake of clarity, let us consider the definitions of the intercut connectivity functions for the cuts k_{2l_2}, k_{1l_1} and k_{1l_1}, k_{2l_2}.

$$f\left(k_{2l_2}, k_{1l_1}\right)=f\left(k_{2l_2}, k_{2l_2+1}\right), f\left(k_{2l_2+1}, k_{2l_2+2}\right), .., f\left(k_{1l_1+1}, k_{1l_1}\right)$$

$$f\left(k_{1l_1}, k_{2l_2}\right)=f\left(k_{1l_1}, k_{1l_1+1}\right), f\left(k_{1l_1+1}, k_{1l_1+2}\right), .., f\left(k_{2l_2-1}, k_{2l_2}\right). \quad (14)$$

If the elements in the cuts k_{2l_2} and k_{1l_1} are uninformative, then for the following intercut connectivity functions, the conditions for determining whether the elements of the cut are informative or not change the meaning. That is, the expressions

$$f\left(k_{2l_2},k_{2l_2+1}\right)\neq\delta,\ f\left(k_{2l_2+1},k_{2l_2+2}\right)\neq\delta,\ldots,f\left(k_{1l_1+1},k_{1l_1}\right)\neq\delta$$

or

$$f\left(k_{1l_1},k_{1l_1+1}\right)\neq\delta,\ f\left(k_{1l_1+1},k_{1l_1+2}\right)\neq\delta,\ldots,f\left(k_{2l_2-1},k_{2l_2}\right)\neq\delta \quad (15)$$

imply, that the elements of the cuts $k_{2l_2+1},k_{2l_2+2},..,k_{1l_1}$ are uninformative. Therefore, for them, the average value of the elements should be subtracted from the elements of the original image. Moreover, for a rough approximation, the elements of the cuts located between the cuts k_{1l_1} and k_{2l_2} are uninformative and the latter are excluded from the original image. If the elements of the cut k_{2l_2} are uninformative, the unit values of this cut are transferred to the next cut k_{2l_2-1} and the intercut connectivity function is determined for this (changed) cut. Further, this iterative process of transferring unit elements of a cut can be continued. If condition (15) is not met, the elements of the cut under consideration are considered image elements.

If we assume that all the elements belonging to an image are interconnected, i.e. correlated in the space-time domain, the following problem arises: how can we optimally implement the multi-stage segmentation operation, assuming that the image elements are correlated in space and time, and the non-informative elements are decorrelated.

The k-means clustering algorithm in pattern recognition tasks. Extracting information from images and understanding it in such a way that the obtained information can be used to perform various tasks is a key aspect of machine learning. Image segmentation is one of the first steps towards understanding images and subsequently identifying different objects within them. Image segmentation involves dividing or partitioning an image into regions with similar attributes. It is one of the most critical components of image analysis and pattern recognition, and still remains one of the most challenging tasks in image processing and analysis. It has applications in multiple fields such as remote image analysis, medicine, traffic monitoring, fingerprint recognition, and more [23-26]. Segmentation methods involving classification approaches face significant challenges in computing the number of clusters present in the object space or in extracting the relevant function. This type of image segmentation is widely used due to its ease of understanding and relatively high accuracy of results. There are several methods, and one of the most popular is the k-means clustering algorithm. This clustering algorithm is unsupervised and is used to segment the region of interest from the background.

When using clustering algorithms, the task arises of determining the number of cluster centers for further analysis. For example, when clustering using the k-means algorithm, which is an exclusive clustering method, the number of centers is set initially and the algorithm works recursively until the formed clusters are balanced according to the proximity of individual data elements to the cluster centre. However, if the data set obtained as a result of experimental research is large enough, it is impossible to determine the optimal number of centers. If a certain number of centers is specified, the clusters formed using the k-means method will not correspond to the internal structure of the data. Therefore, using this approach for recognition tasks will be ineffective. When using, for example, hierarchical clustering methods, the algorithm works until all data is assigned to a single cluster. And there's also the question of which clustering level to stop at so that the number of clusters you get is the best for further analysis.

The paper looked at different ways to pick the best number of clusters, but the most effective one was the one that considered the max density of data assigned to each cluster at different clustering levels. The density was calculated as the ratio of data elements included in the cluster to the volume of this cluster. This approach allows for the structural grouping of data elements and reduces the running time of the clustering algorithm, since it will not be processed to the end (for hierarchical clustering methods).

Detection of overheated axleboxes. As previously noted, the railway industry faces the problem of monitoring the technical condition of axleboxes for safety hazards. Therefore, we propose using a machine vision system to monitor the thermal characteristics of moving train components based on

thermographic cameras and the unsupervised k-means clustering algorithm. For modeling purposes, two images of axleboxes were used: a normal axlebox (Fig. 4(a)) and an overheated axlebox (Fig. 4(b)).

Note on images: since it is not possible to take real images of axle boxes in the infrared range due to the high cost of thermographic cameras, a decision was made to convert ordinary RGB images into a form that visually creates the effect that the image is taken in the thermal range. Therefore, the image of the axle box, which we have conditionally labeled as normal, could actually also be overheated - and, unfortunately, this factor distorts the results of the modeling.

Thus, for modeling, color images of both normal and overheated axle boxes are used for defective segmentation of thermal indicators. Defective segmentation is carried out in two stages. First, pixels are clustered based on their color and spatial characteristics, where the clustering process is performed. Then, the clustered blocks are combined into a certain number of regions. By using this two-step procedure, computational efficiency can be increased by avoiding feature extraction for each pixel in the axle box images. Although color is typically not used for defect segmentation, it provides high discriminative power for different areas of the image. Therefore, this approach provides a reliable solution for segmenting thermal indicators.

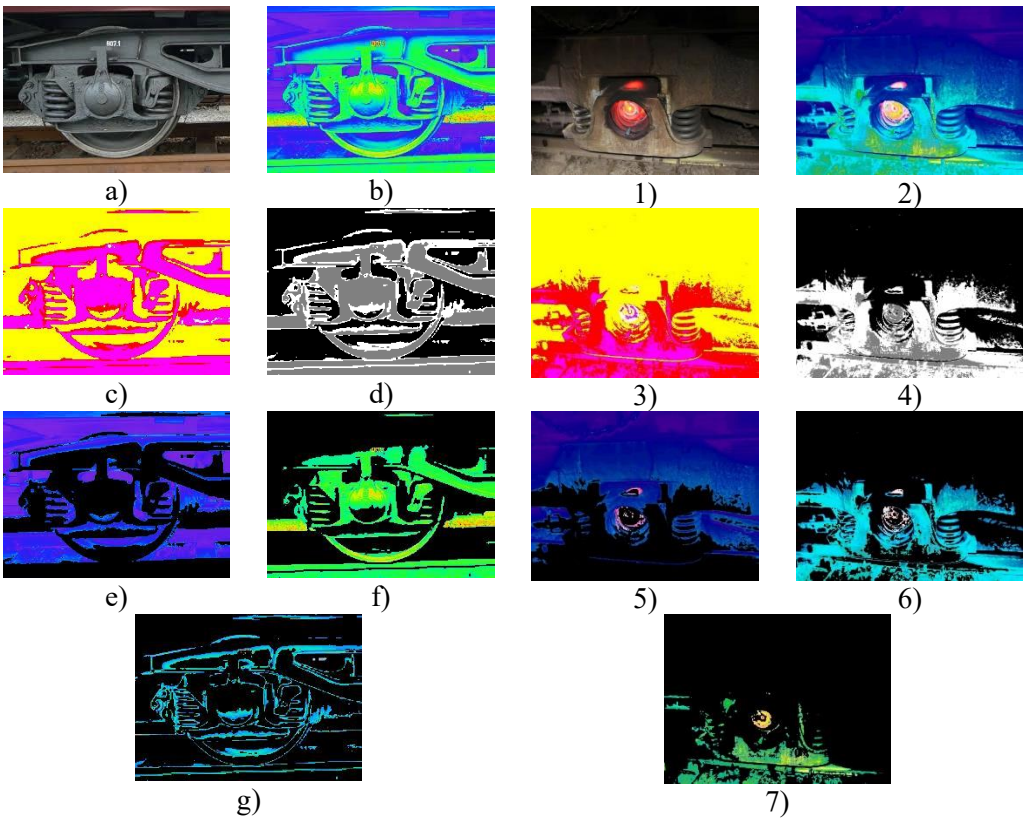

Fig. 4. **Segmentation based on color using the k-means clustering algorithm: a) and 1) - Conditional images of axle boxes; b) and 2) - Illustration of normal and overheated axle boxes in the infrared range; c) and 3) - Thermal images converted from the RGB color space to L*a*b* color space; d) and 4) - Images labeled with cluster indices; e) and 5) - Objects in cluster 1; f) and 6) - Objects in cluster 2; g) and 7) - Objects in cluster 3.**

Experimental results show the effectiveness of the proposed approach for improving the quality of thermal image segmentation in terms of accuracy and computational time. The results of the modeling demonstrate that the proposed approach is promising. Segmentation using the k-means algorithm is very useful for image analysis. An important goal of image segmentation is to separate the object and

background, regardless of whether the image has a blurred boundary. Defective segmentation of thermal characteristics can be considered as an example of image segmentation where the number of segments is unknown. The main goal of the proposed approach is automatic color segmentation using the k-means clustering method and the L*a*b* color space [27-29].

The introduced segmentation structure works in five steps as follows:

1. Reading images in the infrared range.
2. Conversion of the image from RGB color space to L*a*b*. The L*a*b* color space is used because it consists of a luminance layer in the "L" channel and two chromaticity layers in the "a*" and "b*" channels. The use of the L*a*b* color space is uncompromising because all color information is present in "a*" and "b*".
3. Color classification using the k-means clustering algorithm in the "a*b*" space. To measure the difference between two colors, the Euclidean distance metric is used.
4. Labeling each pixel in the image using the results of the k-means algorithm. For each pixel in our input, the algorithm calculates an index corresponding to the cluster. Each pixel in the image will be labeled with the cluster index.
5. Creation of images that segment the input image by color. We need to separate the pixels in the image by color using pixel labels, which will result in different images based on the number of clusters. We program the identification of the index of each cluster that contains the highest temperature readings because the algorithm does not return the same cluster index every time. However, we can do this by using the central value of the clusters, which contains the average "a*" and "b*" values for each cluster.

Conclusions. The k-means clustering algorithm is classified as an unsupervised data clustering algorithm (unsupervised learning). The advantages of this algorithm include its clarity, simplicity, and speed of use. However, its drawbacks include slow performance with large datasets and sensitivity to outliers, which can distort the mean value. The simulation results showed that the k-means algorithm can effectively describe relatively simple shapes. In addition, this algorithm assumes that all clusters have the same ‘diameter’ in a certain sense, it always draws the boundary between clusters so that it passes exactly in the middle between the centres of the clusters.

A scheme for implementing a machine vision system for detecting overheated axle boxes in railway transport using the k-means clustering algorithm has been proposed.

Experimental results of the modeling showed that segmentation based on the color model using the k-means clustering algorithm allows for accurate segmentation of temperature indicators of rolling stock. For example, the image in Fig. 5(e) shows the segmentation of objects in the second cluster and, in comparison with the conditional thermal image (Fig. 5(b)), represents the recognition of the dominant green color, indicating a satisfactory temperature condition of the axle box. This is not the case with the image of the overheated axle box (Fig. 5(6)), where the white color signals an excessive temperature increase, indicating an emergency condition of the axle box.

It should be noted that the application of this algorithm in the development of software for thermographic cameras aimed at recognizing temperature indicators is effective, as this algorithm allows for image compression, which will increase data processing speed and enable monitoring of the thermal characteristics of rolling stock at higher speeds.

REFERENCES

1. Ghaziasgar, M., Bagula, A., & Thron, C. (2020). Computer Vision Algorithms for Image Segmentation, Motion Detection, and Classification. *Implementations and Applications of Machine Learning. Studies in Computational Intelligence*, *782*, 119-138. Springer, Cham. https://doi.org/10.1007/978-3-030-37830-1_5.
2. Hassner, T., & Liu, C. (Eds.). (2016). *Dense image correspondences for computer vision* (pp. 3-14). Springer International Publishing. https://doi.org/10.1007/978-3-319-23048-1.
3. Vishwakarma, A., Dasgupta, A., & Racherla, V. (2025). Detecting and classifying multiple track defects using clustering algorithm. *Engineering Structures*, *334*, 120197. https://doi.org/10.1016/j.engstruct.2025.120197.
4. Pacheco, F., Cerrada, M., Sánchez, R. V., Cabrera, D., Li, C., & de Oliveira, J. V. (2017). Attribute clustering using rough set theory for feature selection in fault severity classification of rotating machinery. *Expert Systems with Applications*, *71*, 69-86. https://doi.org/10.1016/j.eswa.2016.11.024.

5. Jiang, Y., Wang, H., Tian, G., Yi, Q., Zhao, J., & Zhen, K. (2019). Fast classification for rail defect depths using a hybrid intelligent method. *Optik*, *180*, 455-468. https://doi.org/10.1016/j.ijleo.2018.11.053.
6. Rapp, S., Martin, U., Strähle, M., & Scheffbuch, M. (2019). Track-vehicle scale model for evaluating local track defects detection methods. *Transportation Geotechnics*, *19*, 9-18. https://doi.org/10.1016/j.trgeo.2019.01.001.
7. Li, Q., Yao, K., & Zhang, X. (2020). A change-point detection and clustering method in the recurrent-event context. *Journal of Statistical Computation and Simulation*, *90*(6), 1131–1149. https://doi.org/10.1080/00949655.2020.1718149.
8. Gomez, M. J., Castejon, C., Corral, E., & Cocconcelli, M. (2023). Railway axle early fatigue crack detection through condition monitoring techniques. *Sensors*, *23*(13), 6143. https://doi.org/10.3390/s23136143.
9. Amini, A., Entezami, M., Huang, Z., Rowshandel, H., & Papaelias, M. (2016). Wayside detection of faults in railway axle bearings using time spectral kurtosis analysis on high-frequency acoustic emission signals. *Advances in Mechanical Engineering*, *8*(11), 1687814016676000. https://doi.org/10.1177/1687814016676.
10. Lisanti, G., Karaman, S., Pezzatini, D., & Bimbo, A. D. (2018). A multi-camera image processing and visualization system for train safety assessment. *Multimedia Tools and Applications*, *77*, 1583-1604. https://doi.org/10.1007/s11042-017-4351-4.
11. Wei, X., Yang, Z., Liu, Y., Wei, D., Jia, L., & Li, Y. (2019). Railway track fastener defect detection based on image processing and deep learning techniques: A comparative study. *Engineering Applications of Artificial Intelligence*, *80*, 66-81. https://doi.org/10.1016/j.engappai.2019.01.008.
12. Jamshidi, A., Roohi, S. F., Núñez, A., Babuska, R., De Schutter, B., Dollevoet, R., & Li, Z. (2016). Probabilistic defect-based risk assessment approach for rail failures in railway infrastructure. *IFAC-PapersOnLine*, *49*(3), 73-77. https://doi.org/10.1016/j.ifacol.2016.07.013.
13. Yiakopoulos, C. T., Gryllias, K. C., & Antoniadis, I. A. (2011). Rolling element bearing fault detection in industrial environments based on a K-means clustering approach. *Expert Systems with Applications*, *38*(3), 2888-2911. https://doi.org/10.1016/j.eswa.2010.08.083.
14. Botvin, M., Butryk, N., & Gertsiy, O. (2019). K-means clustering algorithm in image recognition tasks. *Collection of scientific works of the State University of Infrastructure and Technologies series "Transport Systems and Technologies"* (34), 199–209. https://doi.org/10.32703/2617-9040-2019-34-2-3.
15. Zhang, C., Zhong, P., Liu, M., Song, Q., Liang, Z., & Wang, X. (2022). Hybrid Metric K-Nearest Neighbor Algorithm and Applications. *Mathematical Problems in Engineering*, *2022*(1), 8212546. https://doi.org/10.1155/2022/8212546.
16. Ando, K., Kuniyoshi, Y., Onogi, N., Uchitane, T., Mukai, N., Iwata, K., Ito, N., & Jiang, Y. (2024). Cluster Detection for Traffic Accidents on Spatiotemporal Networks. *Procedia Computer Science*, *246*, 371-380.. https://doi.org/10.1016/j.procs.2024.09.416.
17. Huang, B., Zhu, Y., Wang, Z., & Fang, Z. (2021). Imbalanced data classification algorithm based on clustering and SVM. *Journal of Circuits, Systems and Computers*, *30*(02), 2150036. https://doi.org/10.1142/S0218126621500365.
18. Timchenko, L. I., Basov, V. I., Gertsiy, O. A., Kokriatskaia, N. I., & Ivasiyk, I.D., (2010). Rospiznavannya pivtonovych zobrazhen za shemoyu "gruboi" - "tochnoi" obrobki: Monografia. [Recognition of halftone images according to the scheme of "rough" - "accurate" processing: Monograph]. *Kyiv: Naukova Dymka,* 180 p. ISBN 978-966-00-0904-6.
19. Timchenko, L. I., Kokriatskaia, N. I., Gertsiy, A. A., Stepaniuk, D. S., Chernyaschuk, N. L., Kotyra, A., & Amirgaliyev, Y. (2019, November). Elaboration of pyramidal methods applying computation technique “rough-fine” image identification. In *Photonics Applications in Astronomy, Communications, Industry, and High-Energy Physics Experiments 2019* (Vol. 11176, pp. 384-391). SPIE. https://doi.org/10.1117/12.2537179.
20. Orazayeva, A., Wójcik, W., Pavlov, S., Tymchenko, L., Kokriatska, N., Tverdomed, V., ... & Semenova, L. (2022, December). Biomedical image segmentation method based on contour preparation. In *Photonics Applications in Astronomy, Communications, Industry, and High Energy Physics Experiments 2022* (Vol. 12476, pp. 21-26). SPIE. https://doi.org/10.1117/12.2657929.
21. Timchenko, L., Kokriatskaya, N., Tverdomed, V., Stetsenko, O., Kaplun, V., Kolesnytskyj, O. K., ... & Zhunissova, U. (2023). Segmentation of multigradation images based on spatial connectivity features. *Informatyka, Automatyka, Pomiary w Gospodarce i Ochronie Środowiska*, *13*(3), 47-50. https://doi.org/10.35784/iapgos.5352.
22. Fan, Z., Xie, J. K., Wang, Z. Y., Liu, P. C., Qu, S. J., & Huo, L. (2021, May). Image classification method based on improved KNN algorithm. In *Journal of physics: Conference series* (Vol. 1930, No. 1, p. 012009). IOP Publishing. https://doi.org/10.1088/1742-6596/1930/1/012009.
23. Gertsiy, O. (2023). Models of criterion evaluation of the image processing systems effectiveness. *Collection of scientific works of the State University of Infrastructure and Technologies series "Transport Systems and Technologies"*, (41), 143-154. https://doi.org/10.32703/2617-9059-2023-41-12.
24. Gertsiy, O. (2024). Research on graphic data formats for compact representation and comparison of images. *Collection of scientific works of the State University of Infrastructure and Technologies series “Transport Systems and Technologies”*, (43), 173–187. https://doi.org/10.32703/2617-9059-2024-43-14.
25. Sacerdoti, F. M., Giordano, A., & Cavaliere, C. (Eds.). (2016). *Advanced imaging techniques in clinical pathology* (No. 9210). Springer New York. https://doi.org/10.1007/978-1-4939-3469-0_2.
26. Burger, W., & Burge, M. J. (2022). *Digital image processing: An algorithmic introduction*. Springer Nature. https://doi.org/10.1007/978-3-031-05744-1.
27. Sinaga, A. S. R. (2019). Color-based Segmentation of Batik Using the L*a*b Color Space. *Sinkron: Jurnal Dan Penelitian Teknik Informatika*, *3*(2), 175-179. https://doi.org/10.33395/sinkron.v3i2.10102.

28. Abbadi, N. K. E., & Razaq, E. S. (2020). Automatic gray images colorization based on lab color space. *Indonesian Journal of Electrical Engineering and Computer Science*, *18*(3), 1501-1509. https://doi.org/10.11591/ijeecs.v18.i3.pp1501-1509.
29. Saifullah, S., Prasetyo, D. B., Dreżewski, R., & Dwiyanto, F. A. (2023). Palm oil maturity classification using K-nearest neighbors based on RGB and L* a* b color extraction. *Procedia Computer Science*, *225*, 3011-3020. https://doi.org/10.1016/j.procs.2023.10.294.

Олександр Герцій[1], Сергій Карнатов[2], Віталій Гладиш[3], Валентина Ткаченко[4]

[1]Доцент, Кафедра Автоматизація та комп'ютерно-інтегровані технології транспорту, Національний транспортний університет, вул. Михайла Омеляновича-Павленка, 2, 01010, м. Київ, Україна. ORCID: https://orcid.org/0000-0002-8634-5880.

[2]Аспірант, Кафедра Автоматизація та комп'ютерно-інтегровані технології транспорту, Національний транспортний університет, вул. Михайла Омеляновича-Павленка, 2, 01010, м. Київ, Україна. ORCID: https://orcid.org/0009-0006-6254-6166.

[3]Аспірант, Кафедра Автоматизація та комп'ютерно-інтегровані технології транспорту, Національний транспортний університет, вул. Михайла Омеляновича-Павленка, 2, 01010, м. Київ, Україна. ORCID: https://orcid.org/0009-0003-5801-056X.

[4]Доцент, Кафедра транспортного права та логістики, Національний транспортний університет, вул. Михайла Омеляновича-Павленка, 2, 01010, м. Київ, Україна. ORCID: https://orcid.org/0000-0001-5147-0772.

Моделювання алгоритму кластеризації зображень для виявлення перегрітих букс вагонів

В статті розглянуто ідентифікацію зображень на основі алгоритму кластеризації для виявлення теплових характеристик букс вагонів. Проведено аналіз перспектив застосування алгоритмів кластерізації в задачах ідентифікації цифрових зображень. Наведено принцип роботи запропонованого алгоритму при сегментації та стисненні графічних зображень, а також при розпізнаванні образів у транспортній сфері. Представлено блок-схему алгоритму і описано принцип його роботи. Пропонується схема реалізації системи машинного зору з використанням даного алгоритму в процесі виявлення перегрітих букс вагонів. Проведено експериментальне моделювання по сегментації на основі кольорових моделей зображень поданих в інфрачервоному діапазоні для виявлення ділянок з підвищеною температурою засобами програми MATLAB. Для експерименту обрані зображення, на яких представлено букси рухомого складу, одна з яких нормальна, а друга - перегріта. В результаті проведеного моделювання виявлено, що сегментація на основі кольорових моделей зображень дозволяє точно сегментувати термозображення букси. Дослідження показали, що застосування запропонованого алгоритму і його програмна реалізація для термографічних камер є ефективним з метою розпізнавання температурних показників. Даний алгоритм також дозволяє представити зображення в компактному вигляді, що приводить до підвищення швидкості його обробки і дозволяє швидко проводити моніторинг теплових характеристик букс рухомого складу.

Ключові слова: *термографічні зображення, кластеризація, сегментація, моніторинг, моделювання, температурні показники, букса.*

DOI: 10.32703/2617-9040-2025-45-7

UDC 656.61.052:629.5.072.8:004.94

Igor Burmaka[1], Olga Petrychenko[2], Bohdan Alieksieichuk[3], Alla Vynohradova[4]

[1]Professor, head of the Ship's handling department, National University «Odessa Maritime Academy», 8, Didrikhson str., Odessa, 65052, Ukraine. ORCID: https://orcid.org/0000-0002-0853-6884.

[2]Associate Professor, Theory and Structure of a Ship Department, National University «Odessa Maritime Academy», 8, Didrikhson str., Odessa, 65052, Ukraine. ORCID: https://orcid.org/0000-0002-4893-8204.

[3] Senior Lecturer of the Ship's Handling Department, National University «Odessa Maritime Academy», 8, Didrikhson str., Odessa, 65052, Ukraine. ORCID: https://orcid.org/0000-0003-1043-5174.

[4]Head of the laboratory of the Ship's handling department, National University «Odessa Maritime Academy», 8, Didrikhson str., Odessa, 65052, Ukraine. ORCID: https://orcid.org/0009-0007-9406-3203.

***Corresponding author**: o.petrychenko@onma.edu.ua.

Analysis of minimum safe approach distances based on vessels navigation safety domain

This article presents an analytical study of changes in the critical allowable approach distance between converging vessels, taking into account the shape of the vessel's safety zone. The research aims to address the important issue of ensuring maritime navigation safety by developing a mathematical approach for precise modeling of vessel domains under various approach scenarios. Analytical expressions are proposed and derived for calculating minimum safe distances for both elliptical zones and zones of complex configuration, allowing flexible assessment of approach situations depending on the relative motion of vessels. The analysis shows that although elliptical and complex-shaped domains differ geometrically, the nature of changes in critical approach distance in both cases remains similar, indicating the possibility of effective application of either model in practical conditions depending on the required level of detail and available computational resources. Graphical representation of the results clearly illustrates the dynamics of distance changes as a function of the angle between the courses of approaching vessels, which can be used in the development of software for navigation systems. The obtained dependencies allow not only quantitative assessment of allowable approach distances but also account for the influence of the approach aspect, which significantly affects the decision-making process by both navigators and automated collision avoidance systems. The results create a foundation for further improvement of collision avoidance algorithms and contribute to increasing the level of automation in navigation processes and overall maritime safety, especially in conditions of heavy traffic or restricted waterways.

Keywords: *safety domain, vessel collision avoidance, approach distance, elliptical domain, collision evasion, vessel traffic management.*

Introduction. In modern maritime transport, ensuring safe and accident-free navigation, particularly in restricted or narrow waterways, represents one of the most critical challenges facing navigational science and practice. The continuous increase in maritime traffic intensity, growing dimensions of modern commercial and passenger vessels, as well as the increasing complexity of navigational conditions in high-density traffic areas create unprecedented challenges for navigators and developers of vessel traffic management systems. Under such conditions, the issue of ensuring reliable collision avoidance between vessels on converging or crossing courses becomes paramount for minimizing collision risks.

Timely and well-founded decision-making regarding course or speed alterations requires precise criteria for evaluating safe distances between vessels. In this context, the concept of a vessel safety domain - a spatial area surrounding a vessel that should not be violated by other watercraft to avoid

dangerous proximity - assumes particular significance. Accurate determination of the shape and dimensions of this zone constitutes a key element for developing effective algorithms for automated collision avoidance systems.

The relevance of this research is emphasized by the fact that in real maritime traffic conditions, vessels rarely approach on strictly opposing courses. Disregarding the approach direction, vessel type, maneuverability, speed, and dimensions inevitably leads to erroneous decisions. Therefore, the task of constructing an adaptive model of the vessel safety domain that accounts for variable parameters of the navigational environment and allows for precise determination of the critical allowable approach distance is not only scientifically interesting but also practically significant for enhancing overall maritime safety.

Despite significant contributions to the development of collision avoidance methods, a critical gap remains in understanding how vessel safety domains should dynamically adapt to changes in navigational conditions, vessel characteristics, and approach scenarios. Current models often employ static, symmetrical safety zones that do not account for the directional nature of collision risk and variable vessel maneuverability under different operational conditions. This research aims to address this gap by developing an adaptive model of vessel safety domains that incorporates multidimensional parameters, including vessel type, size, speed, maneuverability, traffic density, and environmental conditions.

Furthermore, the integration of such adaptive safety domains into automated collision avoidance systems presents significant challenges related to computational efficiency, real-time implementation, and compliance with international maritime regulations. This study proposes a novel framework that combines theoretical rigor with practical applicability in modern vessel traffic management systems, potentially revolutionizing the approach to collision avoidance in increasingly congested waterways.

Analysis of recent research and problem statement. The principles and methods of external control of vessel collision avoidance processes are detailed in works [1-3]. This fundamental research examines not only the primary methods of external control of vessel collision avoidance processes but also their theoretical foundation from the perspective of mathematical modeling and systems analysis. The proposed methods are based on utilizing domains of dangerous courses for approaching vessels and their dangerous speeds for comprehensive assessment of the risk level in approach situations. The authors developed an algorithmic procedure for determining optimal parameters of avoidance maneuvers considering navigational constraints and dynamic characteristics of vessels [4]. Special attention in the work is devoted to issues of coordinating vessel interaction during the execution of avoidance maneuvers and the possibility of accounting for the human factor in decision-making during critical situations. The proposed methodology also includes analytical expressions for evaluating the effectiveness of the selected avoidance maneuver in terms of minimizing loss of voyage time and fuel consumption [5, 6].

The method of vessel collision avoidance at sea by shifting to a line parallel to the path, at a specific angle to the programmed course line, is thoroughly investigated in the monograph [7]. The authors of the monograph presented not only the theoretical foundation of this method but also the results of its experimental verification based on simulation modeling and field trials. The proposed method allows for formalizing the process of selecting a safe maneuver considering hydrometeorological conditions, navigation intensity, and characteristics of the navigation area. As correctly noted in this fundamental work, a significant increase in the effectiveness of vessel collision prevention can be achieved through the development and implementation of innovative avoidance algorithms and intelligent decision support systems. The authors propose the concept of an adaptive collision prevention system capable of adjusting its parameters depending on changing external conditions and the behavior of other vessels [8-9].

Fundamental principles of external and locally-independent control of the collision avoidance process for vessels in dangerous proximity are comprehensively presented in work [10]. The authors thoroughly analyze the advantages and limitations of each control approach, as well as conditions for their effective application in various navigational situations. The work also contains a critical analysis of existing methods for vessel collision prevention and proposes ways to improve them considering modern technical capabilities and regulatory requirements. Special attention is devoted to issues of information support for the decision-making process and reducing uncertainty in assessing vessel movement parameters under conditions of limited visibility and complex navigational environments. The methodology proposed by the authors allows for formalizing the process of selecting an avoidance strategy taking into account the multi-criteria nature of this task and the uncertainty of initial information.

In cases of dangerous approach of a vessel with two targets, which significantly complicates the task of safe collision avoidance, work [11, 12] proposes an innovative method for forming domains of impermissible values of vessel movement parameters with respect to each target. The authors developed a comprehensive procedure for assessing the danger level of the emerging approach situation for each target using special collision risk indicators and a system for their integral evaluation. This research demonstrates the fundamental possibility of selecting an optimal avoidance maneuver through general evasion from both targets based on multi-criteria optimization. Three characteristic situations of a vessel approaching two targets are considered: crossing courses, overtaking, and head-on encounter. For each situation, algorithms for selecting a safe maneuver were developed and verified through simulation modeling methods.

The original description of the vessel collision avoidance process in terms of differential antagonistic game is presented in [13]. The authors formalize the vessel collision avoidance problem as a conflict situation with opposing interests among participants and propose methods for its resolution based on optimal control theory and differential games. This approach allows for consideration of active countermeasures between vessels and uncertainty in their intentions when selecting an avoidance strategy. The study defines necessary and sufficient conditions for the existence of a game solution, and develops effective numerical methods for determining it. The algorithms proposed by the authors can be implemented in onboard decision support systems and ensure guaranteed safe passage of vessels even under conditions of information deficit regarding the intentions of other traffic participants [14].

The work [15] examines in detail the emergency avoidance strategy in critical situations of excessive vessel proximity, when standard methods can no longer be applied due to deficits of time and maneuvering space. The authors propose an innovative approach to selecting parameters for emergency maneuvers, based on the principle of maximizing the vessel's dynamic capabilities while minimizing collision risk. The developed models and algorithms take into account actual vessel handling characteristics, including inertia, control system delay, and maneuvering intensity limitations. Methods for adapting the emergency avoidance strategy to specific navigation conditions and technical capabilities of the vessel are proposed. The results of theoretical research are confirmed by data from field tests and computer modeling.

The issue of selecting the optimal standard collision avoidance maneuver for two vessels is analyzed in detail in [16, 17]. The authors formulate the optimization problem as multi-criteria, taking into account not only the safety of the maneuver, but also its economic efficiency, operational constraints, and compliance with international regulations for preventing collisions at sea. The study develops mathematical models and optimization methods for parameters of standard collision avoidance maneuvers, including course alterations, speed adjustments, or

their combination. Optimality criteria are proposed that account for safety, cost-effectiveness, and regulatory compliance. The results of theoretical research are validated through simulation data of typical vessel encounter situations under various navigational conditions [18].

In [19], innovative distributed algorithms for developing collision avoidance strategies involving multiple vessels in situations of dangerous proximity are presented. The authors propose a decentralized approach to coordinating vessel actions, based on information exchange regarding intentions and parameters of planned maneuvers through automatic identification systems. The developed algorithms ensure coordinated maneuvering of vessels without requiring centralized control, thereby enhancing the reliability and efficiency of the collision avoidance process in complex navigational environments. Paper [20, 21] presents the results of simulation modeling of distributed algorithms in various vessel traffic scenarios and demonstrates their advantages compared to traditional collision prevention methods.

Paper [22, 23] provides rigorous analytical expressions for calculating the boundaries of domains of dangerous courses and dangerous speeds under external control of the vessel collision avoidance process. The authors derived exact formulas for determining the boundaries of prohibited values of one vessel's courses and another vessel's speeds, taking into account their relative positions, dimensions of safety zones, and dynamic characteristics. Special attention is given to the graphical representation of these domains for visualization and operational assessment of the navigational situation. The proposed methods allow for real-time determination of safe vessel movement parameters and selection of optimal collision avoidance maneuvers. The results of theoretical research are confirmed by numerical modeling data and comparison with established empirical rules.

The theoretical foundation for an autonomous vessel collision avoidance system is presented in the fundamental work [24]. The authors developed a comprehensive collision avoidance algorithm based on principles of artificial intelligence and modern methods of optimal control. The study systematizes and generalizes various approaches to vessel control automation in collision prevention tasks. The authors distinguish two main research directions: the first is based on the application of mathematical models and analytical algorithms, while the second utilizes artificial intelligence methods, including neural networks, fuzzy logic, and evolutionary algorithms. A comparative analysis [25, 26] of the effectiveness of these approaches in various navigational situations is conducted, and recommendations for their practical application are formulated. The research also presents a concept for a hybrid collision prevention system that integrates the advantages of both approaches and ensures high reliability of decision-making under conditions of uncertainty in initial information and complex navigational environments. The architectural solutions and algorithms proposed by the authors can serve as a foundation for the development of advanced intelligent maritime safety systems.

The purpose and tasks of the study. Analysis of the current state of the problem indicates the necessity of employing more precise mathematical models and algorithms for determining safe vessel collision avoidance parameters, taking into account their maneuvering characteristics and specific navigational conditions. Traditional approaches to formalizing the vessel collision avoidance process are predominantly based on simplified safety domain models, which do not always adequately reflect actual navigational conditions.

As demonstrated in [27], the condition for safe vessel passage is determined by the equality of the closest point of approach distanceня D_{min} the minimum permissible approach distance D_d, i.e. $D_{min}=D_d$ under the condition that vessels are converging. This fundamental principle serves as the starting point for developing effective algorithms for preventing vessel collisions at sea and forms the basis for mathematical modeling of the collision avoidance process.

Traditionally, the minimum permissible approach distance D_d is independent of the relative positions of converging vessels and is assumed to be constant in magnitude, implying that a vessel's safety domain has a circular shape and is defined in relative motion space. This approach, although characterized by simplicity, fails to account for the maneuvering characteristics of different vessel types and the asymmetry of their safety domains under real navigational conditions.

However, in recent years, more than ten safety domain shapes distinct from circles have been proposed. Their application allows for more accurate modeling of vessel interaction dynamics and more efficient utilization of available navigational space. Therefore, the minimum permissible approach distance D_d when using such domains is not constant but depends on the relative aspect of converging vessels, which significantly complicates algorithms for collision risk assessment and optimal avoidance maneuver selection.

The value of the minimum permissible approach distance between vessels, accounting for the safety domain shape, depends on the side of relative evasion and is determined by the limiting relative courses K_{ot}^{s} and K_{ot}^{p} and the bearing angles. Therefore, we denote D_d^s and D_d^p - as the minimum permissible approach distances for relative evasion to starboard and port respectively, as shown in Fig. 1.

Figure 1 presents a geometric scheme for determining the maximum permissible approach distance between vessels, taking into account the shape of the target's safe domain. The diagram shows two vessels: the own vessel and the target. Around the target, a safe domain in the form of an ellipse is shown, which defines the area within which approach is considered dangerous.

From the own vessel to the target, two directions are drawn, corresponding to possible evasion options - to the right and to the left. For each of these directions, the limiting relative evasion courses are determined: Kotp* - when deviating to the right, Kots* - when deviating to the left. Accordingly, the maximum permissible approach distances for each option are denoted as D_{dp}* (to the right) and D_{ds}* (to the left).

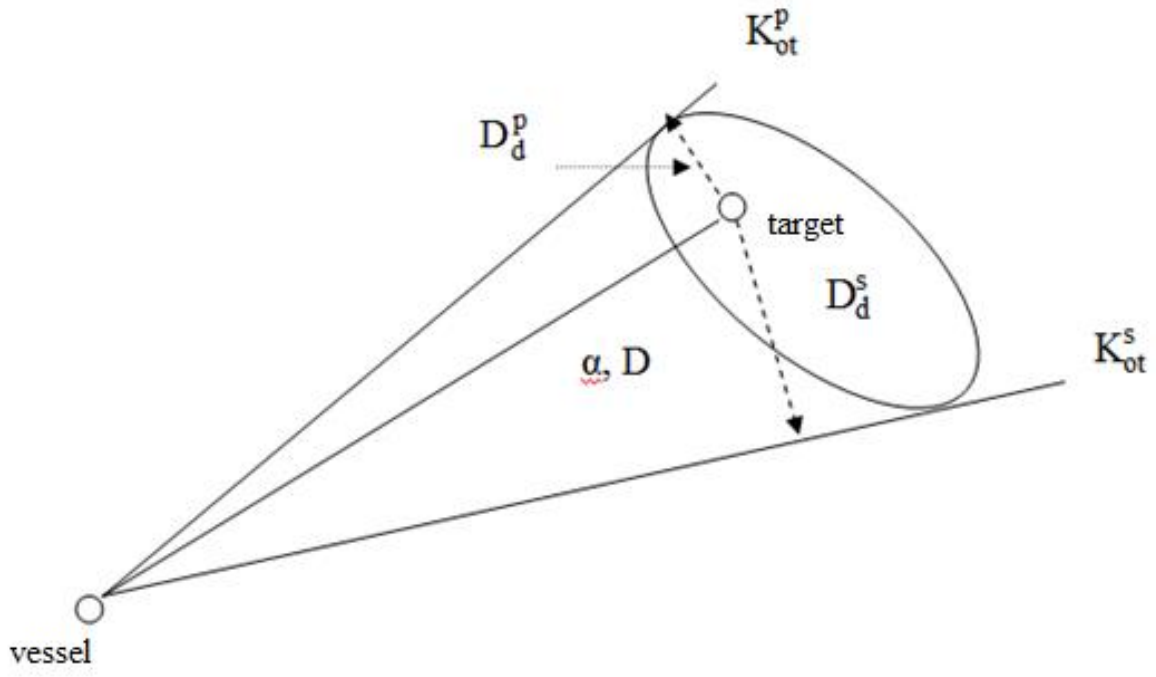

Fig. 1. **Minimum permissible approach distances**

The angle α denotes the course angle to the target, and D represents the current distance between the vessels. Dotted lines show the directions to the points of tangency of trajectories to the boundary of the

safe domain, which determine the values of the maximum permissible approach distances for each evasion option.

Thus, the figure illustrates that the value of the maximum permissible approach distance depends both on the shape of the safe domain and on the chosen side of evasion, and is also determined by the corresponding limiting relative courses and course angles. This allows for obtaining expressions for calculating the maximum permissible approach distances in each specific case of maneuvering.

From this same figure, expressions for determining the minimum permissible approach distances can be derived

$$D_d^s = D|\sin(K_{\text{ot}}^s - \alpha)|, \quad D_d^p = D\left|\sin(K_{\text{ot}}^p - \alpha)\right|,$$

where D and α are the distance to the target and bearing to the target, respectively.

To achieve the stated objective, it is necessary to solve several interrelated tasks. First, to derive analytical expressions for calculating the limiting relative evasion courses of a vessel for various safety domain shapes. Second, to develop algorithms for calculating the minimum permissible approach distance for safety domains of different shapes. Third, to investigate the dependency of the minimum permissible approach distance on target aspect for domains of elliptical and complex shapes. And finally, to conduct a comparative analysis of the characteristics of safety domains of various shapes and determine the most effective domain shape for practical application in decision support systems for vessel collision avoidance [28].

Let us consider two types of domains, for each of which it is necessary to find expressions for the limiting relative evasion courses K_{ot}^s and K_{ot}^p with subsequent development of procedures for calculating the minimum permissible approach distances D_d^s and D_d^p. This task has significant practical importance, as it enables the development of more accurate algorithms for monitoring vessel traffic safety and optimizing their collision avoidance maneuvers.

First, let us examine the analytical expressions for limiting relative evasion courses for a domain of elliptical shape, which we will denote as $D_b^{(\text{El})}$. n this case, the relative course of minimum evasion K_{otymin} is determined by the tangent to the domain boundar $D_b^{(\text{El})}$, he position of which depends on the target aspect. In [14], expressions for calculating the limiting relative evasion courses were derived, which are defined as follows:

$$K_{\text{ot}}^s = max\{\bar{K}_{\text{ymin1}}, \bar{K}_{\text{ymin2}}, \bar{K}_{\text{ymin3}}, \bar{K}_{\text{ymin4}}\}.$$
$$K_{\text{ot}}^p = min\{\bar{K}_{\text{ymin1}}, \bar{K}_{\text{ymin2}}, \bar{K}_{\text{ymin3}}, \bar{K}_{\text{ymin4}}\}.$$

In the last expression:

$$\bar{K}_{\text{ymin1,2}} = arctg\frac{\bar{X}_o \pm b\sqrt{1-\frac{x_1^2}{a^2}}\sin K_c + x_1 \cos K_c}{\bar{Y}_o \pm b\sqrt{1-\frac{x_1^2}{a^2}}\cos K_c - x_1 \sin K_c};$$
$$\bar{K}_{\text{ymin3,4}} = arctg\frac{\bar{X}_o \pm b\sqrt{1-\frac{x_2^2}{a^2}}\sin K_c + x_2 \cos K_c}{\bar{Y}_o \pm b\sqrt{1-\frac{x_2^2}{a^2}}\cos K_c - x_2 \sin K_c}, \quad (1)$$

where

$$x_1 = -\frac{a^2cb}{a^2 + c^2r^2} + \sqrt{(\frac{a^2cb}{a^2 + c^2r^2})^2 - \frac{a^2c^2(b^2 - r^2)}{(a^2 + c^2r^2)}};$$

$$x_2 = -\frac{a^2cb}{a^2 + c^2r^2} - \sqrt{(\frac{a^2cb}{a^2 + c^2r^2})^2 - \frac{a^2c^2(b^2 - r^2)}{(a^2 + c^2r^2)}};$$

$$c = \frac{a^2}{b(\bar{Y}_o \sin K_c - \bar{X}_o \cos K_c)};$$

$$r = (\bar{Y}_o \cos K_c + \bar{X}_o \sin K_c).$$

For calculating the limiting relative evasion courses and minimum permissible approach distances, a computer program was developed that, depending on the angle $\xi = K_{ot}^s - \alpha$ calculates the value of the minimum permissible approach distance $D_d(K_c)$, as shown in Fig. 2. This enabled obtaining quantitative characteristics of the dependency of the minimum permissible approach distance on the relative position of vessels and substantiating the selection of an optimal safety domain shape.

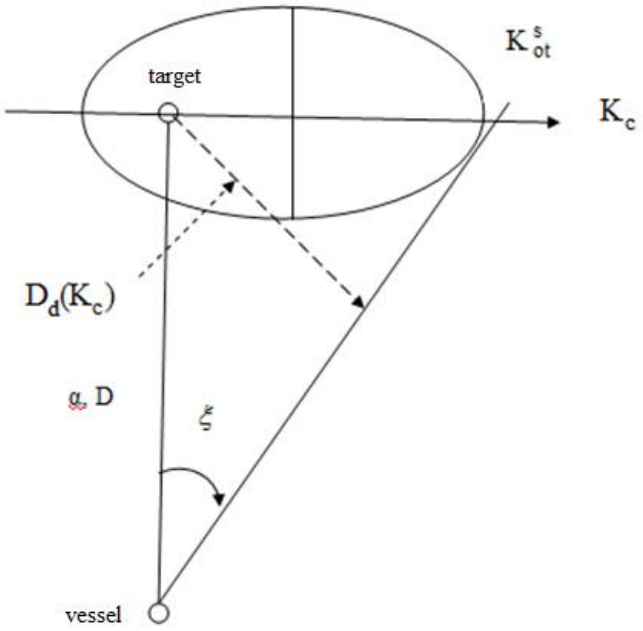

Fig. 2. **Dependence of distance $D_d(K_c)$ on angle ξ**

The figure schematically shows a geometric interpretation of the process of determining the limit distance of a vessel's approach to the target in the plane of relative courses. The oval in the upper part of the figure denotes the safe domain of the target, which is modeled as an ellipse. The center of the ellipse corresponds to the position of the target. Two lines are drawn from the target: one perpendicular to the major axis of the ellipse, the other at a certain angle to this axis, illustrating possible approach trajectories.

From the vessel, located in the lower part of the figure, two vectors are drawn:

- the first vector (solid line) connects the vessel with the target and indicates the current distance D between them;

- the second vector (dashed line) shows the direction to the point of tangency of the vessel's trajectory to the boundary of the target's safe domain, which determines the limit approach distance $D_d(K_c)$.

The angle ξ illustrates the deviation of the vessel's course relative to the target, and α is the angle between the direction to the target and the direction of the vessel's movement. The axis K_c denotes the relative course of the vessel, and K_{ot}^s is the evasion course.

Thus, the figure illustrates the spatial relationship between the vessel, the target, and the safe domain, as well as the geometric approach to determining the limit approach distance for constructing evasion algorithms.

By varying the bearing from від 5° to 360° he program calculated the corresponding values of the limiting relative evasion course K_{ot}^s and distance $D_d(K_c)$. The calculation results are presented in Fig. 3, with the right part showing the graphical dependency of the minimum permissible approach distance on the value of the angle ξ. The obtained results allow us to conclude that there is a significant dependency of the minimum permissible approach distance on the target aspect, which must be taken into account when developing vessel collision avoidance algorithms.

Let us consider the calculation of limiting relative evasion courses for a safety domain $D_b^{(\text{RE})}$ complex shape, which represents a combination of half an ellipse and half a circle. As previously indicated, the limiting relative evasion course of a vessel is the tangent from the vessel's position to the target's safety domain. In [22], it is shown that in the general case, the relative minimum evasion course of a vessel $\bar{K}_{\text{ymin}}$:

$$\bar{K}_{\text{ymin}} = \begin{cases} K_{\text{otn}} + arcsin\dfrac{R_b}{D}, \text{ if } sin\,\beta < 0, \\ max\{\bar{K}_{\text{ymin1}}, \bar{K}_{\text{ymin2}}, \bar{K}_{\text{ymin3}}, \bar{K}_{\text{ymin4}}\}, \text{ if } sin\,\beta > 0, \end{cases}$$

where $\bar{K}_{\text{ymin1}}$, $\bar{K}_{\text{ymin2}}$, $\bar{K}_{\text{ymin3}}$ and $\bar{K}_{\text{ymin4}}$ are determined by expression (1),
β - the bearing angle from the target to the vessel.

In Figure 3, the results of numerical modeling of changes in the maximum permissible approach distance between vessels depending on the target bearing angle with an elliptical shape of the safe domain are presented. The central part of the figure contains a polar diagram, where the elliptical safe domain of the target is highlighted in yellow, modeling the area within which the approach of vessels is considered dangerous. From the center of the domain, numerous radial lines are drawn in different directions, corresponding to different values of the bearing angle (from 5° to 360°). On each line, a point of tangency to the boundary of the ellipse is marked, which determines the maximum permissible approach distance for the corresponding direction.

To the right of the main diagram, a graph shows the relationship between the maximum permissible approach distance and the bearing angle value. The x-axis represents the angle (from 0° to 360°), and the y-axis shows the corresponding distance. The graph demonstrates the non-uniform nature of changes in this distance: maximum values are observed in directions that coincide with the major axis of the ellipse, while minimum values correspond to directions along the minor axis. This indicates a significant dependence of the maximum permissible approach distance on the target's aspect.

The obtained results confirm that when developing algorithms for vessel collision avoidance, it is necessary to consider not only the absolute value of the distance but also its dependence on the approach direction and the geometry of the safe domain. This approach allows for improving the accuracy and reliability of automated collision avoidance systems in complex navigational situations.

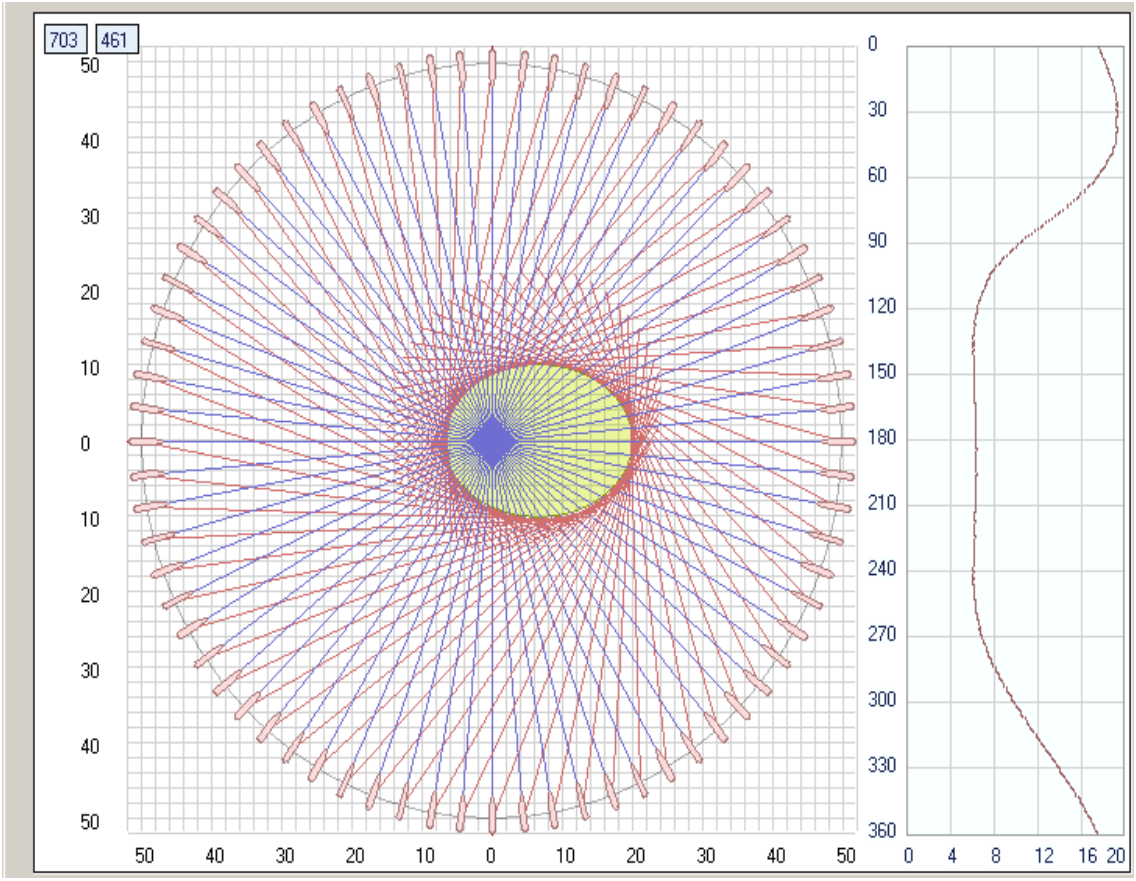

Fig. 3. **Change in distance $D_d(K_c)$ with elliptical domain shape**

As in the previous case, the developed computer program was used to calculate the limiting relative courses and values of the minimum permissible approach distance $D_d(K_c)$ for a domain $D_b^{(RE)}$ of complex shape, the nature of change of which depending on the angle is shown in Fig. 4. In the central part of the figure, a safe domain with a combined, asymmetric shape (green area) is shown, which combines the properties of an ellipse and a semicircle. This domain shape allows for more accurate consideration of the characteristics of vessels' mutual movement in various navigational situations.

From the center of the domain, numerous radial lines (red color) are drawn in all directions, corresponding to different values of the bearing angle from 0° to 360°. On each line, a point of tangency to the boundary of the complex domain is marked, which determines the maximum permissible approach distance for the corresponding direction. This allows for visual assessment of how the safe distance changes depending on the target's aspect.

To the right of the main diagram, a graph shows the relationship between the maximum permissible approach distance and the bearing angle. The x-axis represents the angle (from 0° to 360°), and the y-axis shows the corresponding distance. The graph demonstrates the non-uniform nature of changes in this distance: both maximum and minimum values are observed depending on the approach direction, reflecting the complexity of the domain geometry.

The results presented in Figure 4 allow for evaluating the influence of the safe domain shape on the maximum permissible approach distance and justifying the selection of the optimal domain shape for different types of vessels and navigational situations. This, in turn, contributes to improving the accuracy of collision risk assessment and the effectiveness of choosing the optimal evasion maneuver, which is important for the development of modern intelligent collision prevention systems, including those for autonomous navigation.

These results allow for evaluating the influence of the safe domain shape on the maximum permissible approach distance and justifying the selection of the optimal domain shape for different types of vessels and navigational situations.

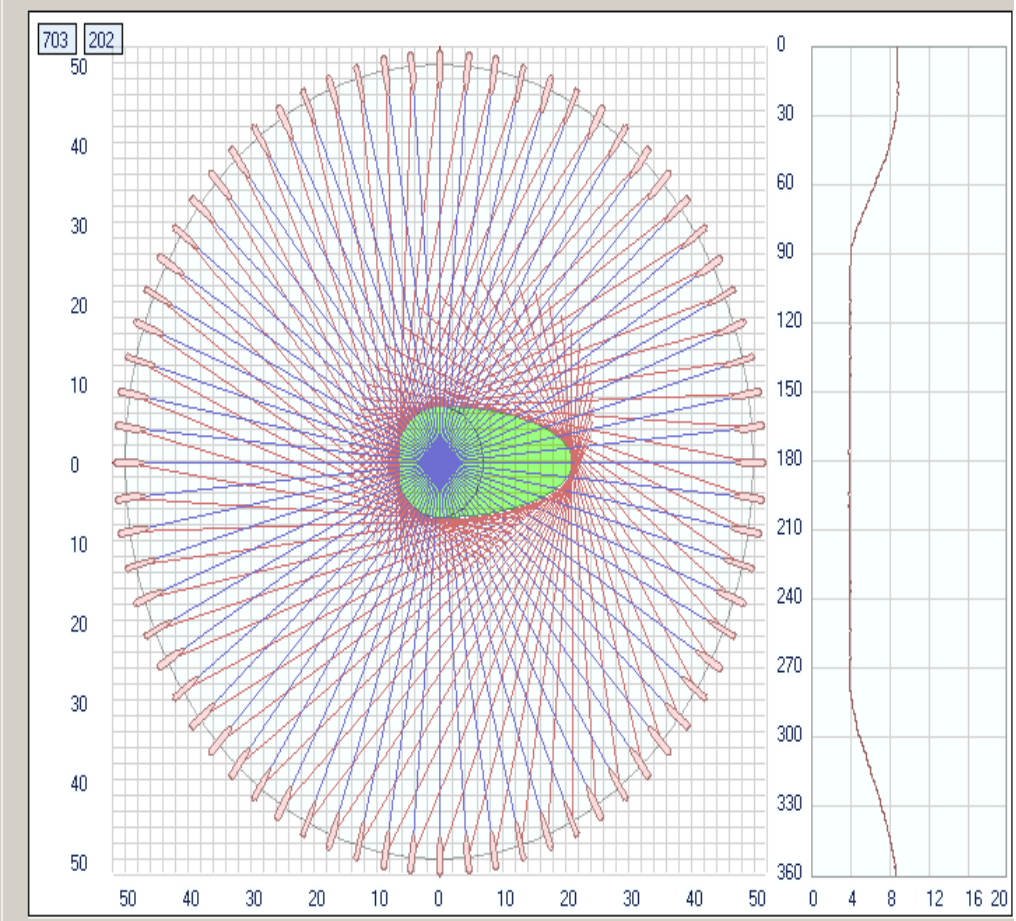

Fig. 4. **Change in distance$D_d(K_c)$ of a complex-shaped domain**

Analyzing the results presented in Figures 3 and 4, it can be noted that both safe domains-elliptical and complex shapes-demonstrate a similar pattern of changes in the maximum permissible approach distance depending on the vessel's aspect. In particular, for both domains, significant variability of this distance is observed depending on the target bearing angle: maximum distance values occur in directions close to the longitudinal axis of the vessel, while minimum values correspond to directions that match transverse aspects. This pattern indicates the necessity of considering the target's orientation when developing collision avoidance algorithms.

At the same time, the complex domain, which combines elements of an ellipse and a semicircle, provides a more flexible and realistic model of the safe zone, allowing for more accurate reproduction of vessel maneuvering characteristics in various navigational situations. However, given the similarity of the obtained results, for practical applications it is advisable to choose the domain that provides an optimal balance between assessment accuracy and computational efficiency. This is especially important for automatic collision prevention systems, where information processing speed and decision-making reliability are critical.

Below is a comparative table and graph illustrating the dependence of the minimum safe approach distance between vessels on the target bearing angle for two different forms of safety domain: elliptical (Fig. 3) and complex (Fig. 4). The data were obtained through numerical modeling and reflect the pattern of distance changes for different approach directions.

Table 1. **Comparison of Minimum Safe Approach Distances for Elliptical and Complex Safety Domains at Different Target Bearing Angles**

Bearing angle (degrees)	Distance (Elliptical domain), miles	Distance (Complex domain), miles
0	3.20	3.00
30	3.17	3.18
60	2.29	2.45
90	0.80	1.00
120	2.29	2.28
150	3.17	3.08
180	3.20	3.00
210	3.17	3.18
240	2.29	2.45
270	0.80	1.00
300	2.29	2.28
330	3.17	3.08
360	3.20	3.00

The graph (Fig. 5.) constructed from these data clearly demonstrates that for both types of domains, the minimum safe approach distance has maximum values at bearings of 0°, 180°, and 360° (i.e., when the target is ahead or behind), and minimum values at bearings of 90° and 270° (target abeam). For the complex domain, the pattern of distance change is more smoothed, and the minimum values are slightly larger, reflecting the greater "width" of the safety zone in the transverse direction.

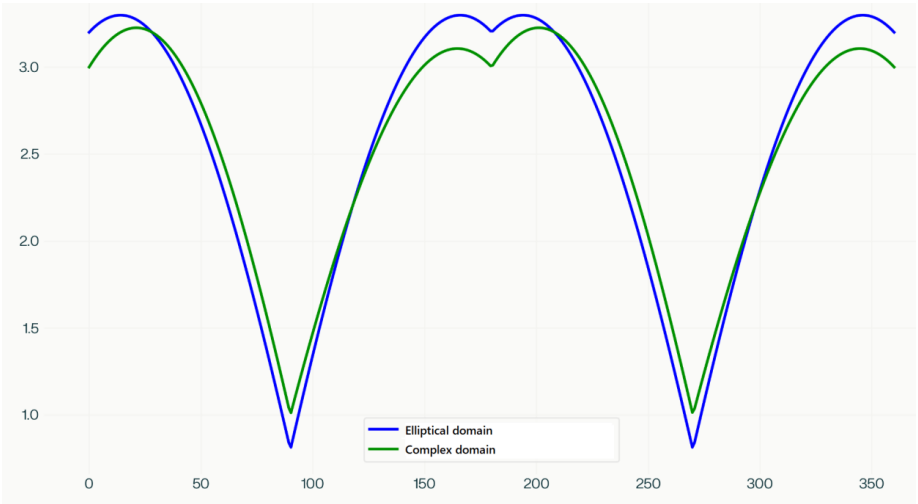

Fig. 5. **Dependence of Minimum Safe Approach Distance on Target Bearing Angle**

The graph shows two curves: blue - for the elliptical domain, green - for the complex domain. The horizontal axis represents the target bearing angle (from 0° to 360°), while the vertical axis shows the maximum allowable approach distance in nautical miles. Both curves have pronounced minimum values in the transverse sectors and maximum values in the bow and stern parts. This confirms the importance of taking into account the direction of approach when calculating the safe distance and selecting the optimal domain shape for different navigational situations.

Solving these tasks will contribute to improving the accuracy of assessing the level of danger during vessel encounters, which, in turn, will enable more effective selection of optimal evasive maneuvers. This approach will not only reduce the risk of emergency situations at sea but also significantly increase the overall level of maritime safety. Furthermore, the developed methods can be integrated into advanced intelligent collision avoidance systems, including autonomous vessel complexes capable of adapting to dynamic changes in the navigational environment and making decisions in real-time.

Conclusions. The analytical study of changes in the maximum permissible approach distance between vessels, taking into account the shape of the vessel domain, has resulted in new analytical dependencies that consider both the safe domain shape and the target aspect angle. The proposed expressions for calculating this distance for both elliptical and complex (combined) domains allow for flexible assessment of approach situations depending on the configuration of vessels' relative movement.

The research established that the nature of changes in the maximum permissible approach distance has a significant dependence on the approach direction, which is confirmed by graphical results of numerical modeling. The analysis showed that while elliptical and complex domains differ geometrically, the pattern of changes in the limiting approach distance remains similar in both cases. This indicates that in practical applications, both domain types can be used as tools for modeling safe space around a vessel, considering the chosen level of detail and available computational resources.

It was determined that using a complex-shaped domain allows for more accurate consideration of vessel maneuvering characteristics in various navigational situations. However, for practical implementation, it is advisable to choose a domain shape that provides an optimal balance between assessment accuracy and computational efficiency.

The obtained dependencies allow not only for quantitative evaluation of the permissible approach distance but also account for the influence of the approach aspect, which significantly affects decision-making by navigators or automated collision avoidance systems. The graphical presentation of results provided a visual demonstration of the distance dynamics depending on the angle between approaching vessels' courses, which can be used in the development of navigation system software.

These results can serve as a foundation for further improvement of collision avoidance algorithms and contribute to increasing the level of automation in navigational processes and overall maritime safety. The proposed approach allows for considering not only the absolute value of distance but also its dependence on the approach direction and safe domain geometry, which is crucial for modern intelligent navigation support systems, including those for autonomous vessels.

REFERENCES

1. Y., Wu, D., Wang, H., & Lou, J. (2025). Dynamic collision avoidance for maritime autonomous surface ships based on deep Q-network with velocity obstacle method. *Ocean Engineering*, *320*, 120335. https://doi.org/10.1016/j.oceaneng.2025.120335.
2. Burmaka, I., Vorokhobin, I., Melnyk, O., Burmaka, O., & Sagin, S. (2022). Method of Prompt Evasive Manuever Selection to Alter Ship's Course or Speed. *Transactions on Maritime Science*, *11*(1), 7-15. https://doi.org/10.7225/toms.v11.n01.w01.
3. Chen, Y., Du, W., Hu, X., Bai, G., & Zhang, J. (2022). USV collision hazard assessment and track planning algorithm. *Ocean Engineering*, *261*, 112149. https://doi.org/10.1016/j.oceaneng.2022.112149.
4. Bolbot, V., Gkerekos, C., Theotokatos, G., & Boulougouris, E. (2022). Automatic traffic scenarios generation for autonomous ships collision avoidance system testing. *Ocean Engineering, 254*, 111309. https://doi.org/10.1016/j.oceaneng.2022.111309.
5. Sahin, S. S., & Sahin, S. V. (2024). Use of a hybrid system for coordinating marine vessel movement during maneuvering in confined waters. *Water Transport*, *3*(41), 208-215. [in Ukraine]. https://doi.org/10.33298/2226-8553.2024.3.41.24

6. Petrychenko, O. A. (2018). Method for choosing divergence maneuver using electronic chart. In *Proceedings of the 10th International Scientific and Practical Conference "Modern Information and Innovative Technologies in Transport (MINTT-2018)"* (pp. 128–130). Kherson: KhDMA.
7. Burmaka, I., Borodulin, A., Fedorov, D., & Petrychenko, O. (2021). External control of the divergence process taking into account the form of the safety domain. *Transport Means - Proceedings of the International Conference, 2021-October*, 579-583.
8. Sahin, S. V., & Sahin, S. S. (2023). Determining the method of marine transport vessel movement management during ensuring their safe divergence. *Water Transport*, *2*(38), 187-195. [in Ukraine]. https://doi.org/10.33298/2226-8553.2023.2.38.20.
9. Vorokhobin, I., Burmaka, I., Fusar, I., & Burmaka, O. (2022). Simulation modeling for evaluation of efficiency of observed ship coordinates. *TransNav: International Journal on Marine Navigation and Safety of Sea Transportation, 16*(1), 137-141.
10. Zhou, J., Ding, F., Yang, J., Pei, Z., Wang, C., & Zhang, A. (2021). Navigation safety domain and collision risk index for decision support of collision avoidance of USVs. *International Journal of Naval Architecture and Ocean Engineering, 13*, 340–350. https://doi.org/10.1016/j.ijnaoe.2021.03.001.
11. Xu, X., Lu, Y., Liu, G., Cai, P., & Zhang, W. (2022). COLREGs-abiding hybrid collision avoidance algorithm based on deep reinforcement learning for USVs. *Ocean Engineering, 247*, 110749. https://doi.org/10.1016/j.oceaneng.2022.110749.
12. Zhou, X., Qu, M., Zhou, C., Wang, C., & Zhao, W. (2024). Personalized active collision avoidance trajectory planning and variable time domain control integrating driver characteristics. Accident Analysis & Prevention, 208, 107764. https://doi.org/10.1016/j.aap.2024.107764.
13. Tsymbal, M., Volkov, E., & Korolyova, T. (2021). Method of ships' collision avoidance by parallel indexing. *TransNav, International Journal on Marine Navigation and Safety of Sea Transportation, 15*(1), 119–126.
14. Mazur, O. M., Volianska, Y. B., Vorokhobin, I. I., Onyshchenko, O. A., & Burmaka, I. O. (2021). On the assessment of energy consumption during course stabilization of an autonomous floating apparatus. In *Proceedings of the First International Scientific and Technical Conference "Progressive Technologies of Transport Means" (pp. 136-137)*. Ukrainian State University of Railway Transport, Myrhorod, Ukraine.
15. Sagin, A. S., & Sagin, S. V. (2024). Experimental determination of optimal phases of fuel supply to the cylinder of marine diesel engines. Water Transport, 1(39), 215-222. https://doi.org/10.33298/2226-8553.2024.1.39.22.
16. Zhang, M., Taimuri, G., Zhang, J., Zhang, D., Yan, X., Kujala, P., & Hirdaris, S. (2025). Systems driven intelligent decision support methods for ship collision and grounding prevention: Present status, possible solutions, and challenges. *Reliability Engineering & System Safety, 253*, 110489. https://doi.org/10.1016/j.ress.2024.110489.
17. He, Z., Liu, C., Chu, X., Wu, W., Zheng, M., & Zhang, D. (2024). Dynamic domain-based collision avoidance system for autonomous ships: Real experiments in coastal waters. *Expert Systems with Applications, 255*(D), 124805. https://doi.org/10.1016/j.eswa.2024.124805.
18. Volianskyi, S. M., Halahan, S. M., Mazur, O. M., Naleva, H. V., Korban, V. K., & Yaremenko, V. A. (2024). Fuzzy control systems for electromechanical systems of small unmanned maritime vessels. *Herald of the Odesa National Maritime University, 3*(74), 68–85. https://doi.org/10.47049/2226-1893-2024-3-68-85.
19. Holikov, V. A., Naleva, H. V., Mazur, O. M., & Onyshchenko, O. A. (2024). Fuzzy controller for autopilot of small unmanned maritime vessel. In *Proceedings of the Scientific and Technical Conference "Marine and River Fleet: Operation and Repair" (pp. 11-15)*. Odesa: National University "Odessa Maritime Academy."
20. Vorozobin, I. I., Burmaka, I. O., Kulakov, M. O., & Petrychenko, O. O. (2021). Method of electronic chart departmenting during external control of ship divergence in VTS responsibility zone. *Navigation, 33*, 24–32.
21. Bao, Y., & Wang, X. (2024). Optimization of forward collision warning algorithm considering truck driver response behavior characteristics. *Accident Analysis & Prevention, 198*, 107450. https://doi.org/10.1016/j.aap.2023.107450.
22. Wang, J., Wang, R., Lu, D., Zhou, H., & Tao, T. (2022). USV dynamic accurate obstacle avoidance based on improved velocity obstacle method. *Electronics, 11*(17), 2720. https://doi.org/10.3390/electronics11172720.
23. Xie, H., Zhang, Y., Xing, S., & Gao, Z. (2021). A method for ship autonomous collision auoidance based on model predictive control. *Ship Engineering*, *43*(8), 23-28.
24. Pechenyuk, A., & Petrychenko, O. (2021). Prediction of Safe Maneuvers in Restricted Waters as Problem of Navigation and Ship Hydrodynamics. In *Transport Means-Proceedings of the International Conference (pp. 239-244)*.
25. Chen, Y.-L., Du, W.-K., Hu, X.-Y., Bai, G.-Q., & Zhang, J.-B. (2022). USV collision hazard assessment and track planning algorithm. *Ocean Engineering, 261*, 112149. https://doi.org/10.1016/j.oceaneng.2022.112149.
26. Vorokhobin, I., Zhuravska, I., Burmaka, I., & Kulakovska, I. (2021). Analysis of the error distribution density convergence with its orthogonal decomposition in navigation measurements. *Journal of Physics: Conference Series, 2090*, 012126. https://doi.org/10.1088/1742-6596/2090/1/012126.
27. Zhou, J., Ding, F., Yang, J., Pei, Z., Wang, C., & Zhang, A. (2021). Navigation safety domain and collision risk index for decision support of collision avoidance of USVs. *International Journal of Naval Architecture and Ocean Engineering, 13*, 340–350. https://doi.org/10.1016/j.ijnaoe.2021.03.001.
28. Ren, J., Zhang, J., & Cui, Y. (2021). Autonomous obstacle avoidance algorithm for unmanned surface vehicles based on an improved velocity obstacle method. *ISPRS International Journal of Geo-Information, 10*(9), 618. https://doi.org/10.3390/ijgi10090618.

Ігор Бурмака[1], Ольга Петриченко[2] , Богдан Алєксєйчук[3], Алла Виноградова [4]

[1]Професор, завідувач кафедри управління судно, Національний університет «Одеська морська академія», 8, вул. Дідрихсона, Одеса, 65052, Україна. ORCID: https://orcid.org/0000-0002-0853-6884.

[2]Доцент, кафедра морських перевезень, Національний університет «Одеська морська академія», 8, вул. Дідрихсона, Одеса, 65052, Україна. ORCID: https://orcid.org/0000-0002-4893-8204.

[3]Старший викладач, кафедра управління судном, Національний університет «Одеська морська академія», 8, вул. Дідрихсона, Одеса, 65052, Україна. ORCID: https://orcid.org/0000-0003-1043-5174.

[4]Завідувач лабораторії кафедри управління судном, Національний університет «Одеська морська академія», 8, вул. Дідрихсона, Одеса, 65052, Україна. ORCID: https://orcid.org/0009-0007-9406-3203.

Адаптивне моделювання суднових доменів безпеки для запобігання зіткненням у морській навігації

*У цій статті представлено аналітичне дослідження змін критичної допустимої дистанції зближення між суднами, що наближаються, з урахуванням форми зони безпеки судна. Дослідження спрямоване на вирішення важливої проблеми забезпечення безпеки морської навігації шляхом розробки математичного підходу до точного моделювання зон суден за різних сценаріїв зближення. Запропоновано та виведено аналітичні вирази для розрахунку мінімально безпечних дистанцій як для еліптичних зон, так і для зон складної конфігурації, що дозволяє гнучко оцінювати ситуації зближення залежно від взаємного руху суден. Аналіз показує, що хоча еліптичні та складні за формою домени відрізняються геометрично, характер змін критичної дистанції зближення в обох випадках залишається подібним, що свідчить про можливість ефективного застосування будь-якої з моделей у практичних умовах залежно від необхідного рівня деталізації та доступних обчислювальних ресурсів. Графічне представлення результатів наочно ілюструє динаміку змін дистанції як функцію кута між курсами суден, що зближаються, що може бути використано при розробці програмного забезпечення для навігаційних систем. Отримані залежності дозволяють не лише кількісно оцінювати допустимі дистанції зближення, але й враховують вплив аспекту зближення, який суттєво впливає на процес прийняття рішень як судноводіями, так і автоматизованими системами уникнення зіткнень. Отримані результати створюють основу для подальшого вдосконалення алгоритмів уникнення зіткнень і сприяють підвищенню рівня автоматизації навігаційних процесів та загальної безпеки мореплавства, особливо в умовах інтенсивного трафіку або обмежених акваторій***.***

Keywords: *домен безпеки, запобігання зіткненням суден, дистанція зближення, еліптичний домен, ухилення від зіткнень, ракурс зближення, управління рухом суден.*

DOI: 10.32703/2617-9040-2025-45-8

UDC 629.4.023

Olena Sorochynska [1], Oleksandr Melnichenko [2], Ivan Kulbovskyi [3], Igor Derehuz[4]

[1]Associate Professor, Department of Ecology and safety of life, National Transport University, Omelianovycha-Pavlenka str. 1, 01010, Kyiv, Ukraine. ORCID: http://orcid.org/0000-0003-2477-1275.

[2]Associate Professor, Department of Manufacturing, Repair and Materials Engineering, National Transport University, Omelianovycha-Pavlenka str. 1, 01010, Kyiv, Ukraine. ORCID: http://orcid.org/0000-0001-9694-9824.

[3]Associate Professor, Department of Automation and computer-integrated technologies of transport, National Transport University, Omelianovycha-Pavlenka str. 1, 01010, Kyiv, Ukraine. ORCID: http://orcid.org/0000-0002-5329-3842.

[4]Postgraduate student, Department of Transport Law and Logistics, National Transport University, Omelianovycha-Pavlenka str. 1, 01010, Kyiv, Ukraine. ORCID: http://orcid.org/0000-0003-3119-3709.

***Corresponding author:** sorochynska_ol@gsuite.duit.edu.ua

Implementation of the occupational health and safety management system model according to DSTU ISO 45001:2018: challenges and opportunities for transport enterprises

The article examines the features of the implementation of the international standard DSTU ISO 45001:2018 "Occupational health and safety management system" specifically at transport enterprises. The focus is on specific challenges associated with a high level of production risks, the mobility of the working environment and the complexity of technological processes in the transport sector. The key problems of implementing the standard are analyzed, in particular, the insufficient level of staff awareness, the need to modernize existing safety systems and adapt to modern occupational safety requirements. The potential benefits of implementing ISO 45001:2018 are identified, including a reduction in the level of occupational injuries, increasing the effectiveness of risk management and strengthening the image of the enterprise. Practical recommendations are proposed for optimizing the process of implementing the standard, taking into account industry specifics.

***Keywords**: occupational health and safety, ISO 45001:2018, transport enterprises, safety management system, risk management, workplace safety, transport systems.*

Introduction. In the current conditions of Ukraine's economic development, ensuring an adequate level of occupational health and safety and preserving employees' health at enterprises –particularly in the transport sector – is gaining particular importance [1]. This sector is among the most hazardous, as it combines complex technological processes, intensive use of equipment, and high staff mobility. In this regard, the implementation of an occupational health and safety management system in accordance with the requirements of the international standard DSTU ISO 45001:2018 is a crucial condition for enhancing the efficiency of transport enterprises, reducing workplace injuries, and improving the overall level of safety.

The ISO 45001:2018 standard is a modern risk management model in the field of occupational health and safety, providing a systematic approach to identifying, assessing, and controlling hazardous factors. Its implementation not only enhances employee safety but also strengthens the reputation of enterprises operating in accordance with international norms and practices. However, despite the evident advantages, enterprises face several challenges on the path to full integration of this standard, including insufficient funding, inadequate staff qualifications, and limited methodological support.

Analysis of recent research and problem statement. The issue of ensuring occupational safety and reducing industrial risks at enterprises across various sectors, including the transport industry, has become particularly relevant in the context of modern European integration processes and increasing demands for working conditions. In academic literature, considerable attention has been devoted to the development of theoretical and practical aspects of occupational safety management, particularly through the implementation of international standards. These topics have been addressed in the works of O.D. Malko, O.V. Bryhada, B.M. Tsymbal, among others. Scholars have also focused significantly on the assessment of occupational risks at enterprises. Research in the field of occupational risk assessment and management has been conducted by R. Trishch, O. Nechuiviter, Sorokolat N., Fateieva L., O.O., Delini M.M., Van Yi., and others. [2-7].

Research emphasizes the importance of integrating the ISO 45001:2018 standard into an enterprise's management system as a factor in improving occupational safety efficiency and fostering a culture of workplace safety. At the same time, studies dedicated to the specific features of implementing DSTU ISO 45001:2018 in transport enterprises are scarce. Existing works pay insufficient attention to the specifics of the organizational and economic conditions under which the transport sector in Ukraine operates, which significantly affects the adaptation of the standard. Moreover, there is a lack of practical models for integrating the standard's requirements into existing management processes, especially considering the limited resources of small and medium-sized enterprises. Therefore, there is a need for an in-depth analysis of the challenges related to the implementation of DSTU ISO 45001:2018 in the transport sector, the identification of obstacles, and the exploration of prospects for developing an occupational health and safety management system, taking into account the current challenges and conditions of industry enterprises.

The purpose and tasks of the study – The purpose and objectives of this study are to determine the appropriate approach to the assessment of occupational risks in production and the effective management of occupational safety at enterprises in the transport sector of Ukraine through the implementation of modern international risk management standards, with the aim of improving workplace safety conditions at enterprises. The study also aims to analyze the main challenges and prospects of implementing DSTU ISO 45001:2018 in the transport industry, and to formulate recommendations for the effective application of this standard at transport enterprises.

Materials and methods of research. The study employs a comprehensive approach that includes the analysis of the regulatory and legal framework, statistical data, and practical experience in implementing the DSTU ISO 45001:2018 standard at transport enterprises in Ukraine.

The main materials for the analysis were:

- the standard DSTU ISO 45001:2018;
- regulatory acts of Ukraine in the field of occupational safety;
- statistical data from the State Labour Service of Ukraine and the State Statistics Service of Ukraine;
- analytical and scientific publications on the topic of occupational health and safety management systems.

The research methods include:

- content analysis, which enabled the examination of the provisions of the standard and regulatory documents;
- a systems approach to identify interconnections between elements of the occupational health and safety management system;
- comparative analysis used to assess the differences between existing practices and the requirements of the standard;
- SWOT analysis, which helped identify strengths, weaknesses, opportunities, and threats regarding the implementation of ISO 45001:2018 in the context of the transport sector.
- The obtained data served as the basis for drawing conclusions regarding the current state, existing issues, and prospects for implementing an occupational health and safety management system based on the requirements of DSTU ISO 45001:2018.

More than 6300 people die every day as a result of an accident at work or an occupational disease, which is a huge burden on organizations and society as a whole. It is an alarming number and is proof that measures need to be taken in the area of occupational safety and health management (OH&S), which will ultimately lead to a reduction in overall accidents and morbidity. One of the important steps is the implementation of the ISO 45001 standard, which employers can apply in order to ensure more effective health and safety.

New approaches in the occupational safety and health management system require that everyone be aware of the risks they face in the workplace and in their daily lives. The employer's obligation is to identify the risks associated with the work process, to implement risk elimination or minimalization measures, and familiarize its employees with residual risks.

The implementation of the ISO 45001 standard is expected to give priority to an overall improvement in occupational safety and a reduction in accidents at work and occupational diseases.

In recent years, occupational safety has been undergoing profound transformations. The management model of occupational safety is evolving toward a system that involves shared social and economic responsibility between businesses and employees in ensuring safe working conditions. The goal is to enhance the role of social partnership in creating a healthy psychological climate in the workplace and maximizing the well-being of both individual employees and the organization as a whole. Improving workplace safety requires the advancement of principles related to occupational health and industrial safety management. This need is defined by current global trends in occupational safety and the requirements of relevant international regulations.

According to World Bank data on nominal global GDP and gross output, annual economic losses caused by poor working conditions, inadequate occupational health, and safety violations are estimated at 4%, amounting to approximately USD 3.0 trillion. In Ukraine, around 4,000 workers are injured annually in workplace incidents, with approximately 400 fatalities. In 74% of these cases, the primary cause is poor work organization. As a result, during the first quarter of 2023, one-time compensation for permanent loss of professional capacity was granted to 853 victims. The total amount spent on these payments reached UAH 17.8 million, with an average payment per victim of UAH 19,100 - UAH 1,700 or 10% more than in the first quarter of the previous year. As of May 2023, monthly insurance payments were being received by 185,600 individuals affected by workplace accidents and their family members. In total, UAH 973.66 million was allocated for these monthly insurance payments.

Expenditures on fines and compensations due to workplace accidents significantly impact an organization's financial performance. Moreover, such incidents negatively affect overall business operations, leading to reputational damage, additional inspections, and increased scrutiny from supervisory and regulatory authorities. За останні роки ситуація з виробничим травматизмом на підприємствах транспортної галузі погіршується, значною мірою на це впливає недосконала система управління охороною праці (Fig. 1.).

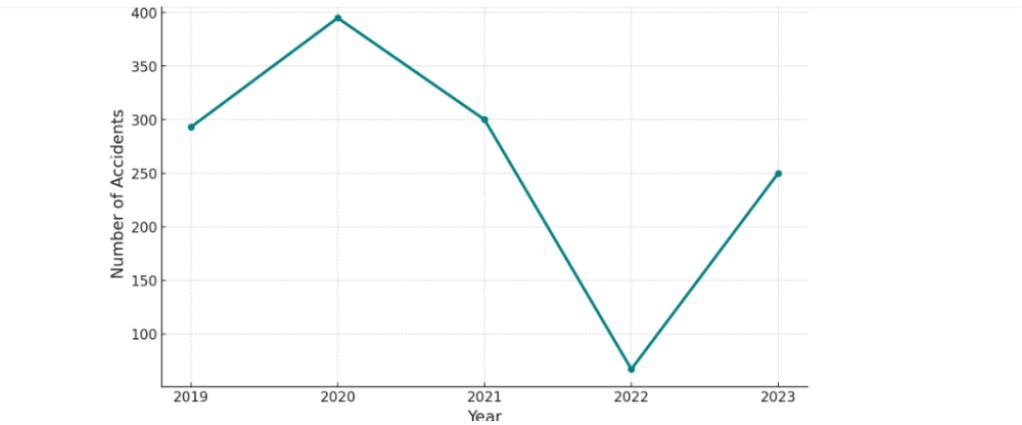

Fig. 1. **Graph of the dynamics of occupational injuries in the transport industry**

Enterprises in the transport sector are considered high-risk for occupational injuries and work-related illnesses. Currently, many transport companies are entering the European market, and therefore must comply with all international standards, including occupational safety requirements.

The study and resolution of issues related to ensuring healthy and safe working conditions is one of the most important tasks in the development of new technologies and production systems. Investigating and identifying potential causes of workplace accidents, occupational diseases, emergencies, explosions, and fires, as well as developing measures and requirements aimed at eliminating these causes, enables the creation of safe and favorable working conditions.

Comfortable and safe working conditions are among the key factors that influence labor productivity, occupational safety, and employee health.

It is globally recognized that the most effective strategy for ensuring and maintaining the highest possible level of workplace safety is the strategy of hazard prevention in the workplace. This strategy involves developing safety measures based on risk assessment procedures.

This approach forms the foundation of occupational health and safety legislation in the industrially developed countries of the European Union and is regularly revised to address current issues related to protecting workers from accidents and occupational diseases.

As part of the Association Agreement with the European Union, Ukraine has committed to gradually reform its regulatory framework over the next few years through the implementation and harmonization of relevant legal acts. Therefore, during this period, all business entities, without exception, will be required to adopt a fundamentally new strategy - based on risk assessment - to ensure safe, healthy, and comfortable working conditions. Timely identification of potential occupational risks will enable the implementation of measures to prevent or minimize them.

Since 1999, the British standard OHSAS 18001 "Occupational Health and Safety Management Systems" [8] has helped enterprises eliminate occupational risk factors. Over the course of its 18 years of implementation, approximately 100,000 enterprises worldwide were certified. OHSAS 18001 earned a positive reputation. However, it was best suited for large industrial and construction organizations and was primarily designed for environments where a basic occupational safety system was already in place.

OHSAS 18001 has since been replaced by a new occupational health and safety standard - ISO 45001:2018 "Occupational Health and Safety Management Systems – Requirements with guidance for use" [9]. This standard was developed using terminology and a unified structure consistent with those of ISO 9001:2015 and ISO 14001:2015.

By applying this standard, an organization assumes responsibility for ensuring safe working conditions and takes all possible measures to prevent negative impacts on individuals (its own employees as well as those affected by the organization's activities – visitors, contractors, etc.). The standard is universal, allowing organizations of any type and size – both manufacturers and service providers – to apply it. According to ISO data, in 2018 alone, 11,952 certificates of conformity to ISO 45001 were issued, demonstrating the effectiveness and strong demand for this standard.

As expected, the standard adopted a new structure, unified across all ISO standards. This enhances the integration of ISO 45001 into other ISO management systems and reduces the audit procedures required for certification.

Key innovations introduced in ISO 45001 include (Fig. *2*):

- Responsibility for the occupational health and safety management system is placed entirely on the organization's leadership – without delegating this authority to occupational safety specialists;
- Risk assessment applies not only to occupational safety but also to the overall management system;
- The organization is accountable for managing the risks associated with its suppliers and contractors, as well as the potential impact of their activities on neighboring facilities within the adjacent territory;
- There is a requirement to identify and manage not only risks but also opportunities;

- In the case of planned changes (to the organization, management system, or processes), whether permanent or temporary, hazard identification and risk assessment must be conducted prior to implementation, with documented information maintained;
- The use of electronic information stored outside the formal document control system is permitted.

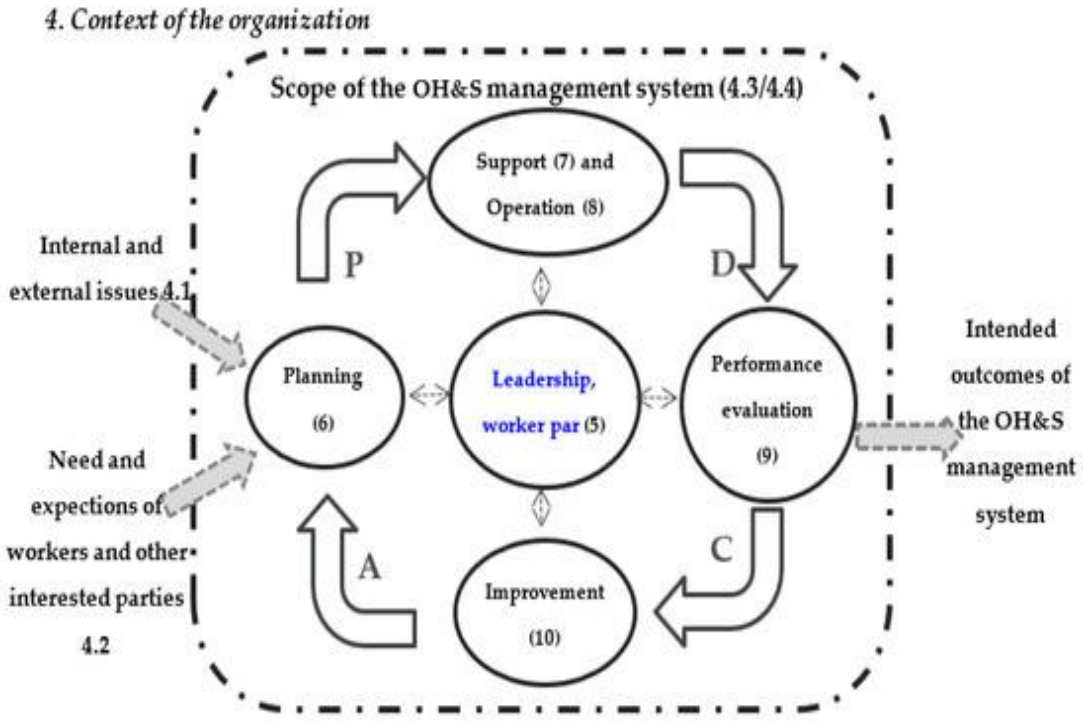

Fig. 2. **Health and safety management system vs. PDCA**

In a more detailed form, this process can be presented as the execution of the following eight stages:

1. Formulating the goals and objectives of risk management and determining the available resources to achieve them.
2. Identifying all potentially possible hazards.
3. Determining the likelihood of the occurrence of a particular hazard and the severity of its manifestation.
4. Assessing the level of risk associated with the identified hazards (quantitative risk assessment).
5. Conducting a criteria-based assessment of risks (based on the acceptability criterion).
6. Prioritizing risks according to their significance.
7. Developing and implementing safety measures and tools.
8. Monitoring and making adjustments [10].

The use of this cycle enables the practical implementation of continuous improvement in the safety aspects of processes, aimed at enhancing organizational efficiency and, as a result, reducing the number of workplace accidents and occupational diseases.

In Fig. 3 it can be seen that, from the point of view of the new standard ISO 45001:2018, the structure of the occupational health and safety management system is at a high level

The main advantages of the new OH&S management system according to ISO 45001:2018 can include [11]:

✓ Elimination of health and safety risks;

- ✓ Development of best practices in the field of occupational safety and health;
- ✓ Reduction in fatalities, accidents at work, and diseases in the workplace
- ✓ Demonstration of leadership and commitment with regard to the OH&S management system;
- ✓ Creation and implementation of health and safety policy and goals;
- ✓ Monitoring and measurement supports supervisory management by providing key performance indicators (KPIs) in measuring the level of performance of the health and safety management system.

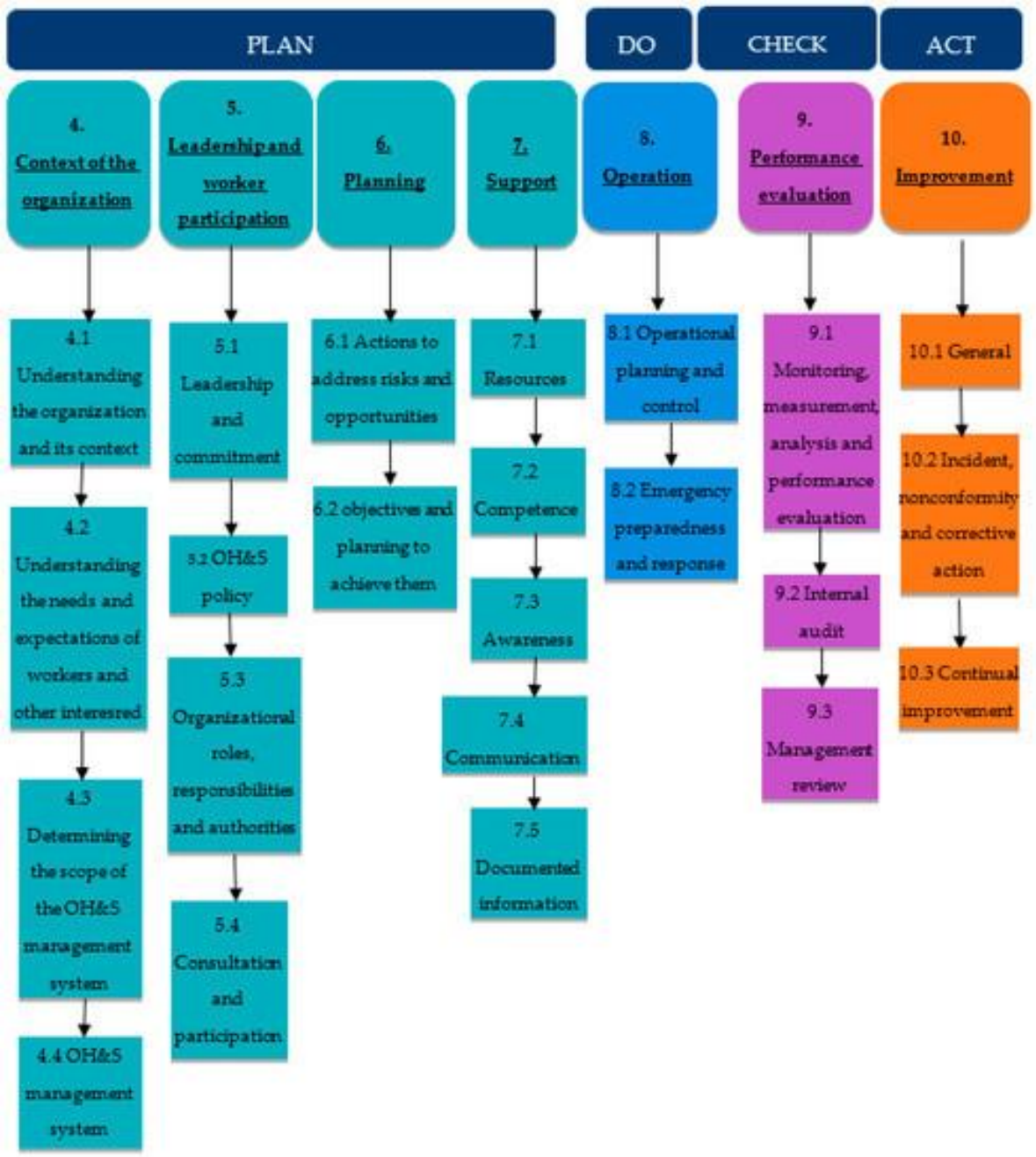

Fig. 3. **The structure of the OH&S according to ISO 45001 from the point of view of PDCA**

However, the ISO 45001:2018 standard is quite complex to understand, and not every enterprise can independently grasp the algorithm for developing an occupational health and safety management system

as outlined in the standard. Since ISO 45001 requires that any occupational health and safety actions correspond to the scale of risks and the nature of activities, the level of documentation is determined by the organization's specific context.

For organizations operating hazardous production facilities, the occupational health and safety policy must also include objectives related to risk identification and assessment at these facilities, as well as goals for implementing measures to reduce accident rates.

ISO 45001 emphasizes the need for risk management within the framework of the occupational health and safety and industrial safety management system. In principle, this requirement is common to all management systems based on ISO standards. In terms of risk assessment, the standard includes a general requirement for planning actions to eliminate risks. This planning involves identifying the risk, steps to minimize its impact, methods for eliminating the risk (if possible), and minimizing or eliminating the consequences of exposure.

In the analysis of risks in the field of occupational health and safety (OHS), commonly used quality management methodologies – such as FMEA analysis - are highly applicable. A key aspect in qualitative risk assessment, identification, and management is adherence to DSTU IEC/ISO 31010:2013 "Risk Management – Risk Assessment Techniques" [12], as well as ISO 31010:2018 "Risk Management – Guidelines" [13].

Current labor legislation does not provide any specific guidance on how exactly an employer should conduct a risk assessment within their enterprise. In practice, the process of "occupational risk assessment," when conducted independently by the employer, often boils down to distributing various questionnaires to departments. These questionnaires typically include items such as: "Has the safety briefing been conducted?", "Are personal protective equipment (PPE) issued?", "Are safety rules followed?" Naturally, lower-level managers answer affirmatively to such questions.

The responsible employee (usually a health and safety specialist), upon receiving the completed questionnaire, typically records a low level of risk - which is exactly what the employer wants. In reality, however, such a procedure has little to do with a genuine risk assessment (unless the employer's sole intention is to formally meet requirements and minimize potential claims from regulatory or inspection authorities). As a result, most enterprises delegate the risk assessment task to external expert organizations that possess the necessary experience, knowledge, and competencies.

The task of experts from such an organization is to inspect the workspace, the organization of workstations, examine the equipment and tools used, familiarize themselves with technological processes, analyze the available results of the special assessment of working conditions and production control, and, when necessary, perform instrumental measurements of the levels and values of hazardous and harmful production factors, as well as carry out many other procedures. Only under these conditions can the results of risk assessment be considered relevant to the actual state of occupational safety.

At present, there are no clearly defined criteria that expert organizations assessing occupational risks must meet. There is also no registry of experts authorized to perform assessments, nor even an approximate list of requirements for them. The most important stage of occupational risk assessment is the study of the process and the identification of hazards. If the process is not sufficiently studied and not considered in all its possible variations (this includes the standard course of the process, rare or irregular operations at a given workplace, non-routine or emergency situations that may occur), then hazards will not be identified. Consequently, risks will not be considered, and potentially important management decisions may be missed. One of the main causes of all accidents is the failure to consider certain hazards.

For high-quality hazard identification, it is necessary to develop a standard list of hazards from which the relevant ones for a specific workplace can be selected. The typical list may include dozens of hazards in just one area of a facility (moving parts of equipment, high temperature, humidity, noise, electromagnetic radiation, dustiness, maximum allowable concentrations, vibration, low lighting, etc.).

At the second stage of risk assessment, a "classical" methodology is usually applied, ranking risks by the probability of occurrence and severity of consequences. Risk assessment procedures must be followed by risk management procedures. Otherwise, the assessment remains just an evaluation, without

implying any measures to reduce the levels of existing hazards, let alone any preventive actions to avoid the emergence of such hazards in the future [14].

During the process of occupational risk assessment, enterprises may face the following challenges:

- Lack of resources for such an extensive and detailed task;
- Insufficient knowledge among responsible personnel for identifying all hazards and conducting further risk assessment;
- Psychological barriers (staff may not always be open to other perspectives, as they are accustomed to standard procedures and reluctant to change).

Implementing and obtaining certification for an occupational health and safety management system can be a demanding task, and many requirements of the ISO 45001 standard may be difficult to quickly grasp.

The implementation stages include numerous steps that require thorough preparation and expertise. It is essential to gain management support and thoroughly study legal requirements.

The ISO 45001 standard sets out the requirements for understanding and maintaining an organization's compliance with legal regulations for the successful implementation of an Occupational Health and Safety Management System (OHSMS). It is necessary to define the scope of the OHSMS (for the entire enterprise or only for a specific department), identify the processes and procedures for risk assessment and management, and later implement these processes and procedures. Employees must be trained and familiarized with ISO 45001. A certification body must be selected. The OHSMS must be used and control records maintained. Internal audits should be conducted. It is essential to apply the "Plan – Do – Check – Act" principle to ensure that final actions are implemented and sustained. Only then can the results of internal audits be considered truly effective. The final steps include management review, development of a corrective action system, and conducting certification audits [15].

These multifaceted and complex tasks can only be effectively performed through collaboration between the company's employees and an expert organization. It is clear that employees who have spent years at their respective workplaces are best positioned to develop a typical list of hazards and professionally identify them. However, the assessment and identification of risks must be carried out by specialists in this field.

As part of the study, a SWOT analysis was conducted, which is considered an effective research method that enables in-depth analysis of internal and external factors influencing the implementation of the ISO 45001:2018 standard in the transport sector. This analysis (Fig. 4) allows not only for the systematization of the key strengths and weaknesses of the organization but also for the identification of potential opportunities and external threats that may impact the effectiveness of the occupational health and safety management system implementation.

The SWOT analysis serves as an analytical tool that forms the basis for making strategic decisions and drawing well-founded conclusions regarding the prospects and challenges of integrating the standard within the modern transportation environment. The analysis identified strengths such as the presence of experienced personnel and existing safety management systems, as well as weaknesses such as the insufficient awareness of employees about the standard's requirements.

Among the opportunities highlighted are increased trust from customers and partners, enhanced corporate image, and optimization of risk management processes. At the same time, threats were identified, including high implementation costs, resistance to change from personnel, and the need for continuous updating of regulatory frameworks.

Despite the recognized effectiveness of the ISO 45001:2018 standard in occupational health and safety management, its implementation in transport enterprises is accompanied by a number of significant challenges. Among the main obstacles are the insufficient awareness of managerial personnel about the advantages of a systematic approach to safety management, limited financial resources that hinder the engagement of qualified specialists and the provision of proper training, as well as the weak integration of the standard's requirements into existing management processes.

STRENGTHS	WEAKNESSES
• **Increased occupational safety** • **Reduced injuries** • **Improved company image** • **International standard = advantage** • **Better risk management**	• **High implementation costs** • **Low staff awareness** • **Resistance to change** • **Difficult integration with other systems**
OPPORTUNITIES	THREATS
• **New contracts thanks to the standard** • **Access to international markets** • **Attracting investments** • **Motivating employees**	• Changes in legislation • Weak state support • **Staff shortage**

Fig. 4. **SWOT Analysis of ISO 45001:2018 Implementation in the Transportation Industry**

Particularly pressing is the issue of employee resistance to change, which is often caused by a low level of corporate safety culture. Additionally, the lack of methodological guidelines and industry-adapted tools for the practical application of the standard within the Ukrainian transport sector further complicates implementation.

A key challenge lies in adapting the standard to the operational activities of the transport industry, where risks are complex and variable. At the same time, there are substantial development prospects: the implementation of digital risk monitoring technologies, automation of safety processes, leveraging international experience, and the creation of sector-specific guidelines for integrating the standard.

With government support, the development of educational initiatives, and the cultivation of a safety culture, an occupational health and safety management system based on ISO 45001:2018 can become an effective tool for reducing workplace injuries and enhancing the competitiveness of transport enterprises.

How should risk identification measures be properly developed at a transport sector enterprise? A very useful tool is the hierarchy of controls, according to which measures are grouped by type and effectiveness (Fig. 5) [16]:

1. Elimination of the hazard – the most effective measure. This means completely removing the source of the hazard. For example, if a road for vehicles passes through a production area, you can redirect traffic along a different route and block off the original road. Elimination is the most effective but often the most expensive type of control measure.

2. Substitution of the hazard – replacing a greater hazard with a lesser one. For example, replacing an old-design pump with a new one equipped with modern safety features (interlocks, protective covers on rotating mechanisms, etc.). This measure does not eliminate the hazard entirely but significantly reduces the risk of injury. Such measures are often less expensive than elimination, but they can still be quite effective.

3. Engineering controls, also referred to as "hazard isolation". If the first two types of measures are not feasible or are too costly, this approach seeks to physically separate the hazard from people as much as possible. A clear example is fencing off an electrical installation and locking the access doors. This prevents unauthorized personnel from entering a dangerous area, granting access only to trained professionals who know how to behave safely. These measures are generally much cheaper than the first two but also less effective.

4. Administrative controls, also known as "organizational measures". These are the cheapest and, therefore, the most commonly used measures. They do not remove the hazard at all but instead aim to influence safe human behavior. For example: the electrical installation is not removed or fenced off, but all workers are instructed to stay away from it, this rule is included in the occupational safety

instructions, and compliance is regularly monitored. These measures are not bad but should ideally be combined with other types of protection.

5. Personal Protective Equipment (PPE). This is also a very popular type of safety measure. It becomes essential when all other protective measures have failed. This type of protection is valid and appropriate. However, it is at the very bottom of the hierarchy of controls because PPE does not prevent an incident from occurring, nor does it stop the hazard from affecting a person - it merely reduces the consequences of the hazard's impact on the body. There are many cases where, to protect workers, reliance is placed solely on the provision of PPE, while other, higher-priority protective measures suggested by the hierarchy are neglected. This is a flawed strategy that, unfortunately, can lead to injuries.

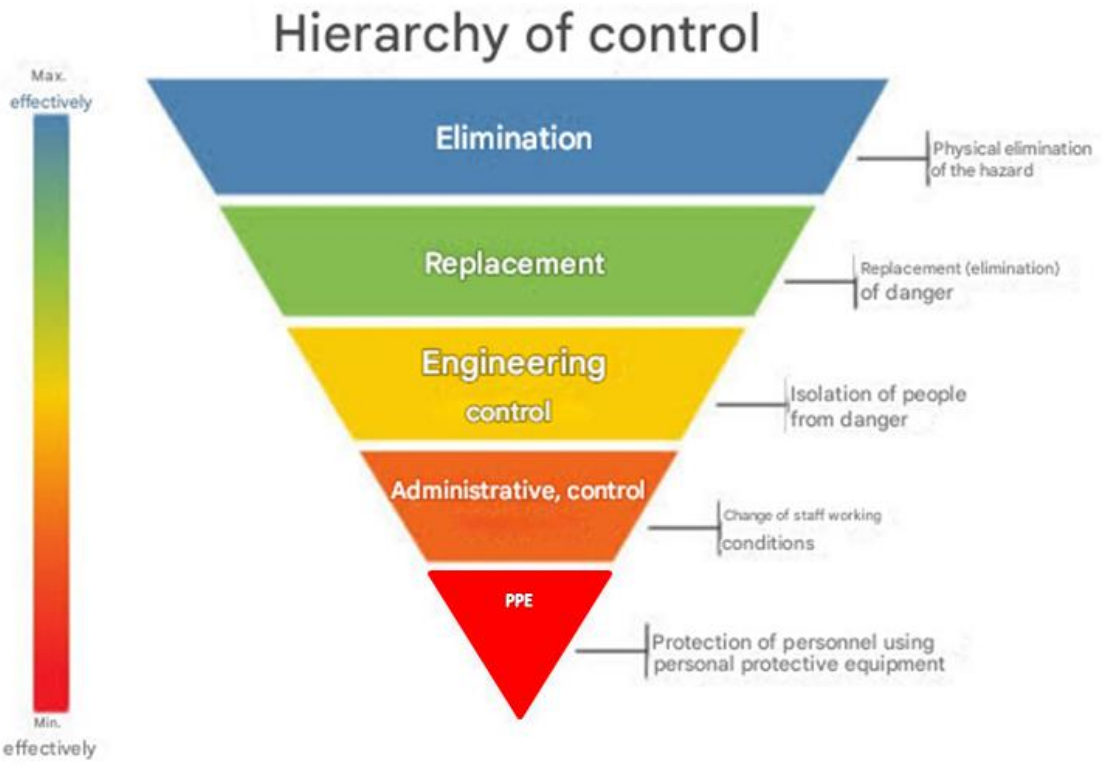

Fig. 5. **Hierarchy of events**

To address existing issues in implementing DSTU ISO 45001 into the occupational health and safety management system of transport enterprises, the following model can be used (Fig. 6).

The implementation of DSTU ISO 45001 at transport enterprises is a key step toward improving worker safety, reducing occupational risks, and ensuring the sustainable development of the industry. The standard sets clear requirements for hazard identification, risk management, and continuous improvement of the occupational health and safety system. In the context of the transport sector, where high risks of accidents, injuries, and external factors are constant challenges, the integration of ISO 45001 not only helps reduce the number of incidents but also enhances the company's reputation, attracts responsible employees, and avoids penalties from regulatory authorities. It is an investment in safety, efficiency, and the competitiveness of enterprises.

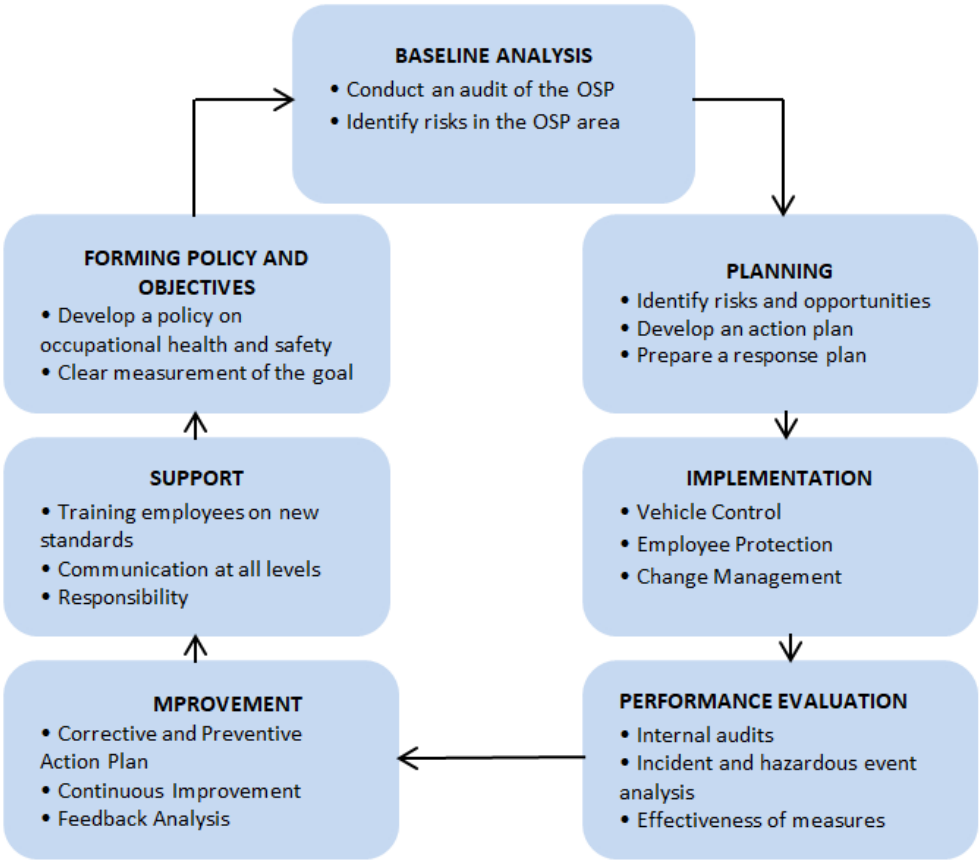

Fig. 6. **Model for integrating DSTU ISO 45001 requirements into the occupational health and safety management system of transport enterprises**

The qualitative analysis of the ISO 45001:2018 standard, based on eight systems thinking principles, indicates that the implementation of the new standard can help organizations move beyond a focus on individual system components, provide a deeper understanding of the entire socio-technical system, and improve workplace safety at the enterprise [17].

Conclusions. Occupational safety is one of the most important issues in today's society, especially at a time when many employers prioritize maximizing profit as quickly and with as little investment as possible. As a result, occupational safety requirements often receive little attention or are completely ignored, which unfortunately leads to an increase in workplace injuries and violations of workers' rights regarding labor protection. Therefore, the introduction of a new occupational safety management model based on the ISO 45001 standard will allow employees to feel that their needs for professional safety are being considered, reduce the risk of accidents, and consequently lower organizational costs. This standard has the potential to fundamentally change the state of occupational safety by introducing best global practices into integrated enterprise management systems. All of this will have a positive impact on building a favorable image of the enterprise.

The implementation of the DSTU ISO 45001:2018 occupational health and safety management system is a critical step for transport enterprises aiming to enhance workplace safety and minimize production risks. This study has highlighted the unique challenges and opportunities associated with the adoption of this standard, including the high-risk nature of transport operations, the complexity of technological processes, and the need for continuous risk assessment.

Key findings of the research include:

- The necessity for comprehensive staff training lies not only in raising awareness of occupational safety requirements but also in implementing a systematic approach to developing competencies in risk-oriented thinking. The scientific novelty consists in the proposed integration of training modules that encompass modern methods of hazard identification, risk management, the application of ISO 45001:2018 standards, and the development of a safety culture through team-based training, case analysis, and risk modeling.
- The modernization of existing safety systems should be carried out by integrating specific elements of leading international practices, such as the application of ISO 31000:2018 for strategic risk management, the use of the HAZOP (Hazard and Operability Study) methodology for identifying hazards in technological processes, the implementation of digital risk monitoring systems and safety dashboards as applied in the Vision Zero concept in Germany, the adoption of Behavior-Based Safety (BBS) models widely used in the USA, Canada, and Australia, and the practice of regular independent audits in accordance with the UK's Health and Safety Executive (HSE) standards. The application of these practices will not only enhance compliance with international requirements but also foster the development of an adaptive and dynamic occupational health and safety management system focused on risk prevention and continuous improvement.
- Effective risk management plays a key role in reducing injuries and improving organizational performance. The scientific novelty of this statement lies in the proposed model for adapting the DSTU ISO 45001:2018 standard to the conditions of transport enterprises, taking into account industry-specific risks. Specific areas for increasing effectiveness include the application of the PDCA cycle (Plan – Do – Check – Act), systematic risk assessment using quantitative criteria, and the prioritized implementation of engineering and organizational protective measures.

Adopting the DSTU ISO 45001:2018 standard not only reduces accident rates and ensures legal compliance but also strengthens the competitive position of enterprises by improving their reputation and operational efficiency. The proposed practical recommendations provide a clear pathway for optimizing the implementation process, considering the specific conditions of the transport sector.

Future research should focus on the development of industry-specific guidelines and the use of digital technologies for risk monitoring, which will further enhance the effectiveness of occupational health and safety systems.

REFERNCES

1. Pro skhvalennya Kontseptsiyi reformuvannya systemy upravlinnya okhoronoyu pratsi v Ukrayini ta zatverdzhennya planu zakhodiv shchodo yiyi realizatsiyi: Rozporyadzhennya Kabinetu Ministriv Ukrayiny vid 12.12.2018 r. № 989-r. [in Ukraine]. https://zakon.rada.gov.ua/laws/show/989-2018-%D1%80?lang=ru#Text.
2. Malko, O, D., Bryhada, O.V., &Tsymbal. B.M. (2022). Adaptatsiia normatyvno-pravovoho zabezpechennia okhorony pratsi do yevropeiskykh standartiv. *Kommunalne hospodarstvo mist*, *6*(173), 160–169. [in Ukraine]. http://repositsc.nuczu.edu.ua/bitstream/123456789/16800/1/26.pdf.
3. Sorokolat, N.A., & Fateieva, L.Yu. (2022). Otsiniuvannia yakosti protsesiv systemy upravlinnia bezpekoiu pratsi, zghidno vymoh mizhnarodnoho standartu ISO 45001:2018. *Mashynobuduvannia*, *29*, 89-96. [in Ukraine]. https://doi.org/10.32820/2079-1747-2022-29-89-96.
4. Trishch, R., Nechuiviter, O., Dyadyura, K., Vasilevskyi, O., Tsykhanovska, I., & Yakovlev, M. (2021). "Qualimetric method of assessing risks of low-quality products", *MM Science Journal*, *4*, 4769-4774. http://doi.org/10.17973/MMSJ.2021_10_2021030.
5. Sánchez-Herrera, I.S., & Donate, M.J. (2019). Occupational safety and health (OSH) and business strategy: *The role of the OSH professional in Spain. Safety Science, 120*, 206–225. https://doi.org/10.1016/j.ssci.2019.06.037.
6. Bochkivskyi, A., & Sapozhnikova, N. (2021). Udoskonalennia klasyfikatsii profesiinykh ryzykiv. *Zbirnyk naukovykh prats ΛΟΓΟΣ*. [in Ukraine]. https://doi.org/10.36074/logos-14.05.2021.v1.23.
7. Delini, M.M., & Van Yi. (2024). Teoretychni zasady formuvannia systemy ryzyk-menedzhmentu pidpryiemstv. *Investytsii: dosvid ta praktyka*, *20*, 40-47. [in Ukraine]. https://doi.org/10.32702/2306-6814.2024.20.40.
8. DSTU OHSAS 18002:2015 Systemy upravlinnya hihiyenoyu ta bezpekoyu pratsi. Osnovni pryntsypy vykonannya vymoh OHSAS 18001:2007 (OHSAS 18002:2008, IDT). [in Ukraine].
9. DSTU ISO 45001:2019 (2019). Systemy upravlinnia okhoronoiu zdorovia ta bezpeky pratsi. Vymohy ta nastanovy shchodo zastosuvannia. Kyiv: DP "UkrNDNTs". [in Ukraine]. https://zakon.isu.net.ua/sites/default/files/normdocs/dstu_iso_45001_2019.pdf.

10. Melnychenko, O.I., Sorochynska, O.L., Kulbovskyi, I.I., Kharuta, V.S., & Holub, H.M. (2023). Metodolohichni aspekty protsesu upravlinnia okhoronoiu pratsi v proiektakh transportu zghidno standartu ISO 45001. Visnyk Natsionalnoho transportnoho universytetu, *2*(52), 76-83. [in Ukraine]. https://doi.org/10.33744/2308-6645-2023-3-57-076-083.
11. Šolc, M., Blaško, P., Girmanová, L., & Kliment, J. (2022). The Development Trend of the Occupational Health and Safety in the Context of ISO 45001:2018. *Standards*, *2*, 294-305. https://doi.org/10.3390/standards2030021.
12. DSTU IES/ISO 31010:2013. Keruvannia ryzykom. Metody zahalnoho otsiniuvannia ryzyku (IES/ISO 31010:2009, IDT). [in Ukraine].
13. ISO (2019). Risk Management – Risk assessment techniques: ISO 31010:2018. Switzerland: ISO.
14. DSTU ISO 31000:2014 (2014). Menedzhment ryzykiv. Pryntsypy ta kerivni vkazivky. Kyiv: DP "UkrNDNTs". [in Ukraine].
15. Sevruk, A. (2025). Metodyka zabezpechennia funktsionuvannia SU OZiBP. *Okhorona pratsi*, *2*, 28-30. [in Ukraine].
16. Ajslev, J.Z.N., Møller, J.L., Andersen, M.F., Pirzadeh, P., &Lingard, H. (2022). The Hierarchy of Controls as an Approach to Visualize the Impact of Occupational Safety and Health Coordination. *Int. J. Environ. Res. Public Health*, 19, 2731. https://doi.org/10.3390/ijerph19052731.
17. Karanikas, N., Weber, D., Bruschi, K., & Brown, S. (2022). Identification of systems thinking aspects in ISO 45001:2018 on occupational health & safety management. *Safety Science, 148*. https://doi.org/10.1016/j.ssci.2022.105671.

Олена Сорочинська[1], Олександр Мельниченко[2], Іван Кульбовський[3], Ігор Дерегуз[4]

[1]Доцент, кафедра «Екологія та безпека життєдіяльності», Національний транспортний університет, вул. Михайла Омеляновича-Павленка, 2, 01010, м. Київ, Україна. ORCID: http://orcid.org/0000-0003-2477-1275.

[2]Професор, кафедра «Виробництво, ремонт та матеріалознавство», Національний транспортний університет, вул. Михайла Омеляновича-Павленка, 2, 01010, м. Київ, Україна. ORCID: http://orcid.org/0000-0001-9694-9824.

[3]Доцент, кафедра «Автоматизація та комп`ютерно-інтегровані технології транспорту» , Національний транспортний університет, вул. Михайла Омеляновича-Павленка, 2, 01010, м. Київ, Україна. ORCID: http://orcid.org/0000-0002-5329-3842.

[4]Аспірант, кафедра «Транспортне право та логістика», Національний транспортний університет, вул. Михайла Омеляновича-Павленка, 2, 01010, м. Київ, Україна. ORCID: http://orcid.org/0000-0003-3119-3709.

Імплементація моделі системи управління охороною праці відповідно до ДСТУ ISO 45001:2018: виклики і можливості для транспортних підприємств

У статті розглядаються особливості впровадження міжнародного стандарту ДСТУ ISO 45001:2018 «Система управління охороною праці та безпекою праці» на транспортних підприємствах. Основна увага приділяється специфічним викликам, пов'язаним з високим рівнем виробничих ризиків, мобільністю робочого середовища та складністю технологічних процесів у транспортному секторі. Проаналізовано ключові проблеми впровадження стандарту, зокрема, недостатній рівень обізнаності персоналу, необхідність модернізації існуючих систем безпеки та адаптації до сучасних вимог охорони праці. Визначено потенційні переваги впровадження ISO 45001:2018, зокрема зниження рівня виробничого травматизму, підвищення ефективності управління ризиками та зміцнення іміджу підприємства. Запропоновано практичні рекомендації щодо оптимізації процесу впровадження стандарту з урахуванням галузевої специфіки.

***Ключові слова**: охорона праці, безпека, стандарт ДСТУ ISO 45001:2018, ризики, стратегія, модель, транспортні підприємства, адаптація, транспортні системи.*

DOI: 10.32703/2617-9040-2025-45-9

UDC 629.5.018.2

Mykola Bulgakov*[1], Oleksiy Melnyk[2]

[1]PhD in Technical Sciences, Associate Professor, Associate Professor at the Navigation and Maritime Safety Department, Odesa National Maritime University, 34, Mechnikova St., Odesa, 65029, Ukraine. ORCID: https://orcid.org/0000-0002-7172-8678.

[2] Doctor of Technical Sciences, Professor, Professor at the Navigation and Maritime Safety Department, Odesa National Maritime University, 34, Mechnikova St., Odesa, 65029, Ukraine. ORCID: https://orcid.org/0000-0001-9228-8459.

***Corresponding author:** npbulgakov2@gmail.com.

Intelligent digital twin utilization for real-time forecasting and optimization of the ship's power system

Abstract. The paper presents the concept and mathematical model of an intelligent digital twin of a ship's power system, designed for real-time operation. The proposed solution integrates dynamic energy balance modeling, telemetry signal processing using a Kalman filter, load forecasting with long short-term memory (LSTM) neural networks, anomaly detection mechanisms, and optimization modules. The digital twin is implemented as a modular software architecture capable of integration with onboard control systems and cloud-based fleet analytics platforms. A series of computational experiments in MATLAB/Simulink simulates both typical and critical operational conditions, including stable load, overloads, generator failures, voltage instability, and energy-saving modes. The results demonstrate strong convergence between simulated and computed values, as well as timely system responses to emerging anomalies and effective optimization decisions. The developed model highlights the potential of digital twin technology to enhance energy efficiency, operational reliability, and environmental sustainability in modern maritime transport. It provides a foundation for advanced autonomous energy management and supports compliance with evolving IMO decarbonization and safety requirements.

Keywords: ship power system, digital twin, telemetry, load forecasting, anomaly detection, energy efficiency, autonomous control, intelligent algorithms, real-time operation, IMO

Introduction. In the context of growing global attention to decarbonization and energy optimization, the maritime industry faces increasing demands for the intelligent management of onboard power systems. Digital twin technology has emerged as a transformative solution for enhancing situational awareness, operational efficiency, and system reliability in real time. By creating a virtual representation of a ship's power infrastructure, digital twins enable continuous monitoring, predictive analytics, and autonomous decision-making based on real-time telemetry and advanced modeling techniques.

This study focuses on the development and implementation of an intelligent digital twin tailored to the dynamic energy system of a marine vessel. Unlike traditional static models, the proposed approach integrates machine learning–based forecasting (LSTM), Kalman-filtered telemetry analysis, and anomaly detection modules within a unified control framework. The digital twin is designed for real-time interaction with shipboard systems, allowing adaptive optimization of energy consumption and improved resilience to operational disruptions. This paper aims to demonstrate the practical feasibility

and benefits of such a system through simulation-based validation under various load and failure scenarios.

Analysis of the latest research and problem statement. Digital twin technologies have recently gained considerable attention as critical tools for real-time monitoring, predictive analysis, and optimization of maritime energy systems. Current research highlights digital twins as foundational elements for enhancing energy efficiency, reliability, and operational sustainability in marine applications.

Li et al. developed an intelligent maintenance platform driven by digital twin technology for large-scale hydro-steel structures. Their research demonstrated the capability of digital twins to significantly improve maintenance effectiveness through predictive analytics and real-time monitoring [1]. Similarly, Liu et al. examined digital twin implementation for shipboard crane operations, highlighting considerable improvements in operational efficiency and safety through advanced predictive maintenance [2]. These studies collectively underline the potential for digital twin systems to dynamically manage and forecast performance and maintenance requirements in maritime infrastructures.

Recent literature also emphasizes the critical role of artificial intelligence (AI) and advanced algorithms in digital twin implementations. For example, Es-haghi et al. (2024) reviewed current methods enabling real-time analytics in digital twins, emphasizing the necessity of robust algorithms capable of rapid adaptation and high accuracy under variable conditions [3]. Ubina et al. further expanded on the integration of AI and the Internet of Things (IoT) within digital twin platforms, demonstrating significant gains in operational predictability and control precision in intelligent fish farming systems [4]. Such findings highlight the adaptability of digital twins to diverse environmental and operational contexts, further underscoring their suitability for marine energy systems.

However, despite these advancements, significant gaps remain. Most existing models rely predominantly on static parameters or averaged data, failing to accurately reflect the dynamic nature of onboard ship energy systems affected by fluctuating load conditions, weather changes, and operational scenarios. This limitation significantly restricts their potential in dynamic real-time control and proactive maintenance management.

Furthermore, Fu et al. emphasized that achieving real-time multi-scale characterization remains a primary challenge due to limitations in computational efficiency and data integration processes [5]. Likewise, Mohanraj and Vaishnavi underscored the ongoing difficulties in managing large volumes of telemetry data and integrating them into coherent real-time digital twin models, particularly under marine operating conditions characterized by continuous variability and environmental uncertainty [6].

Thus, the primary problem addressed in the current study is the absence of comprehensive dynamic models that integrate real-time telemetry, predictive machine learning algorithms, and anomaly detection within a unified digital twin framework. There remains an urgent need for integrated systems capable of real-time adaptive responses to varying ship energy system conditions, which can significantly enhance operational reliability, efficiency, and compliance with stringent IMO decarbonization goals.

This study aims to address these limitations by developing an intelligent digital twin model specifically designed for real-time operation within ship power systems, integrating dynamic energy balance models, LSTM-based predictive analytics, Kalman filtering for telemetry data, and anomaly detection modules. By evaluating this model through simulation scenarios, the study contributes to filling the identified research gaps, providing actionable insights into the practical application of digital twins in maritime energy management.

Problem statement. Existing models of ship energy consumption are usually based on static parameters or calculations of average values. This does not allow to accurately reflect the dynamic behaviour of the ship's energy systems when loads, course, weather conditions, etc. change. The lack of

integration of real telemetry data with virtual models limits the possibilities of adaptive control, fault prediction, and scenario planning of energy consumption.

Research objective. To develop the concept and mathematical model of a digital twin of the ship's power system, which provides real-time monitoring of parameters, efficiency assessment, state prediction, and decision support to reduce fuel consumption and CO_2 emissions.

Summary of the main material. In the context of global digitalisation and increased requirements for energy efficiency in maritime transport, digital twins of ships are becoming a key tool for monitoring, diagnosing and forecasting energy processes in real time. This approach allows not only to monitor the technical condition of ship systems, but also to optimise them based on a large array of data coming from sensors during operation. This topic is especially relevant in the context of strict IMO environmental standards and requirements to reduce greenhouse gas emissions.

The purpose and tasks of the study is to create and verify a thorough mathematical model and conceptual framework for an intelligent digital twin of a ship's power system that can operate efficiently under real-time operating circumstances. By improving the monitoring, anomaly detection, predictive analysis, and optimization of maritime energy systems, the proposed digital twin hopes to greatly boost energy efficiency, minimize CO_2 emissions, and reduce fuel consumption in maritime transportation.

The study establishes the following particular tasks in order to fulfill this purpose:

1. To produce an energy system dynamic mathematical model of the ship that faithfully captures changes in power generation, consumption, and losses in real time.
2. To use a Kalman filter to telemetry signal processing in order to reduce measurement noise and errors and guarantee precise real-time state estimation.
3. Long short-term memory (LSTM) neural networks will be used to create predictive analytics that will allow for accurate shipboard energy consumption forecasts and the identification of possible future states.
4. In order to quickly detect deviations and important events in the ship's power system functioning, an anomaly detection module will be integrated into the digital twin structure.
5. To use computational experiments that mimic common operating scenarios, such as normal loads, overload situations, equipment breakdowns, voltage instabilities, and energy-saving activities, in order to simulate and validate the created digital twin model.
6. To evaluate the digital twin system's accuracy, reactivity, and ability to assist decisions in real time and manage energy on its own in order to determine its viability and efficacy.

By achieving these objectives, the research seeks to address critical existing gaps in maritime energy management and advance the adoption of intelligent digital twin technologies within the maritime industry.

Research materials and methods. The digital twin of a ship's energy system is an integrated mathematical model that displays the dynamic state of energy facilities in real time based on telemetry data to assess, predict, and optimize energy efficiency. The model is based on a system of equations describing the energy balance of a ship:

$$P_{\text{gen}}(t) - P_{\text{load}}(t) - P_{\text{loss}}(t) = \Delta P(t), \tag{1}$$

where $P_{\text{gen}}(t)$ is total capacity of generators;
$P_{\text{load}}(t)$ is continuous power supply of the ship's systems;
$P_{\text{loss}}(t)$ is losses in lines and converters;
ΔP(t) is residual (reserve) capacity.

Evaluation of the efficiency of a diesel generator at any given time by the ratio of useful power to the energy content of the fuel:

$$\eta_{\text{DG}}(t) = \frac{P_{\text{out}}(t)}{\dot{m}_f(t) \cdot LHV}, \tag{2}$$

where $\eta_{\text{DG}}(t)$ is instantaneous generator efficiency;

$\dot{m}_f(t)$ is mass fuel consumption, LHV is lowest heat of combustion.

Telemetry processing, where the Kalman filter is used to filter noisy telemetry signals and refine the estimate of the system's current state based on the previous state and new measurements.

$$\hat{x}_t = \hat{x}_{t-1} + K_t\left(z_t - H\hat{x}_{t-1}\right), \tag{3}$$

$$K_t = \frac{P_{t|t-1}H^T}{HP_{t|t-1}H^T + R}, \tag{4}$$

where $\hat{x}_t$ is assessment of the state;

z_t is measurement (telemetry);

H is observation matrix;

$P_{t\,|t-1|}$ is forecast covariance;

R is sensor noise covariance.

Power consumption prediction (LSTM): The formula reflects the process of predicting the next power consumption value based on the previous n values using a recurrent neural network such as LSTM.

It was clarified that the LSTM model was trained on one month of real ship telemetry data, with features normalized using min-max scaling. The dataset was split 80/20 into training and test subsets. The model architecture includes two LSTM layers of 64 units each, followed by a dense layer of 32 units with L2 regularization. Training proceeded for up to 200 epochs using the Adam optimizer (learning rate = 0.001) and mean squared error (MSE) as the loss function. To prevent overfitting, we applied dropout with a rate of 0.2 and employed early stopping with a patience of 20 epochs. Every 10 epochs, model performance was evaluated on the validation set using both MSE and mean absolute error (MAE), and the final model was selected based on the lowest MAE

$$\hat{E}_{t+1} = f_{\text{LSTM}}(E_t, E_{t-1}, \ldots, E_{t-n}), \tag{5}$$

where $\hat{E}_{t+1}$ is energy consumption forecast;

f_{LSTM} is recursive function of a long-term memory neural network.

Anomaly detection function. A discrete function that is activated (i.e., equal to 1) if the deviation between the predicted and actual load exceeds the specified threshold ε.

$$\delta(t) = \begin{cases} 1, & \text{if } \left|\hat{P}_{\text{load}}(t) - P_{\text{load}}(t)\right| > \varepsilon; \\ 0, & otherwise, \end{cases} \tag{6}$$

where ε is threshold deviation limit for the alarm.

Power system optimization objective function. The objective function that the control system minimizes includes generation costs and the energy imbalance penalty over the entire T time horizon.

$$\min_x \left\{ \sum_{t=0}^{T} \left[C_g(P_{\text{gen}}(t)) + \lambda \cdot \Delta P(t)^2 \right] \right\}, \tag{7}$$

where C_g is generation cost function, λ is imbalance penalty coefficient, x is controllable system variables (loads, generator modes, etc.).

Updating the battery state of charge (SOC), calculating a new battery SOC value based on the energy consumed or accumulated, time, and battery capacity:

$$SOC(t) = SOC(t-1) - \frac{P_{\text{batt}}(t) \cdot \Delta t}{3600 \cdot C_{\text{batt}}}. \tag{8}$$

The mathematical model described above is the analytical basis of the digital twin of the ship's energy system. Each of its components - energy balance calculation, telemetry filtering using Kalman filter, energy consumption forecasting using LSTM, anomaly detection and optimisation function - is implemented as functional modules of the system architecture.

To ensure real-time operation and integration with on-board systems, the model is implemented as a modular software architecture of a digital twin. It receives telemetry data, performs analytical processing, generates forecasts, generates optimisation signals, and transmits the results in the form of visualisations or autonomous control commands.

The architecture of the digital twin of the ship's power system is based on data flows from real sensors to analytical and control modules. At the first level, the system receives data from telemetry sensors covering the main parameters of power plants, generators, batteries, navigation conditions and load. This data is transmitted via standard communication protocols (NMEA, CAN, Modbus) to the internal information exchange bus.

Once collected, the data undergoes pre-processing, which includes noise filtering (e.g. using a Kalman filter) and normalisation. The processed information is fed into the digital twin core of the digital model, which reproduces the current state of the ship's power system in real time. This core includes a predictive model based on neural networks (such as LSTM), which allows predicting energy consumption and generation for several hours or days in advance.

The diagram (fig. 1) shows the architectural structure of the digital twin, which illustrates the key subsystems, data exchange directions and interaction between the analytical core, telemetry, forecasting modules, decision support systems and automatic control.

In parallel, the system visualises data on the crew dashboard and sends it to the optimisation and decision-making modules. If anomalies or potentially inefficient modes are detected, the system either suggests actions to the crew or executes them automatically through an autonomous control module. The digital twin is synchronised with the cloud platform, allowing for fleet-wide analytics comparing the performance of different vessels. Separate units are responsible for model self-learning, monitoring of backup power supplies, predictive maintenance, and event logging for later audit. The architecture of the digital twin of the ship's power system improves reliability, ensures fuel savings and creates the basis for integration with autonomous technologies of the future.

Simulation of the Digital Twin Operation.

The purpose of simulation is to verify the operational effectiveness of the ship's power system digital twin in real-time, analyze forecasting accuracy, and identify potential critical scenarios. For this purpose, a simulation environment was developed in MATLAB/Simulink, which incorporates mathematical

models of shipboard generators, loads, network losses, and an adaptive forecasting module. Telemetry data are simulated as pseudo-random signals that replicate real operational parameters with inherent inaccuracies, including temperature, fuel consumption, generator frequency, voltage, and current at various nodes. External factors such as load variations during maneuvers, malfunctions in cooling systems, and variable marine conditions were introduced to enhance realism.

The digital twin simulation example presented in the graph illustrates the actual consumed power (Pload), forecasted load (LSTM), generator-produced power, and anomaly zones where predictions significantly deviate from the real load. This serves as a demonstration of the implemented model code for real-time analysis.

To verify the effectiveness of the digital twin's energy management algorithms, a simulation of a hybrid ship energy system was carried out in MATLAB. The simulated system includes variable load conditions, photovoltaic generation, a Battery Energy Storage System (BESS), and a diesel generator (DG). The primary control strategy prioritizes the use of renewable energy sources, supplemented by battery discharge, subsequently activating the diesel generator only in cases of energy deficit.

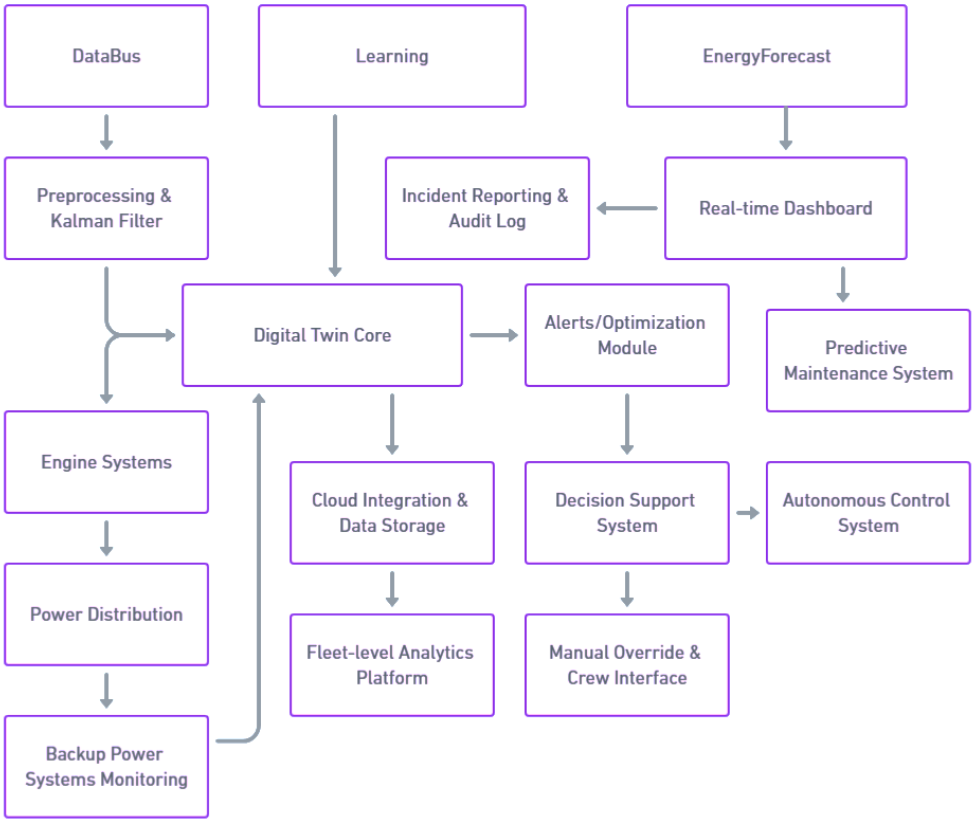

Fig. 1. **Architectural structure of the digital twin**

The model uses a discrete time step of 1 second over a simulated duration of 24 hours. Throughout the simulation, the digital twin continuously updates the energy balance state utilizing a Kalman filter, generates load forecasts for 30 minutes ahead using a trained LSTM model, and compares predicted values against actual readings. It was observed that the average forecasting error for power did not exceed 3.5%, with data update latency under 1.2 seconds.

Five scenarios were simulated: normal operation, overload conditions, failure of a single generator, critical voltage drop, and energy-saving mode. In each case, the digital twin successfully detected

anomalies and visualized potential consequences through an interactive interface. The obtained results confirm that the proposed model serves as an effective tool for dynamic energy management aboard ships. The overall impact suggests moderate effectiveness in optimizing energy system control and maintaining operational stability.

The graph (Fig. 2) demonstrates how the digital twin compares generated and consumed power in real-time, and also generates a short-term forecast based on the LSTM model. It can be observed that the forecast closely follows the actual dynamics, confirming the effectiveness of the digital twin.

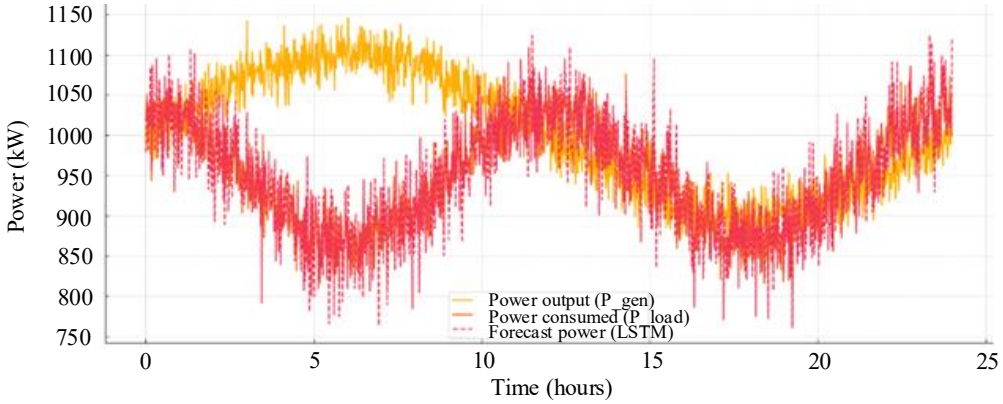

Fig. 2. **Ship Energy Digital Twin Simulation: Real vs Forecasted Load with Anomaly Detection**

The model operates over a time horizon of T=3600 s (1 hour), with a discrete timestep of Δt=1 s. Load and generation signals are modeled as harmonic signals with added noise to closely replicate realistic maritime conditions. The algorithm calculates the energy balance at each timestep, adjusting the battery's state of charge (SOC) and the diesel generator's output power accordingly. The MATLAB implementation of the model is presented in Fig. 3.

```
% Simulation of a hybrid ship power system in MATLAB
T = 3600; dt = 1
P_loag = 1500 + 20 * sin((1:T) * 2 * pi / T);          % Variable load, kW
P_solar = 30 *max(sin((1:T) * 2 * pi / T), 0);         % Solar generation, kW
SOC = zeros(1:T); SOC(1) = 0.5;                        % Initial SOC
P_batt = zeros(1:T); P_DG = zeros(1:T);
    for t = 2:T
        P_deficit = P_loag(t) + P_solar(t);
        if SOC(t - 1) > 0.2 && P_deficit > 0
            P_batt(t) = min(P_deficit, 40);
            SOC(t) = SOC(t - 1) - P_batt(t) * dt / 3600 / 100;
        else if SOC(t - 1) <0.9 && P_solar(t) > P_loag(t)
                P_batt(t) = -min(P_solar(t) > P_loag(t), 40);
                SOC(t) = SOC(t - 1) - P_batt(t) * dt / 3600 / 100;
            else
                P_batt(t) = 0;
                SOC(t) = SOC(t - 1);
        end
        P_DG(t) = P_loag(t) - P_solar(t) - P_batt(t);
        P_DG(t) = max(P_DG(t), 40);
    end
plot(1:T, [P_loag'P_solar'P_batt'P_DG']);
legend('Load', 'Solar energy', 'Battery', 'DG');
xlabel('time, s');
ylabel('Power, kW');
title('Energy balance of a hybrid system')
```

Fig. 3. **MATLAB code implementing the ship's energy balance simulation with forecasting and anomaly detection**

For ease of explanation of the variables used in the code, a table is provided in Fig. 4.

Variable	Description	Units
T	Total simulation time steps	- (integer count)
Dt	Time step duration	seconds (s)
P_load(t)	Electrical load demand profile at time *t*	kilowatts (kW)
P_solar(t)	Solar power generation at time *t*	kilowatts (kW)
P_batt(t)	Battery power (positive for discharge, negative for charge)	kilowatts (kW)
SOC(t)	State of charge of the battery at time t (0 to 1)	- (ratio)
P_DG(t)	Diesel generator output required at time t	kilowatts (kW)
P_deficit	Net power deficit to be covered by battery or DG	kilowatts (kW)

Note: The model assumes priority usage of solar energy, followed by the battery (subject to SOC limits), and finally diesel generation to cover any remaining demand.

Fig. 4. **Description of Variables Used in the MATLAB Hybrid Energy System Model**

Thus, the model demonstrates the basic logic of integrating renewable energy sources (RES), energy storage systems, and a diesel generator (DG) into the overall energy balance of the ship, and can be further extended to incorporate real telemetry data or advanced control optimization strategies within the digital twin framework.

Results and Discussion. The simulation results of the ship's energy system digital twin include five different scenarios. Each scenario illustrates how the system responds to typical and critical conditions during vessel operation.

1. Normal operation. Under stable load conditions, the system demonstrated high accuracy in forecasting power consumption, with an average error of 2.95 percent. The energy balance was visualized correctly, and telemetry updates occurred with a latency of just 0.90 seconds. The system functioned without any disruptions.

2. Overload. The simulation of a sudden connection of additional equipment led to a short-term excess of load over generation. The digital twin identified the anomaly within 4.54 seconds and proposed optimization actions, such as reducing the speed of auxiliary systems.

3. Generator failure. A simulated loss of one of the main generators caused a power imbalance and a voltage drop of 17 percent. The digital twin detected the deviation and generated an early warning 17 minutes before the system reached a critical instability threshold.

4. Critical voltage drop. A voltage spike caused by a switching fault was successfully identified. The system localized the affected nodes and automatically activated the emergency consumption mode.

5. Energy-saving mode. When the system was switched to minimal consumption, the model detected excessive generation of approximately 11 percent and recommended deactivating one of the generators. This confirmed the digital twin's ability to optimize power usage without compromising system balance.

Across all scenarios, the digital twin consistently demonstrated stable performance, rapid adaptation to disturbances, and user-friendly visualization of key indicators. These outcomes confirm its practical potential for integration into modern shipboard power systems.

The simulation of the ship's power system digital twin covered five representative operational scenarios, allowing for evaluation of the model's accuracy, responsiveness, and adaptability. In the normal operating scenario, the average forecasting error was only 2.95%, with a near-instantaneous detection time of 0.9 seconds, confirming the system's stable performance under standard conditions. In the overload case, the digital twin detected a power demand exceeding generation within 4.5 seconds (forecast error 4.12%) and automatically initiated a reduction in the rotational speed of auxiliary systems to lower consumption.

Table 1. **Summary of Scenario-Based Simulation Results for the Ship Energy Digital Twin**

Scenario	Avg Forecast Error (%)	Detection Time (s)	Detected Event	Optimization Action
Normal Operation	2.95	0.9	Stable performance	Monitoring
Overload	4.12	4.5	Load > Generation	Throttle adjustment
Generator Failure	3.87	1020.0	Generator lost	Alert, load balancing
Voltage Drop	3.25	2.3	Voltage spike	Emergency consumption mode
Energy Saving Mode	2.48	6.1	Excessive generation	Generator shutdown

Note: Detection time refers to the time from event onset to system response. Forecast error is based on LSTM prediction versus actual load during simulation.

In the critical scenario of generator failure, the digital twin issued an early warning 1,020 seconds (17 minutes) before reaching a critical instability threshold, with a forecasting error of 3.87%, and suggested load balancing measures. In the voltage drop scenario caused by a switching error, the system identified the issue within 2.3 seconds and switched affected nodes to emergency consumption mode, maintaining a forecasting error of 3.25%. Finally, in energy-saving mode, the model identified an energy surplus (~11%) and recommended deactivating one of the generators, achieving the lowest forecast error of 2.48%.

These results confirm the digital twin's ability to accurately detect and predict critical situations, respond rapidly to changes in power system parameters, and provide relevant recommendations for energy optimization. Its integration into ship systems would enable reliable, dynamic control of energy balance in continuously changing maritime environments.

Conclusions. This study has developed and tested a conceptual model of a digital twin for a ship's power system, designed for real-time operation. The proposed architecture integrates a dynamic energy balance model, adaptive forecasting algorithms based on LSTM, telemetry signal processing using Kalman filtering, and visualization of key energy performance indicators. The simulation results confirm that the digital twin is capable of effectively responding to critical conditions such as overloads, equipment failures, and abnormal voltage fluctuations, offering high prediction accuracy (average error below 4%) and fast detection times (under 5 seconds in most scenarios).

The model demonstrates scalability, modularity, and compatibility with standard shipboard telemetry systems. Its intuitive visual interface supports operator decision-making and facilitates early identification of energy-inefficient operating modes. Based on the results obtained, the digital twin can serve as a practical tool for enhancing energy efficiency, operational reliability, and safety of ship systems.

REFERENCES

1. Li, H., Zhang, R., Zheng, S., Shen, Y., Fu, C., & Zhao, H. (2024). Digital twin-driven intelligent operation and maintenance platform for large-scale hydro-steel structures. *Advanced Engineering Informatics*, *62*, 102661. https://doi.org/10.1016/j.aei.2024.102661.
2. Liu, Z., Chu, Y., Li, G., Hildre, H. P., & Zhang, H. (2024). Shipboard crane digital twin: An empirical study on R/V Gunnerus. *Ocean Engineering*, *302*, 117675. https://doi.org/10.1016/j.oceaneng.2024.117675.
3. Es-haghi, M. S., Anitescu, C., & Rabczuk, T. (2024). Methods for enabling real-time analysis in digital twins: A literature review. *Computers & Structures*, *297*, 107342. https://doi.org/10.1016/j.compstruc.2024.107342.
4. Ubina, N. A., Lan, H., Cheng, S., Chang, C., Lin, S., Zhang, K., Lu, H., Cheng, C., & Hsieh, Y. (2023). Digital twin-based intelligent fish farming with Artificial Intelligence Internet of Things (AIoT). *Smart Agricultural Technology*, *5*, 100285. https://doi.org/10.1016/j.atech.2023.100285.

5. Fu, X., Li, S., Song, H., & Lu, Y. (2025). Digital Twin-driven multi-scale characterization of machining quality: Current status, challenges, and future perspectives. *Robotics and Computer-Integrated Manufacturing*, *93*, 102902. https://doi.org/10.1016/j.rcim.2024.102902.
6. Mohanraj, R., & Vaishnavi, B. K. (2025). Data enabling technology in digital twin and its frameworks in different industrial applications. *Journal of Industrial Information Integration*, *44*, 100793. https://doi.org/10.1016/j.jii.2025.100793.
7. Zou, Y., Liu, Y., Chen, Z., Liu, J., Chen, J., Chen, M., Lv, P., Duan, H., & Li, H. (2024). Data driven digital twin system for the cross-domain vehicle. *Ocean Engineering*, *311*, 118846. https://doi.org/10.1016/j.oceaneng.2024.118846.
8. Shang, G., Xu, L., Li, Z., Zhou, Z., & Xu, Z. (2024). Digital-twin-based predictive compensation control strategy for seam tracking in steel sheets welding of large cruise ships. *Robotics and Computer-Integrated Manufacturing*, *88*, 102725. https://doi.org/10.1016/j.rcim.2024.102725.
9. Liu, J., Zhang, Y., Liu, Z., Leng, J., Zhou, H., Gu, S., & Liu, X. (2024). Digital twins enable shipbuilding. *Alexandria Engineering Journal*, *107*, 915-931. https://doi.org/10.1016/j.aej.2024.09.007.
10. Khaled, I., Vasiukov, D., Shakoor, M., Bennebach, M., & Chaki, S. (2023). Digital Twin for Predicting Progressive Damage in Operating Pressure Vessels. *Procedia Structural Integrity*, *57*, 280-289. https://doi.org/10.1016/j.prostr.2024.03.030.
11. Vashishth, T. K., Sharma, V., Sharma, K. K., Kumar, B., Chaudhary, S., & Panwar, R. (2024). Digital twins solutions for smart logistics and transportation. *Digital Twins for Smart Cities and Villages*, 353-376. https://doi.org/10.1016/B978-0-443-28884-5.00016-6.
12. Javaid, M., & Haleem, A. (2024). Role of digital twin and blockchain in logistics and supply chain management. *Digital Twin and Blockchain for Sensor Networks in Smart Cities*, 243-264. https://doi.org/10.1016/B978-0-443-30076-9.00012-1.
13. Majidi Nezhad, M., Neshat, M., Sylaios, G., & Astiaso Garcia, D. (2024). Marine energy digitalization digital twin's approaches. *Renewable and Sustainable Energy Reviews*, *191*, 114065. https://doi.org/10.1016/j.rser.2023.114065.
14. Onishchenko, O., Bulgakov, M., Melnyk, O., Volianska, Y., Storchak, O., & Kovalchuk, M. (2024). Environmental sustainability in maritime transportation through the development of strategies to reduce emissions from marine internal combustion engines. In Studies in Systems, Decision and Control, 561, 509–534. https://doi.org/10.1007/978-3-031-68372-5.
15. Bulgakov, M., Melnyk, O., Kuznichenko, S., Zaporozhets, A., Sagaydak, O., & Shcheniavskyi, G. (2025). Assessing the effectiveness of deoxygenation methods in ballast water treatment. In Studies in Systems, Decision and Control (Vol. 580, pp. 107–119). Springer. https://doi.org/10.1007/978-3-031-82027-4_7.

Микола Булгаков*[1], Олексій Мельник[2]

[1]Кандидат технічних наук, доцент, доцент кафедри судноплавства та безпеки мореплавства, Одеський національний морський університет, вул. Мечникова, 34, Одеса, 65029, Україна. ORCID: https://orcid.org/0000-0002-7172-8678.

[2]Доктор технічних наук, професор, професор кафедри судноплавства та безпеки мореплавства, Одеський національний морський університет, вул. Мечникова, 34, Одеса, 65029, Україна. ORCID: https://orcid.org/0000-0001-9228-8459.

Використання інтелектуального цифрового двійника енергосистеми судна для прогнозування та оптимізації в реальному часі

У статті представлено концепцію та математичну модель інтелектуального цифрового двійника енергетичної системи морського судна, розраховану на функціонування в режимі реального часу. Розроблена система поєднує динамічне моделювання енергобалансу, обробку телеметричних даних із застосуванням фільтра Калмана, прогнозування навантаження на основі нейронних мереж типу LSTM, а також механізми виявлення аномальних режимів і модулі оптимізації. Архітектура цифрового двійника реалізована у вигляді модульної програмної системи з підтримкою інтеграції до суднових платформ управління та хмарних аналітичних сервісів. У середовищі MATLAB/Simulink проведено серію комп'ютерних експериментів, що охоплюють типові та аварійні режими енергоспоживання судна. Отримані результати

засвідчили високу збіжність розрахункових та модельованих значень, оперативне реагування системи на зміни технічного стану та ефективність запропонованих рішень. Розроблена модель цифрового двійника може бути використана як інструмент підвищення енергоефективності, надійності та безпеки експлуатації суден в умовах змінного морського середовища.

Ключові слова: *цифровий двійник, енергетична система судна, прогнозування навантаження, телеметрія, фільтр Калмана, LSTM, виявлення аномалій, енергоефективність, автономне управління, морський транспорт.*

DOI: 10.32703/2617-9040-2025-45-10

UDC 004.925.4

Serhii Karnatov[1], Oleksandr Gertsiy[2]

[1] Postgraduate student of the Department of Automation and Computer-Integrated Transport Technologies, National Transport University, Omelianovycha-Pavlenka str. 1, 01010, Kyiv, Ukraine. ORCID: https://orcid.org/0009-0006-6254-6166.

[2]Associate Professor, Department of Automation and Computer-Integrated Transport Technologies, National Transport University, Omelianovycha-Pavlenka str. 1, 01010, Kyiv, Ukraine. ORCID: https://orcid.org/0000-0002-8634-5880.

Corresponding author: serafim@ukr.net

Comparative analysis of the quality of fractal image compression with JPEG and JPEG2000 standards

This paper presents a comparative analysis of three image compression methods: JPEG, JPEG2000, and fractal compression (FIC). The theoretical foundations of each method are reviewed, including the discrete cosine transform (DCT) for JPEG, the discrete wavelet transform (DWT) for JPEG2000, and the iterated function system (IFS) for FIC. The performance of the algorithms is evaluated using a set of metrics: compression ratio (CR), peak signal-to-noise ratio (PSNR), structural similarity index (SSIM), and the learned fragment image similarity metric (LPIPS). The analysis shows that JPEG2000 generally provides better quality at a given bitrate than JPEG, especially at high compression ratios, and offers additional features such as scalability, but this advantage is rather small. JPEG remains popular due to its simplicity and speed, but suffers from block artifacts. Fractal compression, despite its theoretical advantages, such as potential resolution independence, has significant drawbacks, including extremely slow encoding and often uncompetitive quality on general images. The application areas, reasons for limited implementation, and the current relevance of FIC are discussed. It is concluded that it is necessary to use various metrics for comprehensive quality assessment and that the choice of the optimal compression method depends on the specific requirements of the application.

Keywords*: image, compression, lossy, lossless, fractal compression, LPIPS, PSNR, SSIM.*

Introduction. In the digital age, visual information plays an extremely important role in many areas, from everyday communication and entertainment to highly specialized industries such as medicine, remote sensing of the Earth, and scientific research. The rapid growth of the volume of generated and processed digital images in various fields, including multimedia and consumer technology, places an urgent need for efficient methods of their storage and transmission. Despite the constant improvement of hardware, the volume of uncompressed images often exceeds the available memory resources and bandwidth of communication channels, making image compression not just a useful option, but an urgent necessity. The basis for solving this problem are image compression algorithms, the goal of which is to reduce data redundancy while preserving visually meaningful information. The effectiveness of any compression algorithm is determined by the balance between the achieved compression ratio (Compression Ratio, CR) and the quality of the restored image.

There are many approaches to image compression, each with its own characteristics and applications. One of the most widely used and versatile standards is JPEG, which has gained widespread acceptance for its effectiveness for photographic images, especially in the web and consumer electronics. Its successor, JPEG 2000, offered significant improvements, including better quality at high compression ratios, scalability, and support for lossless compression, making it valuable in critical areas such as

medical imaging, high-quality image archiving, and professional graphics processing. In addition to transformation-based standards, alternative methods have been explored, including fractal compression, which uses the principles of image self-similarity and can be effective for certain types of visual data, although it is more computationally intensive [1]. The choice of the optimal compression method depends on the specific quality, speed, and purpose of the compressed image.

Analysis of recent research and problem statement. Fractal concepts find application even in the field of lossless compression (lossless compression), especially for specific data types. The CompaCT algorithm is designed for efficient lossless compression of high bit depth medical images (e.g. 12-bit monochrome DICOM images such as CT scans). CompaCT is claimed to demonstrate significantly better compression ratios than standard lossless compression methods used in medicine such as JPEG2000-Lossless (approximately 37% more space efficient), while guaranteeing full recovery of the original data [2]. CompaCT's success in lossless compression of medical images using fractal scanning challenges the historical association of fractals with primarily lossy compression. This highlights the usefulness of space - filling fractal curves), to optimize the data order before the next standard encoding steps (delta, entropy). The significant improvements compared to standard lossless methods demonstrate the practical value of such fractal preprocessing in the lossless compression pipeline. This broadens the scope of fractal techniques in compression, showing their relevance even where perfect recovery is required [2].

Fractal ideas also penetrate the field of generative modeling. The concept of Fractal Generative Models (Fractal Generative Models), where a generative model is built by recursively calling models of the same type within itself. For example, an autoregressive model can consist of modules that are themselves autoregressive models. This recursive strategy leads to complex architectures with self-similarity at different levels of modules, similar to fractal structures in nature or biological neural networks. This approach is potentially suitable for modeling non-sequential data with internal multi-scale structure. Its effectiveness has been demonstrated on the complex problem of pixel-by-pixel image generation, where it showed high generation quality and accuracy of likelihood estimation [3, 4].

There are several approaches to compression, among which JPEG and JPEG2000 are the most common, while fractal compression (FIC) offers an alternative approach based on image self-similarity [1]. However, comparing the performance of these methods is complicated by their different underlying principles and the types of artifacts they introduce. Traditional quality metrics, such as PSNR, often correlate poorly with human subjective perception of quality. Therefore, the problem arises of objectively and comprehensively assessing the quality and performance of fractal compression compared to JPEG and JPEG2000. This problem requires the use of a set of metrics that include both objective indicators (CR, PSNR) and metrics that better reflect human perception (SSIM, LPIPS) to analyze the trade-offs between compression rate, image quality, and computational complexity, as well as to determine the practical feasibility and potential niche applications of fractal compression in a modern context.

The purpose and tasks of the study. The main goal of this study is to conduct a comprehensive comparative analysis of the effectiveness of fractal image compression (FIC) relative to the widely used JPEG and JPEG2000 standards, using a set of objective and perceptual quality metrics. To present in detail the theoretical foundations and algorithmic steps of JPEG (DCP-based), JPEG2000 (DVP-based), and fractal compression (SIF-based) compression methods. To analyze the types of artifacts characteristic of each method. To analyze the strengths and weaknesses of each method, including the computational complexity of encoding and decoding. To separately consider potential areas of application and reasons for the limited implementation of fractal compression.

Materials and methods of research. Among the main compression methods that have gained popularity and are widely used are the J PEG and J PEG2000 methods. The fractal compression method is much less common and no less interesting. Let's consider them in more detail.

*JPEG compression standard***.** JPEG (Joint Image File Format) Photographic Experts Group) is a lossy compression standard based on dividing an image into 8x8 pixel blocks and applying a Discrete Cosine Transform (DCT) to each block. The purpose of DCT is to correlate pixel values within a block,

concentrating most of the signal energy in the low-frequency coefficients.
The JPEG compression process includes the following steps:

1. Color space conversion: Typically, an image is converted from RGB to YCbCr. This allows for chroma thinning to be applied. subsampling), reducing the resolution of the Cb and Cr components, since human vision is less sensitive to color details than to brightness.
2. Block division: The image is divided into non-overlapping blocks of 8x8 pixels.
3. Discrete Cosine Transform (DCT): DCT is applied to each 8x8 block, converting pixel values from the spatial domain to the frequency domain. The first coefficient (DC) represents the average brightness of the block, the rest (AC) represent high-frequency details.
4. Quantization: This is the key step where data loss occurs. Each DCT coefficient is divided by the corresponding value from the quantization table (larger values for higher frequencies, resulting in greater information loss) and rounded to the nearest integer. This process is controlled by the quality parameter (quality factor).
5. Zigzag scanning: The quantized coefficients are reordered from low frequencies to high frequencies in a zigzag pattern. This groups zero coefficients together, which increases the efficiency of the next stage.
6. Entropy coding: A lossless compression method (usually Huffman coding, sometimes arithmetic coding) is applied to the reordered coefficients to efficiently represent the quantized data stream.

Advantages: Easy to implement, widespread, fast decoding.

Disadvantages: At low bitrates (high compression ratios), characteristic "block artifacts" appear due to independent processing of 8x8 blocks. The standard does not provide scalability or robust error tolerance compared to JPEG2000 [5].

JPEG's reliance on fixed 8x8 blocks and DCT is both its strength (simplicity) and its weakness. The characteristic block artifacts that appear at the boundaries of these blocks when quantized heavily are its visual signature. This predictability makes it a useful baseline for comparison, but also highlights its limitations, especially compared to methods that use other approaches such as JPEG2000 (based on wavelets, which produces smoother artifacts) or FIC (with potentially other types of artifacts related to the self-similarity mapping). Understanding this type of artifact is key to interpreting comparative metric scores (e.g., SSIM may penalize blocking more heavily than PSNR).

*JPEG2000 compression standard***.** JPEG2000 uses a Discrete Wavelet Transform (DWT) applied to the entire image or large tiles, providing a multi-level representation of the signal. This overcomes the blocky artifacts characteristic of JPEG and provides better concentration of signal energy.
The JPEG2000 algorithm includes the following steps:

1. Color space conversion: Various conversions are supported, including reversible (for lossless compression) and irreversible (for lossy compression).

2. Tiling (optional): The image can be divided into rectangular tiles that are processed independently. This improves memory efficiency for large images.

3. Discrete Wavelet Transform (DWT): Applied to tiles (or the entire image). DWT decomposes the image into different frequency subbands at multiple resolution levels (e.g. using the Cohen-Daubechy-Favo 9/7 wavelet for lossy compression or the LeGall 5/3 wavelet for lossless compression).

4. Quantization: Scalar quantization is applied to the wavelet coefficients in each subband. This allows for precise control of the bitrate.

5. Entropy Coding (EBCOT): Embedded Block Coding with Optimized Truncation (Embedded Block Coding with Optimized Truncation). Coefficients within subbands are grouped into code blocks that are coded bit-by-bit independently. This creates an embedded bitstream where layers can be truncated to achieve the desired bitrate or resolution. This multi-layer coding provides scalability.

Advantages: Higher compression efficiency, usually achieves better quality than JPEG at the same bitrate, especially at low bitrates. Lossy and lossless compression possible, supports both modes within a single standard. Scalability, progressive transmission by quality (SNR scalability) or resolution (resolution) scalability). Regions of interest (ROI) coding is also implemented, which allows coding certain areas of the image with higher accuracy. Increased error tolerance, better handling of errors in

the bitstream compared to JPEG [1, 6].

Disadvantages: At low bitrates the characteristic "blocking artifacts" still appear.

JPEG2000 limitations and advantages: higher computational complexity of encoding and decoding compared to JPEG, less widespread native support in web browsers and basic image viewers. A key advantage of JPEG2000, resulting from the use of DVP and EBCOT, is its intrinsic scalability. A single compressed file can serve different purposes (thumbnail, screen resolution, full quality) without the need for re-encoding. This is in sharp contrast to JPEG (where separate files are required for different qualities/ resolutions) and FIC (where decoding is iterative and resolution independence is theoretical, but practical scaling may require repeated decoding). EBCOT organizes the bitstream into quality layers, allowing the decoder to stop reading the stream at any point and restore the image at the appropriate quality or resolution. This property fundamentally changes the way compressed data is used compared to JPEG, where the entire file must be decoded to obtain a complete image. This makes JPEG2000 particularly suitable for applications such as medical image archives or content delivery networks (CDNs) [7, 8].

Fractal Image Compression (FIC). Fractal compression is based on the mathematics of Systems of Iterated Functions (SIF) and the Collage Theorem (Barnsley). The basic idea is that the redundancy of an image can be described by finding parts of the image (domain blocks, DB) that, after simple geometric and contrast transformations (affine mappings), can approximate other parts of the image (rank blocks, RB). The image is represented by a set of these transformations, rather than by pixel values [9].

Coding process.

1. Image partitioning: The image is partitioned into non-overlapping 'rank blocks' (RBs). A separate collection of potentially larger, possibly overlapping 'domain blocks' (DBs) is created.
2. Self-similarity search: For each rank block, the encoder searches among the domain blocks for the best match after applying an affine transformation (typically involving scaling, rotation/reflection, brightness shift, contrast scaling). This search is the computational bottleneck of the algorithm.
3. Transformation parameters: The parameters of the best affine transformation (spatial compression, isometry, brightness/contrast settings) and the location of the best domain block are stored for each rank block. Quantization is applied to these parameters.

Decoding process.

1. It starts with an arbitrary initial image.
2. iteratively applied to the current image, mapping the contents of the domain blocks (transformed) to the corresponding positions of the rank blocks.
3. Due to the compressibility property of transformations, this iterative process converges to a stable attractor – an image that is a restored approximation of the original.

Key features:

- Potential for high compression ratios, especially for images with significant self-similarity (e.g. textures).
- Resolution independence (theoretical), since the image is represented by transforms, decoding can potentially occur at a higher resolution than the original, generating plausible details (though not necessarily accurate high-frequency information).
- Extremely slow coding due to extensive search process, there are various optimization methods (e.g. block classification), but this remains the main drawback.
- Typically faster than encoding, but the iterative nature may be slower than basic JPEG decoding.
- Artifacts may differ from JPEG/JPEG2000, with possible loss of fine texture or "fractal-like" artifacts if the conversions are inaccurate.

The fundamental asymmetry between slow encoding and faster decoding in FIC is a direct consequence of its reliance on self-similarity search. Encoding requires exhaustive search, while decoding is a deterministic iterative application of the found transforms. This significant time difference (encoding is slow, decoding is faster) has profoundly affected the practical implementation of FIC. Scenarios that require fast encoding (e.g., digital cameras, real-time video conferencing) are poorly

suited to FIC. It may be more viable for archival scenarios (encode once, decode many times), but even there it competes with standards that offer better overall performance or functionality [10].

Although resolution independence is often cited as a key advantage of FIC, its practical value is debatable. Higher-resolution decoding essentially interpolates data based on learned self-similarities. This can generate visually plausible details, especially for textures, but does not recover high-frequency information lost during encoding. Modern super-resolution methods (often based on deep learning) may offer more efficient ways to increase image resolution. The benefits of this approach should be assessed in terms of achievable quality and compared to alternative upscaling methods [11].

Image quality assessment metrics. Evaluating the performance of compression algorithms with different underlying mechanisms (DCP, DVP, SIF) requires metrics that capture different aspects of reproduction accuracy and perceptual image quality.

Compression ratio (CR) - the ratio of the size of the original uncompressed image to the size of the compressed file. Measures the primary goal of compression - reducing the amount of data. Higher CR means stronger compression. Does not provide information about quality.

Peak signal-to-noise ratio (PSNR) is based on the mean square error (MSE) between the original (I) and reconstructed (K) images of size M×N.

$$MSE = \frac{1}{M \times N} \sum_{i=0}^{M-1} \sum_{j=0}^{N-1} \left[I(i,j) - K(i,j) \right]^2 \tag{1}$$

$$PSNR = 10 \cdot \log_{10} \left(\frac{MAX_I^2}{MSE} \right) \tag{2}$$

where MAX_I is the maximum possible pixel value (for example, 255 for an 8-bit gradation image).

Historically, the standard metric, which is easy to compute, measures per-pixel accuracy. A higher PSNR typically indicates lower per-pixel error. But the metric has a poor correlation with human perception of quality; it penalizes all errors equally, regardless of image content or structure. It can be misleading when comparing different types of artifacts (e.g., blurring versus blocking) [12].

The Structural Similarity Index (SSIM) measures perceived similarity based on structural information by comparing local patterns pixel intensities, normalized by brightness and contrast. Computed locally and averaged.

$$SSIM(x,y) = \left[l(x,y)^{\alpha} \cdot c(x,y)^{\beta} \cdot s(x,y)^{\gamma} \right] \tag{3}$$

Typically α=β=γ=1. Component l compares brightness, c compares contrast, s compares structure (using covariance /correlation).

Designed to better match human visual perception than PSNR, focusing on structural changes. Values range from -1 to 1 (or 0 to 1), where 1 represents perfect similarity. The metric has some limitations: it is still based on relatively simple statistical comparisons of image fragments; it may not accurately capture complex texture distortions or suprathreshold artifacts [12, 13].

Trained image fragment similarity metric (LPIPS). A "perceptual distance" metric that uses deep convolutional neural networks (CNNs, e.g., VGG, AlexNet) pre-trained on large image datasets (such as ImageNet). It computes the distance between activations at intermediate layers of the network for fragments of the reference and distorted images. Lower LPIPS values indicate greater perceptual similarity. It uses features learned by deep networks that are known to correlate well with human object and texture recognition, thus aiming for better agreement with human perceptual similarity/quality estimates than PSNR or SSIM. Particularly useful for evaluating generative models or distortions that are poorly captured by traditional metrics. Limitations of the metric - requires pre-trained networks, is computationally more expensive than PSNR/SSIM, and performance may depend on the specific network architecture and training data. Its interpretation as a universal quality metric is still evolving.

The selected metrics form a hierarchy of complexity and perceptual relevance. CR measures efficiency. PSNR measures per-pixel error. SSIM measures structural error. LPIPS measures perceptual distance based on deep features. Using them together provides a more holistic view. For example, FIC may achieve high CR but lower PSNR/SSIM than JPEG2000 at the same CR, but LPIPS may evaluate it differently depending on the nature of the artifacts, potentially revealing cases where its distortions are perceptually less unpleasant despite per-pixel /structural differences. Comparing algorithms such as JPEG (blocking), JPEG2000 (blurring), and FIC (potential texture/self-similarity artifacts) requires such a multifaceted approach, as each metric may evaluate different types of artifacts differently.

The progression from PSNR to SSIM and then to LPIPS reflects the ongoing research effort in computational modeling of human visual perception. The limitations of PSNR motivated the development of SSIM, and the quest for even better perceptual correlation, especially for complex distortions, led to the emergence of learning-based metrics such as LPIPS. This evolution emphasizes that "image quality" is not a fixed concept, and our tools for measuring it are constantly improving. This means that evaluating compression algorithms requires the use of metrics that reflect current understanding of perceptual quality, making LPIPS particularly relevant alongside established standards [14, 15, 16].

Quality assessment of compression methods on samples. For compression comparison, samples of 512x512 pixels were taken and compressed with the same compression ratio. The first sample for the study is a photograph of brickwork (Fig. 1). The applied compression ratio (CR) for all algorithms for this image is 6.5. Fig. 2.1, 2.2., in an enlarged form, show the distortions that occur when compressing JPEG, JPEG 2000, FIC, respectively.

The figures clearly show minimal distortion when compressing FIC, preserving boundaries and colors. The JPEG sample clearly shows 8 x 8 areas, and JPEG 2000 compression shows strong blurring. But brickwork is an example of an image with a large number of similar fragments that can be used in compression due to affine transformation. Table 1 shows comparative metrics. PSNR is indicated in dB (the higher, the better), the pixel-by-pixel restoration accuracy of all methods is very close and is within 2.4%, although the visual difference is very noticeable. This indicates the weakness of this metric for evaluating compression algorithms. The structural similarity index (SSIM, the closer to 1, the better) is a perceptual metric that evaluates the structural similarity between the original and restored images, taking into account brightness, contrast and structure, but it also gives a difference of 2.1%. Moreover, the SSIM metric gives an advantage to the SSIM algorithm even with an obvious blur factor. LPIPS is a similarity metric of image fragments, designed for better correlation with the human perception of image similarity. It is it that gives an advantage to the FIC algorithm with a gap of 58% and 25% over JPEG and JPEG2000, respectively. Judging by the examples given, it is this metric that most accurately shows the similarity of images from a human perspective.

Table 1. **Comparison of JPEG, JPEG2000 and Fractal compression (FIC) of Figure 1**

Compression ratio (CR)	Algorithm	PSNR (dB)	SSIM	LPIPS
6.5:1	JPEG	28.7013	0.7704	0.1352
	JPEG2000	29.1834	0.7915	0.1067
	FIC	28.4859	0.7767	0.0854

The second example for comparing compression algorithms is a lung X-ray, which is widely used in medicine (Fig. 3).

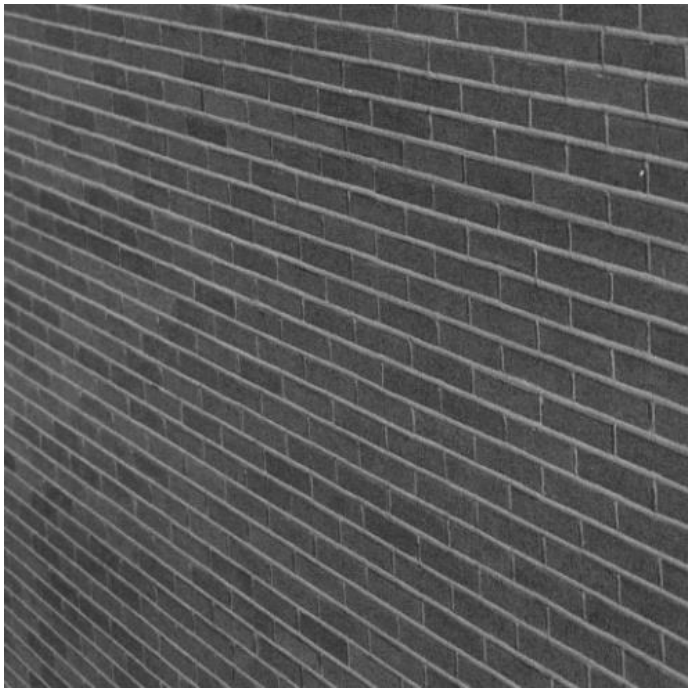

Fig. 1. **Brickwork**

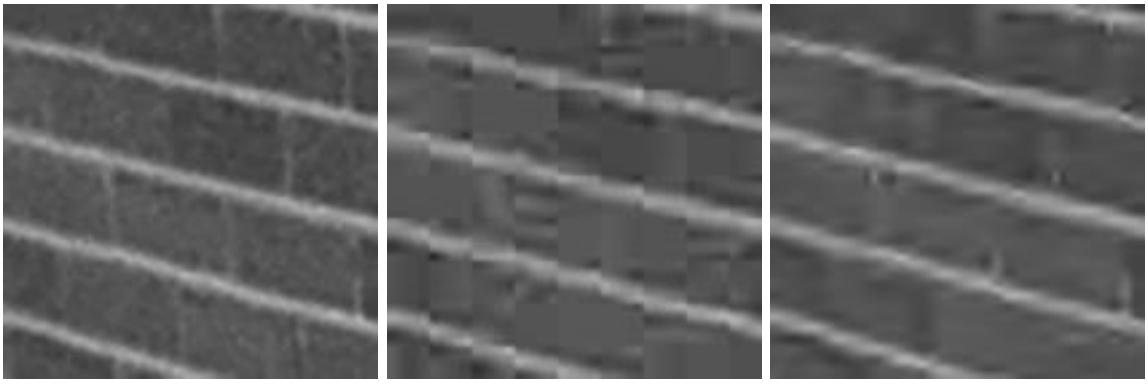

Fig. 2.1. **Brickwork. Original image, compressed JPEG, compressed JPEG 2000**

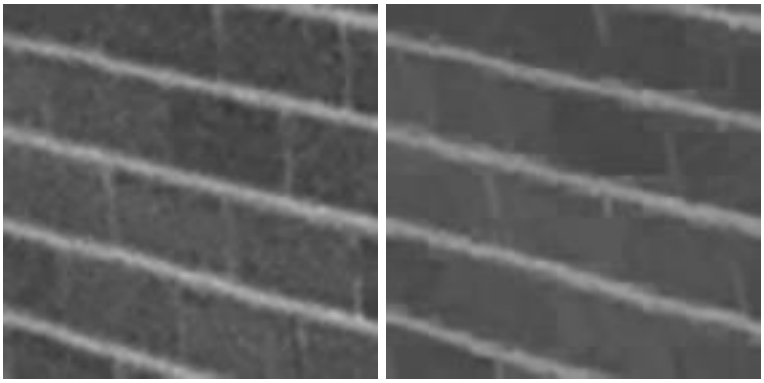

Fig. 2.2. **Brickwork. Original image, image compressed FIC**

Fig. 3. **Lung X-ray**

The applied compression ratio (CR) for all algorithms for this image is 5.2. Fig. 3.1, 3.2., in an enlarged form, show the distortions that occur when compressing JPEG, JPEG 2000, FIC.

The figures clearly show minimal distortion when compressing JPEG and JPEG 2000, the edges and colors are preserved. The FIC sample clearly shows 8 x 8 areas. X-ray is an example of an image with clear boundaries, a large number of areas filled with a gradient. Table 2 shows comparative metrics. Although the image reproduction quality in all algorithms is very high, the PSNR of FIC is worse than JPEG and JPEG2000 by 15% and 17%, SSIM is worse by 1.7%. LPIPS is almost 6 times worse, but this is not very noticeable from a human point of view because the level of 0.0383 is very close to 0. Nevertheless, for X-rays, FIC performed worse than the JPEG family. This is explained by the small number of similar fractals, although it seems that the edges are almost the same, not all fragments can be converted to similar ones by affine methods.

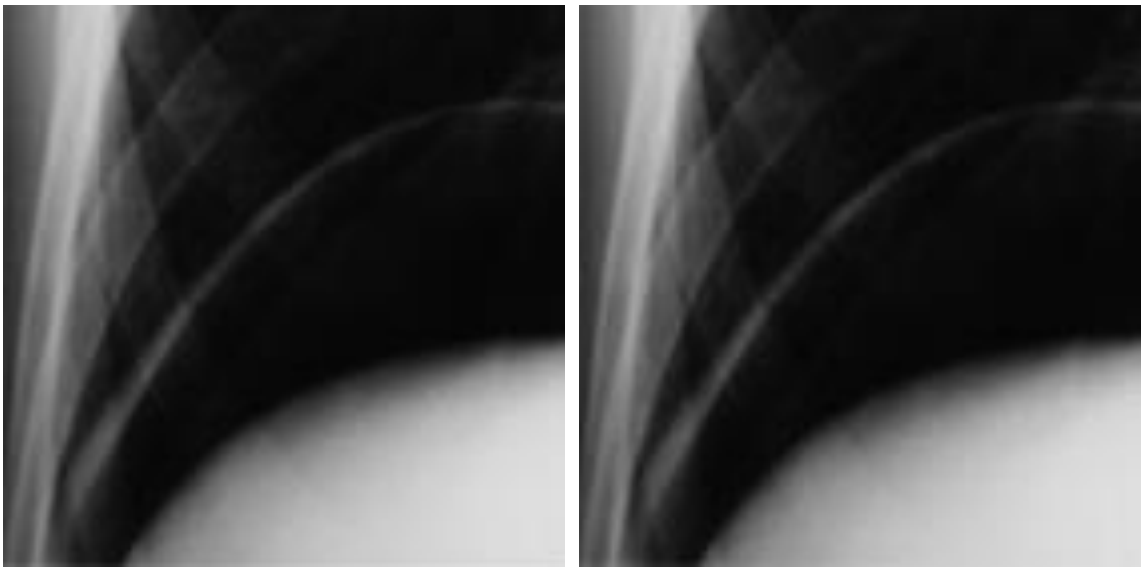

Fig. 3.1. **Lung X-ray. Original image, compressed JPEG**

Fig. 3.2. **Lung X-ray. Image compressed JPEG 2000, compressed FIC**

Table 2. **Comparison of JPEG, JPEG2000 and Fractal compression Compression (FIC) of Figure 3**

Compression ratio (CR)	Algorithm	PSNR (dB)	SSIM	LPIPS
5.2:1	JPEG	46.3723	0.9905	0.0056
	JPEG2000	47.2023	0.9900	0.0066
	FIC	40.2540	0.9730	0.0383

The third example for comparing compression algorithms is a satellite image (Fig. 4).

Fig. 4. **Satellite image**

The applied compression ratio (CR) for all algorithms for this image is 5.2. Fig. 4.1, 4.2., in an enlarged form, show the distortions that occur when compressing JPEG, JPEG 2000, FIC.

Fig. 4.1. **Satellite image. Original image, JPEG compressed**

The figures clearly show the worse quality of the FIC compression algorithm, which can be explained by the rather large size of the rank block of 8 x 8 pixels, which does not allow reproducing small details. But when the block is reduced to 4 x 4 pixels, the number of blocks and, accordingly, the size of the compressed file increases 4 times. It is precisely for the purpose of comparison that the CR algorithms were brought to the same level. Comparative metrics are shown in Table 3.

Fig. 4.2. **Satellite image. Image compressed JPEG 2000, compressed FIC**

Small details revealed the weakness of the FIC algorithm compared to JPEG and JPEG2000 at the same CR. The main LPIPS metric is more than 2 times worse in FIC compared to JPEG, this is very noticeable on small details, although the overall level of 0.1653 is high.

Table 3. **Comparison of JPEG, JPEG2000 and Fractal compression Compression (FIC) of Figure 4**

Compression ratio (CR)	Algorithm	PSNR (dB)	SSIM	LPIPS
5.2:1	JPEG	31.0731	0.8334	0.0771
	JPEG2000	31.6100	0.8364	0.1042
	FIC	27.2289	0.7250	0.1653

The analysis shows an inevitable trade-off between compression efficiency (CR), objective quality (PSNR), structural quality (SSIM), perceptual quality (LPIPS), and computational cost (encoding/decoding time). JPEG2000 generally offers the best balance of quality and compression for natural images, but at the expense of higher complexity compared to JPEG. JPEG remains popular due to its simplicity and speed, despite quality limitations at high CRs [17, 18]. FIC, despite its theoretical advantages, suffers from extremely slow encoding and often uncompetitive quality on general images.

Although JPEG2000 generally dominates the "bitrate-to-distortion" ratio for natural images, FIC's unique mechanism exploiting self-similarity suggests that it could have a niche for images rich in repeating patterns or textures. Theoretically, for such images, the self-similarity model could be more efficient than the frequency model (DCP/DVP), potentially resulting in better compression or quality for these specific images. However, empirical data often shows it to lag behind. This suggests that FIC's strengths, if they exist, are likely limited to specific classes of images, making it less suitable as a universal standard.

Including LPIPS can potentially change the perceived rating, especially between FIC and JPEG. If FIC produces artifacts that look "unnatural" but do not destroy the structure as much as blocking (less impacting SSIM) or pixel values (less impacting PSNR), LPIPS may penalize it heavily. Conversely, if its artifacts are perceptually smoother or less obtrusive than strong blocking, LPIPS may rate it higher than a relatively low-quality JPEG than PSNR/SSIM. This highlights the importance of using metrics that are consistent with the intended application (e.g., human viewing vs. machine analysis).

The choice of the "best" method depends heavily on the specific requirements of the application: the required quality, the constraints on encoding speed, the need for features such as scalability, etc. Today, FIC is mostly considered a niche technique with historical significance. Although research into optimizing FIC algorithms or exploring hybrid approaches is ongoing, it is not a mainstream compression method [19]. Its basic ideas (the use of self-similarity) may find application in other areas such as analysis or texture generation, or potentially inspire aspects of future compression schemes [20]. Even if FIC has failed as a mainstream compression standard, the basic concept of exploiting structural self-similarity in data is powerful. This idea finds resonance in other areas of computer vision and graphics, such as texture synthesis, image augmentation (inpainting), and potentially in the development of generative models. FIC research, even if commercially unsuccessful, contributed to a broader understanding of image statistics and redundancy. Texture synthesis techniques explicitly search for and reproduce similar patterns. Image redrawing algorithms can fill in missing areas by copying and transforming similar existing regions. Generative adversarial networks (GANs) learn complex data distributions, which implicitly involves capturing repeating structures. Thus, the intellectual contribution of FIC goes beyond its direct application in compression, influencing related fields dealing with the modeling and manipulation of image structure.

Although FIC represents an intellectually exciting approach to CIF-based image compression, its practical limitations, including coding complexity and inconsistent performance advantages over standardized methods such as JPEG2000, have prevented its widespread adoption. JPEG2000 remains a technically superior standard compared to JPEG, although its adoption has been constrained by factors beyond pure performance. The history of these compression standards illustrates the phenomenon of path dependence (dependency): Early choices (like JPEG standardization) create ecosystems and user bases that make it difficult to completely supplant technically more advanced but later or more complex technologies (like JPEG2000 or FIC), even if they offer advantages.

Conclusions. The study compared the effectiveness of three image compression algorithms – JPEG, JPEG2000, and fractal compression (FIC) – on different types of samples (texture, medical image, satellite image) at the same compression ratios.

The analysis showed that the effectiveness of each method significantly depends on the characteristics of the image itself. Fractal compression demonstrated the best visual results and LPIPS perceptual metric performance on an image with a high degree of self-similarity (brickwork), significantly outperforming JPEG and JPEG2000 (by 58% and 25%, respectively) in terms of human

perception of quality, despite the close values of the traditional PSNR and SSIM metrics. This emphasizes the limitations of PSNR and SSIM for a complete assessment of visual quality and the superiority of LPIPS in reflecting human perception. However, on images with fewer repeating fractal elements, clear boundaries (lung X-ray) or a large number of fine details (satellite image), FIC significantly lost ground to the JPEG family algorithms, LPIPS is 60% lower in FIC compared to JPEG2000. Visually, the FIC method also created more distortions - the appearance of blocky artifacts, loss of detail. For such images, JPEG and JPEG2000 provided significantly higher reproduction quality at a given compression ratio.

The study confirms that the choice of the optimal compression method is a trade-off between compression ratio, quality (objective, structural, and perceptual), and computational complexity, especially considering the extremely high encoding time for FIC. Although JPEG2000 often offers a better balance of quality and compression compared to JPEG, the latter remains popular due to its simplicity and speed.

Fractal compression, despite its theoretical potential for certain classes of images, remains niche due to practical drawbacks (slow encoding, uncompetitive quality on general images). The choice of compression algorithm remains application-specific, requiring a balance between quality, compression ratio, functionality, and computational resources.

REFERENCES

1. Russ, J. C. (2006). *The image processing handbook*. CRC press.
2. Patel, N., & Sadleir, R.J. (2023). CompaCT: Lossless medical image compression via fractal pixel traversal and dynamic segmentation. *arXiv preprint arXiv:2308.13097*. https://arxiv.org/abs/2308.13097.
3. Li, T., Sun, Q., Fan, L., & He, K. (2025). Fractal generative models. *arXiv preprint arXiv:2502.17437*. https://arxiv.org/html/2502.17437v1.
4. Xiao, S., Guo, Y., Peng, H., Liu, Z., Yang, L., & Wang, Y. (2025). Generalizable AI-Generated Image Detection Based on Fractal Self-Similarity in the Spectrum. *arXiv preprint arXiv:2503.08484*. https://arxiv.org/html/2503.08484v1.
5. Gertsiy, O., (2024). Research on graphic data formats for compact representation and comparison of images. *Collection of scientific works of the State University of Infrastructure and Technologies series "Transport Systems and Technologies"*, (43), 173–187. https://doi.org/10.32703/2617-9059-2024-43-14.
6. Shrestha, B. (2005). *Evaluation of JPEG2000 for lossless medical image compression*. Mississippi State University Libraries. https://www.gri.msstate.edu/publications/docs/2005/03/4328BijayShrestha_2005.pdf.
7. Garmash, V.V., Kulyk, A.Y. (2010). Blocking Artifacts Reduction Method in JPEG- images. *Artificial Intelligence*, (4), 177-184.
8. Gonzalez, R. C. (2009). *Digital image processing*. Pearson education india.
9. Welstead, S. T. (1999). *Fractal and wavelet image compression techniques* (Vol. 40). Spie Press.. https://doi.org/10.1117/3.353798.
10. Zhu, L., Zeng, X., Chen, B., Chen, P., Li, Y. H., & Wang, S. (2025). Leveraging Diffusion Knowledge for Generative Image Compression with Fractal Frequency-Aware Band Learning. *arXiv preprint arXiv:2503.11321*. https://arxiv.org/html/2503.11321v1.
11. A. Djeacoumar, A., Mujkanovic, F., Seidel, H. P., & Leimkühler, T. (2025, April). Learning Image Fractals Using Chaotic Differentiable Point Splatting. In *Computer Graphics Forum* (p. e70084). https://arxiv.org/html/2502.17230v1.
12. Chen, C. H., Yao, Y., Page, D. L., Abidi, B., Koschan, A., & Abidi, M. (2006). Objective Image Quality Evaluation for JPEG, JPEG 2000, and Vidware Vision TM. In *Advances in Image and Video Technology: First Pacific Rim Symposium, PSIVT 2006, Hsinchu, Taiwan, December 10-13, 2006. Proceedings 1* (pp. 751-760). Springer Berlin Heidelberg. https://doi.org/10.1007/11949534_75.
13. Kim, J,H,, Lee K,H,, Kim, B., & Yoo, S,K, (2010). Evaluation of JPEG2000 compression efficiency by using physical factors in computed radiography images. *Journal of the Korean Physical Society, 56*(3), 856–861. https://doi.org/10.3938/jkps.56.856.
14. Gertsiy, O., & Butryk, N. (2021). Comparative analysis of compact methods representations of graphic information. *Collection of scientific works of the State University of Infrastructure and Technologies series "Transport Systems and Technologies"*, (37), 130–143. https://doi.org/10.32703/2617-9040-2021-37-13.
15. Singh, S., Singh, BK, & Mohan, A. (2024). Perceptual quality assessment of compressed images using different JPEG standards. *Information, 15*(5), 261. https://doi.org/10.3390/info15050261
16. Zhang, K., Liang, J., Van Gool, L., & Timofte, R. (2021). Designing a practical degradation model for deep blind image super-resolution. In *Proceedings of the IEEE/CVF international conference on computer vision* (pp. 4791-4800). https://doi.org/10.48550/arXiv.2103.14006.
17. Breger, A., Biguri, A., Landman, M. S., Selby, I., Amberg, N., Brunner, E., ... & Schönlieb, C. B. (2025). A study of why

we need to reassess full reference image quality assessment with medical images. *Journal of Imaging Informatics in Medicine*, 1-26. https://healthmanagement.org/c/imaging/News/the-limits-of-image-quality-measures-in-healthcare.
18. Arabboev, M., Begmatov, S., Rikhsivoev, M., Nosirov, K., & Saydiakbarov, S. (2024). A comprehensive review of image super-resolution metrics: classical and AI-based approaches. *Acta IMEKO*, *13*(1), 1-8. https://doi.org/10.21014/actaimeko.v13i1.1679.
19. Patel, Y., Appalaraju, S., & Manmatha, R. (2021). Saliency driven perceptual image compression. In *Proceedings of the IEEE/CVF winter conference on applications of computer vision* (pp. 227-236). https://openaccess.thecvf.com/content/WACV2021/papers/Patel_Saliency_Driven_Perceptual_Image_Compression_WACV_2021_paper.pdf.
20. Chen, B., Li, Y., Zeng, N., & He, W. (2019). Fractal lifting wavelets for machine fault diagnosis. *IEEE Access*, *7*, 50912-50932. https://doi.org/10.1109/ACCESS.2019.2908213.

Карнатов Сергій[1], Олександр Герцій[2]

[1]Аспірант кафедри автоматизації та комп'ютерно-інтегрованих транспортних технологій, Національний транспортний університет, вул. Михайла Омеляновича-Павленка, 2, 01010, м. Київ, Україна. ORCID: https://orcid.org/0009-0006-6254-6166.

[2]Доцент кафедри автоматизації та комп'ютерно-інтегрованих транспортних технологій, Національний транспортний університет, вул. Михайла Омеляновича-Павленка, 2, 01010, м. Київ, Україна.. ORCID: https://orcid.org/0000-0002-8634-5880.

Порівняльний аналіз якості фрактального стиснення зображень із стандартами JPEG та JPEG2000

У цій статті представлено порівняльний аналіз трьох методів стиснення зображень: JPEG, JPEG2000 та фрактального стиснення (FIC). Розглянуто теоретичні основи кожного методу, включаючи дискретне косинусне перетворення (ДКП) для JPEG, дискретне вейвлет-перетворення (ДВП) для JPEG2000 та системи ітерованих функцій (СІФ) для FIC. Ефективність алгоритмів оцінюється за допомогою набору метрик: коефіцієнт стиснення (CR), пікове відношення сигналу до шуму (PSNR), індекс структурної подібності (SSIM) та навчена метрика подібності фрагментів зображення (LPIPS). Аналіз показує, що JPEG2000 зазвичай забезпечує кращу якість при заданому бітрейті порівняно з JPEG, особливо при високих коефіцієнтах стиснення, та пропонує додаткові функції, такі як масштабованість, але ця перевага досить невелика. JPEG залишається популярним завдяки простоті та швидкості, але страждає від блокових артефактів. Фрактальне стиснення, незважаючи на теоретичні переваги, такі як потенційна незалежність від роздільної здатності, має суттєві недоліки, зокрема надзвичайно повільне кодування та часто неконкурентоспроможну якість на загальних зображеннях. Обговорюються сфери застосування, причини обмеженого впровадження та сучасна актуальність FIC. Робиться висновок про необхідність використання різноманітних метрик для комплексної оцінки якості та про те, що вибір оптимального методу стиснення залежить від конкретних вимог програми.

***Ключові слова**: зображення, стиснення, з втратами, без втрат, фрактальне стиснення, LPIPS, PSNR, SSIM.*

DOI: 10.32703/2617-9040-2025-45-11

UDC 629.4.053

Oleksandr Gorobchenko[1], Denys Zaika[2*], Sergiy Maliuk[3], Oleksander Arkhypov[4], Oleksandr Nevedrov[5]

[1]Professor, Electromechanics and Rolling Stock of Railways Department, National Transport University, 1, M. Omelianovycha-Pavlenka str., Kyiv, 01010, Ukraine. ORCID: https://orcid.org/0000-0002-9868-3852.

[2]Assistant, Electromechanics and Rolling Stock of Railways Department, National Transport University, 1, M. Omelianovycha-Pavlenka str., Kyiv, 01010, Ukraine. ORCID: https://orcid.org/0000-0003-0693-9580.

[3]Senior Lecturer, Electromechanics and Rolling Stock of Railways Department, National Transport University, 1, M. Omelianovycha-Pavlenka str., Kyiv, 01010, Ukraine. ORCID: https://orcid.org/0000-0003-1777-2384.

[4]Postgraduate student, Electromechanics and Rolling Stock of Railways Department, National Transport University, 1, M. Omelianovycha-Pavlenka str., Kyiv, 01010, Ukraine. ORCID: https://orcid.org/0009-0009-8873-8643.

[5]Senior Lecturer, Electromechanics and Rolling Stock of Railways Department, National Transport University, 1, M. Omelianovycha-Pavlenka str., Kyiv, 01010, Ukraine. ORCID: https://orcid.org/0000-0001-9347-0973.

***Corresponding author:** zaika_do@gsuite.duit.edu.ua.

Research of theoretical basis of implementation of intelligent control systems for locomotive traction transmission

The paper presents an analysis of existing automated control systems based on artificial intelligence theory. These systems employ methods such as fuzzy logic, artificial neural networks, and genetic algorithms. The application of these techniques enables the development of more adaptive and efficient control systems compared to traditional approaches. The main areas of artificial intelligence application in railway transport are identified, particularly in locomotive control systems and optimization of operational modes. The fundamental stages of artificial intelligence-based model development are outlined, including data collection and model training. Key directions for modeling intelligent systems are established. A generalized approach is proposed for the development of an intelligent traction transmission control system for shunting locomotives, taking into account the rolling stock characteristics and operational conditions. For solving control tasks, the use of a production model is proposed, which integrates elements of both logical and network-based approaches. A production model is proposed for solving control tasks.

Keywords: *railway transport, rolling stock, control, artificial intelligence, Mamdani method, risk, traction electric transmission, safety*

Introduction. Modern intelligent control systems have recently undergone significant progress in many areas of human development [1-3]. These systems are distinguished by their ability to "understand" and learn, adapting to the characteristics of the control object, its operating conditions and environmental influences. Their main difference is the presence of mechanisms for complex knowledge processing. The architectural feature that distinguishes intelligent systems from traditional ones is the ability to accumulate, store and analyze knowledge for the effective performance of control functions. Increasingly, such systems that use fuzzy logic methods, artificial neural networks and genetic algorithms are being introduced into various areas, including railway transport. Thanks to these technologies, adaptive, reliable and efficient systems have been created that cope better with changing conditions and uncertainty compared to traditional control approaches [4,5].

Analysis of recent research and problem statement. According to A. Bayen's research, artificial intelligence can control a vehicle in a way that is not intuitive to humans, but is generally more efficient. F. You's work explores the combination of quantum computing with artificial intelligence to solve complex optimization problems in energy systems. A multi-level optimization framework combined with machine learning is presented for planning the transition of energy systems, such an approach allows for detailed planning of energy capacities with hourly accuracy.

Innovative projects for the implementation of intelligent systems in rail transport can be conditionally divided into implemented ones, as well as promising technologies with a implementation period of up to 2030 [6]. The implemented ones include "Smart Locomotive" – a system that combines artificial intelligence, the Internet of Things (IoT) and big data analysis for monitoring the technical condition of locomotives, predicting faults and optimizing routes [7]; "Smart train" refers to intelligent trains, such as the Chinese Yiqun from CRRC, equipped with autonomous control modules, energy-efficient systems and adaptive interfaces for passengers [8]; "Smart depot" refers to depots that use robotic systems and AI to diagnose, maintain and repair rolling stock, which allows to reduce downtime and increase service efficiency [9]. In the metros of Santiago, Paris, Hong Kong and Beijing, Alstom is implementing its development based on implemented projects. An additional example of the implementation of such technologies is the Copenhagen metro. It is unique in that there is no driver in the metro trains, and control is carried out thanks to the fully automated ATC (Automatic Train Control) system [10]. This system is designed to eliminate the possibility of human error, as well as to more accurately control the distance between trains (thanks to the precisely set value of braking and acceleration). The ATC system consists of three subsystems:

- ATS (Automatic Train Supervisory) subsystem – a system for monitoring and controlling train routes and directions. It is this system that selects the train route. The ATS subsystem, depending on the situation, selects a scenario for movement. For example, there are different scenarios: normal movement, movement at night, movement during track maintenance. Information about train movement and routes is displayed on the monitors of the control center. The ATS also stores information about errors and malfunctions, repair and maintenance activities.
- ATO (Automatic Train Operation) subsystem – a system for controlling movement at stations, namely train stops, opening doors, waiting for a certain period of time, closing doors, and continuing movement. This part of the system is an analogue of an autopilot and performs the physical function of a train driver. The ATO subsystem operates at a very high level and cannot independently change its parameters, such as braking speed or waiting interval at the station.
- ATP (Automatic Train Protection) subsystem – a system for protecting subway passengers and personnel from accidents (in particular, derailments, train collisions, opening doors during movement). The system checks and controls the speed limit (three speed switch positions: start of movement or acceleration, movement and braking), the distance between trains, the switch and the free path (presence of foreign objects on the path, repair work or maintenance work).

The development of unmanned train movement in rail transport is actively implemented thanks to intelligent systems such as Cognitive Rail Pilot, which use artificial intelligence to improve safety and efficiency of transportation [11]. These systems are aimed at achieving high levels of automation, in particular GoA 3 (control without a driver, but with the presence of personnel on board) and GoA 4 (fully autonomous control without personnel on board). Cognitive Rail Pilot, a system developed by Cognitive Pilot, is designed to help drivers prevent dangerous errors that can lead to accidents. It uses artificial intelligence to analyze the environment and make decisions in real time. Promising technologies with an implementation deadline of 2030 include the GoA 4 automation level, which requires not only technical improvements, but also adaptation of the regulatory framework. New standards such as ANSI/UL 4600 are considered as the basis for certification of autonomous control systems based on artificial intelligence methods [12]. Additionally, Knorr-Bremse and Rail Vision are currently testing an obstacle recognition system for shunting locomotives in Switzerland [13]. This system includes optical sensors, artificial intelligence and machine learning elements, and is capable of recognizing switches, traffic light readings and track obstacles at a distance of up to 200 meters,

classifying objects in real time and issuing warnings to the driver. Research is also being conducted on the use of SLAM technologies (lidar and visual) to obtain additional data on the location of locomotives [14]. Obstacle detection is carried out using lidar data, stereo vision and neural networks, which allows to increase the accuracy and reliability of the system. In [15], the pragmatic and neurobiotic approaches to the use of artificial intelligence were analyzed. In [16], the creation of a knowledge base for intelligent locomotive DSS was theoretically substantiated. The authors proposed an approach and structure of a self-learning system for intelligent DSS, the main advantage of which is the use of a fuzzy classifier. This classifier operates according to specified criteria and forms a fuzzy image of the current situation during train movement. In article [17], the main control algorithms of an automated train control system are analyzed. In particular, control based on artificial neural network algorithms is considered, as well as fuzzy control using a fuzzy controller. The latter plays a key role in the system, which includes the stages of fuzzification, defuzzification, a knowledge base and a fuzzy logical inference unit. In article [18], the development of the structure of an intelligent decision support system for locomotives is presented. Formal indicators of the efficiency of the train control process are determined. The method of establishing weight coefficients for each individual control quality criterion is also theoretically justified. In work [19], a mathematical model of an automated traction control system for a shunting locomotive is presented. Using fuzzy logic methods, a fuzzy knowledge base of the system was formed and theoretically substantiated. A scheme of an automated system for controlling the traction transmission of a shunting locomotive with the possibility of self-learning was developed. The obtained results of the system operation allow implementing quite diverse modes of controlling the traction transmission of a shunting locomotive, which differ from those adopted in traction calculations and indicated in the mode maps.

Analyzing the above literature, it can be noted that the process of controlling locomotives using artificial intelligence methods is in a stage of constant development. The advantages of the works include the prepared theoretical basis for creating intelligent control systems. Each work investigates the factors that affect the movement of the locomotive and the control signals necessary for individual elements of the control system. The disadvantages include: the lack of consideration of the operation of each of the locomotive elements separately.

The purpose and tasks of the study. The main purpose of this work is to analyze existing methods and approaches to the development of automated control systems based on the theory of artificial intelligence, as well as to conduct applied research on the development of an intelligent locomotive traction control system.

To solve this problem, the main directions of using artificial intelligence methods in railway transport have been formed. The main stages of developing a model based on artificial intelligence have been identified and the main directions of modeling intelligent systems have been formed. It is proposed to use production models for rolling stock management tasks, and the Mamdani Algorithm to build a model of automated control of the traction transmission of shunting locomotives.

The main tasks.

1. To analyze the current state of development of intelligent technologies in railway transport and determine the main areas of application of artificial intelligence.

2. To study the theoretical foundations of existing decision-making methods by the intelligent control system of traction rolling stock.

3. To develop a generalized approach to the development of an intelligent control system for the traction transmission of shunting locomotives.

Materials and methods of research. The analysis of existing works devoted to the development of digital technologies in railway transport allows to systematize the areas of application of intelligent technologies and form Table 1 [15].

Table 1 **Main areas of use of artificial intelligence in railway transport**

Conversational artificial intelligence, automation of manual processing of typical applications, appeals	Infrastructure and rolling stock	Traction rolling stock	Automation of routine operations
Interactive artificial intelligence, capable of conducting a dialogue in natural language, as well as automating the processing of standard requests, applications and appeals. Such a system significantly reduces the workload on staff, increases the speed of response and provides 24/7 user support. In addition, it can learn based on the history of interactions, gradually improving the accuracy of responses and adapting to the specifics of tasks.	Predictive diagnostics. Maintenance and repair	Locomotive control using artificial intelligence methods	Technical support. Reporting. Maintaining regulatory information

The first in the field of implementing AI-based systems were A. Simon and A. Newell, who argue that research in the field of AI is like a heuristic search in the state space. Each node represents a task, and each path in the graph is a project aimed at solving this task. Based on this, it is possible to distinguish the main stages of developing any AI model (Fig. 1.).

The AI concept is quite multifaceted and sometimes even contradictory, but based on them, two basic directions in modeling intelligent systems can be distinguished (Fig. 2.).

The pragmatic or informational approach consists in the optional copying of all the principles of natural intelligence, data can be represented only in symbolic, not in numerical form. The solution algorithm in the general case is presented as a "black box", which in turn may be inapplicable in the light of a certain set of constraints. The objective function in these tasks is either complex or not formalized at all. All this does not allow the use of existing methods and algorithms when solving problems. The informational approach allows modeling only the properties of intelligence associated with information processing and heuristic analysis.

Neurobionics is based on the mandatory computer implementation of problem-solving processes by natural intelligence, and the adequacy of using AI theory to define them. The main idea of this approach is that successful reproduction of intellectual processes is impossible without reproducing their material carriers, that is, the creation of AI is inextricably linked with the modeling of brain processes. The key direction in this approach is the analysis of decision-making, formalization of tasks and parameters, which closely connects neurobionics with psychology, as a result of which psychonics emerged.

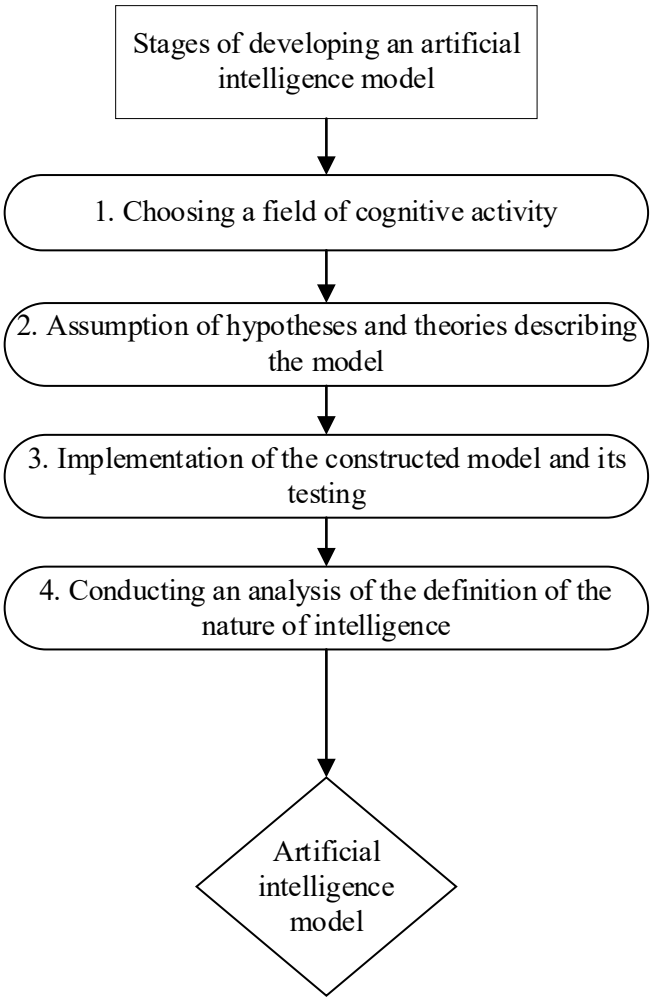

Fig. 1. **Stages of developing an artificial intelligence model**

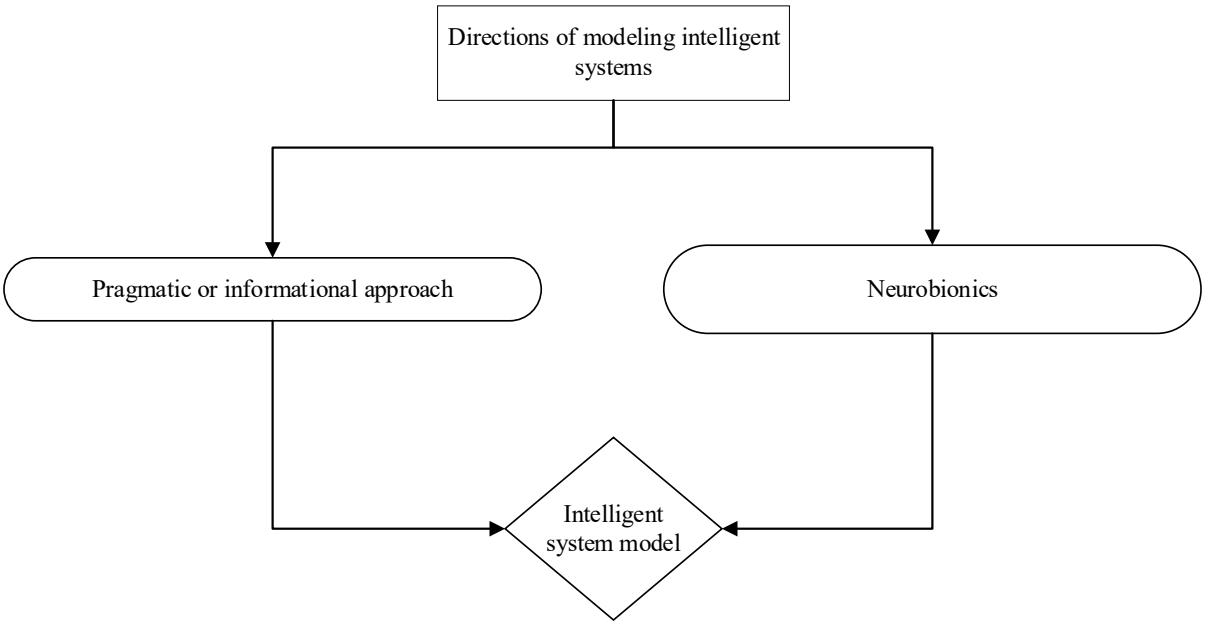

Fig. 2. **Directions of modeling intelligent systems**

The study [20] presents a structural diagram of the application of artificial intelligence on high-speed railways. The structural diagram includes the following blocks:

1) Mechanical and electrical system. This block includes intelligent manufacturing of trains and key components; forecasting of railway maintenance using artificial intelligence; optimization of energy consumption on railways and trains using artificial intelligence.

2) Communication and signal control. This block includes communication security using artificial intelligence methods; reliability of information exchange using artificial intelligence; modeling and evaluation of communication channels using artificial intelligence.

3) Railway transport management. This block includes passenger traffic planning based on artificial intelligence; traffic flow forecasting based on artificial intelligence. "Smart" platform for high-speed railway based on artificial intelligence.

To create intelligent systems based on artificial intelligence methods, a database and a knowledge base are required. To formalize and represent knowledge in the memory of information systems, a number of models are used, which can be structured as follows:

- Logical models – use formal logical systems, where knowledge is represented in the form of facts and rules, with the help of which conclusions are drawn. They are based on logical operators and form the basis for building logical conclusions.
- Network models – represent knowledge in the form of graphs or networks, where nodes correspond to objects, and the connections between them reflect relationships. An example is a semantic network, which illustrates the relationships between concepts.
- Frame models – knowledge is organized in the form of frames, which are data structures for representing stereotypical situations. A frame contains slots corresponding to the attributes of an object and values describing the state of the object. Frames are useful for modeling knowledge in the context of situations or scenarios.
- Production models – use a set of “if-then” rules (productions) that determine what actions should be performed under certain conditions. These rules allow to make inferences and make decisions based on the available information.

Each of the models of knowledge representation in artificial intelligence has its limitations and shortcomings. Let's consider the main shortcomings of logical, network, frame and production models:

Logical models:

- Difficulty in scaling.
- Lack of flexibility.
- Sensitivity to incomplete data.

Network models:

- Difficulty in building and maintaining.
- Limited expression of complex concepts.
- Performance problems:

Frame models:

- Rigidity of structure.
- Problems with uncertainty handling.
- Problems with frame interaction.

Production models:

- Complexity of managing a large number of rules.
- Problems with efficiency.
- Maintenance and updating.

For the rolling stock management problem, it is proposed to use a production model that combines elements of logical and network approaches. The concept of inference rules, called products, is borrowed from logical models, and the representation of knowledge in the form of a semantic network is borrowed from network models.

One of the most convenient programming tools in the field of fuzzy logic is the Fuzzy Logic environment of the Matlab application package [21-26]. The main advantage of this method is visual modeling, when it is possible to create quite complex programs without writing program code. To create simulation programs in Matlab (Fuzzy Logic), Mamdani or Sugeno algorithms [27] are used.

The Sugeno algorithm [28] formalizes decision-making processes under uncertainty when the input data are imprecise or fuzzy (Fig. 3).

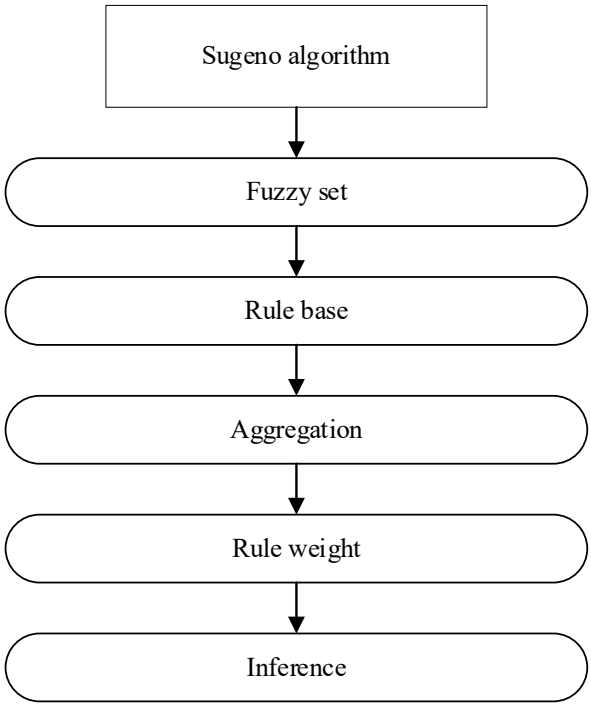

Fig. 3. **Class diagram of the Sugeno algorithm**

All input variables are converted into degrees of membership in fuzzy sets (fuzzification):

$$x_1 = high(0.8),\ medium(0.2)$$
$$x_2 = low(1.0) \quad (1)$$

Кожне правило має вигляд:

$$If\ \mathrm{x}_1 \in A_1\ \mathrm{i}\ \mathrm{x}_2 \in A_2, then\ \mathrm{y}=f(\mathrm{x}_1,\mathrm{x}_2), \quad (2)$$

where x_1, x_2 – the input variables of the system;
A_1, A_2 – the fuzzy set that describes the linguistic values of these variables (for example, “High”, “Medium”, “Low”;
$f(\mathrm{x}_1,\mathrm{x}_2)$ – the consequence function (linear or constant).

For example, there is the variable “Engine Temperature (x1)”. A1= “Low” is a fuzzy set with a certain membership function:

$$\mu_{A_1}(x_1) = \max(0, \min(1, (\frac{30 - x_1}{10}))), \quad (3)$$

where μ_{A_1} – the membership function of the element x to the fuzzy set A.

That is, the lower the temperature, the higher the degree of membership to “Low”. Unlike Mamdani Algorithm, Sugeno conclusion is not a fuzzy concept, but is usually a linear or constant function.

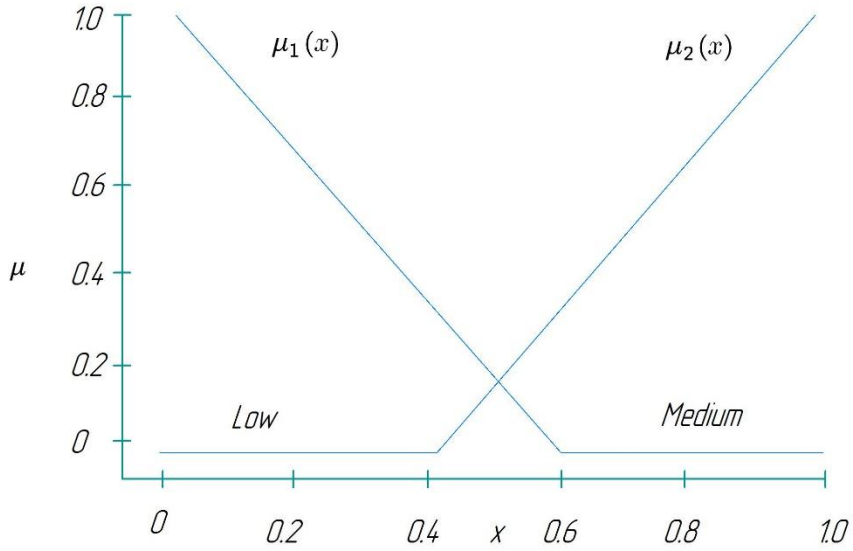

Fig. 4**. Diagram of the membership function A_1, A_2**

Instead of weight cents, as in Mamdani, a weighted average is used:

$$y = \frac{\sum_{i=1}^{n} w_i \cdot f_i(x)}{\sum_{i=1}^{n} w_i}, \tag{4}$$

where w_i – the degree of activation (weight) of the rule;
$f_i(x)$ – the result of the consequence function of the rule.

Mamdani algorithm [29-32] describes several stages that are executed sequentially. At the same time, each subsequent stage receives the values obtained at the previous step as input. The algorithm works according to the “black box” principle [33]. At the intermediate stages, the fuzzy logic apparatus and the theory of fuzzy sets are used. To implement the algorithm, the diagram shown in Fig. 5 is used, which indicates the most significant connections and relationships between the classes involved in the algorithm.

Rules consist of conditions and conclusions, which in turn are fuzzy statements. A fuzzy statement includes a linguistic variable and a term represented by a fuzzy set. A membership function is defined on the fuzzy set, the value of which can be obtained using the get Value method. This method is defined in the FuzzySetlface interface. When executing the algorithm, it will be necessary to use an “activated” fuzzy set (ActivatedFuzzySet), which in some way redefines the membership function of the fuzzy set (FuzzySet). The algorithm also uses the union of fuzzy sets (UnionOfFuzzySets). The union is also a fuzzy set, and therefore has a membership function (defined by FuzzySetlface). Mamdani Algorithm includes all stages and uses a rule base (List<Rule>) as input data. The algorithm also involves the use of "activated" fuzzy sets (ActivatedFuzzySet) and their unions (UnionOfFuzzySets).

Formation of a rule base. A rule base is a set of rules, where each subconclusion corresponds to a certain weight coefficient.

A rule base can have the following form (for example, rules of different constructions are used):

RULE_1: IF «Condition_1» THEN «Conclusion_1» (F1) AND «Conclusion_2» (F2);

RULE_2: IF «Condition_2» AND «Condition_3» THEN «Conclusion_3» (F3);

RULE_n: IF «Condition_k» THEN «Conclusion_(q-1)» (Fq-1) AND «Conclusion_q» (Fq),

Fi - are weight coefficients, which denote the degree of confidence in the truth of the obtained subconclusion (i = 1..q). By default, the weight coefficient is taken equal to 1. Linguistic variables present in the conditions are called input, and in the conclusions - output.

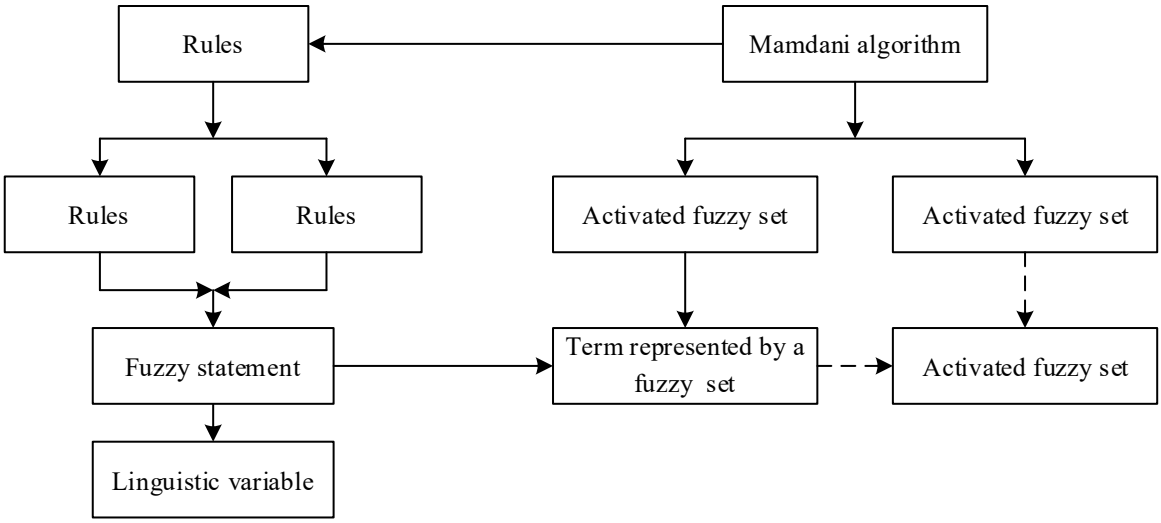

Fig. 5. **Mamdani algorithm implementation class diagram**

Aggregation of subconclusions. The purpose of this stage is to determine the degree of truth of the conditions for each rule of the fuzzy inference system [19]. Formally, it looks like this:

$$c_j = \min\{b_i\} \tag{5}$$

where j=1...n (n – the number of fuzzy production rules);
i – a number from the set of sub-condition numbers in which the j-th input variable participates

Activation of subconclusions. This method is called min-activation, which is formally written as follows:

$$\mu_i^{'}(x) = \min\{d_i, \mu_i(x)\}, \tag{6}$$

where $\mu_i(x)$ – the "activated" membership function;
$\mu_i(x)$ – the membership function of the term;
d_i – the degree of truth of the i-th subconclusion.

Accumulation of conclusions. The purpose of this stage is to obtain fuzzy sets (or their union) for each of the output variables [10]. The union of two fuzzy sets is represented as a third fuzzy set with the following membership function:

$$\mu_i^{'}(x) = \max\{\mu_1(x), \mu_2(x)\}, \tag{7}$$

where $\mu_1(x)$, $\mu_{12}(x)$ – the membership functions of the combined sets.

Defuzzification of output variables. The purpose of defuzzification is to obtain a quantitative value (crisp value) for each of the output linguistic variables [19]. This implementation of the algorithm uses the center of gravity method, according to which the value of the i-th output variable is calculated by the formula:

$$y_i = \frac{\int_{Min}^{Max} x \cdot \mu_i(x) dx}{\int_{Min}^{Max} \mu_i(x) dx}, \quad (8)$$

where $\mu_i(x)$ – the membership function of the corresponding fuzzy set E_i;
Min and *Max* – the boundaries of the universe of fuzzy variables;
y_i – the defuzzification result.

For a simple interpretation, close to human logic, in the process of controlling the traction transmission of shunting locomotives, it is proposed to use the Mamdani Algorithm, which will allow obtaining a clearer graphical representation.

In work [19], an intelligent model of controlling the traction transmission of shunting locomotives is proposed, the basis of which is the Mamdani Algorithm. To create a knowledge base, rules in the form of logical products "If condition, then action" were used. The number of connected TEDs at partial loads was chosen as actions. All input signals were normalized in the interval [0;1]. To represent them in the form of fuzzy values, a set of characteristic functions was assigned to each input signal. Fig. 6 and 7 show the fuzzification of the values "Speed", "Traction generator current", "They are represented by the following fuzzy values: "very_low", "low", "middle", "high", "very_high".

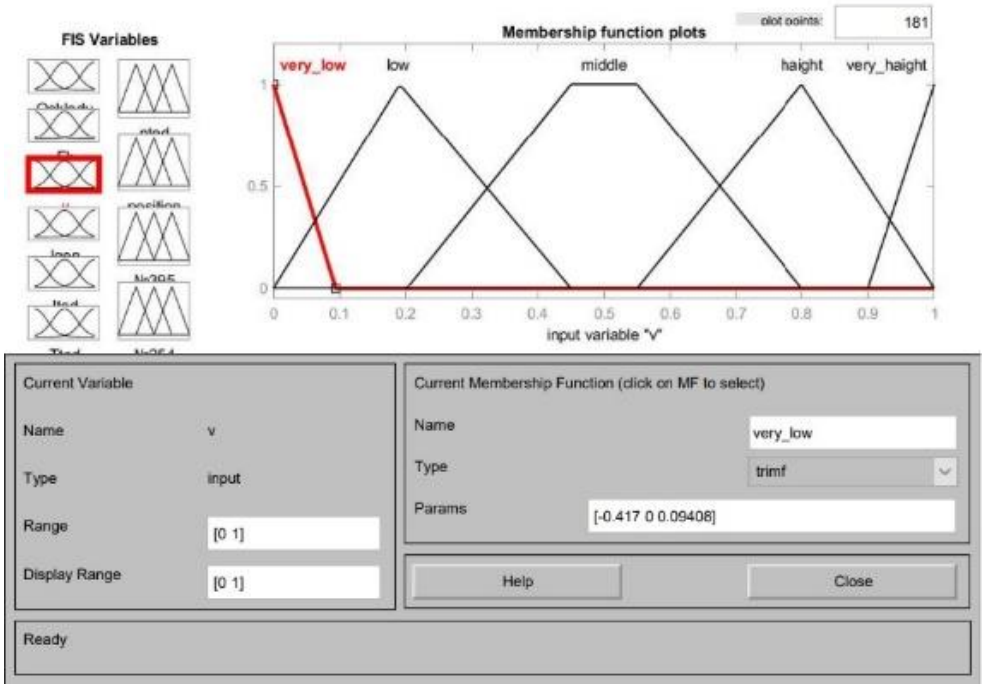

Fig. 6. **Fuzzification of the "Speed" value**

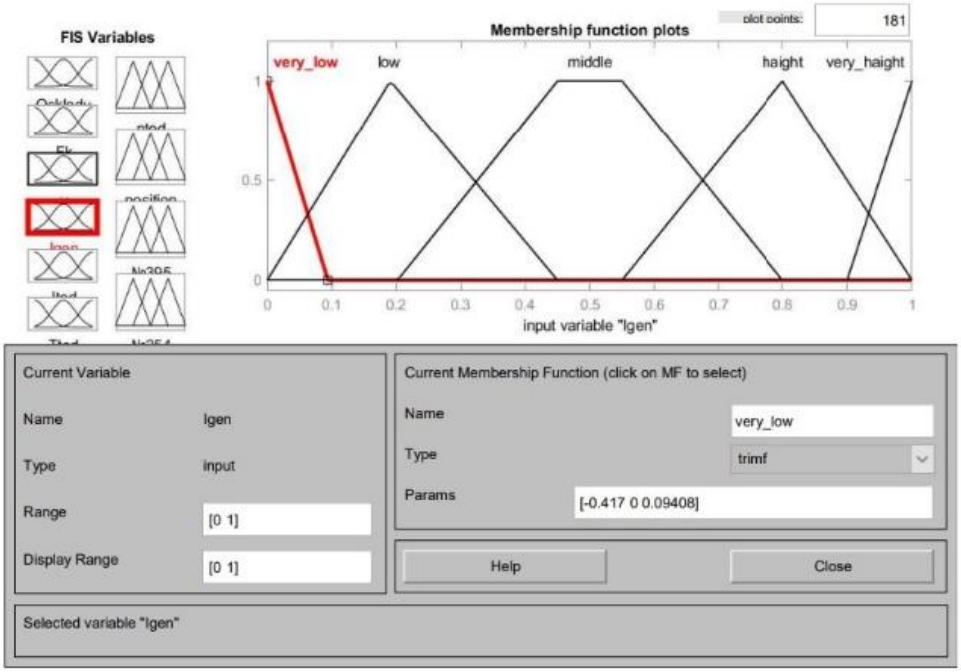

Fig. 7. **Fuzzification of the "Traction generator current" value**

Fig. 8 and 9 present the defuzzification of the "Number of connected TEM" and "Position of the driver's controller handle No. 254" output values

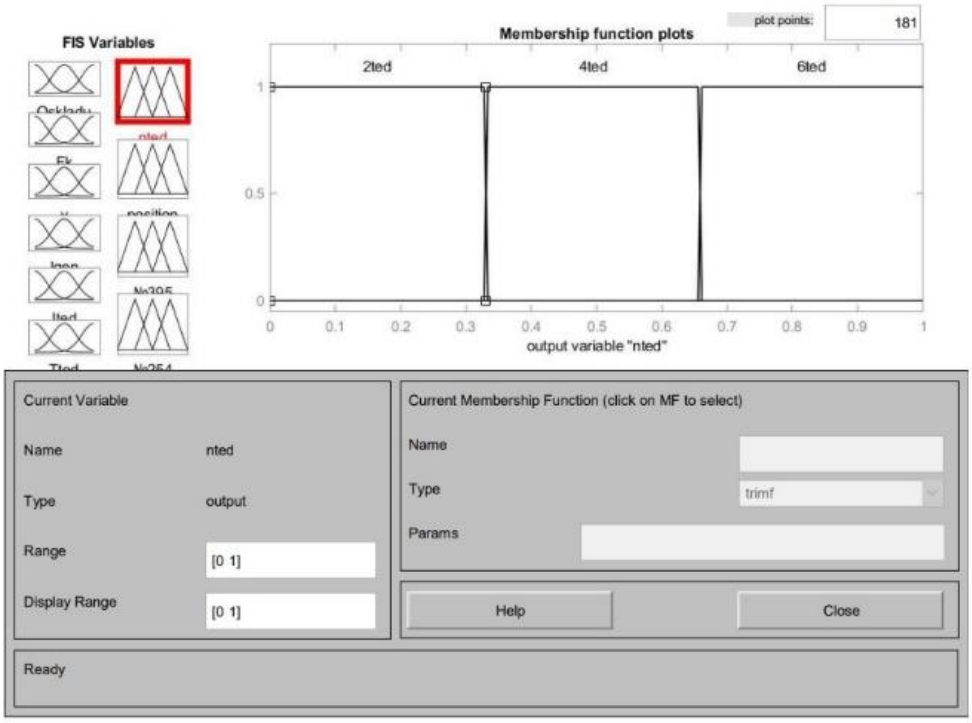

Fig. 8. **Defuzzification of the "Number of connected TEM" value**

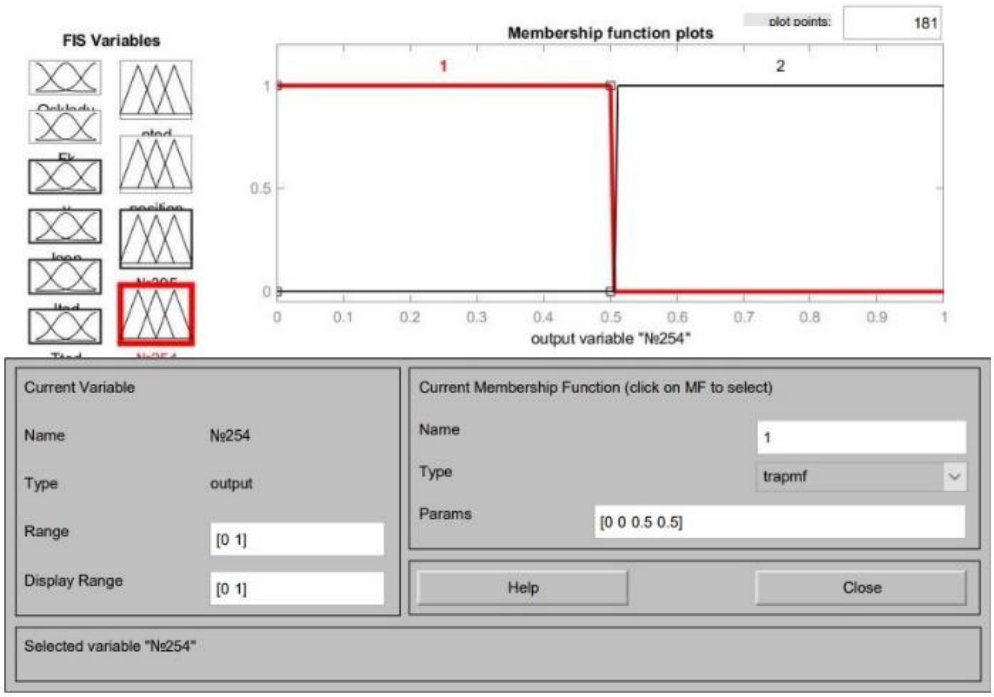

Fig. 9. **Defuzzification of the "Position of the driver's controller handle No. 254" value**

Using the method of expert assessments and traction rolling stock control logic, a list of logical rules for this control system has been developed. For example, one variant of the developed logical rules is shown, which has the following form:

If(IF) (Qskladu(Train mass) is very_low) and(I) (Fk(Traction force) is very_high) and(I) (v(Speed) is very_high) and(I) (Igen(Generator current) is high) and(I) (Ited(Traction electric motor current) is high) and(I) (Tted(Temperature above ambient for TED Д) is low) then(then) (nted(Number of connected TEMs is 6ted)(position(Locomotive position is 5ps) (№395(Driver's controller position No.395) is 2)(№254(Driver's controller position No 254) is 2) (1);

The results of modeling the automated traction control system of shunting locomotives based on a mathematical model allow to analyze the relationship between the input parameters and the output variable of the system. This approach allows to identify patterns in the behavior of the system under different operating modes. In particular, using the Fuzzy Logic Surface Viewer tool, it is possible to construct three-dimensional dependencies that clearly reflect the nature of changes in the output signal depending on variations in the input variables. This allows to:

- visualize fuzzy dependencies between parameters;
- identify critical areas of operation;
- optimize control based on graphical analysis;
- compare the effectiveness of different traction control strategies.

Thus, the use of fuzzy logic in modeling provides flexibility, adaptability and more accurate accounting for uncertainties in the operation of the locomotive, which is especially important for shunting modes.

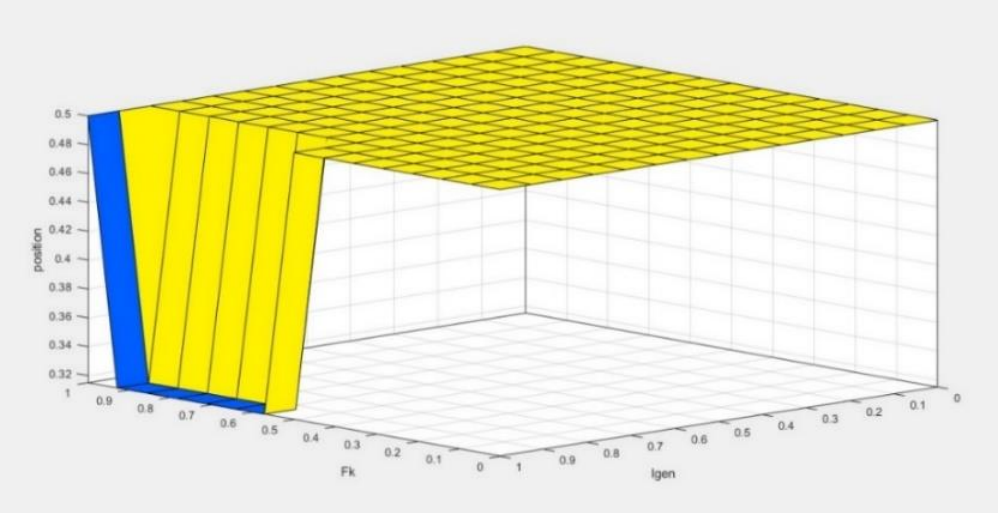

Fig. 10. **Three-dimensional surface of the dependence of the "Driver's controller position" output variable on the "Traction force" and "Traction generator current" inputs**

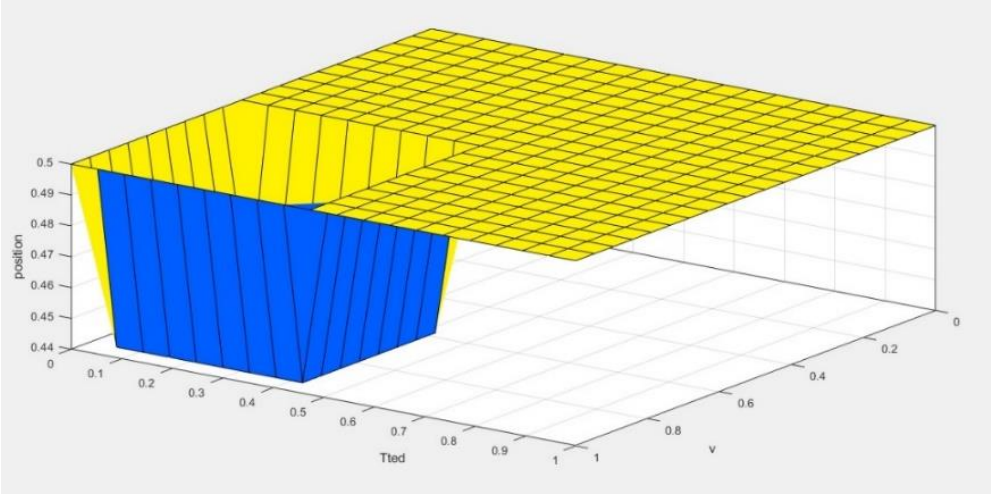

Fig. 11. **Three-dimensional surface of the dependence of the "Driver's controller position" output variable on the "Temperature above ambient for TED" and "Speed" inputs**

Assessment of shortcomings and prospects for the development of the above research. In the process of analyzing existing automated rolling stock control systems based on artificial intelligence methods, the main shortcomings can be identified, such as limited consideration of locomotive components, existing works have created effective models for controlling individual nodes, but do not take into account the interaction with other key subsystems of the locomotive (braking, cooling system, electrical network, etc.), which reduces the complexity of the model. An additional disadvantage is the complexity of scaling and maintenance. With an increase in the number of rules and variables, the system becomes more complicated, becomes difficult to administer, and the possibility of conflicts between rules increases. The works lack a clear description of experimental testing of the model on real equipment or in simulation conditions, which makes it difficult to assess its practical effectiveness. In addition, there is a problem with providing an analysis of the time delay in the operation of the control system, which is critical in real conditions of railway transport. In further research, the models should be expanded to a full digital twin of the locomotive, combining the developed models with other digital modules, which will allow the implementation of the "Smart Locomotive" concept. Additionally, integration with machine learning and reinforcement learning is required, which will allow the use of

self-learning models for automatic generation or correction of production rules, and the creation of a dynamic knowledge base that will adapt to new train situations.

Conclusions. The conducted analysis allowed to form the main directions of application of artificial intelligence in railway transport, to highlight the main stages of developing a vehicle control model based on artificial intelligence. Based on the analysis conducted, it is proposed to use a production model for traction rolling stock control tasks. The conducted analysis of the theoretical foundations of existing decision-making methods demonstrates the effective application of the Mamdani algorithm, which is closest to human logic, but has the potential for significant development – both in the direction of expanding functionality and in improving adaptability and practical application. Based on the conducted research, a generalized approach to creating an intelligent traction control system for shunting locomotives is presented. The model has demonstrated its adequacy and effectiveness, it has significant potential for further development.

REFERENCES

1. Fernández, P. M., Sanchís, I. V., Yepes, V., & Franco, R. I. (2019). A review of modelling and optimisation methods applied to railways energy consumption. *Journal of Cleaner Production, 222*, 153-162. https://doi.org/10.1016/j.jclepro.2019.03.037.
2. Aredah, A., Du, J., Hegazi, M., List, G., & Rakha, H. A. (2024). Comparative analysis of alternative powertrain technologies in freight trains: A numerical examination towards sustainable rail transport. *Applied Energy*, 356. https://doi.org/10.1016/j.apenergy.2023.122411.
3. Aredah, A., Fadhloun, K., & Rakha, H. A. (2024). Energy optimization in freight train operations: Algorithmic development and testing. *Applied Energy*, 364. https://doi.org/10.1016/j.apenergy.2024.123111.
4. Aredah, A. S., Fadhloun, K., & Rakha, H. A. (2024). NeTrainSim: a network-level simulator for modeling freight train longitudinal motion and energy consumption. *Railway Engineering Science*, 1-19. https://doi.org/10.1007/s40534-024-00331.
5. Jing, S. H. A. N. G., Yong, L. I. U., & Fan, J. I. A. N. G. (2023). Research and application of locomotive automatic operation technology. *Electric Drive for Locomotives, 1*, 1–12. https://doi.org/10.13890/j.issn.1000-128X.2023.01.001.
6. Ткаченко, О. І., & Куліш, С. А. (2024). Проблеми та перспективи впровадження геоінформаційних систем на залізничному транспорті. *IT Synergy*, (2), 155-169. https://doi.org/10.53920/ITS-2024-2-10.
7. R. Lakshmi Devi, G. Saravanan, K. Sangeetha, S. Pavithra and S. Thiyagarajan, (2021). Smart Train Accident Detection And Prevention System Using Iot Technology. *International Conference on System, Computation, Automation and Networking (ICSCAN)*, Puducherry, India, 2021, pp. 1-3. https://doi.org/10.1109/ICSCAN53069.2021.9526413.
8. Flammini, F., De Donato, L., Fantechi, A., & Vittorini, V. (2022, May). A vision of intelligent train control. In International Conference on Reliability, Safety, and Security of Railway Systems (pp. 192-208). Cham: Springer International Publishing. https://doi.org/10.1007/978-3-031-05814-1_14.
9. Liu, Q., Li, N., Tang, H., & Jia, X. (2023). An Analysis of Intelligent Operation and Maintenance for Rail Transit Electric Locomotives. Engineering Advances, 3(3). https://doi.org/10.26855/ea.2023.06.002.
10. Morin, X., Olsson, N. O., & Lau, A. (2024). Managerial Challenges in Implementing European Rail Traffic Management System, Remote Train Control, and Automatic Train Operation: A Literature Review. Future Transportation, 4(4), 1350-1369. https://doi.org/10.3390/futuretransp4040065.
11. Krawczyk, J. (2021). The era of the unmanned vevicles is coming. Przegląd Nauk O Obronności, 11, pp. 27-42. http://dx.doi.org/10.37055/pno/142494.
12. Taguchi, K., & Ishikawa, F. (2021). Experimental Conformance Evaluation on UBER ATG Safety Case Framework with ANSI/UL 4600. In Computer Safety, Reliability, and Security. SAFECOMP 2021 Workshops, (pp. 272-283). Springer International Publishing. https://doi.org/10.1007/978-3-030-83906-2_22.
13. Jung H-S, Eschmann F, Schindler C. (2023). Experimental investigation on RFID-odometer-based localization of an automated shunting vehicle. Proceedings of the Institution of Mechanical Engineers, Part F. 238(1), pp. 14-23. https://doi.org/10.1177/09544097231176464.
14. Wang, Y., Song, W., Zhang, Y., Huang, F., Tu, Z., Li, R., ... & Lou, Y. (2024). Four years of multimodal odometry and mapping on the rail vehicles. Journal of Field Robotics, 41(2), 227-257. https://doi.org/10.1002/rob.22256.
15. Gorobchenko, O., & Zaika, D. (2022). Review of methods and prospects of using artificial intelligence in railway transport. Innovations and prospects of world science. Springer. pp. 184–192.
16. Gorobchenko, O., Holub, H., & Zaika, D. (2024). Theoretical basics of the self-learning system of intelligent locomotive decision support systems. Archives of Transport, 71(3), pp. 169–186. https://doi.org/10.61089/aot2024.gaevsp41
17. Zhou, K., Song, S., Xue, A., You, K., & Wu H. (2022). Smart train operation algorithms based on expert knowledge and reinforcement learning. IEEE Transactions on Systems, Man, and Cybernetics: Systems, 52(2). pp. 716–727. https://doi.org/10.1109/TSMC.2020.3000073
18. Gorobchenko, O. & Nevedrov, O. (2020). Development of the structure of an intelligent locomotive DSS and assessment of its effectiveness. Archives of Transport, 56(4), pp. 47–58. https://doi.org/10.5604/01.3001.0014.5517

19. Gorobchenko, O., & Zaika, D. (2024). Creation of a model of automated traction control of shunting locomotives by using artificial intelligence methods. Transport Systems and Technologies, (44), pp. 8–26. https://doi.org/10.32703/2617-9059-2024-44-1
20. Li, X., Zhu, M., Zhang, B., Wang, X., Liu, Z., & Han, L. (2024). A review of artificial intelligence applications in high-speed railway systems. High-speed Railway, 2(1), pp. 11-16. https://doi.org/10.1016/j.hspr.2024.01.002
21. Herpratiwi, H., Maftuh, M., Firdaus, W., Tohir, A., Daulay, M. I., & Rahim, R. (2022). Implementation and Analysis of Fuzzy Mamdani Logic Algorithm from Digital Platform and Electronic Resource. TEM Journal, 11(3), pp. 1028-1033. https://doi.org/10.18421/TEM113-06
22. Zadeh, L. A. (2023). Fuzzy logic. In Granular, Fuzzy, and Soft Computing. New York: NY: Springer US. https://doi.org/10.1007/978-3-642-27737-5_234
23. Kaczorek, M., & Jacyna, M. (2022). Fuzzy logic as a decision-making support tool in planning transport development. Archives of Transport, 61(1). 51–70. https://doi.org/10.5604/01.3001.0015.8154
24. Ciani, L., Guidi, G., Patrizi, G., & Galar, D. (2021). Improving Human Reliability Analysis for railway systems using fuzzy logic. IEEE Access, (9). 128648–128662. DOI: 10.1109/ACCESS.2021.3112527
25. Alnuman, H. H., Gladwin, D. T., Foster, M. P., & Ahmed, E. M. (2022). Enhancing energy management of a stationary energy storage system in a DC electric railway using fuzzy logic control. International Journal of Electrical Power & Energy Systems, (142). 108345. https://doi.org/10.1016/j.ijepes.2022.108345
26. Rodriguez, R., Trovão, J. P. F., & Solano, J. (2022). Fuzzy logic-model predictive control energy management strategy for a dual-mode locomotive. Energy Conversion and Management, (253). 115111. https://doi.org/10.1016/j.enconman.2021.115111
27. Eckert, J. J., Pavani Teodoro, Í., Valente Lopes, M., Wu, Q., & Santos, A. A. (2024). Multi-objective optimization of electro-pneumatic braking process with fuzzy logic control for heavy haul railway applications. International Journal of Rail Transportation, 1–20. https://doi.org/10.1080/23248378.2024.2338837
28. Apriyanto, R. A. N., & Samudra, D. I. (2022). Perbandingan Simulasi Kontrol Kecepatan Kereta Api Dengan Logika Fuzzy Metode Mamdani dan Sugeno. Telekontran: Jurnal Ilmiah Telekomunikasi, Kendali dan Elektronika Terapan, 10(1), pp. 18-29. https://doi.org/10.34010/telekontran.v10i1.7238.
29. Wang, L., Han, M., Li, X., Zhang, N., & Cheng, H. (2021). Review of classification methods on unbalanced data sets. IEEE Access, (9). 64606–64628. https://doi.org/10.1109/ACCESS.2021.3074243
30. Zhang, D., Mohammed, S., & Calvi, A. (2021). Fuzzy logic systems for transportation engineering. Journal of Intelligent & Fuzzy Systems, 41(4), 4705–4712. https://doi.org/10.3233/JIFS-189957
31. Herpratiwi, H., Maftuh, M., Firdaus, W., Tohir, A., Daulay, M. I., & Rahim, R. (2022). Implementation and Analysis of Fuzzy Mamdani Logic Algorithm from Digital Platform and Electronic Resource. TEM Journal, 11(3), 1028–1033. https://doi.org/10.18421/TEM113-06
32. Gorobchenko, O., Zaika, D., Holub, H., & Kulbovskyi, I. (2024). Development of an intelligent control model for a maneuvering locomotive using the Mamdani method. Innovations and Prospects of World Science. Proceedings of the I International Scientific and Practical Conference: Current Trends in Scientific Research Development, Boston, USA, August 22–24, 2024 (pp. 70–77).
33. Kacimi, M. A., Guenounou, O., Brikh, L., Yahiaoui, F., & Hadid, N. (2020). New mixed-coding PSO algorithm for a self-adaptive and automatic learning of Mamdani fuzzy rules. Engineering Applications of Artificial Intelligence, 89. https://doi.org/10.1016/j.engappai.2019.103417

Олександр Горобченко[1], Денис Заіка[2], Сергій Малюк[3], Олександр Архипов[4], Олександр Неведров[5]

[1]Професор, Кафедра електромеханіки та рухомого складу залізниць, Національний транспортний університет, М. Омеляновича-Павленка, 1, м. Київ, 01010, Україна. ORCID: https://orcid.org/0000-0002-9868-3852.

[2]Асистент, Кафедра електромеханіки та рухомого складу залізниць, Національний транспортний університет, М. Омеляновича-Павленка, 1, м. Київ, 01010, Україна. ORCID: https://orcid.org/0000-0003-0693-9580.

[3]Старший викладач, Кафедра електромеханіки та рухомого складу залізниць, Національний транспортний університет, М. Омеляновича-Павленка, 1, м. Київ, 01010, Україна. ORCID: https://orcid.org/0000-0003-1777-2384.

[4]Аспірант, Кафедра електромеханіки та рухомого складу залізниць, Національний транспортний університет, М. Омеляновича-Павленка, 1, м. Київ, 01010, Україна. ORCID: https://orcid.org/0009-0009-8873-8643.

[5]Старший викладач, Кафедра електромеханіки та рухомого складу залізниць, Національний транспортний університет, М. Омеляновича-Павленка, 1, м. Київ, 01010, Україна. ORCID: https://orcid.org/0000-0001-9347-0973.

Дослідження теоретичних основ впровадження інтелектуальних систем управління тяговою передачею локомотивів

В роботі виконано аналіз існуючих систем автоматизованого управління на основі теорії штучного інтелекту. Дані системи використовують методи нечіткої логіки, штучні нейроні мережі та генетичні алгоритми. Використання даних методів дозволяє створювати більш адаптивні та ефективні системи управління в порівнянні з традиційними методами. Сформовано основні напрямки застосування методів штучного інтелекту на залізничному транспорті, зокрема в системах управління локомотивами, та оптимізації режимів руху. Виділено основні етапи розробки моделей на основі штучного інтелекту, включаючи збір даних та навчання моделей. Сформовано основі напрямки моделювання інтелектуальних систем. Представлено узагальнений підхід для розробки інтелектуальної системи управління тяговою передачею маневрових локомотивів, який враховує характеристики рухомого складу та умови експлуатації. Для задачі управління пропонується використовувати продукційну модель.

Keywords: *залізничний транспорт, рухомий склад, управління, штучний інтелект, метод Мамдані, ризик, тягова електрична передача, безпека.*

DOI: 10.32703/2617-9040-2025-45-12

UDC 629.4.023.14

***Igor Martynov*[1*], *Yuri Kalabukhin*[2], *Alyona Trufanova*[3], *Stanislav Martynov*[4]**

[1]Department of wagons engineering and product quality, Ukrainian State University of Railway Transport, Feuerbach Square, 7, Kharkov, 61050, Ukraine. ORCID: https://orcid.org/0000-0002-0481-3514.

[2]Department of marketing, business activity and economic theory", Ukrainian State University of Railway Transport, Feuerbach Square, 7, Kharkov, 61050, Ukraine. ORCID: https://orcid.org/0000-0003-3693-7607.

[3]Department of wagons engineering and product quality, Ukrainian State University of Railway Transport, Feuerbach Square, 7, Kharkov, 61050, Ukraine. ORCID: https://orcid.org/0000-0003-1702-1054.

[4]Department of operation and repair of rolling stock, Ukrainian State University of Railway Transport, Feuerbach Square, 7, Kharkov, 61050, Ukraine. ORCID: https://orcid.org/0000-0003-1826-6053.

[*]**Corresponding author:** martinov.hiit@gmail.com.

Study of stress-strain state of passenger car body

The article presents the stress-strain state analysis results of the load-bearing elements of the body and frame of the 61-779 model passenger car. To assess the strength of the car body, the finite element method was used with the ANSYS software package. In the model, the body is represented as a system consisting of beam, shell, and solid finite elements. The connections are modeled using rigid links. The model contains a total of 890,436 nodes and 321,874 finite elements. Boundary conditions include restrictions of freedom in support nodes (fixed support) and applied external loads. The main load-bearing element of the car structure is the center sill, made of I-beam profile No. 30. Additional fastening elements are used to increase the stiffness of the connections between the center sill and the crossbeams. The sheathing is made of structural and stainless sheet steel. Corrugated metal 2 mm thick is used as the outer sheathing. A study was conducted on the stress-strain state of the car body with nominal dimensions. The highest stress under load occurs in the bolster beam at the point of contact with the end beam of the frame and amounts to 258 MPa. The stress in the body sheathing between window openings is 65 MPa. The results obtained will further determine the direction of research on the optimization of load-bearing structures of the frame and body.

Key words: *railway transport, passenger car, body, reliability, load, wear, stresses, optimization.*

Introduction. Railway transport remains the leading link in the country's transport system. Despite the decline in passenger traffic for well-known reasons, most passenger transportation is still carried out by railways. Therefore, passenger cars must ensure traffic safety and comfortable conditions for passengers.

Unfortunately, the current state of the passenger industry at the moment does not meet the requirements for the effective implementation of Ukraine's European integration course. The fleet of passenger cars owned by the Passenger Company branch of JSC Ukrzaliznytsia has largely worked out its standard service life and exhausted its resource. The average age of a passenger car exceeds thirty years. The cars are outdated both morally and physically. The major repairs carried out to extend the service life can no longer provide the required reliability and modern level of comfort.

Ukraine needs new innovative passenger cars. But traditional approaches to car design are based on assessing the safety margin. However, the loads acting in operation are of a probabilistic nature. As a result, a deterministic approach to designing primarily bodies turns out to be insufficiently effective in terms of ensuring both the reliability of a passenger car and its efficiency.

Analysis of recent research and problem statement. A number of studies have been devoted to the issues of ensuring the strength and reliability of passenger car bodies both in our country and abroad. Thus, articles [1, 2] present an overview of the technical condition of the passenger car fleet owned by the branch of JSC "Passenger Company" Ukrzaliznytsia. The authors come to the conclusion that a

radical renewal of the passenger car fleet is necessary. Moreover, the cars that are designed must meet all the requirements of the European Union regulatory documents [3].

The results of statistical analysis of the amounts of wear and damage to the metal structures of the frame and body of passenger cars from different years of manufacture are presented in the works [4, 5]. Dependencies characterizing the amount of corrosion wear on the operating time are obtained. It is proven that the lower parts of the side and end walls are most often subject to corrosion damage. The results of strength analysis of the passenger car metal structures, taking into account their wear, are presented.

Ways to reduce the tare weight of a passenger car are considered in the articles [6, 7]. The authors performed multi-variant calculations of the strength of a body with different skin thicknesses. It was established that the body of a passenger car has a sufficient margin of safety and, due to the rational use of elements of the car's metal structures, it is possible to achieve a reduction in the tare weight.

The article [88] describes calculation of the main standard dynamic characteristics for a new passenger car. All standardized dynamic indicators of the passenger car model 61-779 do not exceed the permissible values, and the stability indicators have a sufficient reserve, which indicates good running qualities of the car.

In article [9], the authors propose a method for theoretical study of the strength of double-decker car bodies, the selection of rational design schemes and parameters.

Study [10] discusses a method for assessing the durability of a passenger car body under the influence of random dynamic loads. The main focus is on the use of fatigue analysis using the finite element method. Taking into account dynamic stress and a nonlinear damage accumulation model, the service life and level of fatigue damage to the body are determined. The simulation results were experimentally confirmed.

The authors of the study [11] propose a method for testing the fatigue strength of a passenger car body frame. The tests are carried out under laboratory conditions with accurate simulation of loads corresponding to real operating conditions. The authors examined in detail the process of simulation on a vibration test rig during motion.

Study [12] presents a methodological approach to assessing the reliability of passenger car structures using the finite element method. The authors analyze the impact of various loads on the durability of the car body and propose approaches to optimizing structures to improve their reliability.

The paper [13] considers issues of determining the durability of a passenger car body under dynamic loads. The study is based on the finite element method and allows for high-precision modeling of the real dynamic properties of the body structure.

The article [14] presents the results of the analysis of the metal structures of passenger cars taking into account their operation. It has been proven that the lower parts of the side and end walls are most often subject to corrosion damage. The authors of the article [15] propose a new approach to dynamic optimization of the design of passenger car bodies under static loads.

The study [16] presents a methodology for predicting the safety level of passenger cars using well-known software products. The works [17, 18] assess the accident rate and provide proposals for the modernization of a railway passenger car. Using the finite element method, the authors simulated a collision of a passenger car with a rigid wall. As a result, a car design with better accident properties was obtained.

The purpose and tasks of the study. The purpose of this work is to conduct research for optimization calculations of the structures of bodies of new generation passenger cars. To achieve this, it is necessary to build a computational 3D model of the body and frame of the 61-779 railcar and, using the finite element method, analyze the stress-strain state of the load-bearing elements of the body and frame, taking into account possible wear during operation.

Materials and methods of research. The Finite Element Method (FEM) is currently one of the most essential computational techniques for solving problems in solid mechanics. It operates by discretizing a continuous object into a finite number of smaller regions, known as finite elements, to facilitate the numerical solution of continuum mechanics equations. These equations are assumed to hold true within

each individual element.

Finite elements may represent physical segments of the structure or be abstract mathematical representations – such as elements used to model rods, beams, plates, or shells. Each element is assigned specific physical properties (e.g., stiffness, strength, material density) and is used to describe key field variables relevant to solid mechanics, such as displacements, strains, and stresses.

These field variables are typically defined at the nodes of the element. Interpolation functions are then used to estimate their values at any location within the element or along its boundaries. The core of the FEM formulation involves establishing mathematical relationships between the nodal values – primarily displacements and the corresponding forces in the context of continuum mechanics. A rigid compartment passenger car was selected for the calculation. The frame design is based on a spine beam configuration with additional reinforcement along the entire perimeter of the frame. The main load-bearing element of the structure is the spine beam, made from I-beam profile No. 30. Cross beams made of channel sections are welded to it. To increase the rigidity of the joints between the spine and cross beams, additional fastening elements in the form of triangles are used.

Longitudinal beams present in the structure are intended for installation of undercarriage equipment. The end part of the frame consists of two channel sections, and the lower frame binding is also made from channel section No. 20. The load-bearing elements efficiently combine traditional structural and low-alloy steels commonly used in railcar manufacturing. The sheathing consists of sheet-rolled structural and stainless steels. Corrugated metal with a thickness of 2 mm is used as the exterior cladding. The roof frame consists of 26 arch-shaped cross beams with a Z-shaped profile. For reinforcement, each of them is additionally welded to an unequal-angle bar along the base of the arch and two reinforcement elements. The car floor is made of two corrugated trapezoidal sheets.

The calculation scheme is shown in Fig. 1

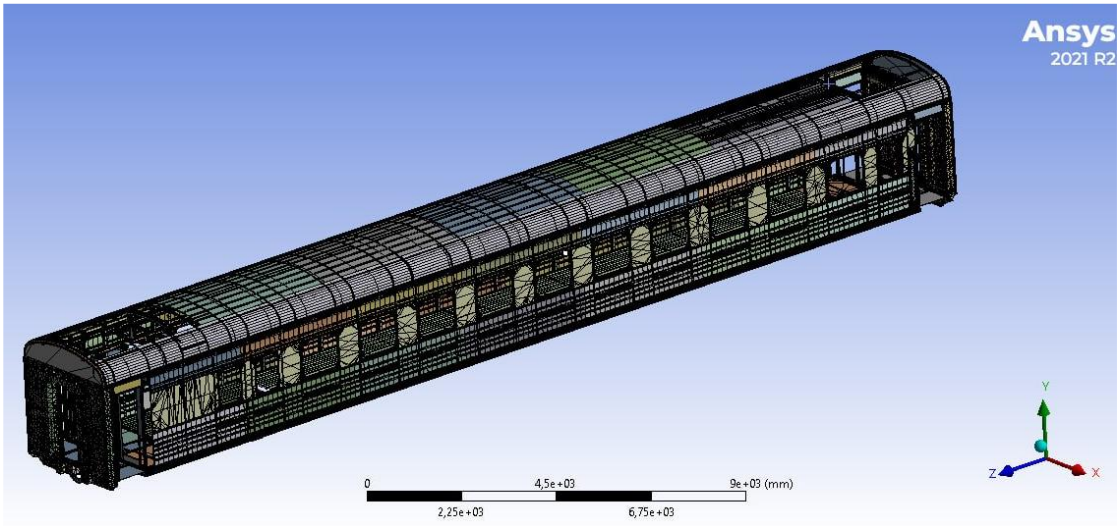

Fig. 1. **Passenger car 61-779 body model**

The load-bearing elements rationally combine traditional structural and low-alloy steels used in railcar construction. Sheathing is a rolled sheet made of structural and stainless steel.

To assess the strength of the body, the method of finite elements was applied using the ANSYS software complex in accordance with the requirements of the DSTU [19]. In the model, the body is presented as a system consisting of beam, shell and solid finite elements.

The calculation scheme of the body (without roof) is shown in Fig. 2 (view from below).

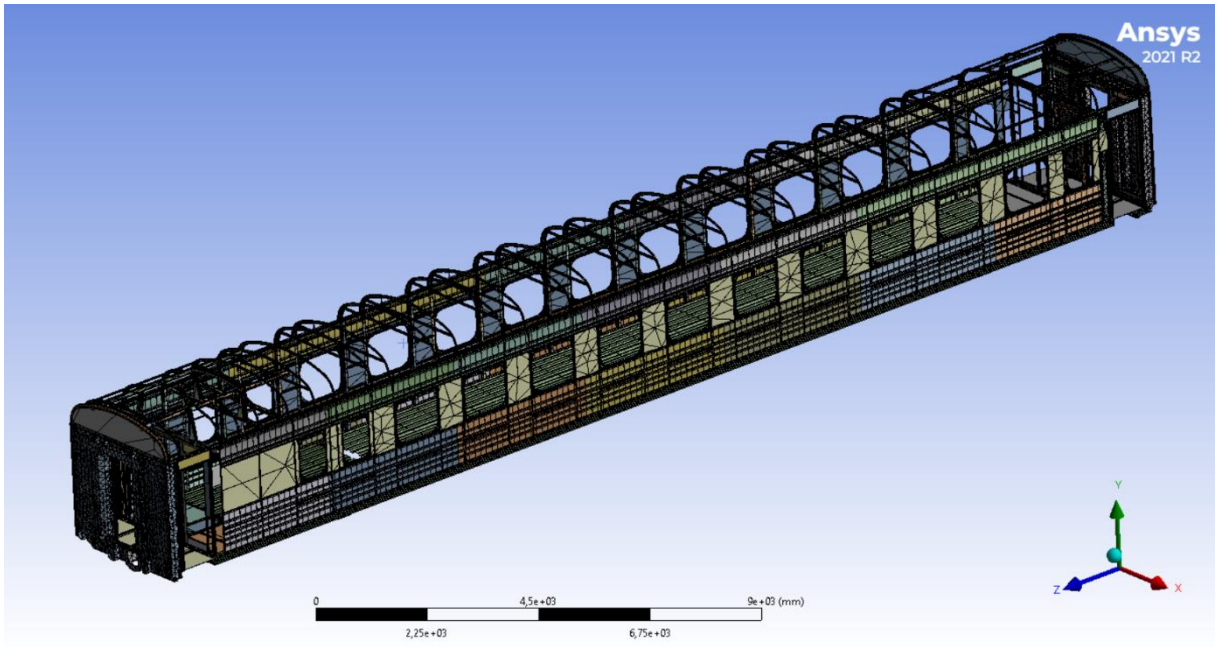

Fig. 2. **Passenger car 61-779 body model** (without roof)

The scheme of the body fastening in the thrust bearing unit is shown in Fig. 3 (view from below).

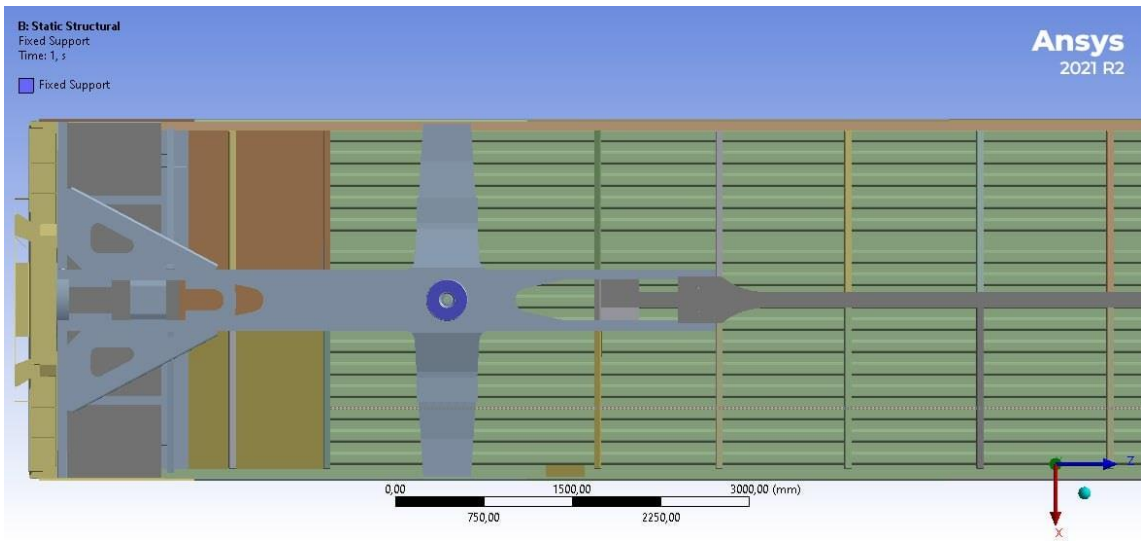

Fig. 3. **Passenger car 61-779 body model (view from below)**

Beam elements include risers, lower sidewall trim, roof arches, etc. Elements such as the upper trim, wall and roof trim, and floor were modeled using shell elements. Solid elements were used to describe structures of complex geometry such as (under the handrails) or end walls. Beam elements perceive all types of loads (tension, bending in two planes and torsion). Each node of such an element has three linear and three angular degrees of freedom. Beam elements - each node of such elements is endowed with six degrees of freedom: three linear displacements along the axes of the local reference system and three angles of rotation around these axes. Since the nodes of solid finite elements have only three degrees of freedom, all applied external moments are reduced to zero. Therefore, each finite element transfers only forces and linear displacements to neighboring elements.

The modeling of connections is implemented through a rigid connection. In total, the model contains

890,436 nodes and 321,874 finite elements.

The boundary conditions include restrictions of freedom in the supporting nodes (fixed support) and applied external loads.

According to the requirements of [19] for passenger cars, external loads include: the self-gravity of the structure (container), in particular objects and equipment, the gravity of passengers and personnel and luggage; inertial forces caused by oscillatory accelerations of masses during the movement of the wagon on a track with irregularities; forces arising during the movement of the wagon as a result of the interaction of the wagon and the track in curved sections of the track and switches, quasi-static wind pressure forces; static and dynamic forces of interaction between cars, between a car and a locomotive, traction and braking forces arising during transient modes, longitudinal forces of inertia and others.

Regarding longitudinal forces, the following load modes are established: I mode (conditional safety mode) and III mode – operational mode. Each of these modes includes appropriate load combinations that allow you to simulate different operating options.

The vertical loads acting on the body of a passenger car include the body's own weight, the mass of installed internal equipment, the stock of operating materials, and the mass of passengers with their luggage. These loads are supplemented by dynamic components that arise during the movement of the car due to vertical accelerations caused by track irregularities, vibrations, and other dynamic effects.

The vertical dynamic load is determined using the vertical dynamic coefficient. The coefficient of vertical dynamics k_{dv} is considered in [19] as a random function with a probability distribution of the form

$$P(k_{dv}) = 1 - exp\left(-\frac{\pi}{4} \cdot \frac{k_{d.v.}^2}{\overline{k}_{d.v.}^2} \cdot \beta^2\right). \quad (1)$$

The coefficient k_{dv} is defined as the quantile of this function with the calculated one-sided probability $P(k_{dv})$ according to the formula

$$k_{dv} = \overline{k}_{dv} \sqrt{\frac{4}{\pi} ln \frac{1}{1 - P(k_{dv})}}, \quad (2)$$

where $\overline{k}_{dv}$ is the average value of the vertical dynamic coefficient (mathematical expectation of the random process of changing the vertical dynamics coefficient $k_{dv}(t)$;
$P(k_{dv})$ – confidence probability. It is equal to $P(k_{dv})$=0.97.

The average value of the vertical dynamic coefficient $\overline{k}_{dv}$ визначається за наступною формулою

$$\overline{k}_{dv} = a + 3{,}6 \cdot 10^{-4} \cdot b \frac{V - 15}{f_{\text{ст}}}, \quad (3)$$

where a is an empirical coefficient, which for car bodies is equal to a=0.05;
b – coefficient depending on the number of axles in the cart (for biaxial carts b is equal to 1);
f_{st} – static deflection of spring suspension;

V – speed of movement in m/s.

$$f_{\text{ст}} = \frac{Q_{b.p.} + 2(Q_b + 0.333Q_1)}{2C_{b1}} + \frac{Q_{b.p.} + 2\left(Q_k + Q_1 + Q_{b.f.} + 0.333Q_2\right)}{2C_{b2}}, \quad (4)$$

where $Q_{b.p.}$ - body weight with passengers ($Q_{b.p.} = 518\ kN$);
Q_b - bolster weight ($Q_b = 6\ kN$);
Q_1 - weight of central spring suspension springs of one bogie ($Q_1 = 0.307\ kN$);
Q_2 - weight of axle box springs suspension of one bogie ($Q_2 = 0.312\ kN$);
C_{b1} - vertical rigidity of the central spring suspension of one bogie ($C_{b1} = 2659.22\ kN$);
C_{b2} - vertical rigidity of axle box spring suspension of one bogie ($C_{b2} = 6567.064\ kN$);
Q_k - empty body weight ($Q_k = 476\ kN$);
$Q_{b.f.}$ - weight of the bogie frame ($Q_{b.f.} = 14.68\ kN$);

After entering the corresponding values into formula (4), for a fully loaded passenger carwe obtain $f_{\text{ст}}$ 0.13 m.

During the calculations, it was assumed that the car moves at a maximum speed of 160 km/h and the third calculation mode is used.

Thus, for movement at a speed of 44.4 m/s, the average value of the coefficient of vertical dynamics $\overline{k}_{dv}$ was

$$\overline{k}_{dv} = 0{,}05 + 3{,}6 \cdot 10^{-4} \cdot 1\frac{44{,}4 - 15}{0{,}13} = 0{,}124.$$

$$k_{\text{дв}} = 0{,}124\sqrt{\frac{4}{3{,}14} ln \frac{1}{1 - 0{,}97}} = 0{,}263.$$

The gravitational force Q acting on the body is defined as the difference between the total (gross) mass of the car and the total mass of its bogies. During the calculations, the weight of the metal structure of the body itself and the massive units that make up the main equipment was initially taken into account.

The residual part of the force Q – that is, the difference between the total gravitational force and the already taken into account masses of structures and equipment — was evenly distributed over the floor area in the form of a surface load. This approach allows you to correctly model the influence of passengers and small equipment on the overall load distribution.

The action of the lateral load should be taken into account only when calculating according to mode III. The force, which is equal to the difference of the centrifugal force and the horizontal component of the gravity force, which arises as a result of the elevation of the outer rail, for passenger cars is 10% of the gross force of gravity. Then for a body with passengers

$$F_b = 0.1Q_{b.p.}. \quad (5)$$

$$F_b = 0.1 \cdot 518 = 51.8\ kN.$$

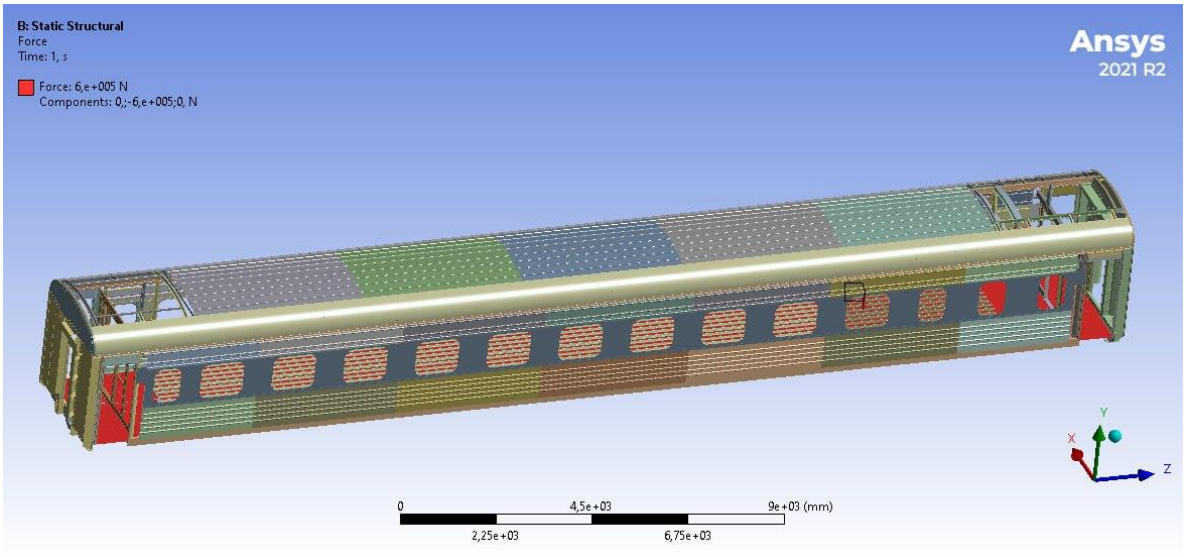

Fig. 4. **Scheme of application of a vertical load on the body of a passenger car**

Also taken into account is the force of wind pressure, which divides the area of the side projection of the body by the specific wind pressure (500 N/m^2).

For the body of a passenger car

$$F_b = p_w \cdot F, \tag{6}$$

where p_w - specific wind pressure ($p_w = 0.5\ kN/m^2$);
F - lateral projection area of the car body ($F = 98\ m^2$).

Then for the body of a passenger car force of wind pressure will be equal

$$F_b = 0.5 \cdot 98 = 49\ kN$$

Thus, the total lateral load will be 100.8 kN. It is applied to the upper and lower lining of the side walls.

Two load application options were considered during the calculations. The first corresponds to Calculation Mode I, while the second corresponds to Calculation Mode III at a speed of 160 km/h.

The distribution of stresses over the car body is shown in Fig. 5.

The highest stresses under loading occur in the pivot beam at the point of support on the end beam of the frame and amount to 258 MPa. Stresses in the roof elements do not exceed 57 MPa. In the side walls, the pillars are the most heavily loaded element. In them, the maximum stress does not exceed 69 MPa. Stresses in the body sheathing in the openings between the windows amount to 65 MPa. The maximum stress in the body occurs in the end walls – 160 MPa.

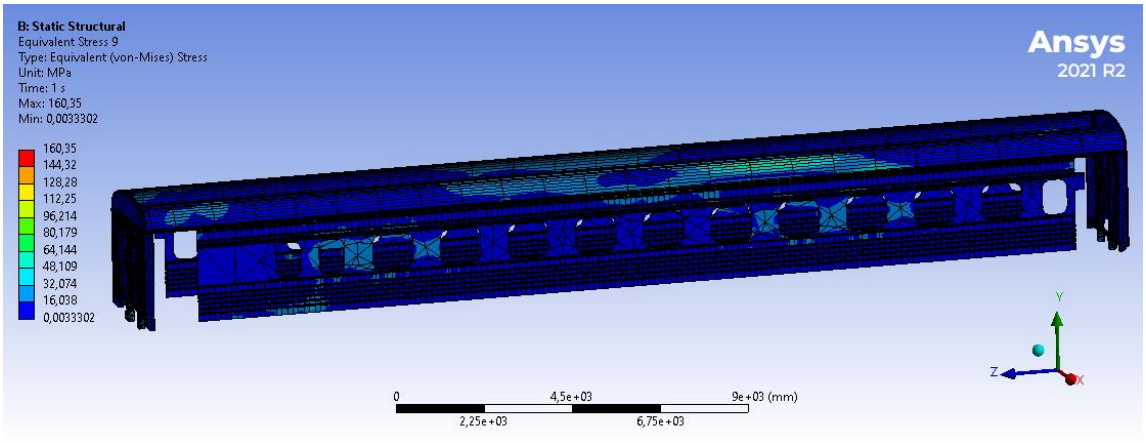

Fig. 5. **Stress distribution graph for the car body**

The distribution of stresses over the pivot beam and the bolster assembly is shown in Fig. 6.

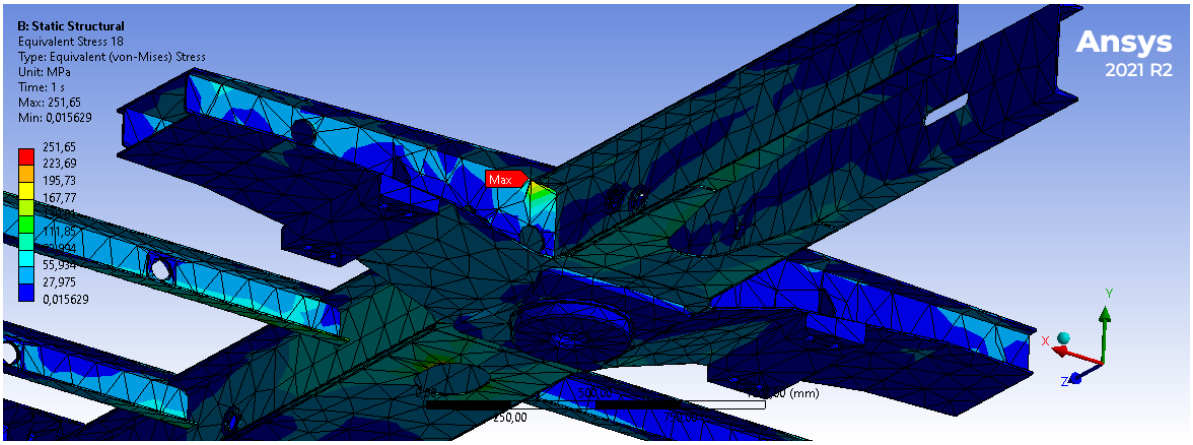

Fig. 6. **Diagram of stress distribution in the frame pivot assembly passenger car 61-779**

Stresses occurring in the center sill do not exceed 98 MPa, and they are localized at the junction with the end part of the frame. The average value of stresses arising in the center sill is 9.6 MPa. The most heavily loaded is the pivot beam. The stresses in the cross beams do not exceed 90 MPa. Except for the first row of cross beams supported by the end frame. In it, the maximum stresses reach 200 MPa in the contact zone with the center sill.

The developed model was verified. In the initial stage, calculations were performed for the structure with standard sheathing thicknesses. The results were then compared with experimental data from strength tests. The close agreement between the results confirmed the accuracy of the model.

For comparison, on Fig. 7 is shown stress distribution in the frame pivot assembly passenger car 47D [**Ошибка! Источник ссылки не найден.**]. The maximum stresses in the kingpin beam are localized near the bolster assembly and do not exceed 191 MPa.

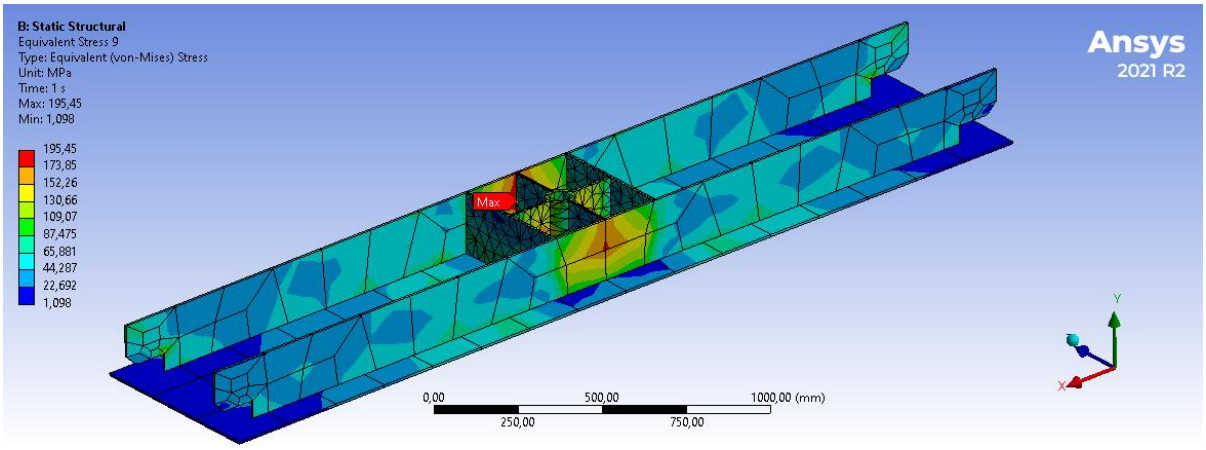

Fig. 7. **Diagram of stress distribution in the frame pivot assembly passenger car 47D**

The distribution of stresses in the center sill is shown in Fig. 8.

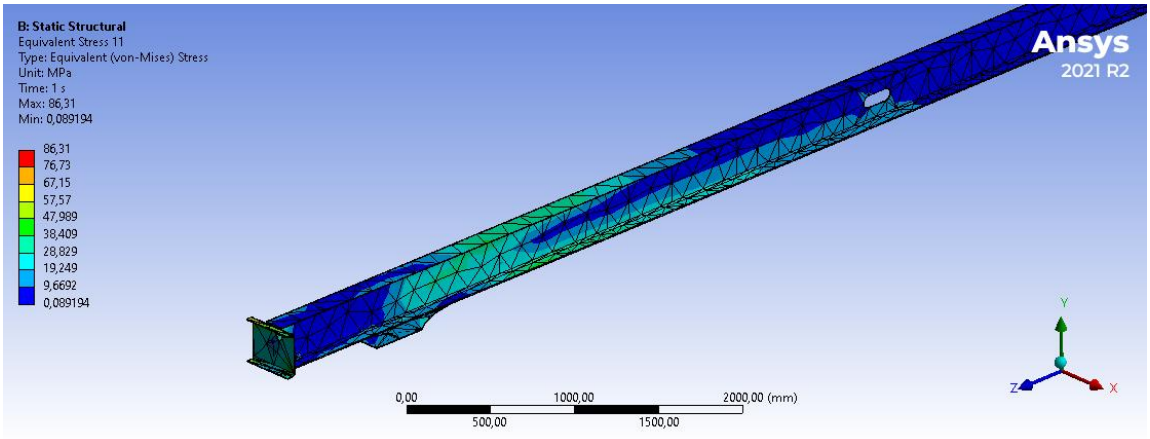

Fig.8. **Diagram of stress distribution in the center sill passenger car 61-779**

In the center sill of the 61-779 model railcar, the maximum stresses are also localized in the area of the pivot beam node and amount to 98 MPa.

The results obtained made it possible to compare the stress-strain state of the 61-779 model car with the 47D model car (Table 1).

Table 1. **Comparison of stresses in passenger car units**

	47D	61-779
Pivot beam	195,4	251,6
Longitudinal beam	258,7	-
Center sill	-	97,8
Cross beam	74,8	89,6
Body sheathing	125,1	65
End wall	143,3	160,3
Upper binding	46,3	57

Due to the fundamental differences in frame design, different elements are subjected to the highest loads. In model 47D, it is the longitudinal beam with 258.7 MPa, whereas in the 61-779 model, the most heavily loaded element is the pivot beam. In both designs, the maximum stresses occur near the bolster assembly. The overall stress values in the car body are similar, differing only in the side wall sheathing. The obtained stress values do not exceed the allowable limits.

Conclusion.

1. A finite element model was constructed based on the 3D model of the body of the rigid compartment car 61-779. The strength calculations of the body were performed using the finite element method. Beam, shell and solid finite elements were used to model the body elements.

2. A study was conducted of the stress-strain state of the body at nominal dimensions with standard skin thicknesses. The highest stresses under loading occur in the pivot beam at the point of support on the end beam of the frame and amount to 258 MPa. The stresses in the body sheathing in the openings between the windows are 65 MPa.

3. The results obtained will further determine the direction of research on the optimization of the supporting structures of the frame and body.

REFERENCES

1. Bozhok, N. O., Bulgakova, Y. V., & Pularia, A. L. (2014). Research on the current state of the passenger car fleet. *Review of transport economics and management*, (8), 78-87. [in Ukrainian].
2. Loboyko, L. N., & Barash, Yu. WITH. (2007). State of the wagon park and wagon repair base in Ukraine. Science and progress of transport. *Bulletin of the Dnipropetrovsk National University of Railway Transport*, (19), 176-182. [in Ukrainian].
3. Kirpa, G. M. (2004). *Integration of Ukrainian railway transport into the European transport system*. D.: Publishing house of Dnipropetrovsk National University of Railway Transport named after Acad. V. Lazaryan. [in Ukrainian].
4. Martynov, I., Trufanova, A., Petukhov, V., & Serhiienko, M. (2021). Research of the dependence of operation of carrying elements of passenger cars. *Transport Systems and Technologies*, (36), 72–81. [in Ukrainian]. https://doi.org/10.32703/2617-9040-2020-36-8.
5. Martynov, I. E., Trufanova, A. V., Pavlenko, Yu. S., & Sergienko, M. O. (2018). Analysis of the technical condition of passenger car bodies. *Bulletin of the National Technical University of KhPI. Series: New solutions in modern technologies*, (45), 41-46. https://doi.org/10.20998/2413-4295.2018.45.06. [in Ukrainian].
6. Myamlin, S. V., Yagoda, P. A., Dedaeva, T. A., & Shkabrov, O. A. (2006). Reducing the weight of metal structures of passenger cars for high-speed transportation. *Bulletin of the Dnipropetrovsk National University of Health Transport named after Academician V. Lazaryan*, (13), 118-120. [in Ukrainian].
7. Prikhodko, V. I., Shkabrov, O. A., Myamlin, S. V., & Yagoda, P. A. (2007). Improving the design of passenger car bodies for high-speed transportation. *Bulletin of the Dnipropetrovsk National University of Health Transport named after Academician V. Lazaryan*, (14), 152-156. [in Ukrainian].
8. Prikhodko, V. I. (2006). Calculation of dynamic indicators of a passenger car. Science and progress of transport. *Bulletin of the Dnipropetrovsk National University of Health Transport named after Academician V. Lazaryan*, (12), 146-152. [in Ukrainian].
9. Sun, W., Zhou, J., Gong, D., & You, T. (2016). Analysis of modal frequency optimization of railway vehicle car body. *Advances in Mechanical Engineering*, *8*(4), 1687814016643640. https://doi.org/10.1177/1687814016643640.
10. Sharma, S. K., Sharma, R. C., & Lee, J. (2022). In situ and experimental analysis of longitudinal load on carbody fatigue life using nonlinear damage accumulation. *International Journal of Damage Mechanics*, *31*(4), 605-622. https://doi.org/10.1177/10567895211046043/.
11. Song, Y., Wu, P., & Jia, L. (2016). Study of the fatigue testing of a car body underframe for a high-speed train. *Proceedings of the Institution of Mechanical Engineers, Part F: Journal of Rail and Rapid Transit*, *230*(6), 1614-1625. https://doi.org/10.1177/0954409715618425.
12. de Cisneros Fonfría, J. J. J., Olmeda, E., Sanz, S., Garrosa, M., & Díaz, V. (2024). Failure analysis of a train coach underframe. *Engineering Failure Analysis*, *156*, 107756. https://doi.org/10.1016/j.engfailanal.2023.107756.
13. Bingrong Miao, & Dingchang Jin. (2009). Evaluation of Railway Vehicle Car Body Fatigue Life and Durability using a Multi-disciplinary Analysis Method. *International Journal of Vehicle Structures and Systems,* 1(4). https://doi.org/10.4273/ijvss.1.4.05.
14. Martynov, I., Kalabukhin, Y., Trufanova, A., & Martynov, S. (2024). Analysis of stress state of passenger car bodies. *Transport systems and technologies*, (43), 111-120. [in Ukrainian]. https://doi.org/10.32703/2617-9059-2024-43-9.

15. Cascino, A., Meli, E., & Rindi, A. (2023). Dynamic size optimization approach to support railway carbody lightweight design process. *Proceedings of the Institution of Mechanical Engineers, Part F: Journal of Rail and Rapid Transit*, *237*(7), 871-881. https://doi.org/10.1177/09544097221140933.

16. Kobishanov, V.V., Lozbinev, V.P., Sakalo, V.I., Antipin, D.Y., Shorohov, S.G., & Vysocky, A.M. (2013). Passenger Car Safety Prediction. *World Applied Sciences Journal*, *24*, 208–212. https://www.idosi.org/wasj/wasj24(1)/ 2013.htm.

17. Baykasoglu, C., Sunbuloglu, E., Bozdag, S. E., Aruk, F., Toprak, T., & Mugan, A. (2012, April). Numerical static and dynamic stress analysis on railway passenger and freight car models. In *International Iron & Steel Symposium* (pp. 02-04)..

18. Baykasoğlu, C., Sünbüloğlu, E., Bozdağ, S. E., Aruk, F., Toprak, T., & Mugan, A. (2011). Railroad passenger car collision analysis and modifications for improved crashworthiness. *International Journal of Crashworthiness*, *16*(3), 319-329.https://doi.org/10.1080/13588265.2011.566475.

19. DSTU 7774:2015. (2017). *Mainline passenger locomotive-drawn wagons. General technical standards for the calculation and design of mechanical parts of wagons*. Ministry of Economic Development of Ukraine. [in Ukrainian].

20. Martynov, I. E., Trufanova, A. V., Shovkun, V. O., Martynov, S. I., & Ostapenko, Ya. V. (2023). Modeling the stress-strain state of a rigid-compartment passenger car body. Collection of scientific papers "Rail rolling stock", (27), 59-69. https://doi.org/10.47675/2304-6309-2023-27-59-69.

***Ігор Мартинов*[1], *Юрій Калабухін*[2], *Альона Труфанова*[3], *Станіслав Мартинов*[4]**

[1]Кафедра інженерії вагонів та якості продукції, Український державний університет залізничного транспорту, пл. Фейєрбаха, 7, Харків, 61050, Україна. ORCID: https://orcid.org/0000-0002-0481-3514.

[2]Кафедра маркетингу, комерційної діяльності та економічної теорії, Український державний університет залізничного транспорту, пл. Фейєрбаха, 7, Харків, 61050, Україна. ORCID: https://orcid.org/0000-0003-3693-7607.

[3]Кафедра інженерії вагонів та якості продукції, Український державний університет залізничного транспорту, пл. Фейєрбаха, 7, Харків, 61050, Україна. ORCID: https://orcid.org/0000-0003-1702-1054.

[4]Кафедра експлуатації та ремонту рухомого складу, Український державний університет залізничного транспорту, пл. Фейєрбаха, 7, Харків, 61050, Україна. ORCID: https://orcid.org/0000-0003-1826-6053.

Дослідження напружено-деформованого стану кузова пасажирського вагона

У статті викладено результати аналізу напружено-деформованого стану несучих елементів кузова та рами пасажирського вагона моделі 61-779. Для оцінки міцності кузова застосовано метод скінчених елементів з використанням програмного комплексу ANSYS. У моделі кузов представлений у вигляді системи, що складається з балкових, оболонкових та об'ємних кінцевих елементів. Всього модель містить 890436 вузлів і 321874 кінцевих елемента. Граничні умови включають обмеження свободи в опорних вузлах (нерухома опора) та зовнішні навантаження. Основним несучим елементом конструкції вагона є хребтова балка, виконана з двотаврового профілю № 30. До неї приварені поперечні балки зі швелерів. Для підвищення жорсткості з'єднань хребтової та поперечних балок використовуються додаткові елементи кріплення. Зовнішня обшивка кузова виконана з листових конструкційних та нержавіючих сталей товщиною 2 мм. Проведено дослідження напружено деформованого стану кузова при номінальних розмірах. Найбільші напруження при навантаженні виникають у шворневій балці у місці обпирання на кінцеву балку рами і становлять 258 МПа. Напруження в обшивці кузова в отворах між вікнами становлять 65 МПа. Отримані результати надалі визначать напрямок досліджень з оптимізації несучих конструкцій рами та кузова.

Ключові слова: *залізничний транспорт, пасажирський вагон, кузов, надійність, спрацювання, напруження, оптимізація.*

CONTENT

Dashdamirli N. Cross-platform development for microcontrollers: design of a virtual machine based portable programming language. **8**

Bal O., Tverdomed V., Kovalchuk O., Solodiak L., Borys N. Implementation of TSI requirements in railway infrastructure modernization projects of Ukraine in the context of EU transport system integration. **22**

Ishchenko V., Braikovska N., Shcherbyna Iu., Demchenko Yu.. Modern requirements for refrigeration agents in transport air conditioners. **37**

Riabov Ie., Overianova L., Kondratieva L., Plyutin O., Overianov A.. Comparative assessment of resonant frequencies of the floor of suburban electric train cars. **53**

Dashdamirov F., Verdiyev T. Study of the ınfluence of coordınated regulatıon on the traffıc flow parameters on ıntersectıng streets. **70**

Gertsiy O., Karnatov S., Gladish V., Tkachenko V. Modeling an Image Clustering Algorithm For Detecting Overheated Railway Axle. **81**

Burmaka I., Petrychenko O., Alieksieichuk B., Vynohradova A. Analysis of minimum safe approach distances based on vessels navigation safety domain. **94**

Sorochynska O., Melnichenko O., Kulbovskyi I., Derehuz I. Implementation of the occupational health and safety management system model according to DSTU ISO 45001:2018: challenges and opportunities for transport enterprises. **108**

Bulgakov M., Melnyk O. Intelligent digital twin utilization for real-time forecasting and optimization of the ship's power system. **121**

Karnatov S., Gertsiy O. Integration of Ukrainian railways into Trans-European Transport Network (TEN-T) – problems and solutions. **132**

Gorobchenko O., Zaika D., Maliuk S., Arkhypov O., Nevedrov O. Research of theoretical basis of implementation of intelligent control systems for locomotive traction transmission. **145**

Martynov I., Kalabukhin Yu., Trufanova A., Martynov S. Study of stress-strain state of passenger car body. **161**

Наукове видання

Scientific edition

ЗБІРНИК НАУКОВИХ ПРАЦЬ
ДЕРЖАВНОГО УНІВЕРСИТЕТУ ІНФРАСТРУКТУРИ ТА ТЕХНОЛОГІЙ
COLLECTION OF SCIENTIFIC PAPERS
OF THE STATE UNIVERSITY OF INFRASTRUCTURE AND TECHNOLOGIES

Серія «Транспортні системи і технології»
Series "Transport Systems and Technologies"

Випуск 45
Issue 45

Відповідальний за випуск С. О. Гулак
Редактор Н. В. Щербак
Макет і верстка В. О. Зорьки

Підписано до видання 01.06.2025.
Ум. друк. арк.8,1. Обл.-вид. арк. 12,00.
Наклад 50 прим. Зам. № 24/16.

Надруковано в друкарні редакційно-видавничого відділу
Державного університету інфраструктури та технологій.
Ідентифікатор медіа - R30-05246

03049, м. Київ-49, вул. І. Огієнка, 19.
https://tst.duit.in.ua/